



Terms and Conditions of Use of Digitised Theses from Trinity College Library Dublin

Copyright statement

All material supplied by Trinity College Library is protected by copyright (under the Copyright and Related Rights Act, 2000 as amended) and other relevant Intellectual Property Rights. By accessing and using a Digitised Thesis from Trinity College Library you acknowledge that all Intellectual Property Rights in any Works supplied are the sole and exclusive property of the copyright and/or other IPR holder. Specific copyright holders may not be explicitly identified. Use of materials from other sources within a thesis should not be construed as a claim over them.

A non-exclusive, non-transferable licence is hereby granted to those using or reproducing, in whole or in part, the material for valid purposes, providing the copyright owners are acknowledged using the normal conventions. Where specific permission to use material is required, this is identified and such permission must be sought from the copyright holder or agency cited.

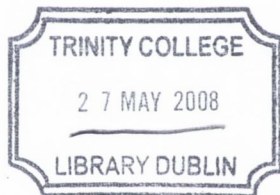
Liability statement

By using a Digitised Thesis, I accept that Trinity College Dublin bears no legal responsibility for the accuracy, legality or comprehensiveness of materials contained within the thesis, and that Trinity College Dublin accepts no liability for indirect, consequential, or incidental, damages or losses arising from use of the thesis for whatever reason. Information located in a thesis may be subject to specific use constraints, details of which may not be explicitly described. It is the responsibility of potential and actual users to be aware of such constraints and to abide by them. By making use of material from a digitised thesis, you accept these copyright and disclaimer provisions. Where it is brought to the attention of Trinity College Library that there may be a breach of copyright or other restraint, it is the policy to withdraw or take down access to a thesis while the issue is being resolved.

Access Agreement

By using a Digitised Thesis from Trinity College Library you are bound by the following Terms & Conditions. Please read them carefully.

I have read and I understand the following statement: All material supplied via a Digitised Thesis from Trinity College Library is protected by copyright and other intellectual property rights, and duplication or sale of all or part of any of a thesis is not permitted, except that material may be duplicated by you for your research use or for educational purposes in electronic or print form providing the copyright owners are acknowledged using the normal conventions. You must obtain permission for any other use. Electronic or print copies may not be offered, whether for sale or otherwise to anyone. This copy has been supplied on the understanding that it is copyright material and that no quotation from the thesis may be published without proper acknowledgement.

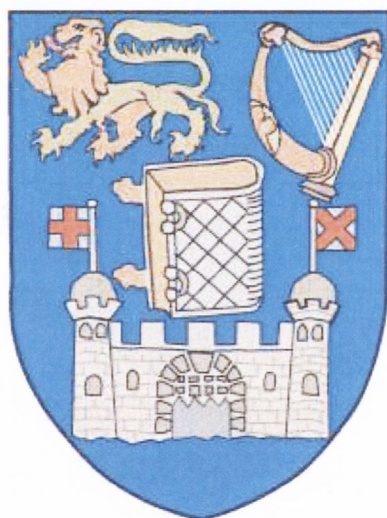


140512
8398

**Synthesis, biological evaluation and
subsequent SAR of four novel families of
alkyliphatic twin drugs**

Jonathan Corcoran

January 2007

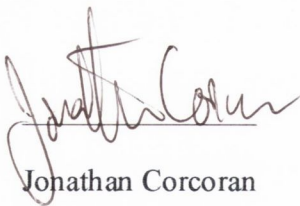


Based on research carried out under the direction of

Dr. Isabel Rozas

*A thesis presented to Trinity College Dublin for the degree of
Doctor of Philosophy*

I hereby declare that this thesis has not been submitted as an exercise for a degree at this or any other university. The work contained herein is entirely my own, except where otherwise cited, referenced, acknowledged or accredited. I agree that the library of the University of Dublin, may at their discretion lend or copy the thesis upon request.



Jonathan Corcoran

January 2007

Trinity College Dublin

Abstract

The I₂-IBS is a well known binding site widely distributed in the body of both animals and humans. It is suspected that they are an allosteric binding site of MAO-B. They have also been linked to several conditions such as Alzheimer's and neuro protection. Their main physiological function appears to be the ability of I₂-IBS ligands to attenuate the tolerance to opioid drugs. This link between the I₂-IBS and the μ -opioid receptor system has made I₂-IBS binding sites of pharmacological importance.

Many of the existing I₂-IBS ligands to date have been aromatic derivatives of the first IBS ligands, clonidine and idazoxan. There have been very few aliphatic ligands of note synthesized to date and most of them have been prepared by Rozas' group. One of the first aliphatic I₂-IBS ligands to be reported was the endogenous ligand agmatine. Previous research by Rozas' group reported the synthesis of four aliphatic *bis*-guanidines based on the structure of agmatine. These compounds acted as I₂-IBS ligands and showed a higher I₂-IBS / α_2 -ARs selectivity than the I₂-IBS prototype ligand idazoxan.

This thesis was divided into eight chapters. Chapter one discusses the discovery of the I₂-IBS binding sites and the development of I₂-IBS ligands since they were first reported in 1982 by Pascal Bousquet. In chapter two we report the synthesis of further aliphatic *bis*-guanidines. In synthesizing and pharmacologically tested these compounds we have investigated the hypothesis that as the length of the aliphatic linker between the guanidine moieties increases the I₂-IBS / α_2 -ARs selectivity will increase as well.

Amiloride, an interesting IBS ligand, is an aromatic guanidino carbonyl derivative. Due to the structural similarity between the guanidino carbonyl and guanidine functional groups we have synthesized a new family of potential I₂-IBS ligands similar to the aliphatic *bis*-guanidines but using the guanidino carbonyl functional group. Chapter two reports the synthesis of these derivatives.

Of the few existing aliphatic ligands, S15430 and pentamidine were of particular interest to our group. Pentamidine is an aliphatic and aromatic twin ligand for I₂-IBS (pK_i I₂-IBS = 7.85). It possesses two amidine functional groups bonded to an aromatic phenyl group at either end of a short aliphatic chain. Due to the high I₂-IBS affinity showed by pentamidine and the similarity of the amidine and guanidine functional groups we have synthesized a series of related compounds with no aromatic moieties present and based on the aliphatic *bis*-guanidines. Moreover, S15430 is an aliphatic 2-imidazoline with the heterocyclic functional group located at the end of a methylene chain with seven carbons. This ligand is highly selective for the I₂-IBS over the α₂-ARs (I₂-IBS /α₂-ARs selectivity = 110). The 2-imidazoline functional is also related to the amidine functional group and hence we decided to prepare a new family of I₂-IBS ligands based on the structure of S15430 and the aliphatic *bis*-guanidines. Chapter four discusses the synthesis of both the aliphatic *bis*-2-imidazolines and the aliphatic *bis*-amidines.

The syntheses and pharmacological evaluations these four families of aliphatic ligands (*bis*-guanidines, *bis*-guanidino carbonyls, *bis*-2-imidazolines and *bis*-amidines) have allowed us to extrapolate a structure activity relationship for aliphatic twin compounds for the I₂-IBS. This is important because existing SAR only discuss the pharmacophoric elements required for aromatic I₂-IBS ligands. Therefore, we have performed a conformational analysis of the four ligand families. Chapter five reports the results of these conformational analyses and a hypothesis for the interaction of the ligands with the I₂-IBS receptor site is formulated.

Chapter six discusses the biological assays results (both binding to I₂-IBS and, in some cases, selectivity over α₂-adrenoceptors) for all four ligand families and their implication on the SAR discussed in chapter five. Using these results we further refined the SAR and report the results herein. Chapter seven summarizes the results obtained in this thesis and discusses potential future work. Finally, chapter eight contains the experimental procedures and characterisation of the compounds prepared in this thesis.

Acknowledgements

I would like to sincerely thank my supervisor Dr. Isabel Rozas for all her support, cajoling, understanding and, most of all, for the opportunity to work on this project.

I would like to thank Dr. Luis F. Callado, Dr. Javier Meana and Dr. Fernando Rodriguez for all of the biological tests they have performed for me over the past four years and their patience while I synthesized the compounds.

I would like to thank Dr. John O' Brien for all the help with my NMRs. I would also like to thank all the support staff in the chemistry department, particularly; Corrine, Tess, Helen, Patsy, Fred, Martin, Ed, Peggy and all the cocker staff.

To the friends that I have come to know and love in the department, especially Sergio, Mick, Serena, Ann-marie, Danni, Gary and Sally thank you. Without you all I would not be here thank you. To Ruairi, Kevin and John, thank you for the pints and reminders throughout the thesis.

Finally, to my family, dad, Luke, Annette, Anne and especially Adam a special thanks. You have supported me throughout this labour of love and I owe each of you a heartfelt thanks.

Table of Contents

Abbreviations	xi
Chapter 1 <i>Introduction</i>	1
1.1 Introduction	2
1.2 I₁-Imidazoline Binding Sites	3
1.2.1 I₁- Imidazoline Binding Sites ligands	3
1.3 I₃- Imidazoline Binding Sites and Their ligands	4
1.4 I₂- Imidazoline Binding Sites	5
1.5 I₂-Imidazoline Binding Sites ligands	9
1.5.1 Endogenous I₂- Imidazoline Binding Sites ligands	9
1.5.2 Synthetic I₂- Imidazoline Binding Sites ligands	11
1.5.2.1 Imidazoline I₂- Imidazoline Binding Sites ligands	12
(a) Benzo Fused Heterocyclic ligands	12
(b) Cirazolines	16
(c) 2-Trans-styrylimidazolines	18
(d) 2-Aryl and 2-Heterocyclic Imidazolines	19
1.5.2.2 Aromatic and Aliphatic 2-Aminoimidazolines	20
1.5.2.3 Amidines	21
1.5.2.4 Guanidine Derivatives	23
(a) Aromatic Guandines	23
(b) Aliphatic Guandines	24
1.5.2.5 Miscellaneous ligands	26
1.6 Project aims	27
1.7 References	29
Chapter 2 <i>Synthesis of the alkyl bis-guanidines</i>	36
2.1 Introduction	37
2.2 General methods for the synthesis of guanidines	38
2.3 Description of alkyl bis-guanidine syntheses	45

(a) Route 1	46
(b) Route 2	48
(c) Route 3	51
(d) Route 4	52
2.4 Summary and Conclusions	57
2.5 References	59
Chapter 3 <i>Synthesis of the alkyl bis-guanidino carbonyls</i>	61
3.1 Introduction	62
3.2 Existing synthetic routes for guanidino carbonyls	62
(i) <i>From carbamate derivatives</i>	63
(ii) <i>From carboxylic acid derivatives</i>	66
3.3 Preparation of the alkyl <i>bis</i> -guanidino carbonyls	67
(a) Route 1	67
(b) Route 2	69
(c) Route 3	71
3.4 Summary and conclusions	74
3.5 References	76
Chapter 4 <i>Synthesis of the alkyl bis-2-imidazolines and the alkyl bis-amidines</i>	77
4.1 Introduction	78
4.2 General synthesis of 2-Imidazolines	78
(i) <i>Diamines and a one carbon fragment</i>	80
(ii) <i>Aziridines</i>	82
(iii) <i>Reaction of a nitrile, amide or imidate with an aminoalcohol derivative</i>	83
(iv) <i>Amidines plus two carbon electrophiles</i>	84
(v) <i>Isonitriles and imines</i>	85
(vi) <i>CCNC biselectrophile</i>	85
4.3 Synthesis of the alkyl <i>bis</i> -2-imidazoline	86

(a) Route 1	86
(b) Route 2	91
4.4 General Synthesis of Amidines	94
(i) <i>Amidines synthesised from amides</i>	95
(ii) <i>Amidines synthesized from carboxylic acids</i>	96
(iii) <i>Amidine synthesized from nitriles</i>	96
(iv) <i>Amidines synthesized from esters</i>	97
4.5 Amidine synthesis	97
4.6 Summary and conclusions	98
4.7 References	100
Chapter 5 <i>Conformation analysis of the alkyl bis-guanidines, alkyl bis-guanidino carbonyls, alkyl bis-2-imidazolines and alkyl bis-amidines</i>	102
5.1 Introduction	103
(i) <i>Systematic searches</i>	104
(ii) <i>Random conformational searches</i>	105
5.2 Methodology of the Random search analysis	106
5.3 Conformational analysis of the alkyl <i>bis</i> -guanidines	113
5.4 Conformational analysis of the alkyl <i>bis</i> -guanidino carbonyls	117
5.5 Conformational analysis of the alkyl <i>bis</i> -2-imidazolines	121
5.6 Conformational analysis of the alkyl <i>bis</i> -amidines	126
5.7 Summary and conclusions	130
5.8 References	133
Chapter 6 <i>Biological assay results for the alkyl bis-guanidines, alkyl bis-guanidino carbonyls, alkyl bis-2-imidazolines and alkyl bis-amidines</i>	134
6.1 Introduction	135
6.2 Biological results for the alkyl <i>bis</i> -guanidines	136
6.3 Biological results for the alkyl <i>bis</i> -guanidino carbonyl	137
6.4 Biological results for the alkyl <i>bis</i> -imidazolines	138
6.5 Biological results for the alkyl <i>bis</i> -amidines	140

6.6 Structure Activity Relationships I ₂ -IBS affinity	142
6.7 Structure Activity Relationship I ₂ -IBS/ α_2 -ARs selectivity	146
6.8 Summary and conclusions	149
6.9 References	151
Chapter 7 <i>Thesis Summary and Future Work</i>	152
7.1 Synthesis of the ligands in Chapters 2-4	153
7.2 Conformational analysis, biological assay results and subsequent SAR	154
7.3 Future work	155
7.4 References	157
Chapter 8 <i>Experimental</i>	158
8.1 General Conditions	159
8.2 General synthetic procedures	159
8.2.1 Procedure 1; synthesis of the alkyl diamines	159
8.2.2 Procedure 2; synthesis of the alkyl bis-guanidines	160
8.2.3 Procedure 3; synthesis of the alkyl <i>bis</i> -Boc protected <i>bis</i> -guanidines	160
8.2.4 Procedure 4; removal of the Boc group	160
8.2.5a Procedure 5a; synthesis of the alkyl boc protected guanidines using the Mitsunobu protocol A	161
8.2.5b Procedure 5b; synthesis of the alkyl boc protected guanidines using the Mitsunobu protocol B	161
8.2.6 Procedure 6; synthesis of alkyl <i>bis</i> -methyl esters	161
8.2.7 Procedure 7; synthesis of the alkyl di-alcohols	162
8.2.8 Procedure 8; synthesis of the alky bis-guanidinylamides picrate salts	162
8.2.9 Procedure 9; synthesis of the alkyl <i>bis</i> -guanidinylamides	162
8.2.10 Procedure 10; synthesis of the alkyl bis-guanidino carbonyl hydrochloride salts	163

8.2.11 Procedure 11; synthesis of the Boc protected alkyl bis-guanidino carbonyls	163
8.2.12 Procedure 12; Synthesis the alkyl bisguanido carbonyl hydrochloride salts	163
8.2.13 Procedure 13; Synthesis of the alkyl <i>bis</i> -2-imidazolines	163
8.2.14 Procedure 14; Synthesis of the alkyl <i>bis</i> -2-imidazoline oxalate salts	164
8.2.15 Procedure 15; Synthesis of the alkyl bis-amidines	164
8.3 Synthesis and characterisation of compounds in Chapter 2	164
8.4 Synthesis and characterisation of compounds in Chapter 3	177
8.5 Synthesis and characterisation of compounds in Chapter 4	189
8.6 Biological Assays	200
8.7 References	202
Appendix	203

Abbreviations

%	Percentage
[]	Concentration
3-D	Three dimensional
Å	Ångstrom
α_{2A} -AR	α_{2A} adrenoceptor
α_2 -AR	α_2 adrenoceptor
α_{2B} -AR	α_{2B} adrenoceptor
α_{2C} -AR	α_{2C} adrenoceptor
AER	Anion exchange resin
Am	Amide
aq	Aqueous
ATP	Adenosine tri-phosphate
BAC	Biological active conformation
BBB	Blood Brain Barrier
Boc	<i>tert</i> Butoxy carbonyl
BOP	Benzotriazole-1-yloxytrisdimethylamino hexafluorophosphate
br	Broad
CDI	Carbodiimidazole
cDNA	Coding deoxyribose nucleic acid
CDS	Clonidine displacing substance
CNS	Central Nervous System
δ	Chemical shift
Db	Debyes
DCC	Dicyclohexyl carbodiimide
DCM	Dichloromethane
DIAD	Diisopropylazodicarboxylate
DMF	<i>N, N</i> -dimethylformamide
DMSO	Dimethyl sulphoxide
EDA	Ethylene diamine
EDCI	<i>N</i> -(3-dimethylaminopropyl)- <i>N'</i> -ethyl carbodiimide
eq	Equivalents
ESMS	Electrospray mass spectroscopy
FAD	Flavine adenosine diphosphate
GFAP	Glial fibrillary acid protein
GMEC	Global minimum energy conformation

GMEC	Global minimum energy conformation
GPCR	G Protein coupled receptor
h	Hours
HPLC	High performance liquid chromatography
I	Imidazoline
I ₁ -IBS	I ₁ Imidazoline Binding Site
I _{2A} -IBS	I _{2A} Imidazoline Binding Site
I _{2B} -IBS	I _{2B} Imidazoline Binding Site
I ₂ -IBS	I ₂ Imidazoline Binding Site
I ₃ -IBS	I ₃ Imidazoline Binding Site
IPS	Imidazoline Preferring Sites
K _a	Dissociation constant
kcal	Kilocalorie
kDa	Kilo dalton
K _i	Inhibition constant
LC	Locus Corruleus
M	Molar
m	Multiplet
m/z	Mass charge ratio
MAO-A	A isoform Monoamine oxidase
MAO-B	B isoform Monoamine oxidase
min	Minutes
mol	Mole
NF-L	Immunolabelled neurofilament proteins
NMR	Nuclear magnetic resonance
pH	$-\text{Log}_{10}[\text{H}^+]$
pK _a	$-\text{Log}_{10}[K_a]$
pK _i	$-\text{Log}_{10}[K_i]$
ppm	Parts per million
PPSE	Polyphosphoric acid trimethylsilylester
PSA	Polar surface energy
PyAOP	(7-azabenzotriazol-1-yloxy)-trispyrrolidino phosphonium hexafluorophosphate
PyBOP	Benzotriazol-1-yloxytripyrrolidinophosphonium hexafluorophosphate
q	Quartet
qt	Quintet
RCS	Random conformational analysis
rt	Room temperature
RVLM	Rostro Ventrolateral Medulla

S.M.	Starting material
SAR	Structure activity relationship
t	Triplet
TBAF	Tetra- <i>n</i> -butylammonium fluoride
TBTU	O-(benzotriazol-1-yl)- <i>N,N,N',N'</i> -tetramethyl uranium tetrafluoro borate
TEA	Triethylamine
<i>tert</i>	Tertiary
TFA	Trifluoroacetic acid
TFL	Tail flick tendencies
THBC	Tetrahydro- β -carboline
THF	Tetrahydrofuran
tlc	Thin layer chromatography

Chapter 1

Introduction

1.1 Introduction

Since their discovery in 1984 by Bousquet *et al.*¹ Imidazoline Binding Sites (IBS) have perplexed, frustrated and brought no end of joy to scientists around the world. Bousquet and co-workers discovered that clonidine (Figure 1.1) not only interacted with the α_2 -adrenoceptors (α_2 -AR) in the central nervous system (CNS) but also through a secondary site located in the rostral ventrolateral medulla (RVLM). This secondary binding site was distinct from the α_2 -AR because they were not activated by catecholamines. Bousquet and co-workers provisionally labelled these sites Imidazoline Preferring Sites (IPS) although this denomination has since been changed to the more recent, IBS.

Despite Bousquet's proposal of a distinct site separate from α_2 -ARs, it was not until the work by Emsberger *et al.*² on the radioligand binding of [³H] *para*-aminoclonidine (Figure 1.1) in bovine brainstem that this theory was proved. In fact, further investigation of these sites revealed that they formed at least two populations, labelled I₁-IBS and I₂-IBS. More recently a third subtype has been identified in pancreatic β cells, labelled I₃-IBS.³

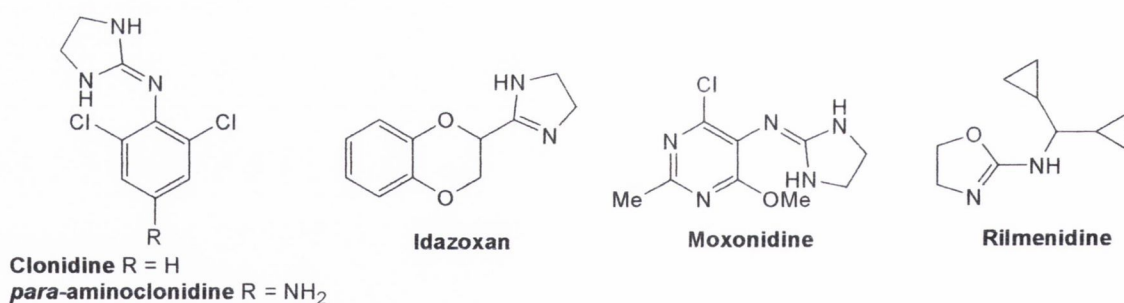


Figure 1.1.- The structures of clonidine, *para*-aminoclonidine, idazoxan, moxonidine and rilmenidine

Since the different IBS subtypes differ in their ligand recognition properties, location and even in their structural properties⁴⁻⁶ they are now recognized as a heterogenous family of sites. One of the most interesting roles of the entire imidazoline receptor system is they are upregulated in depressed patients. While the role and function of this upregulation

still remains unclear it is an exciting prospect that targeting IBS could provide a treatment to help depressed patients. Unfortunately, the full three dimensional (3-D) structure of any of the IBS subtypes still remains unknown. In the next section we will discuss the different IBS subtypes, their location, pharmacological function and ligands. We will discuss the I₂-IBS in the final section because they are the selected target for this body of work.

1.2 I₁-Imidazoline Binding Sites

It is known that the I₁-IBS are G-protein coupled receptors (GPCR, also known as seven transmembrane receptors, are a large protein family of transmembrane receptors that sense molecules outside the cell and activate inside signal transduction pathways)^{7,8} and the best candidate for the cloned I₁-IBS receptor in the human brain is a protein of 43 KDa.⁹ I₁-IBS are, like all GPCR, embedded in the membrane of the cell. In the body, depending on species, they can be found in different tissues such as the brain stem, RVLM, kidney, prostate, thrombocytes and lung.

The role of the I₁-IBS is dependent on their location. In the RVLM the I₁-IBS ligands inhibit the sympathetic excitatory neurones lowering the blood pressure. However, since these ligands also possess affinity towards α_2 -ARs the belief that the I₁-IBS are the ones eliciting this response is not without debate. In the Locus Coeruleus (LC), I₁-IBS increase the activity of noradrenergic neurones; this is an indirect effect mediated by I₁-IBS located on paragigantocellularis neurones, which project to the LC releasing excitatory amino acids as neurotransmitters. I₁-IBS in the kidney are involved in sodium secretion and its ligands have a natriuretic effect by lowering that secretion. These effects appear to be mediated through a GPCR, independent of α_2 -AR.

1.2.1 I₁- Imidazoline Binding Sites ligands

I₁-IBS show high affinity for ligands like clonidine, which is an imidazolidine derivative (Figure 1.1) and medium affinity towards idazoxan, which is an imidazoline derivative

(Figure 1.1). The main therapeutic role for I₁-IBS is to elicit an effect on hypertension, with the majority of I₁-IBS ligands acting as antihypertensive agents. In this sense, the most important ligands are rilmenidine and moxonidine (Figure 1.1). Moxonidine is a potent derivative of clonidine.^{10,11} Rilmenidine, however, is an imidazoline derivative and was the first I₁-IBS ligand to enter clinical trials as an antihypertensive agent.¹² Rilmenidine acts both centrally and in the kidneys. The affinity of these compounds for I₁-IBS, I₂-IBS and α₂-ARs is presented in Table 1.1. For a more complete overview of I₁-IBS ligands one should consult the review of Dardonville and Rozas.¹³

Table 1.1.- Summary of Affinities of Compounds in Sections 1 through 1.1.1

Ligand	I ₁ -IBS Affinity (pKi)	I ₂ -IBS Affinity (pKi)	α ₂ -AR Affinity (pKi)	Selectivity IBS/α-AR
clonidine	7.25	6.02	7.21 (α _{2A}) 7.16 (α _{2B}) 6.87 (α _{2C})	0.06 (I ₂ /α _{2A}) 0.07 (I ₂ /α _{2B}) 7.08 (I ₂ /α _{2C})
<i>para</i>-aminoclonidine		<5	8.1 (α _{2A}) 7.53 (α _{2B}) 7.67 (α _{2C})	1259 (I ₂ /α _{2A}) 339 (I ₂ /α _{2B}) 468 (I ₂ /α _{2C})
idazoxan	5.9	8.37	7.72	4.5 (I ₂ /α ₂)
rilmenidine	7.22	5.96	6.9	18 (I ₁ /I ₂), 2 (I ₁ /α ₂)
moxonidine	8.37	<5	<5	

1.3 I₃- Imidazoline Binding Sites and Their ligands

It has recently been established that certain drugs containing imidazoline groups can stimulate insulin secretion from pancreatic β cells.^{14,15} This secretion seems to be related to targeting a certain imidazoline binding site, which differs from both I₁-IBS and I₂-IBS. While there is some evidence linking I₂-IBS to pancreatic cells¹⁵ it has also been proven that I₂-IBS sites cannot account for the insulin secretion induced by the IBS ligands. Radio labelled experiments using [³H] RX821002 (Figure 1.2) identified a low affinity site with I₃-IBS characteristics.¹⁶ While the location of the I₃-IBS sites is known their structure is not. However, it is suspected that there is a relationship between I₃-IBS and ATP sensitive potassium channels.¹⁶ More recent evidence suggests that I₃-IBS control a

distal step in the exocytotic pathway.¹⁷ Two ligands have been identified as potential I₃-IBS ligands, these are efaroxan (Figure 1.2) and KU-14R (Figure 1.2).

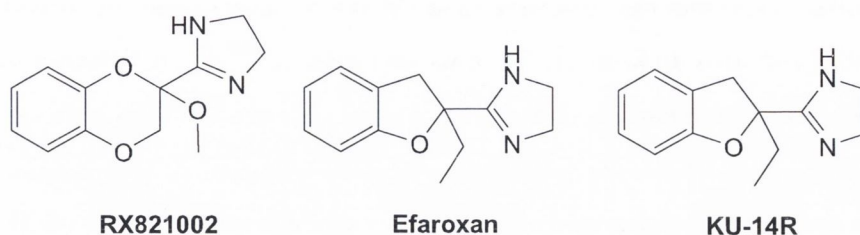


Figure 1.2.- The structures of RX821002, efaroxan and KU-14R

1.4 I₂- Imidazoline Binding Sites

Despite evidence of their existence since 1987 the full physiological structure, location and role of I₂-IBS has not yet been totally elucidated. Radioligand binding and affinity studies by Ernsberger *et al.*² using [³H] *para*-aminoclonidine showed that I₂-IBS were of a heterogenous nature and could be subdivided into two further subtypes called I_{2A}- and I_{2B}-IBS. These subdivisions were based on their tissue distribution, localisation within the cell and ligand recognition properties. I_{2A}-IBS shows high affinity for amiloride (Figure 1.3) and I_{2B}-IBS little or no affinity for the same compound (p*K*_i).^{1,15}

Initial research into the I₂-IBS showed a wide and varied tissue distribution pattern. They can be found in the lung,¹⁷ adipocytes,¹⁸ placenta,¹⁹ pancreatic islet,²⁰ adrenal chromaffin cells,¹⁵ as well as the CNS.²¹ Of all those sites, binding studies performed using rabbit and human tissue showed that the highest density of I₂-IBS can be found in the adipocytes,¹⁸ liver, kidney and brain.¹⁹ At a cellular level, research suggests that I₂-IBS can be found in the cell membrane (primarily in trophoblasts²⁰ and rabbit renal proximal tube²²) as well as on the outer mitochondrial membrane.¹⁷

In a particular study on the purification of I₂-IBS by Tesson *et al.*,²³ it was shown that I₂-IBS density positively correlated with MAO activity. Monoamine Oxidases (MAO) are flavin dependent isozymes that catalyse the oxidative deamination of neurotransmitters such as serotonin, norepinephrine, epinephrine, phenethylamine and dopamine (Figure

1.3) as well as exogenous arylalkylamines such as benzylamine (Figure 1.3). The mammalian form of these isozymes can be found on the outer mitochondrial membrane.²⁰ MAO can be divided into two subtypes MAO-A, found in the liver, gastrointestinal tract and the placenta, and MAO-B, which can be found in blood platelets. Both can also be found in neurons and astroglia.²¹ Several subsequent studies have directly linked MAO and I₂-IBS:

1. The molecular weights of I₂-IBS proteins isolated match those of MAO-A and MAO-B²⁴
2. The amino acid sequencing of purified I₂-IBS shows homology to that of MAO⁵
3. When the coding DNA (cDNA) for the amino acid sequence of MAO was transfected into yeast cells, in order to produce the MAO protein, not only was MAO expressed but they also found that the I₂-IBS were as well.²⁵
4. Photoaffinity labelled I₂-IBS from human placenta and liver tissue immunoprecipitate with monoclonal antibodies directed against both MAO-A and MAO-B²⁶

From these studies the I₂-IBS appears to be a ligand binding domain located on MAO. It is neither the active site nor the flavine adenosine diphosphate site (FAD).²⁷ This would suggest the possibility of I₂-IBS being an allosteric binding site of a subpopulation MAO-B^{21,28,29} although this hypothesis is not without debate.^{30,31} Recently, the full structure of MAO-B has been elucidated³¹ and while there have been no recent publications in the area hopefully the theory of I₂-IBS being an allosteric binding site of MAO-B may soon be solved.

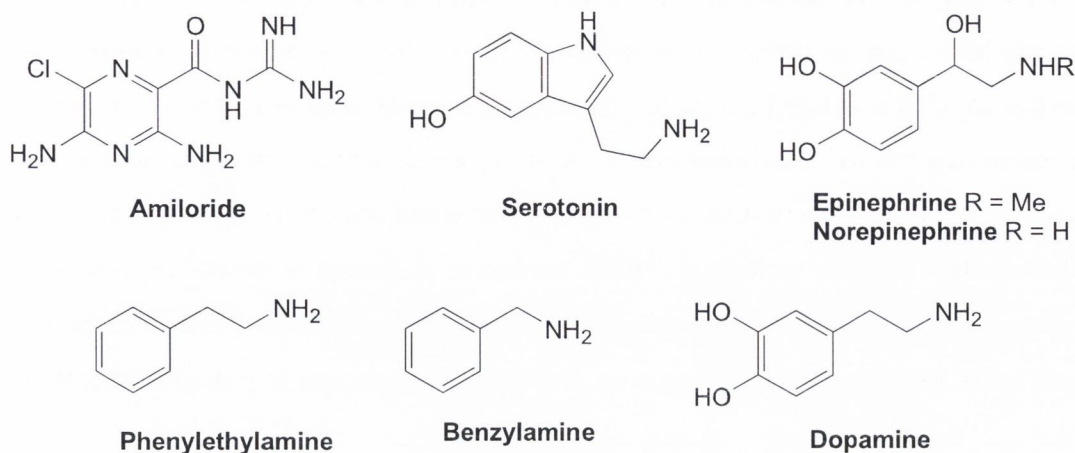


Figure 1.3.- The structures of amiloride, serotonin, epinephrine, norepinephrine, phenylethylamine, benzylamine and dopamine

Despite the evidence proposing I_2 -IBS as an allosteric binding site of MAO, their full pharmacological role has yet to be determined. It has been shown that I_2 -IBS ligands inhibit MAO but require large concentrations in order to elicit such an effect.^{25,32} This would indicate that I_2 -IBS plays some role in the regulation of MAO. This belief is supported by the fact that both MAO-B and I_2 -IBS show a marked increase in density in the brains of Alzheimer's patients.^{33,34} However, these are not the only physiological roles that I_2 -IBS have been linked with.

In rats it has been shown that stimulation of I_2 -IBS in astrocytes leads to an increase in Glial Fibrillary Acid Protein (GFAP).³⁵⁻³⁷ The GFAP content of a cell is seen as a marker for the activity of a glial cell since glial cells produce both neurotrophic substances and growth factors.³⁸ An increase in the activity of glial cells is seen as a repair mechanism after stroke^{39,40} indicating the potential neuro-protective role of I_2 -IBS. It has also been shown that stimulation of the I_2 -IBS increases food consumption in rats.^{41,42} An interesting possible physiological role is the decrease of I_2 -IBS in the human putamen of Huntington's disease patients⁴³ but an increase in depressed suicide victims.⁴⁴

Despite the varied physiological roles for I_2 -IBS it is their link with the opioid system, which is the most interesting. The repeated use of opioid drugs is well known to lead to tolerance as well as a loss of anti-nociceptive efficacy.⁴⁵ In rats in particular this loss of

efficacy is observed as a marked decrease in immunolabelled neurofilament proteins (NF-L). In a study in 1998 by Garcia-Sevilla *et al.*²⁹ they showed that treatment with a number of known I₂-IBS ligands could attenuate the tolerance of rats to morphine. Also by measuring the tail-flick latencies (TFL's) of rats they found that pre treatment with idazoxan before administration of morphine prevented morphine tolerance developing. Other I₂-IBS ligands, including 2-BFI, produced a similar response. α_2 -AR ligands, however, failed to produce any response indicating the specific involvement of the I₂-IBS over the α_2 -ARs in attenuating and even preventing tolerance to morphine. Other ligands, such as the endogenous ligand agmatine, produce spinal antinociception when administered as an intrathecal injection in rats.²⁸ More recently further evidence has been provided by Garcia-Sevilla *et al.*²⁷ supporting the link between the μ -opioid system and I₂-IBS. In this article it was shown that norharmane (Figure 1.4), a member of the endogenous β -carboline family, can block the behavioural and biochemical effects of opiate withdrawal.

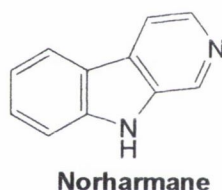


Figure 1.4.- The structure of norharmane

I₂-IBS have been linked with several other physiological phenomena and all are listed in Table 1.2. From this list it can be envisaged that I₂-IBS ligands are a diverse family and are discussed in the following section.

Table 1.2.- Summary of IBS location and Physiological Roles

IBS Subtype	Species	Tissue	Function	Reference
I ₁	Rat, primate	Hepatocytes	Inhibit cholesterol synthesis	46
I ₁	Rat	Brain	Antinociception	47
I ₁	Cat, Rat, Rabbit, Human	RVLM	Hypotension	1, 6, 48-51
I ₁ /I ₂	Rat, Rabbit	Kidney	Natriuresis	52-56
I ₂	Pig, Dog, Human	Kidney	MAO inhibition	57-59
I ₂	Rat	Dorsal Horn	Antinociception	60
I ₂	Rat	Glial Cells	Neuroprotection	28
I ₂	Rat	Brain, Liver	Block effect of opiate withdrawal	40
I ₂	Mouse	n/s	Analgesia of visceral pain	29
I ₂ (yet to be confirmed)	Human	Platelets	Anti-hyper-reactivity to catecholamines	61
I ₃	Rat	Suprspinal	Inhibit spinal segment reflexes	62
I ₃	Man, Mouse	Kidney, Stomach	Inhibition of 5-HT ₃	63
I ₃	Mouse, Rat	Pancreatic Islets	Increase in insulin secretion	64-67

1.5 I₂-Imidazoline Binding Sites ligands

1.5.1 Endogenous I₂- Imidazoline Binding Sites ligands

In the 1980s, Atlas *et al.*⁶⁸⁻⁷⁰ isolated a substance that could displace the α_2 -AR ligand clonidine but not the α_1 -AR ligand prazosin or the β -AR ligand cyanopondolol. This substance was labelled Clonidine Displacing Substance (CDS). CDS was proposed as an endogenous ligand for IBS first by Ernsberger *et al.*,^{71,72} since it displayed a 30 fold selectivity for IBS over α_2 -ARs (pK_i IBS = 6.7, pK_i α_2 = 8.2) and later by Atlas *et al.*⁷³ who showed CDS has only a weak affinity towards the inhibitory G-protein. The work of Atlas *et al.*⁷³ further strengthened the belief that CDS is an endogenous ligand for IBS and it is now considered a realistic proposition. The full structure of CDS was never

discovered and this led to several compounds being proposed as the active component of CDS.

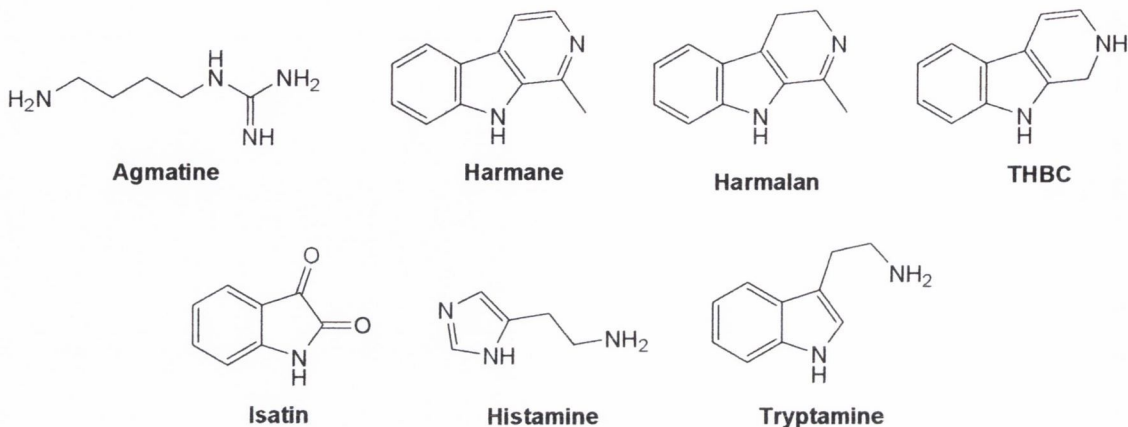


Figure 1.5.- The structures of agmatine, harmane, harmalan, THBC, isatin, histamine, tryptamine

Among the first compounds to be proposed as an active component of CDS was agmatine (Figure 1.5).⁷⁴ Agmatine is biosynthesized by decarboxylation of L-arginine by argininedecarboxylase and metabolised by diamine oxidase. It is widely distributed throughout the body and has been proposed as a neurotransmitter although this is not without serious debate.^{9,75,76} While agmatine shows affinity for both α_2 -ARs and IBS ($pK_i \alpha_2 < 5$, $pK_i I_1 = 7.48$, $pK_i I_2 < 5$) its selectivity for IBS over α_2 -ARs rules it out as the active component of CDS because of the affinity and selectivity shown towards IBS over α_2 -ARs by CDS itself.

Another family of endogenous ligands are the β -carbolines first reported as I₂-IBS ligands by Husbands *et al.*⁷⁷ in 1999. Several β -carbolines bind with high affinity and selectivity towards all IBS⁷⁷⁻⁷⁹ and some are found endogenously (believed to be the side product of a secondary metabolism but can be synthesised via condensation reactions), these include harmane ($pK_i I_1 = 6.52$, $pK_i I_2 = 6.31$, $pK_i \alpha_2 = 3.69$) and harmalan ($pK_i I_1 = 6.34$, $pK_i I_2 = 5.83$, $pK_i \alpha_2 = 3.99$) (Figure 1.5, Table 1.3). In a recent publication, and by means of ESMS, NMR and HPLC, it was reported that these two endogenous ligands are active components of CDS.³⁰ Through the synthesis of derivatives of harmane and

harmalan, Husbands *et al.*⁷⁷ also found a tetrahydro- β -carboline (THBC, Figure 1.5) possessing good affinity for I₂-IBS but only showing low affinity towards I₁-IBS (Table 1.3). Despite the fact that harmane and harmalan are active components of CDS and agmatine is not does not rule out agmatine as an endogenous ligand of IBS, especially in light of its affinity towards I₁ -IBS.

Other endogenous compounds have been tested as potential I₂-IBS ligands these include isatin, histamine and tryptamine (Figure 1.5), all of which are endogenous indolamines.⁸⁰ Isatin and histamine only displayed moderate affinity towards I₂-IBS unlike tryptamine, which was of higher affinity (Table 1.3). Again the affinity of the compounds mentioned in this section for I₁-IBS, I₂-IBS and α_2 -ARs can be seen in table 1.3.

Table 1.3.- Summary of the Affinities of the Endogenous I₂-IBS ligands Mentioned in Section 1.4.1

Ligand	I ₁ -IBS Affinity (pK _i)	I ₂ -IBS Affinity (pK _i)	α_2 -AR Affinity (pK _i)
agmatine	7.48	<5	<5
harmane	6.52	6.31	3.75
harmalan	6.34	5.83	3.99
THBC	6.7	8.27	n/d
tryptamine		4.57, 5.52 (rat and rabbit respectively)	

1.5.2 Synthetic I₂- Imidazoline Binding Sites ligands

Existing synthetic I₂-IBS ligands can be generally subdivided into five different families based on their structures. These are β -carbolines (which were already discussed in the previous section 1.5.1) imidazolines, amidines, 2-aminoimidazolines and guanidines.

1.5.2.1 Imidazoline I₂- Imidazoline Binding Sites ligands

Most research on I₂-IBS ligands has focused on imidazolines. This is apparent when one considers the wide and varied type of imidazoline ligands produced: benzofurans, cirazolines, 2-*trans*styrylimidazolines and 2-heterocyclic imidazolines.

(a) Benzo Fused Heterocyclic ligands

The benzo fused heterocyclic ligands are the largest subtype of the imidazoline ligands. The reason for this is the development of idazoxan (Figure 1.1), which has good affinity for both I₂-IBS and α_2 -ARs but only marginal selectivity for I₂-IBS (pK_i I₂ = 8.37, pK_i α_2 = 7.72, I₂/ α_2 = 4.5).^{6,81} This ligand opened the door to the development of several more potent families of ligands such as benzodioxanes,⁸² benzofurans,^{82,83} and benzooxazines⁸⁴ (Figure 1.6). Using idazoxan as a template Chapleo *et al.*⁸⁵ modified several aspects of this ligand and found the following structure activity relationships (SAR):

- a) Halogen substituents at positions 6-, 7- or 8- on the aromatic ring increased selectivity towards I₂-IBS and were favoured over aliphatic substituents at any position on the aromatic ring (**1a-j**, Figure 1.6). This increase in selectivity was primarily due to a decrease in affinity for α_2 -ARs as opposed to an increase in affinity for I₂-IBS (Table 1.4).
- b) By changing the position of the 4-oxygen of idazoxan to position 5, RX821029, (Figure 1.6), affinity and selectivity towards I₂-IBS over α_2 -ARs was increased (Table 4).
- c) Modifying the size of the benzodioxane ring resulted in low affinity and only moderate selectivity over α_2 -ARs (RX791042, RX801024, Figure 1.6 & Table 1.4).
- d) Examining chromanyl analogues revealed that removal of the 4-oxygen, RX801025 (Figure 1.6) had little or no effect on the affinity for both the I₂-IBS and α_2 -ARs. However, removal of the 2-oxygen, RX801026 (Figure 1.6),

decreased the affinity for both I_2 -IBS and α_2 -ARs (four fold and ten fold, respectively, Table 1.4).

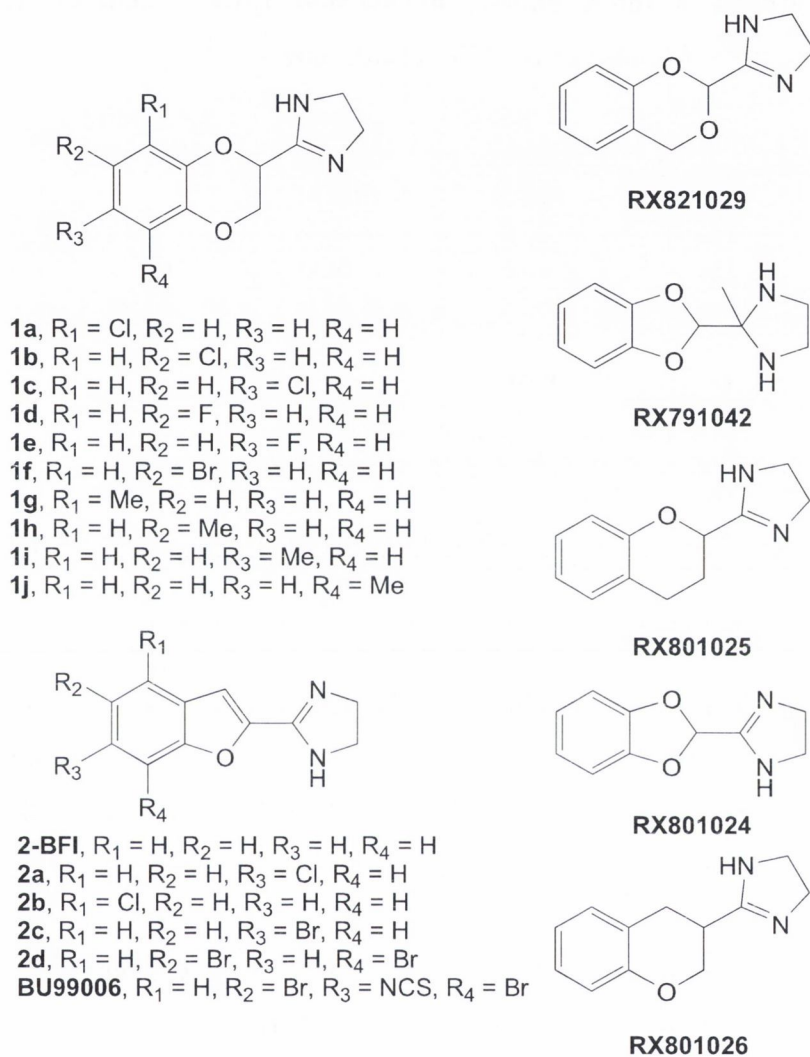


Figure 1.6.- Compounds synthesized by Chapleo *et al.*^{83,85} and Hudson *et al.*^{82,86,87}

Further research by Hudson *et al.*⁸² discovered the highly selective ligand **2-BFI** (Figure 1.6, $pK_i I_2 = 8.89$, $pK_i \alpha_2 = 4.57$, $I_2/\alpha_2 = 2874$). Again halogen substituents at any position on the aromatic ring are tolerated and result in similar affinity and selectivity compared to the parent compound (**2a-d**, Figure 1.6, Table 1.4). Another derivative of 2-

BFI gave an irreversible ligand, BU99006 (Figure 1.6), proving to be very selective and for I₂-IBS over I₁-IBS and α_2 -ARs (Table 1.4).^{86,87}

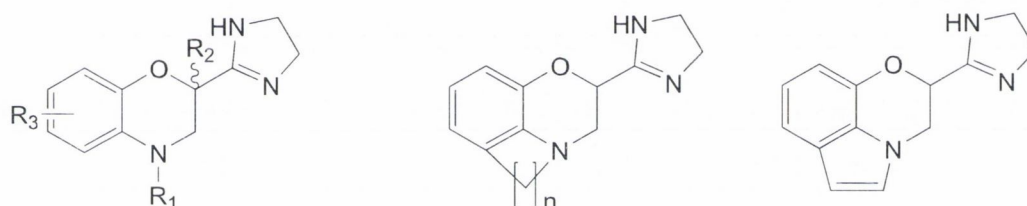
Table 1.4.- Summary of the Affinities of the Synthetic I₂-IBS ligands Synthesized by Chapleo *et al.*^{83,85} and Hudson *et al.*^{82,86,87}

Ligand	I ₂ -IBS Affinity (pK _i)	α_2 -AR Affinity (pK _i)	Selectivity IBS/ α -AR
1a	7.31	5.84	29.1
1b	6.68	5.66	10.5
1c	6.6	5.41	13.9
1d	7.1	5.44	41.3
1e	6.94	5.8	13.7
1f	6.6	5.44	13.7
1g	6.2	5.5	5.2
1h	6	5	9.1
1i	6.2	5.5	5.4
1j	6.1	5.75	2.2
RX821029	8.57	5.36	161.5
RX791042	5.95	4.3	44.8
RX801024	6.5	5	28.7
RX801025	7.1	6.4	5
31RX801026	7.4	5.4	10
2-BFI	8.89	4.57	2,874
2b	6.4	4.26	142.5
2c	7.55	4.2	2192.5
2d	6.77	4.51	183.1
2e	7.21	4.7	361.1
BU99006	8.6	3.8	63,095

While this research was performed in the 1980s, Touzeau *et al.*⁸⁴ recently still used idazoxan as a template to create a series of compounds and investigated their SAR. The results revealed that:

- a) Replacing the 4-oxygen with nitrogen (**3a**, Figure 1.7), while retaining the original affinity towards I₂-IBS, dramatically increased the selectivity over α_2 -ARs (Table 1.5).

- b) Introducing substituents on the 4-nitrogen and at the 2-carbon (**3b-c**, Figure 1.7) drastically reduced the affinity and selectivity towards I₂-IBS (Table 1.5).⁸⁸
- c) Substitution on the 4-nitrogen by methyl groups and larger groups, such as benzyl (**3d-f**, Figure 1.7) reduce the selectivity towards I₂-IBS over α_2 -ARs (Table 1.5).
- d) Mono substitution on the aromatic ring by a methyl group (**3g**, Figure 1.7) resulted in good affinity towards I₂-IBS (Table 1.5).
- e) Mono substitution on the aromatic ring by an ester group (**3h**, Figure 1.7) resulted in excellent selectivity towards I₂-IBS (Table 1.5).
- f) Finally tricyclic derivatives containing a five member ring (**4a**, Figure 1.7) showed good affinity and even better affinity when a double bond was introduced into this ring (**5**, Figure 1.7). Larger rings (**4b**, Figure 1.7) proved to be detrimental to the affinity towards I₂-IBS (Table 1.5).



- 3a**, R₁ = R₂ = R₃ = H
3b, R₁ = Me, R₂ = n-Pr, R₃ = H
3c, R₁ = Me, R₂ = Me, R₃ = H
3d, R₁ = Me, R₂ = H, R₃ = H
3e, R₁ = Bn, R₂ = H, R₃ = H
3f, R₁ = n-Pr, R₂ = H, R₃ = H
3g, R₁ = Me, R₂ = H, R₃ = Me
3h, R₁ = Me, R₂ = H, R₃ = CO₂Me

- 4a**, n = 2
4b, n = 3

5

Figure 1.7.- Structures of the ligands **3a-h**, **4a-b** and **5**

Table 1.5.- Summary of the Affinities of the Synthetic I₂-IBS ligands Synthesized by Touzeau *et al.*^{84,88}

Ligand	I ₁ -IBS Affinity (pK _i)	I ₂ -IBS Affinity (pK _i)	α ₁ -AR Affinity (pK _i)	α ₂ -AR Affinity (pK _i)
3a	5.1	7.29	<4	<4
3d	6.25	7.1	5	6.13
3e	4.4	4.8	4.5	6.89
3f	5.35	5.8	<4	5.9
3g	6.67	7.7	<4	6.15
3h	6.1	7.15	<4	4.12
3c	<4	<4	<4	<4
3b	4.25	4.1	<4	<4
4a	6.32	6.5	<4	6.6
4b	5.8	7	5.25	5.5
5	7.88	8.45		6.44

(b) Cirazolines

Another ligand, cirazoline (Figure 1.8) despite being a potent agonist/antagonist for α₁-AR and α₂-AR also shows good affinity and selectivity towards I₂-IBS (Figure 1.8, Table 1.6).^{89,90} Pignini *et al.*^{81,90-92} produced several SAR studies synthesizing several ligands possessing potent affinity with high selectivity over α₂-ARs. They found that;

- The cyclopropyl moiety was not essential for I₂-IBS affinity and could be easily replaced by aliphatic alkyl groups with no loss of affinity towards I₂-IBS (**6b-c**, Figure 1.8, Table 1.6).⁸¹
- The insertion of a second phenyl ring resulted in a dramatic reduction of the affinity towards I₂-IBS (**7** and **8a**, Figure 1.8, Table 1.6).⁹³
- By replacing the oxygen atom in the bridge linking the aromatic and imidazoline moieties with a methylene group (**6a**, Figure 1.8) reduced α₁-AR affinity and eliminated α₂-AR affinity while the affinity towards I₂-IBS remained similar to the parent compound (Table 1.6).⁹¹

- d) Substitution at the β position of the bridge (**8b**, Figure 1.8) yielded compounds with a decreased affinity and selectivity towards both I₂-IBS and α_2 -ARs (Table 1.6).⁹³
- e) The introduction of a methyl substituent on the imidazoline ring (**6b – c**, Figure 1.8) either eliminated or reduced I₂-IBS affinity but also reduced α_1 -AR agonist activity (Table 1.6).⁹¹

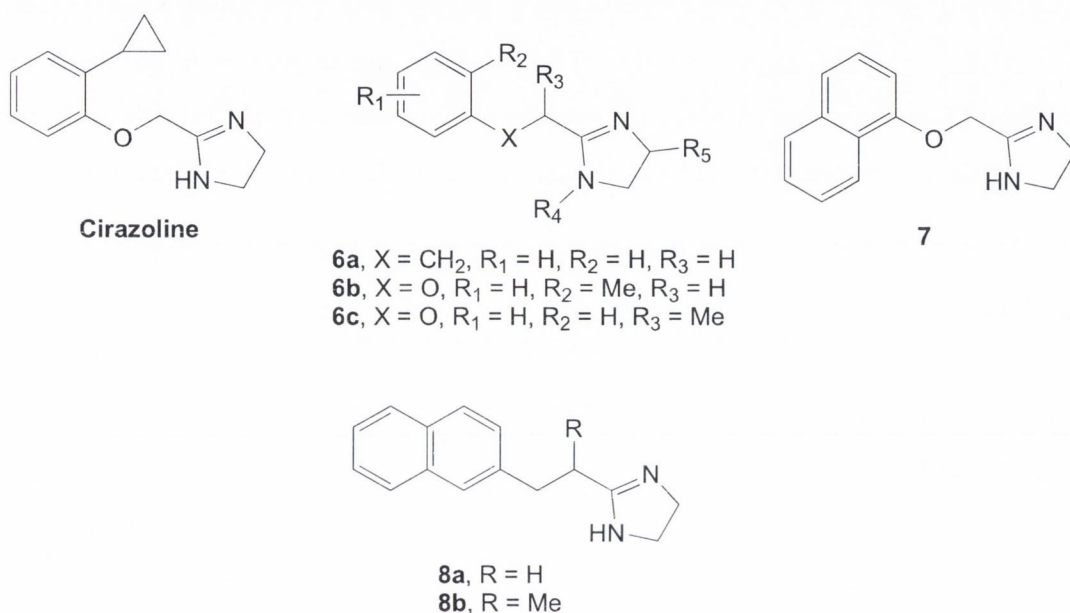


Figure 1.8.- The structure of the compounds discussed in section 1.5.2.1(b)

Table 1.6.- Summary of the Affinities of the Synthetic I₂-IBS ligands in Section 1.5.2.1(b)

Ligand	I ₂ -IBS Affinity (pK _i)	α_1 -AR Affinity (pK _i)	α_2 -AR Affinity (pK _i)	Selectivity IBS/ α -AR
cirazoline	7.9, 8.41	7.33	7.77	25 (I ₂ / α_1), 4.4 (I ₂ / α_2)
6a	8.6		5.7	794
6b	i/a		i/a	
6c	5.96		4.72	17
7	8.72		7.17	35
8a	8.4		5.96	275
8b	5.44		5.39	1.1

(c) 2-*Trans*-styrylimidazolines

The 2-*trans*-styrylimidazolines were discovered by Pigni *et al.*⁹² when they restricted the flexibility of the linker between the aromatic and imidazoline moieties of compound **8a** (Figure 1.8) with a double bond to give tracizoline (Figure 1.9), which possesses good affinity and excellent selectivity ($pK_i I_2 = 8.74$, $I_2/\alpha_2 = 7,762$, $I_2/\alpha_1 = 2,344$). However, substitution of the *trans*-styryl bridge with a second phenyl ring produced the ligand benazoline (Figure 1.9), which possesses unprecedented selectivity towards I_2 -IBS ($pK_i I_2 = 9.07$, $I_2/\alpha_2 = 18,621$, $I_2/\alpha_1 = 2,691$).⁹² Unfortunately, benazoline could not distinguish between IBS subtypes but this was resolved by substituting the naphthyl ring with either quinoline or isoquinoline (BU224 and BU226, respectively, Figure 1.9, Table 1.7).^{94,95}

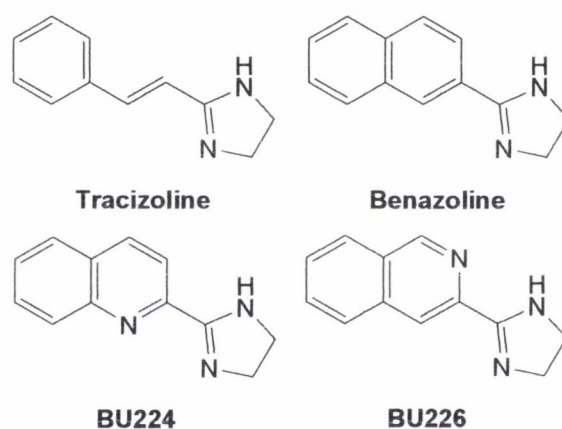


Figure 1.9.- The structure of the compounds discussed in section 1.5.2.1(c)

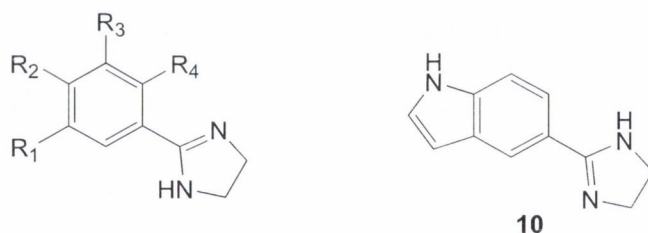
Table 1.7.- Summary of the Affinities of the Synthetic I_2 -IBS ligands in Section 1.5.2.1(c)

Ligand	I_1 -IBS Affinity (pK_i)	I_2 -IBS Affinity (pK_i)	α_1 -AR Affinity (pK_i)	α_2 -AR Affinity (pK_i)	Selectivity IBS/ α -AR
tracizoline	7	8.74		4.13	
benazoline		9.07			18,621 (I_2/α_2), 2,691 (I_2/α_1)
BU224	7.38	8.7		<5	832 (I_2/I_1)
BU226		8.85	<5	<5	380 (I_2/I_1)

(d) 2-Aryl and 2-Heterocyclic Imidazolines

Research by Anastassiadou *et al.*⁹⁶ revealed that linking an aromatic substituent to the 2-position of an imidazoline ring produced compounds with no α -ARs affinity. Their results also indicated that introduction of a substituent at the *para*-position of the phenyl ring provided ligands with affinity towards I₂-IBS while having substituents at the *ortho*- or *meta*-positions provided ligands with affinity towards I₁-IBS (**9a-k**, **9m** and **9l** respectively, Figure 1.10, Table 1.8). A prime example of this is where the methyl group is located at the *para*-position (**9l**, Figure 1.10). This compound possesses high affinity and selectivity towards I₂-IBS. However, when the methyl group is at the *ortho*-position (**9m**, Figure 1.10) the compound is selective towards I₁-IBS (Table 1.8).

Heterocyclic derivatives in general, showed low affinity towards IBS with no affinity towards α -ARs except in the case of the 5'-indolyl-2-imidazoline derivative (**10**, Figure 1.10), which showed similar affinity to 2-BFI (Table 1.8).



- 9a**, R₁ = H, R₂ = Me, R₃ = H, R₄ = H
9b, R₁ = H, R₂ = n-Pr, R₃ = H, R₄ = H
9c, R₁ = H, R₂ = i-Pr, R₃ = H, R₄ = H
9d, R₁ = H, R₂ = Bu, R₃ = H, R₄ = H
9e, R₁ = H, R₂ = t-Bu, R₃ = H, R₄ = H
9f, R₁ = H, R₂ = Ph, R₃ = H, R₄ = H
9g, R₁ = H, R₂ = OMe, R₃ = H, R₄ = H
9h, R₁ = H, R₂ = OPh, R₃ = H, R₄ = H
9i, R₁ = H, R₂ = SMe, R₃ = H, R₄ = H
9j, R₁ = H, R₂ = CF₃, R₃ = H, R₄ = H
9k, R₁ = H, R₂ = OCF₃, R₃ = H, R₄ = H
9l, R₁ = H, R₂ = Me, R₃ = F, R₄ = H
9m, R₁ = F, R₂ = H, R₃ = H, R₄ = Me

Figure 1.10.- The structure of the compounds discussed in section 1.5.2.1(d)

1.5.2.2 Aromatic and Aliphatic 2-Aminoimidazolines

Traditionally, 2-aminoimidazolines act as α_2 -AR ligands, there are, however, exceptions to this rule. One of these exceptions is the ligand brimonidine (Figure 1.11), which shows good affinity towards I₂-IBS over α -ARs.^{9,97} Another exception is the compound RS45041 (Figure 1.11) although in this derivative the 2-aminoimidazoline is included in the isoindoline moiety, which could explain its unusual affinity and selectivity towards I₂-IBS (Table 1.9).^{98,99} Saczewski *et al.*¹⁰⁰ prepared a series of ligands similar to RS45041, introducing a second nitrogen on the isoindoline moiety. Indazim (Figure 1.11), the parent compound, showed medium affinity towards I₂-IBS but the introduction of a chloro substituent on the aromatic ring increased the affinity and selectivity towards I₂-IBS (**11**, Figure 1.11, Table 1.9).

Table 1.8.- Summary of the Affinities of the Synthetic I₂-IBS ligands in Section 1.5.2.1(d)

Ligand	I ₁ -IBS Affinity (pK _i)	I ₂ -IBS Affinity (pK _i)	α_1 -AR Affinity (pK _i)	α_2 -AR Affinity (pK _i)
9a	5.89	8.04	<5	<5
9b	6.22	7.16	<5	<5
9c	5.66	7.09	<5	<5
9d	6.04	6.77	<5	<5
9e	5.05	6.25	<5	<5
9f	6.69	8	6	<5
9g	7.46	8.28	<5	<5
9h	6.34	7.34	5.11	5.26
9i	7.75	8.42	<5	<5
9j	5.96	7.28	6.89	<5
9k	6.04	7.07	<5	<5
9l	<5	8.53	<5	<5
9m	7.64	5.3	<5	<5
10		8.57		

Previous research by Rozas' group resulted in the preparation of a series of twin drugs (both aliphatic and aromatic) containing the 2-aminoimidazolinium moiety (**12a-d** and **13a-d** respectively, Figure 1.11).¹⁰¹ The affinity of the aliphatic 2-aminoimidazolines

towards I₂-IBS increased as the length of the aliphatic chain increased with the compound **12d**, the ligand with the longest aliphatic chain in this series, showing the highest affinity (pK_i I₂-IBS = 6.42). The affinity of this molecule while lower than that of idazoxan contradicts the fact that it possesses a six fold increase in selectivity when compared to the same compound (pK_i α_2 -ARs = 7.30, Selectivity I₂/ α_2 = 1.35 [idazoxan], pK_i α_2 -ARs = 6.42, Selectivity I₂/ α_2 = 6.03 [**12d**]). Unfortunately, this same selectivity was not observed in the aromatic *bis*-(2-aminoimidazolines) (**13a-d**, Figure 1.11) synthesized in the same study. Although the compounds prepared showed a similar affinity towards I₂-IBS they also showed a higher affinity towards α_2 -ARs especially in the case of compounds **13a** and **13c** (pK_i I₂-IBS = 6.29, pK_i α_2 -ARs = 7.24, Selectivity I₂/ α_2 = 0.11 [**13a**], pK_i I₂-IBS = 6.19, pK_i α_2 -ARs = 8.80, Selectivity I₂/ α_2 = 0.002 [**13c**]).

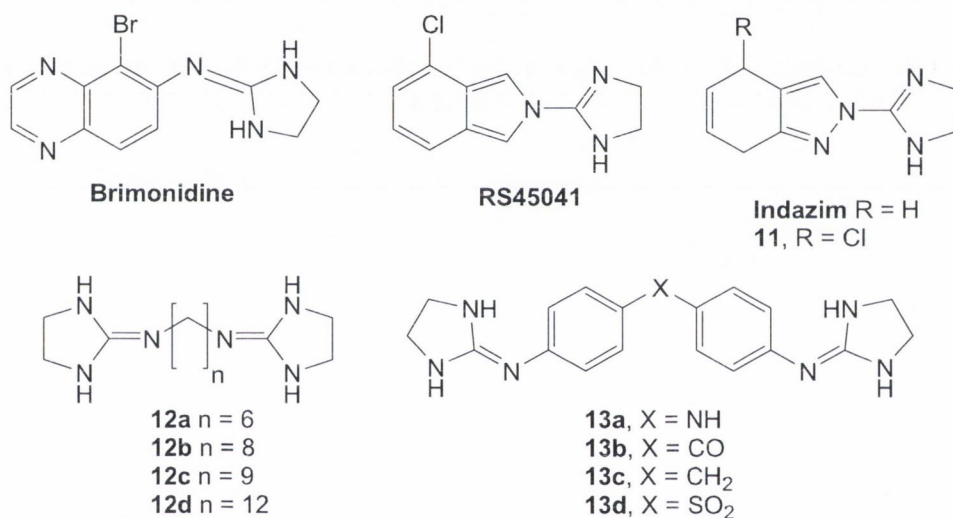


Figure 1.11.- The structure of the compounds discussed in section 1.5.2.2

1.5.2.3 Amidines

Amidine derivatives form another small family of I₂-IBS ligands, with only three ligands of note, pentamidine and the amidine analogues of both RX821029 and idazoxan (Figure 1.12).^{102,103} The amidine analogues of RX821029 and idazoxan show far less affinity towards IBS than their parent compounds (145 and 20 times less, respectively, Table 1.9). Wood *et al.*¹⁰³ showed that pentamidine was a potent I₂-IBS ligand but this affinity

relied strongly on the presence of both benzamidine moieties and loss of one moiety resulted in a 228 fold decrease in affinity towards I₂-IBS (Table 1.9).¹⁰⁴

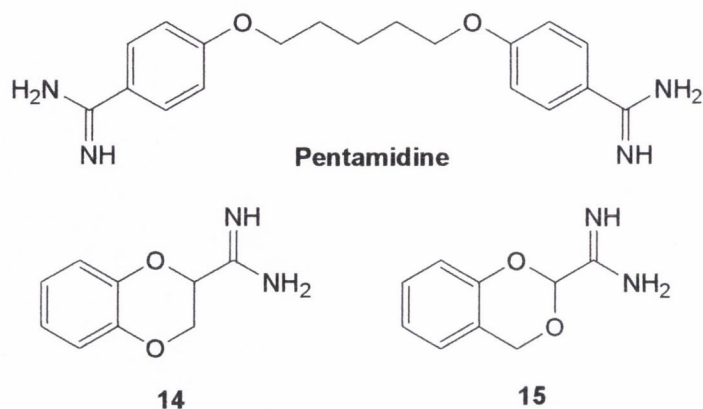


Figure 1.12.- The structure of the amidines discussed in section 1.5.2.3

Table 1.9.- Summary of the Affinities of the Synthetic I₂-IBS ligands in Section 1.5.2.2 and 1.5.2.3

Ligand	I ₂ -IBS Affinity (pK _i)	α ₂ -AR Affinity (pK _i)	Selectivity IBS/α-AR
brimonidine	7.47	6.67 (α _{2A}) 6.02 (α _{2B}) 5.71 (α _{2C})	6.3 (α _{2A}) 28 (α _{2B}) 57 (α _{2C})
RS45041	9.37	<5	23,000
indazim	5.7	<4	46
11	6.5	<4	3076
12a	5.6		
12b	6.37	6.22	1.41
12c	6.80	6.44	2.29
12d	7.20	6.42	6.03
13a	6.29	7.24	0.11
13b	6.05		
13c	6.19	8.8	0.002
13d	<5		
pentamidine	7.85		

1.5.2.4 Guanidine Derivatives

(a) Aromatic Guanidines

Guanidine ligands such as amiloride and guanabenz (Figure 1.13) are important guanidine ligands, which have been used to characterise IBS and in particular amiloride can distinguish between the two I_2 -IBS subtypes, I_{2A} -IBS and I_{2B} -IBS.¹⁰⁵ The selectivity towards I_{2B} over I_{2A} could be tuned by the introduction of various alkyl groups. The introduction of an *iso*-propyl group favoured the I_{2A} -IBS subtype (**16a** > **16b** > **16c** > **16d**), while the introduction of a methyl group favoured the I_{2B} -IBS subtype (**16c** > **16b** > **16d** > **16a**) (Figure 1.13, Table 1.10).

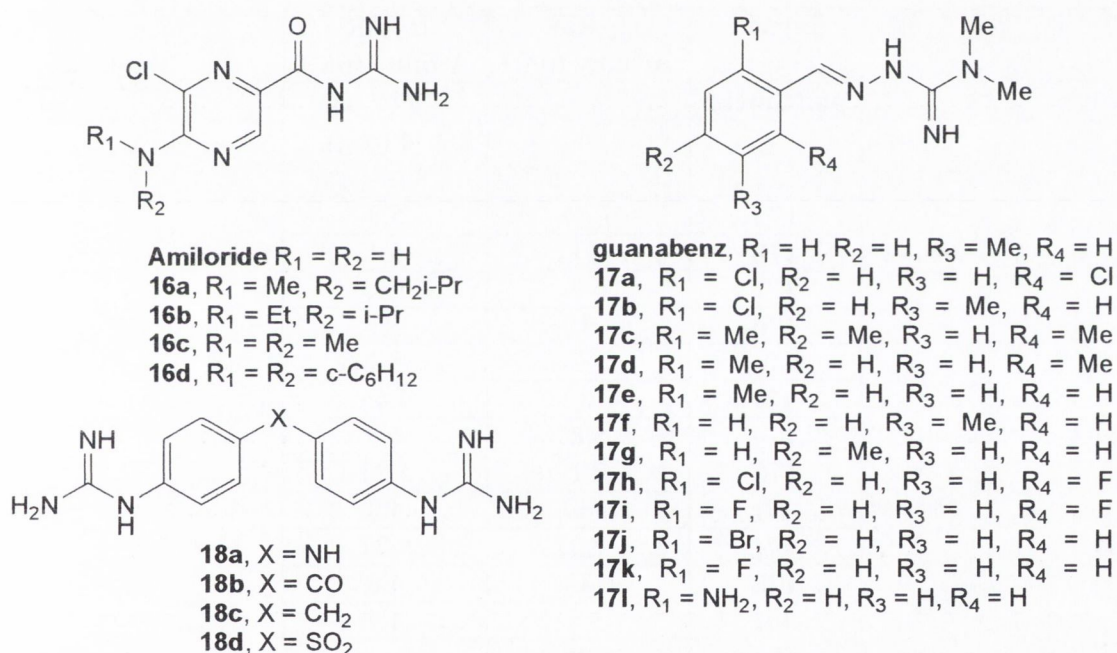


Figure 1.13.- The structure of the aromatic guanidines discussed in section 1.5.2.4(a)

Wikberg *et al.*¹⁰⁶ synthesised a series of Schiff bases similar to guanabenz, which featured various substituents on the aromatic ring (**17a-m**, Figure 1.13). The results showed that, in general, 2-substituted and 2,6-disubstituted ligands had the best affinity and selectivity towards I_2 -IBS and for the 2-substituted compounds the order was: 2-Br > 2-Cl > 2-Me > 2-F > 2-NH₂ (Figure 1.13, Table 1.10) but that the two N-methyl

substituents were vital for the affinity. For the 2,6-disubstituted ligands the presence of a methyl group at the *para*-position disfavoured I₂-IBS activity, which is opposite to the trend observed in the *para*-substitution of the 2-arylimidazolines as reported by Anastassiadou *et al.*⁹⁶

Very few aromatic *bis*-guanidines have been reported as I₂-IBS ligands. One family of such compounds was synthesized by our group in 2002 (**18a-d**, Figure 1.13). The aromatic *bis*-guanidines prepared did not show high affinity for I₂-IBS and were never tested for their affinity towards α_2 -ARs.

Table 1.10.- Summary of the Affinities of the Synthetic I₂-IBS ligands in Section 1.5.2.4(a)

Ligand	I ₂ -IBS Affinity (pK _i)	α_2 -AR Affinity (pK _i)
guanabenz		7.7 (α_{2A}), 7.54 (α_{2B}), 8 (α_{2C})
17a	7.44	5.7
17b	7.1	5.1
17c	6.4	5.33
17d	7	5.7
17e	6.88	5.1
17f	6	4.45
17g	5.8	4.3
17h	7.1	5.23
17i	6.37	4.8
17j	7.3	5.27
17k	6.33	4.6
17l	5.5	4.7
18a	5.28	
18b	5.98	
18c	5.93	
18d	5.35	

(b) Aliphatic Guanidines

Aliphatic guanidines are again a small family of ligands, which is surprising bearing in mind the biological importance of the endogenous ligand agmatine as previously

discussed. Early research by Rozas' group has revealed that a series of agmatine like twin drugs such as **19a-d** (Figure 1.14) showed an improved affinity towards I₂-IBS when compared to the aliphatic *bis*-(2-aminoimidazolines) **12a-d** previously prepared by the group (Table 1.9). In general, again similar to the *bis*-(2-aminoimidazolines) **12a-d**, it was found that increasing the length of the alkyl chain increased the affinity towards I₂-IBS and lowered the affinity towards α₂-ARs.¹⁰¹ In a direct comparison to the *bis*-(2-aminoimidazolines) **12a-d**, the compound **19c** shows a similar selectivity to the most potent *bis*-(2-aminoimidazoline), **12d** (pK_i I₂ = 6.89, pK_i α₂-ARs = 6.07, I₂/α₂ = 6.61 [**19c**], pK_i I₂ = 7.20, pK_i α₂-ARs = 6.42, I₂/α₂ = 6.03 [**12d**]). However, once again it was the compound with the longest chain length, **19d**, that showed the best affinity and selectivity towards I₂-IBS (pK_i I₂ = 7.48, pK_i α₂-ARs = 6.29, I₂/α₂ = 15.5). These results compared favourably to those obtained for idazoxan. A similar series of mono substituted guanidine derivatives (**20a-c**, Figure 1.13) were prepared and tested but were found to be inactive at both the I₂-IBS and α₂-AR sites.

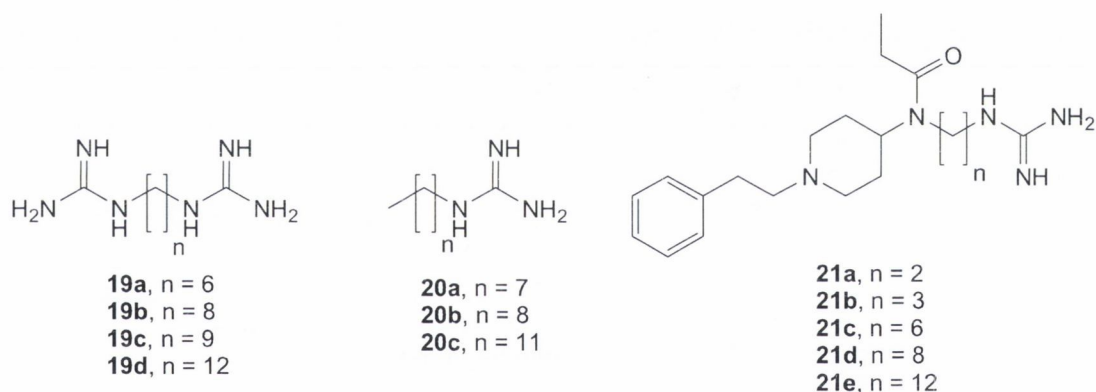


Figure 1.14.- The structure of the aliphatic guanidines discussed in section 1.5.2.4(b)

Recent research by Dardonville *et al.*¹⁰⁷ has also revealed the potential of one ligand acting at both the I₂-IBS and μ-opioid receptors. These are a series of fentanyl derivatives with a guanidine located at the end of a long alkyl chain (**21a-e**, Figure 1.14), again similar to the aliphatic *bis*-guanidines prepared by our group the best results have been obtained with the longest aliphatic chain linking the two moieties, **21e** (pK_i I₂-IBS = 8.24).¹⁰⁸

Table 1.11.- Summary of the Affinities of the Synthetic I₂-IBS ligands in Section 1.5.2.4(b)

Ligand	I ₂ -IBS Affinity (pK _i)	α ₂ -AR Affinity (pK _i)	Selectivity IBS/α-AR
19a	5.23		
19b	6.2	6.27	0.87
19c	6.89	6.07	6.61
19d	7.48	6.29	15.49
20a	<4	5.35	
20b	<4	4.84	
20c	4.49	4.83	0.46
21a	4.69	6.43	0.02

1.5.2.5 Miscellaneous ligands

Due to the evidence linking MAO and IBS it is no surprise that several MAO inhibitors have been tested as potential IBS ligands.¹⁰⁸ This research to date has given mixed results. The irreversible MAO inhibitor clorgyline (Figure 1.15) has good affinity towards I₂-IBS and can distinguish between I₂-IBS subtypes (Table 1.12).

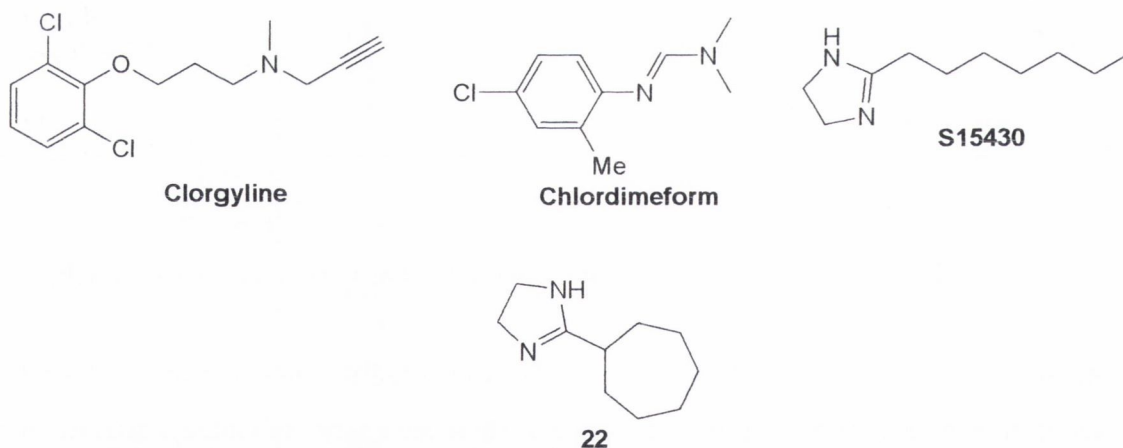


Figure 1.15.- The structure of the compounds discussed in section 1.5.2.5

The reversible MAO inhibitor, chlordimeform (Figure 1.15), also holds good affinity towards I₂-IBS but cannot distinguish between subtypes. One interesting ligand is S15430, an aliphatic 2-imidazoline, which possesses good affinity towards I₂-IBS but not as high as its cyclic counterpart **22** (Figure 1.15, Table 1.12).^{102,106,109}

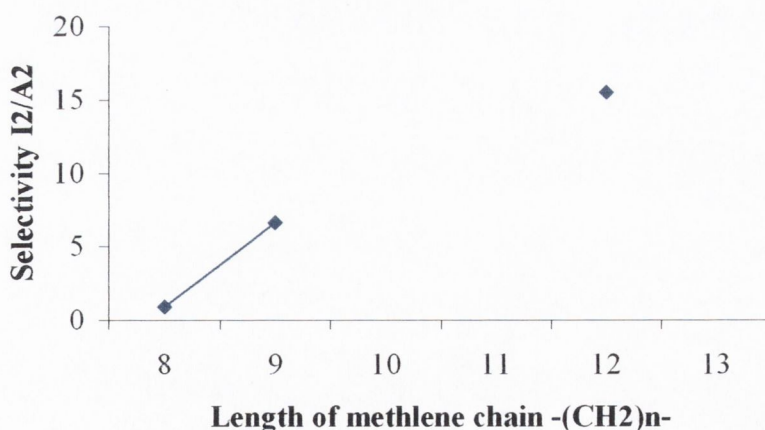
Table 1.12.- Summary of the Affinities of the Synthetic I₂-IBS ligands in Section 1.5.2.5

Ligand	I ₂ -IBS Affinity (pK _i)	α ₂ -AR Affinity (pK _i)	Selectivity IBS/α-AR
clorgyline	5.45 (I _{2A}) 7.27 (I _{2B})	<4	66.6 (I _{2A} /I _{2B}) 19.9 (I _{2A} /α ₂)
chlorodimeform	8.22		
S15430	6.9	<4	110
22	7.4		

1.6 Project Aims

As stated earlier, previous research by Rozas' group revealed that the compounds **19a-d** acted as I₂-IBS ligands. It also revealed that as the length of the methylene linker chain increased the selectivity and affinity towards I₂-IBS over α₂-ARs increased as well (Graph 1.1). From this trend we concluded that some form of Structure Activity Relationship (SAR) between chain length and affinity/selectivity towards I₂-IBS over α₂-ARs existed. Two hypotheses can be proposed from this data;

- if the methylene chain is further lengthened the relationship between selectivity and chain length will eventually reach an optimum or
- the optimum has been reached by either **19d** or possibly where n = 10 or 11 (**19e-f**, Figure 1.16).



Graph 1.1.- Selectivity of the alkyl *bis*-guanidines **19b-d** towards I₂-IBS over α₂-ARs

The results obtained in the present project are presented in the following chapters and can be divided into four parts based on these two hypotheses. In Chapter two the results of further elongating the methylene chain linking both guanidine groups and preparation of **19e-g** are presented. Chapters three and four deal with the synthesis of three new families of potential I₂-IBS ligands, **23a-f**, **24a-f** and **25a-f** (Figure 1.16), based on the *bis*-guanidines and one of three other ligands; amiloride, S15930 and pentamidine. Chapter five deals with the methodology and results obtained by performing conformational analysis on all four families to investigate any possible SAR between members of families and between families themselves. Chapter six presents the results obtained from the biological assays of these compounds regarding their affinity towards I₂-IBS and, where it was warranted (based on affinity towards I₂-IBS), their selectivity over α₂-ARs.

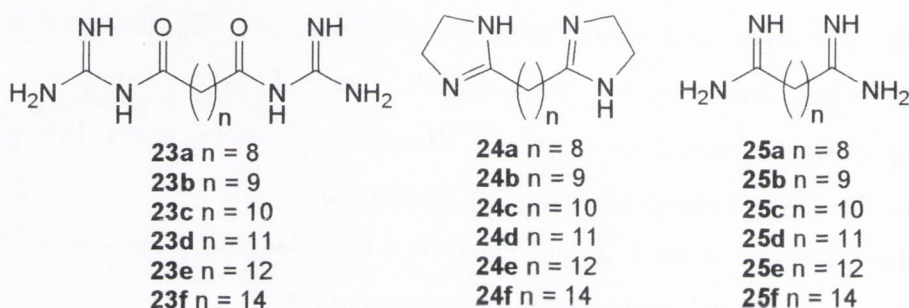


Figure 1.16.- Structure of the ligands **23a-f**, **24a-f** and **25a-f**

1.7 References

1. Bousquet, P.; Feldman, J.; Schwartz, J. *J. Pharmacol. Exp. Ther.* **1984**, *230*, 230.
2. Emsberger, P.; Meeley, M. P.; Mann, J. *J. Eur. J. Pharm.* **1987**, *134*, 1.
3. Morgan, N. G.; Chan, S. L. F.; Brown, C. A.; Tsoli, E. *Ann. New York Acad. Sci.* **1995**, *763*, 531.
4. French, N. *Pharmacol. Ther.* **1995**, *68*, 175.
5. Parini, A.; Moudanos, C. G.; Pizzinat, N.; Lanier, S. M. *Trends Pharmacol. Sci.* **1996**, *17*, 13.
6. Regunathan, S.; Reis, D. J. *Annu. Rev. Pharmacol. Toxicol.* **1996**, *36*, 511.
7. Molderings, G. J.; Moura, D.; Fink, K.; Bonisch, H.; Gothert, M. *NauNew Yorkn-Schmied. Arch. Pharmacol.* **1993**, *348*, 70.
8. Dontenwill, M.; Vonthron, C.; Greney, H.; Magnier, C.; Heemskerk, F.; Bousquet, P.; *Ann. New York Acad. Sci.* **1999**, *881*, 123.
9. Eglen, R. M.; Hudson, A. L.; Kendall, D. A.; Nutt, D. J.; Morgan, N. G. Wilson, V. G.; Dillon, M. P. *Trends Pharmacol. Sci.* **1998**, *19*, 9, 381.
10. Piletz, J. E.; Zhu, H. Chikkala, D. N. *J. Pharmacol. Exp. Ther.* **1996**, *279*, 2, 694.
11. Reid, J. L. *Am. J. Hypertens.* **2000**, *13*, 6, 106S.
12. Chan, S. L. F.; Brown, C. A.; Scarpello, K. E.; Morgan, N. G. *Br. J. Pharmacol.* **1996**, *117*, 1749.
13. Dardonville, C.; Rozas, I. *Med. Research Review.* **2004**, *24*, 5, 639.
14. Morgan, N. G.; Chan, S. L. F. *Drug Design Rev.* **2004**, *1*, 3, 185.
15. Regunathan, S.; Meeley, M. P.; Reis, D. J. *Biochem. Pharmacol.* **1993**, *45*, 1667.
16. Mitoma, J.; Ito, A. *J. Biochem.* **1992**, *111*, 20.
17. Tesson, F.; Limon, I. Parini, A. *Eur. J. Pharmacol.* **1992**, *219*, 335.
18. Langin, D.; Paris, H.; Lafontan, M. *Mol. Pharmacol.* **1990**, *37*, 876.
19. Diamant, S.; Eldar-Geva, T. Atlas, D. *Br. J. Pharmacol.* **1992**, *106*, 101.
20. Lacombe, C.; Viallard, V.; Paris, H. *Let. J. Biochem.* **1993**, *25*, 1077.
21. Escriba, P. V. *Neurosci. Lett.* **1994**, *178*, 81.
22. Coupry, I.; Atlas, D.; Podevin, R. A.; Lizielli, I.; Parini, A. *J. Pharmacol. Exp. Ther.* **1989**, *252*, 293.

23. Tesson, F.; Buus, C. P.; Lemoine, A.; Pegorier, J. P. Parini, A. *J. Biol. Chem.* **1991**, *266*, 155.
24. Lanier, S. M.; Ivkovic, B.; Singh, I.; Neumever, I.; Rakthavachalam, V. *J. Biol. Chem.* **1993**, *268*, 16047.
25. Tesson, F. *J. Biol. Chem.* **1995**, *270*, 9856.
26. Raddatz, R.; Parini, A.; Lanier, S. M. *J. Biol. Chem.* **1995**, *270*, 27961.
27. Miralles, A.; Esteban, S.; Sastre-Coll, A.; Moranta, D.; Asensio, V. J.; Garcia-Sevilla, J. A. *Eur. J. Pharm.* **2005**, *518*, 234.
28. Diaz, A.; Mayet, S.; Dickenson, A. H. *Eur. J. Pharmacol.* **1997**, *333*, 9.
29. Boronat, M. A.; Olmos, G.; Garcia-Sevilla, J. A. *Br. J. Pharmacol.* **1998**, *125*, 175.
30. Parker, C.; Anderson, N. J.; Robinson, E. S. J.; Price, R.; Tyacke, R. J.; Husbands, S. M.; Dillon, M. P.; Eglen, R. M.; Hudson, A. L.; Nutt, D. J.; Crump, M. P.; Crosby, J. *Biochem.* **2004**, *43*, 16385.
31. Binda, C.; Newton-Vinson, P.; Hubalek, F.; Edmondson, D. E.; Mattevi, A. *Nat. Struct. Biol.* **2002**, *9*, 1, 22.
32. Carpena, C. *J. Pharmacol. Exp. Ther.* **1995**, *272*, 681.
33. Saura, J. *Neurosci.* **1994**, *62*, 15.
34. Sastre, M.; Ventayol, P.; Garcia-Sevilla, J. A. *Neuroreport.* **1996**, *7*, 509.
35. Wang, H.; Regunathan, S.; Ruggiero, D. A.; Reis, D. J. *Mol. Pharmacol.* **1993**, *43*, 509.
36. Olmos, G.; AlemaNew York, R.; Escriba, P. V.; Garcia-Sevilla, J. A. *Br. J. Pharmacol.* **1994**, *111*, 997.
37. Regunathan, S.; Feinstein, D. L.; Reis, D. J. *J. Neurosci. Res.* **1993**, *34*, 681.
38. Oderfeld-Nowak, B.; Bacia, A.; Gardkowska, M. *Neurochem. Int.* **1992**, *21*, 455.
39. Molderings, G. J. *Drugs Fut.* **1997**, *22*, 7, 757.
40. Martin-gomez, J. I.; Ruiz, J.; Barrondo, S.; Callado, L. F.; Meana, J. J. *Life Sci.* **2005**, *78*, 205.
41. Brown, C. M. *Br. J. Pharmacol.* *116*, 1737.
42. Jackson, H. C.; Nutt, D. J. Drug Receptor Subtypes and Ingestive Behaviour (Cooper, S. J. and Clifton, P. G.; eds) pp. 267 – 283 Academic Press.

43. Reynolds, G. P.; Boulton, R. M.; Pearson, S. J.; Hudson, A. L.; Nutt, D. J. *Eur. J. Pharmacol.* **1996**, *301*, R19.
44. Meana, J. J.; Barturen, F.; Martin, I.; Garcia-Sevilla, J. A. *Biol Psych.* **1993**, *34*, 498.
45. Self, D. W.; Nestler, E. J. *Annu. Rev. Neurosci.* **1995**, *18*, 463.
46. Venteclef, N.; Guillard, R.; Issandou, M. *Biochem. Pharmacology* **2005**, *69*, 1041.
47. Santos, A. R. S.; Gadotti, V. M.; Oliveira, G. L.; Tibola, D.; Paszcuk, A. F.; Neto, A.; Spindola, H. M.; Souza, M. M.; Rodrigues, A. L. S.; Calixto, J. B. *Neuropharm.* **2005**, *48*, 1021.
48. Bousquet, P. J. *Cardiovasc. Pharmacol.* **1995**, *26* (Suppl. 2), S1.
49. Ernsberger, P.; Collins, L. A.; Graves, M. E.; Dreshaj, I. A.; Hiu, M. A. Lung Biology in Health and Disease, 82. Truth, C. O.; Mills, R. M.; Kiwull-Schone, H. F.; Schljake, M. E. (Eds.). Marcel Dekker: New York **1995**, 319.
50. Guyenet, P. G.; Allen, A. M.; Lynch, K. R.; Rosin, D. L.; Stor, R. L. Lung Biology in Health and Disease, 82. Truth, C. O.; Mills, R. M.; Kiwull-Schone, H. F.; Schljake, M. E. (Eds.). Marcel Dekker: New York **1995**, 281.
51. Ernsberger, P.; Giuliano, R.; Willette, R. N.; Reis, D. J. *J. Pharmacol. Exp. Ther.* **1990**, *253*, 408.
52. Allan, D. R.; Penner, S. B.; Smyth, D. D. *Br. J. Pharmacol.* **1996**, *117*, 29 – 34.
53. Li, P.; Smyth, D. D. *J. Pharmacol. Exp. Ther.* **1993**, *267*, 1395.
54. Smyth, D. D.; Li, P.; Blandford, D. E.; Penner, S. B. *J. Pharmacol. Exp. Ther.* **1992**, *261*, 1080.
55. Darkwa, F. K.; Smyth, D. D. *Pharmacology*, **1995**, *51*, 347.
56. Smyth, D. D.; Penner, S. B. *J. Cardiovasc. Pharmacol.* **1995**, *26* (Suppl. 2), S63.
57. Bidet, M.; Poujeol, P.; Parini, A. *Br. J. Biophys. Acta.* **1990**, *1024*, 173.
58. Penner, S. B.; Smyth, D. D. *Cardiovasc. Drugs Ther.* **1994**, *8*, 43.
59. Lachaud-Pettiti, V.; Podevin, R. A.; Chretien, Y.; Parini, A. *Eur. J. Pharmacol. – Mol. Pharmacol. Sect.* **1991**, *206*, 23.
60. Ivkovic, B.; Batkthavachalam, V.; Zhang, W. *Mol. Pharmacol.* **1994**, *46*, 15.

61. Mac Kinnon, A. C.; Stewart, M.; Olverman, H. J.; Spedding, M.; Brown, C. M. *Eur. J. Pharmacol.* **1993**, *232*, 79 – 87. Atlas, D.; Burstein, Y. *Eur. J. Biochem.* **1984**, *144*, 287.
62. Sabetkasaie, M.; Vala, S.; Khansefid, N.; Hosseini, A. R.; Ladjevardi, M. A. R. S. *Eur. J. Pharm.* **2004**, *501*, 95.
63. Kino, Y.; Tanabe, M.; Honda, M.; Ono, H. *J. Pharmacol. Sci.* **2005**, *99*, 52.
64. Molderings, G. J.; Schmidt, K.; Bonisch, H.; Gothert, M. *Arch. Pharmacol.* **1996**, *354*, 245.
65. Dunne, M. J. *Br. J. Pharmacol.* **1991**, *103*, 1847.
66. Chan, S. L. F. *Clin. Sci.* **1993**, *85*, 671.
67. Olmos, G.; Kulkarni, R. N.; Haque, M.; Mac Dermot, J. *Eur. J. Pharmacol.* **1994**, *262*, 41.
68. Atlas, D.; Burstein, Y. *Eur. J. Biochem.* **1984**, *144*, 287.
69. Atlas, D.; Burstein, Y. *FEBS Lett.* **1984**, *170*, 387.
70. Atlas, D.; Diamant, S.; Fales, H. M.; Pannell, L. *J. Cardiovasc. Pharmacol.* **1987**, *10* (Suppl 12), S122.
71. Ernsberger, P.; Meeley, M. P.; Reis, D. J. *Brain Res.* **1988**, *441*, 309.
72. Ernsberger, P.; Feinland, G.; Meeley, M. P.; Reis, D. J. *Am. J. Hypertens.* **1990**, *3*, 90.
73. Atlas, D. *Biochem. Pharmacol.* **1991**, *41*, 1541.
74. Li, G.; Regunathan, S.; Barrow, C. J.; Eshraghi, J.; Cooper, R.; Reis, D. J. *Sci.* **1994**, *263*, 5149, 966.
75. Raasch, W.; Schafer, U.; Chun, J.; Dominiak, P. *Br. J. Pharmacol.* **2001**, *133*, 755.
76. Raasch, W.; Schafer, U.; Qadri, F.; Dominiak, P. *Br. J. Pharmacol.* **2001**, *135*, 633.
77. Husbands, S. M.; Glennon, R. A.; Gorgerat, S.; Gough, R.; Tyacke, R.; Crosby, J.; Nutt, D. J.; Lewis, J. W.; Hudson, A. L. *Drug Alcohol Depend.* **2001**, *64*, 203.
78. Morgan, N. G.; Cooper, E. J.; Squires, P. E.; Hills, C. E.; Parker, C. A.; Hudson, A. L. *Ann. New York Acad. Sci.* **2003**, *1009*, 167.
79. Glennon, R. A.; Grella, B.; Tyacke, R. J.; Lau, A.; Westaway, J.; Hudson, A. L. *Bioorg. Med. Chem. Lett.* **2004**, *14*, 999.

80. Hudson, A. L.; Luscombe, S.; Gouch, R. E.; Nutt, D. J.; Tyacke, R. J. *Ann. New York Acad. Sci.* **1999**, *881*, 212.
81. Carrieri, A.; Brasili, L.; Leonetti, F.; Pignini, M.; Giannella, M.; Bousquet, P.; Carotti, A. *Bioorg. Med. Chem.* **1997**, *5*, 5, 843.
82. Hudson, A. L.; Chapleo, C. B.; Lewis, J. W.; Husbands, S.; Grivas, K.; Mallard, N. J.; Nutt, D. J. *Neurochem. Int.* **1997**, *30*, 1, 47.
83. Nutt, D. J.; French, N.; Handley, S. Hudson, A. L.; Husbands, S.; Jackson, H.; Jordan, S.; Lalies, M. D.; Lewis, J.; Lione, L. *Ann. New York Acad. Sci.* **1995**, *763*, 125.
84. Touzeau, F.; Arrault, A.; Guillaumet, G.; Scalbert, E.; Pfeiffer, B.; Rettori, M. C.; Renard, P.; Merour, J. Y. *J. Med. Chem.* **2003**, *46*, 10, 1962.
85. Chapleo, C. B.; Myers, P. L.; Butler, R. C.; Davis, J. A.; Doxey, J. C.; Higgins, S. D.; Myers, M.; Roach, A. G.; Smith, C. F.; Stillings, M. R. *J. Med. Chem.* **1984**, *27*, 5, 570.
86. Coates, P. A.; Grundt, P.; Robinson, E. S.; Nutt, D. J.; Tyacke, R.; Hudson, A. L.; Lewis, J. W.; Husbands, S. *Bioorg. Med. Chem. Lett.* **2000**, *10*, 6, 605.
87. Tyacke, R. J.; Robinson, E. S.; Nutt, D. J.; Hudson, A. L. *Neuropharmacol.* **2002**, *43*, 1, 75.
88. Langin, D.; Paris, H.; Dauzats, M.; Lafontan, M. *Eur. J. Pharmacol.* **1990**, *188* (4 – 5), 261.
89. Ruffolo, R. R. Jr.; Waddell, J. E. *J. Pharmacol. Exp. Ther.* **1982**, *222*, 1, 29.
90. Brasili, L.; Pignini, M.; Marucci, G.; Quaglia, W. Malmusi, L.; Lanier, S. M.; Lanier, B. *Bioorg. Med. Chem.* **1995**, *3*, 11, 1503.
91. Pignini, M.; Bousquet, P.; Carotti, A.; Dontenwill, M.; Giannella, M.; Moriconi, R.; Piergentili, A.; Quaglia, W.; Tayebati, S. K.; Brasili, L. *Bioorg. Med. Chem.* **1997**, *5*, 5, 833.
92. Pignini, M.; Bousquet, P.; Brasili, L.; Carrieri, A.; Cavagna, R.; Dontenwill, M.; Gentili, F.; Giannella, M.; Leonetti, F.; Piergentili, A.; Quaglia, W.; Carotti, A. *Bioorg. Med. Chem.* **1998**, *6*, 12, 2245.

93. Gentili, F.; Bousquet, P.; Brasili, L.; Caretto, M.; Carrieri, A.; Dontenwill, M.; Giannella, M.; Marucci, G.; Perfumi, M.; Piergentili, A.; Quaglia, W.; Rascente, C.; Pignini, M. *J. Med. Chem.* **2002**, *45*, 1, 32.
94. Bruban, V.; Feldman, J.; Dontenwill, M.; Greney, H.; Brasili, L.; Giannella, M.; Pignini, M.; Bousquet, P. *Ann. New York Acad. Sci.* **1999**, *881*, 102.
95. Hudson, A. L.; Gough, R.; Tyacke, R.; Lione, L.; Lalies, M.; Lewis, J.; Husbands, S.; Knight, P.; Murray, F.; Hutson, P.; Nutt, D. J. *Ann. New York Acad. Sci.* **1999**, *881*, 81.
96. Anastassiadou, M.; Danoun, S.; Cane, L.; Baziard-Mouysset, G.; Payard, M.; Caignard, D-H.; Rettori, M-C.; Renard, P. *Bioorg. Med. Chem.* **2001**, *9*, 3, 585.
97. Jasper, J. R.; Lesnick, J. D.; Chang, L. K.; Yamanishi, S. S.; Chang, T. K.; Hsu, S. A.; Daunt, D. A.; Bonhaus, D. W.; Eglon, R. M. *Biochem. Pharmacol.* **1998**, *55*, 7, 1035.
98. Brown, C. M.; Mac Kinnon, A. C.; Redfern, W. S.; Williams, A.; Linton, C.; Stewart, M.; Clague, R. U.; Clark, R.; Spedding, M. *Br. J. Pharmacol.* **1995**, *116*, 2, 1737.
99. Mac Kinnon, A. C.; Redfern, W. S.; Brown, C. M. *Br. J. Pharmacol.* **1995**, *116*, 2, 1729.
100. Saczewski, F.; Hudson, A. L.; Tyacke, R. J.; Nutt, D. J.; Man, J.; Tabin, P.; Saczewski, J. *Eur. J. Pharm. Sci.* **2003**, *20*, 2, 201.
101. Dardonville, C.; Rozas, I.; Callado, L. F.; Meana, J. J. *Bioorg. Med. Chem.* **2002**, *10*, 5, 1525.
102. Baurin, N.; Vangrevelinghe, E.; Morin-Allory, L.; Merour, J. Y.; Renard, P.; Payard, M.; Guillaumet, G.; Marot, C. *J. Med. Chem.* **2000**, *43*, 6, 1109.
103. Wood, D. H.; Hall, J. E.; Rose, B. G.; Tidwell, R. R. *Eur. J. Pharmacol.* **1998**, *353*, 1, 97.
104. Wood, D. H.; Hall, J. E.; Rose, B. G.; Boykin, D. W.; Tidwell, R. R. *Ann. New York Acad. Sci.* **1999**, *881*, 110.
105. Olmos, G.; AlemaNew York, R.; Boronat, M. A.; Garcia-Seville, J. A. *Ann. New York Acad. Sci.* **1999**, *881*, 144.
106. Wikberg, J. E. S.; Hudson, A. L. *Neurochem. Int.* **1996**, *30*, 1, 95.

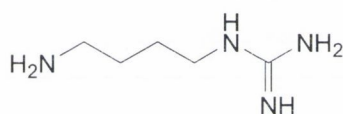
107. Dardonville, C.; Jagerovic, N.; Callado, L. F.; Meana, J. J. *Bioorg. Med. Chem. Lett.* **2004**, *14*, 2, 491.
108. Montero, A.; Goya, P.; Jagerovic, N.; Callado, L. F.; Meana, J. J.; Giron, R.; Goicoechea, C.; Martin, I. *Bioorg. Med. Chem.* **2001**, *10*, 1009.
109. Carpena, C.; Collon, P.; Remaury, A.; Cordi, A.; Hudson, A. L.; Nutt, D. J.; Lafontan, M. J. *J. Pharmacol. Exp. Ther.* **1995**, *272*, 2, 681.

Chapter 2

Synthesis of the alkyl bis-guanidines

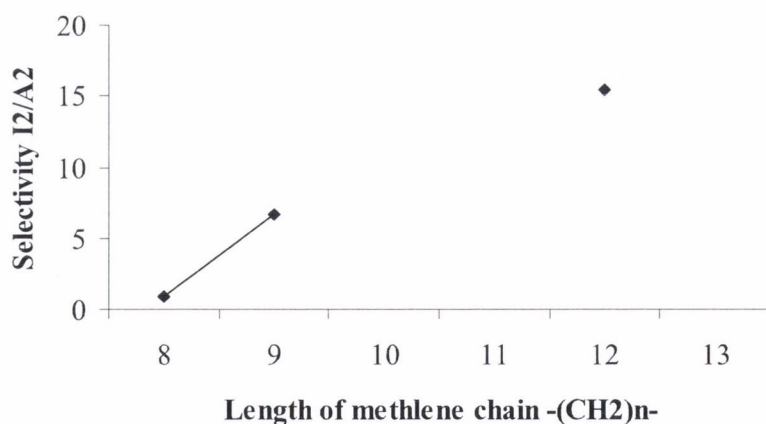
2.1 Introduction

Agmatine (Figure 2.1) is an endogenous ligand with medium affinity towards both I₁-IBS and I₂-IBS (pK_i I₁-IBS = 7.48, pK_i I₂-IBS < 5) and was once considered a candidate for the active component of CDS. Part of what makes **agmatine** unique is the aliphatic chain linking the guanidine group and the amine group at either end of the molecule. It was this I₂-IBS ligand that was used as a template for the synthesis of the alkyl *bis*-guanidines previously prepared by Rozas' group. The alkyl *bis*-guanidines, **19a-d**, previously synthesized by our group were prepared following the method described in the literature¹¹⁰⁻¹¹² as having been synthesized from commercial diamines and S-methyl pseudothiourea in an S_N2 reaction (Scheme 2.1). These alkyl *bis*-guanidines proved to possess higher affinity towards I₂-IBS than **agmatine** and were also more selective vs. α_2 -ARs (Graph 2.1).



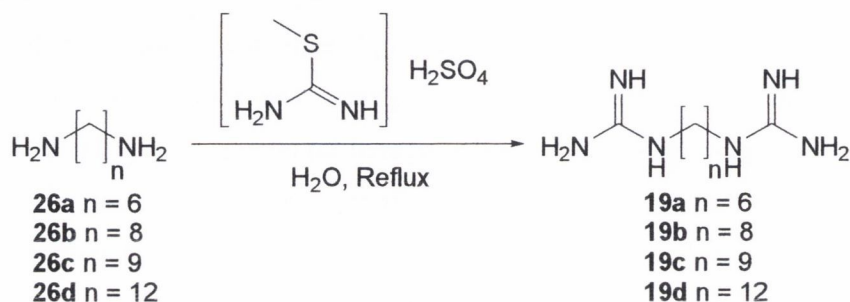
Agmatine

Figure 2.1.- Structure of **agmatine**



Graph 2.1.- Selectivity of the alkyl *bis*-guanidines **19b-d** towards I₂-IBS over α_2 -ARs

The data may also suggest that as the length of the methylene linker chain increases the selectivity towards I₂-IBS over α₂-ARs also increases. We planned to synthesize more alkyl *bis*-guanidines by elongating the alkyl linker chain to investigate this trend. In order to accomplish this we looked for the commercial availability of the corresponding alkyl diamines in order to use the original procedure shown in Scheme 2.1.

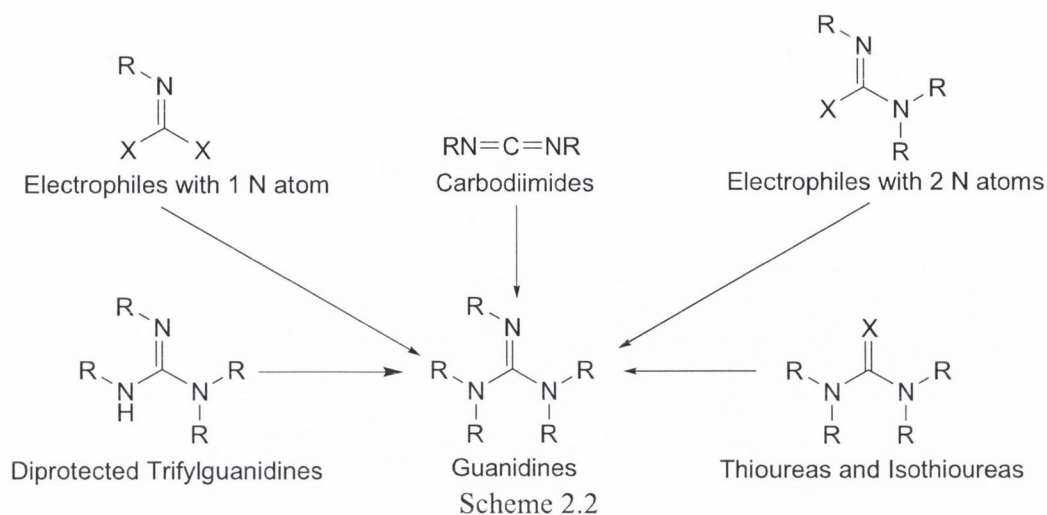


Scheme 2.1

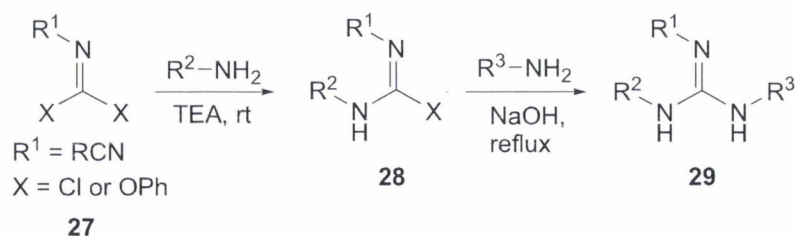
Unfortunately, diamines with linkers of 13 and 14 methylene groups were not commercially available so alternative routes needed to be investigated. The following section is a brief summary of general methods for the synthesis of guanidines. For a more complete review of the preparation of guanidines the reviews of Katritzky *et al.*¹¹³, Anslyn *et al.*¹¹⁴ and Burgess *et al.*¹¹⁵ should be consulted. In the next section the different methods of preparation of the proposed alkyl *bis*-guanidines is presented.

2.2 General Methods for the Synthesis of Guanidines

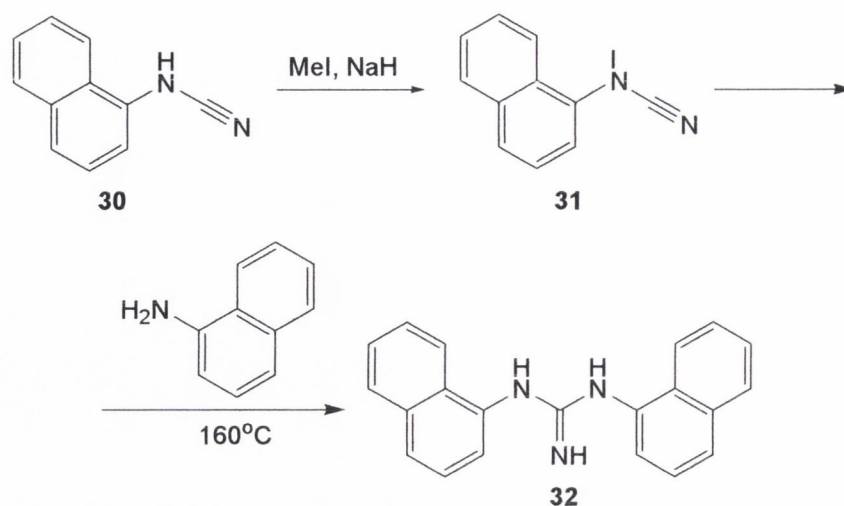
In Scheme 2.2 different routes for the preparation of guanidines are presented according to the different starting functional groups. These routes will be described in detail in this section.



Functionalised imidocarbonyl dichlorides (an electrophile containing one nitrogen atom), such as **27** (Scheme 2.3) can be converted into guanidines in a stepwise manner using mild conditions. However, the reaction will only proceed if **27** is functionalised with an electron withdrawing group such as a cyanate (Scheme 2.3).^{116,117} It has also been shown that the presence of the chloride groups are not necessary since moieties other than chlorine have been used giving similar results (Scheme 2.3).¹¹⁸

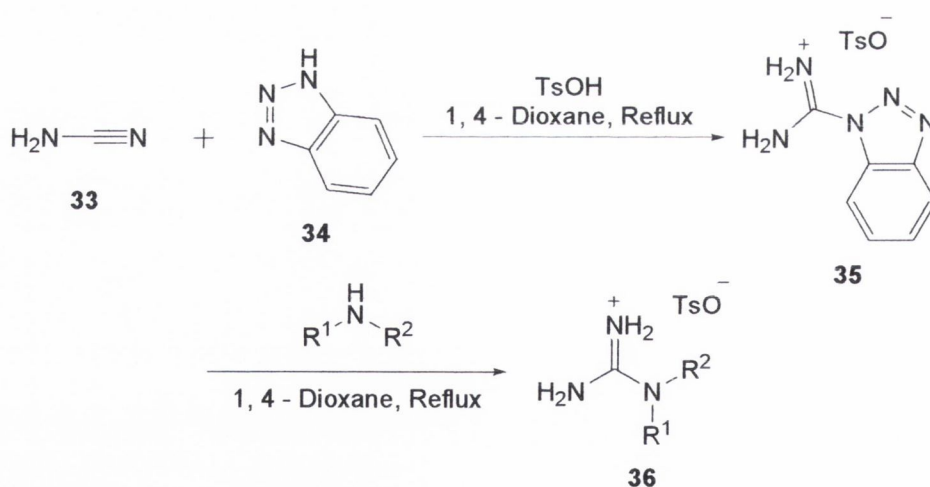


Cyanamides such as **30** (an example of an electrophile containing two nitrogen atoms) were originally converted into guanidines by using alkylating reagents such as methyl iodide followed by reaction with an amine (Scheme 2.4).¹¹⁹ Unfortunately, these reactions require high temperatures to provide the desired guanidines.



Scheme 2.4

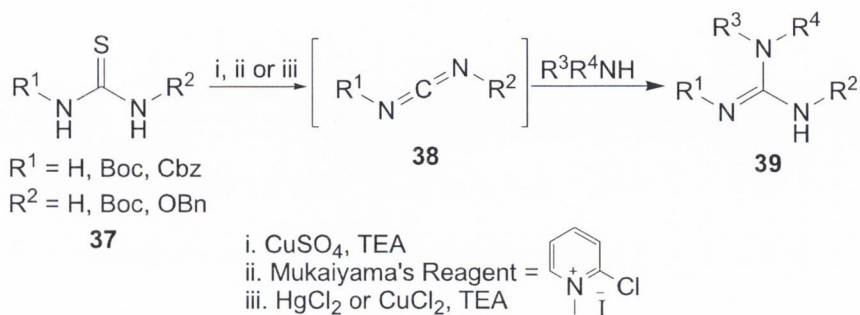
However, work by Katritzky *et al.*¹²⁰ showed that the reaction of **33** with benzotriazole, **34**, gives benzotriazole-1-carboxamidinium tosylate, **35**, which, undergoes facile substitution reactions to yield mono and disubstituted guanidines, **36** (Scheme 2.5). Both primary and secondary amines can be used in this reaction to produce the corresponding guanidines in good yield (55 – 86%).



Scheme 2.5

It is well known that thioureas, **37**, can be converted into guanidines by reacting with amines and this reaction has been thoroughly documented.¹²¹⁻¹²⁶ These reactions proceed

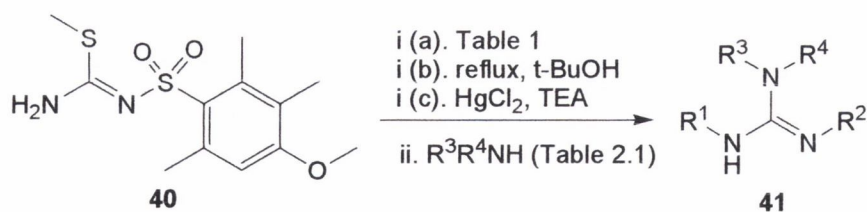
through the formation of a carbodiimide intermediate, **38**, which then reacts with either a primary or secondary amine to form the guanidine, **39**, in good to excellent yield (57 – 90%, Scheme 2.6).



Scheme 2.6

The reaction can be improved by introducing strong electron withdrawing groups into the thiourea fragment. One of the most typical electron withdrawing groups to be introduced into the thiourea fragment is the tert-Butoxy carbonyl (Boc) protecting group, which then, can be easily removed by standard methods (Scheme 2.6). However, other protecting groups, such as benzyl formate (Cbz) and benzyl groups, have also been used.¹²²⁻¹²⁶ To form the guanidine it is necessary to promote the formation of the carbodiimide intermediate and several different compounds have been reported to produce this intermediate, they include; copper sulphate,¹⁰ Mukaiyama's reagent¹¹ and mercury/copper chloride.¹²⁴⁻¹²⁶

S-methylisothiureas, **40**, have been widely used as guanylation reagents because of their easy preparation and availability. Similar to the thioureas, the presence of electron withdrawing groups on the isothiourea fragment promotes the formation of the guanidine product, **41**, although in most cases it is a substitution reaction, which occurs as opposed to the formation of a carbodiimide intermediate, **38** (Scheme 2.7).^{127,128} Again similar to the reaction from the thioureas, mercury (II) chloride is used to promote these reactions, but, when using mercuric perchlorate higher yields have been reported for a range of guanidines (Scheme 2.7, Table 2.1).^{127,129,130}

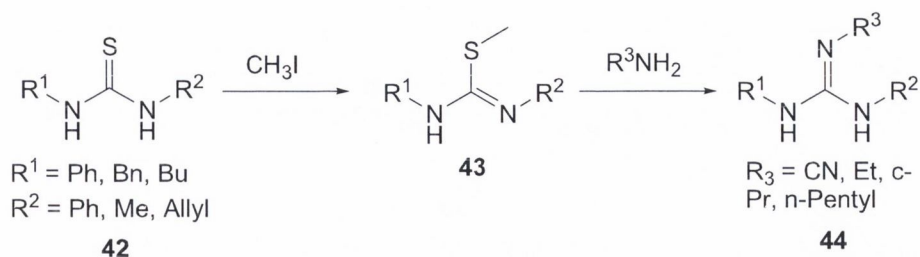


Scheme 2.7

Table 2.1.- Summary of Yields Obtained when varying Conditions (i) in Scheme 2.7

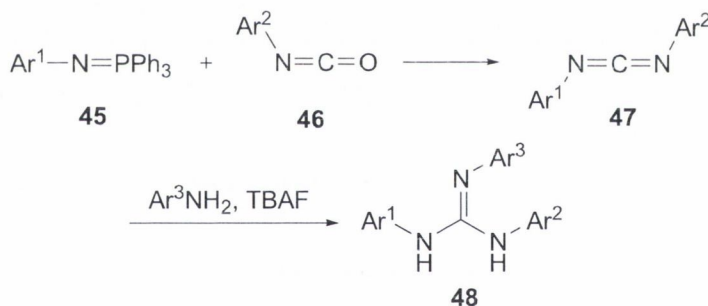
R ³ R ⁴ NH	Conditions	% Yield
	HgCl ₂ (1.1 eq), THF, Reflux	42
	HgCl ₂ (1.1 eq), Et ₃ N (2 eq), Tol, Reflux	37
	Hg(ClO ₄) ₂ (1.1 eq), Et ₃ N (2 eq), Tol, Reflux	62
	Ag(ClO ₄) ₂ (1.1 eq), Et ₃ N (2 eq), Tol, Reflux	46
	Hg(ClO ₄) ₂ (1.1 eq), Et ₃ N (2 eq), THF, Reflux	80
	HgCl ₂ (1.1 eq), Et ₃ N (2 eq), Tol, Reflux	>20
	Hg(ClO ₄) ₂ (1.1 eq), Et ₃ N (2 eq), Tol, Reflux	47
	HgCl ₂ (1.1 eq), Et ₃ N (1.5 eq), THF, Reflux	51
	Ag(ClO ₄) ₂ (1.1 eq), Et ₃ N (2 eq), Tol, Reflux	71
	Hg(ClO ₄) ₂ (1.1 eq), Et ₃ N (2 eq), THF, Reflux	93

Other guanidines have been obtained by reaction of a thiourea, **42**, with methyl iodide to first synthesize the S-methylisothiurea **43** before further reacting this fragment in the presence of amines (Scheme 2.8).^{128,129} The reaction produces the guanidines **44** in good yield (67 -77%) although the guanidines that have been synthesized to date are limited in their structure and are all tri-substituted.



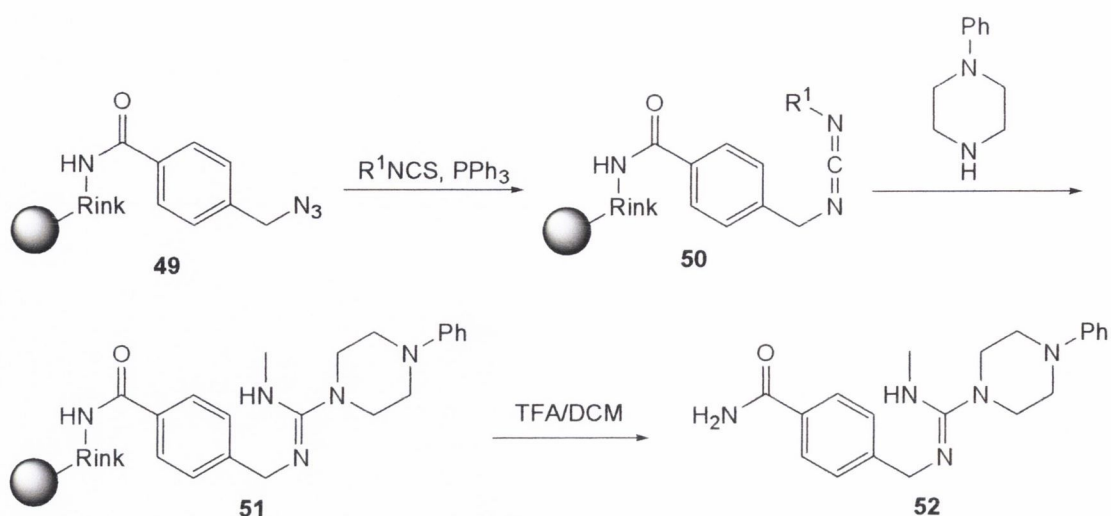
Scheme 2.8

As stated earlier in the preparation of guanidines, thioureas undergo a rearrangement to form a carbodiimide intermediate. Hence, it is not surprising that there has been recent research into synthesizing carbodiimides as precursors for the preparation of guanidines (although it has been limited to aromatic guanidine derivatives). Molina *et al.*¹³⁰ reacted *N*-aryliminophosphanes, **45**, with isocyanates, **46**, to form a *N*¹, *N*²-diarylcarbodiimide intermediate, **47**, which when treated with amines in the presence of one equivalent of tetra-*n*-butylammonium fluoride (TBAF) for ten minutes gave the desired guanidines, **48**, in good yield (52 – 80%, Scheme 2.9).



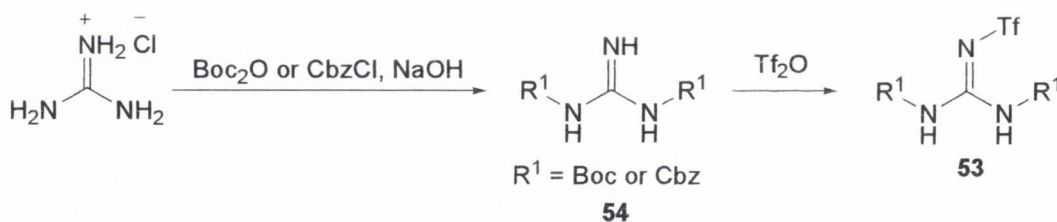
Scheme 2.9

An interesting solid phase synthesis using carbodiimides has been reported by Drewry *et al.*¹³¹ A *p*-bromomethyl benzoic acid is coupled to a rink extended macrocrown primary amine to give a *p*-bromomethylbenzamide. The *p*-bromomethylbenzamide then undergoes a nucleophilic displacement with azide to form an α -azido-*p*-toluamide, **49**, which when treated with triphenylphosphine and phenylisothiocyanate yields the carbodiimide, **50**. Reaction of **50** with *N*-phenylpiperazine gives a polymer bound guanidine, **51**, in a 63% yield (Scheme 2.10).



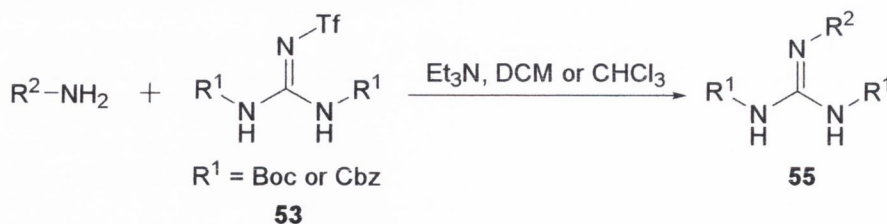
Scheme 2.10

Diprotected tritylguanidines, **53**, were first reported as guanylation reagents in 1998 by Feichtinger *et al.*^{132,133} The reaction of guanidine first with Boc-anhydride or Cbz-Cl to give a di-protected guanidine, **54**, and then with triflic anhydride give the desired diprotected tritylguanidines (Scheme 2.11).



Scheme 2.11

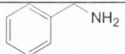
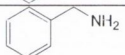
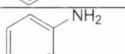
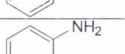
Feichtinger *et al.*^{132,133} reported the conversion of a variety of amines into their corresponding guanidines, **55**, through the use of the diprotected tritylguanidines (Scheme 2.12).



Scheme 2.12

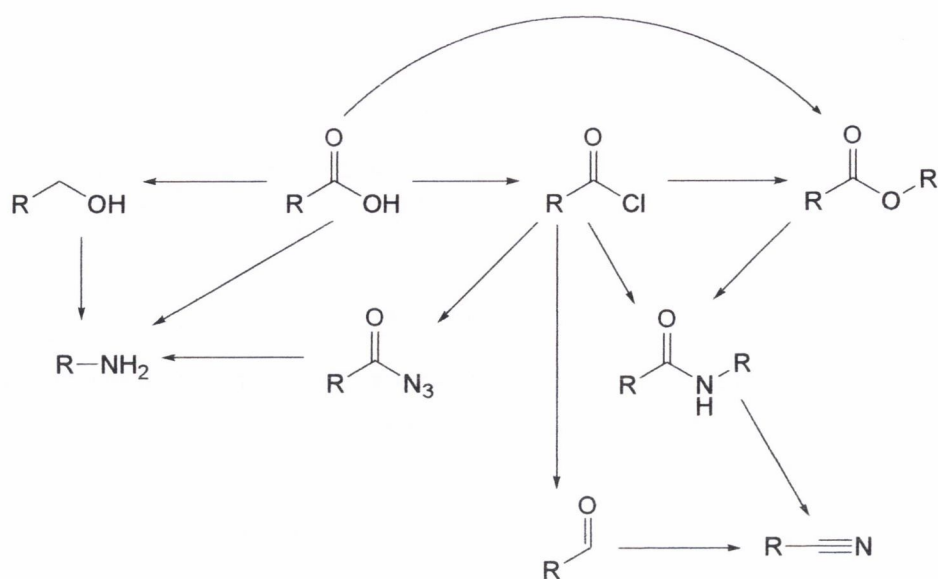
They reported that the reaction proceeds in good yield with polar and non-polar solvents, although higher yields were reported for non-polar solvents. It is believed that these guanylation reagents act as both electrophiles and weak acids. In the presence of polar solvents it is possible for the guanylation reagent to be deprotonated by the amine slowing the reaction down, to avoid this triethylamine was added. This resulted in a faster reaction time although the reaction remained slower than when carried out in non-polar solvents (benzene and acetonitrile) although this data was not provided (Table 2.2).

Table 2.2.- Summary of the yields of the Reactions in Scheme 2.12

Amine	Conditions	% Yield
	DCM, 0.5h, rt, R ¹ = Boc	100
	CHCl ₃ , 1h, rt, R ¹ = Cbz	94
	DCM, 0.5h, rt, R ¹ = Boc	99
	CHCl ₃ , 1h, rt, R ¹ = Cbz	98

2.3 Description of alkyl bis-guanidine syntheses

While these methods provided inspiration for the synthesis of guanidines we still did not have a viable long chain aliphatic starting material. Further search into potential commercially available long chain aliphatic compounds revealed that the corresponding dicarboxylic acids **27a-d** were available. This is very useful since carboxylic acids are one of the most versatile functional groups in organic chemistry, and can be converted into numerous other functional groups such as, alcohols, aldehydes (*via* reductions), esters, amides (*via* dehydration), amines (*via* the Curtius reaction) and even nitriles (Scheme 2.13).¹³⁴ Hence, we decided to use the commercially available dicarboxylic acids as our starting material.

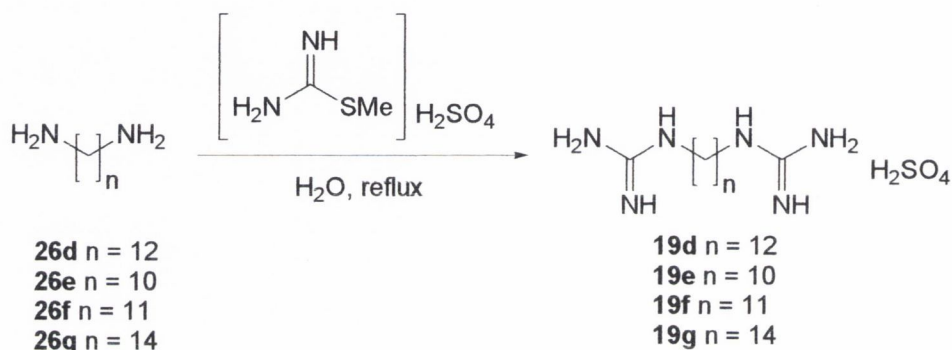


Scheme 2.13

(a) Route 1

As stated earlier in chapter 1 the alkyl *bis*-guanidines, **19a-d**, previously prepared by our group were synthesized via an S_N^2 reaction between aliphatic diamines, **26a-d**, and *S*-methylpseudothiourea. Using the same reaction conditions we decided to synthesize several other aliphatic *bis*-guanidines to investigate the effect of elongating the aliphatic linker chain on affinity towards I_2 -IBS and the selectivity towards I_2 -IBS over α_2 -ARs. As mentioned before the corresponding diamines were not commercially available, therefore, we decided to use the aliphatic dicarboxylic acids, **56a-d**. The dicarboxylic acids, **56a-d**, were converted into the alkyl diamines, **26d-g**, using a procedure reported by Wikberg et al.¹⁰⁶ who synthesized 2-phenylbicyclo[1.1.1]pentane from 2-phenylbicyclo[1.1.1]pentan-2-ol. The dicarboxylic acids, **56a-d**, were heated at reflux in the presence of concentrated sulphuric acid and sodium azide for two hours. The pH of the reaction mixture was then raised to 13, the mixture was filtered and the organic layer washed and dried to produce the desired alkyl diamines, **26d-g**, in good yield (Table 2.3).

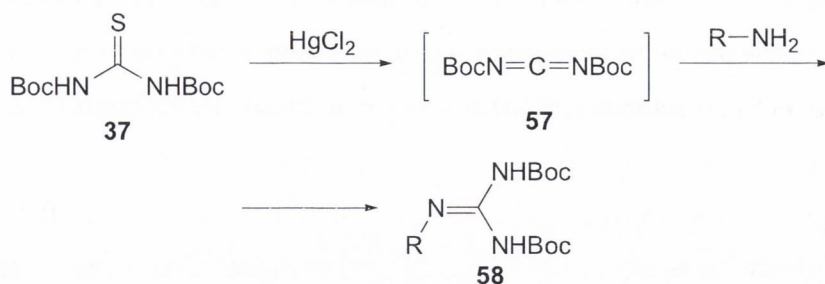
vary both the reaction time and the equivalents of *S*-methylpseudothiourea used. Refluxing the reaction for 20 h instead of 12 h increased the yield to 13% and further increases in the reflux time (48h) resulted in only a slightly higher yield of 14%. Varying the equivalents of *S*-methylpseudothiourea had a similar effect on the yield of the reaction. Using five equivalents of *S*-methylpseudothiourea gave a yield of 17% and increasing the equivalents of *S*-methylpseudothiourea further (to ten equivalents) lowered the yield to 11%.



Scheme 2.15

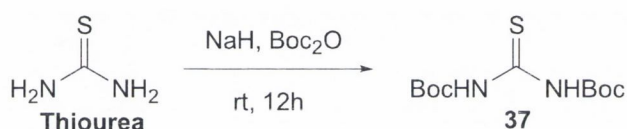
(b) Route 2

After the disappointing yields of the previous reactions we decided to explore other possible synthetic routes for the synthesis of the alkyl bis-guanidines, **19d-g**. The first of these routes was previously described for the synthesis of aromatic guanidines, **18a-d**, prepared by our group. Thus, a Boc-protected thiourea (**37**, Scheme 2.16) was reacted with a primary amine in the presence of mercury (II) chloride and a base. The reaction was originally reported by Kim *et al.*¹²³ who synthesized a series of guanidines from primary and secondary amines in good yields. They postulated that **37** forms a *bis*-Boc carbodiimide intermediate, **57**, which undergoes nucleophilic attack by the amines to form the corresponding *bis*-Boc-protected guanidine, **58** (Scheme 2.16).



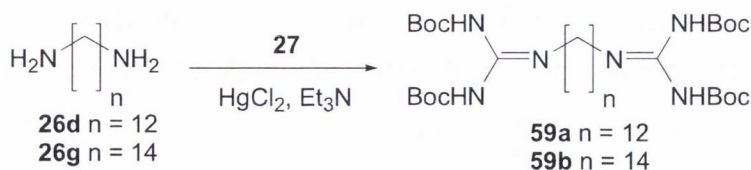
Scheme 2.16

Before attempting this reaction using the aliphatic diamines, **26d-g**, we needed to synthesize **37**. This was accomplished in a good yield (70%) by reacting thiourea with sodium hydride and Boc anhydride at room temperature overnight (Scheme 2.17).



Scheme 2.17

The primary alkyl diamines, **26d-g**, were prepared from the alkyl dicarboxylic acids, **27a-d**, as previously described. The aliphatic diamines, **26d-g**, were left to react with **37**, mercury (II) chloride and triethyl amine in an inert atmosphere for 12 hours at room temperature (Scheme 2.18). The product, an aliphatic *bis*-Boc protected *bis*-guanidine, **59a-b**, was purified by flash chromatography and isolated in good yield (Table 2.4). The best result was obtained for **59b**, which gave the aliphatic *bis*-Boc protected *bis*-guanidine in a yield of 83%.

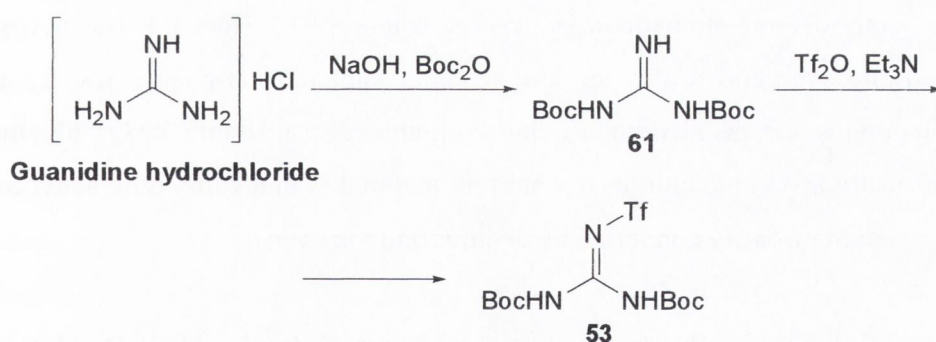


Scheme 2.18

(c) Route 3

After the success of the use of **37** for the synthesis of the alkyl *bis*-guanidines, **59a-b**, we decided to investigate a similar reaction that had been recently reported as a facile synthesis of guanidines in high yield. This reaction used a triflyl *bis*-Boc protected guanidine, **53**, as a replacement for the compound **37** and did not use any metal salts to promote the reaction. As discussed earlier, due to the presence of the triflate, the nitrogen carbon double bond is sufficiently weakened to allow a nucleophilic substitution using weak nucleophiles.

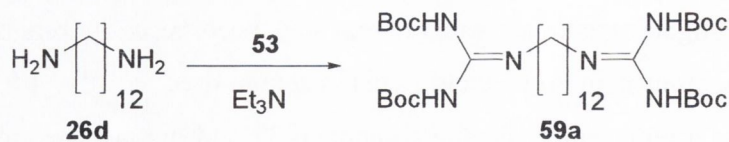
Compound **53** was easily prepared in two steps (Scheme 2.20). First, guanidine hydrochloride is dissolved in a solution of sodium hydroxide, dioxane and Boc anhydride and stirred at room temperature for 6 hours. This gave a *bis*-Boc-protected guanidine, **61**, in 60% yield (slightly higher than the reported value of 58% by Zapf *et al.*¹³⁵). Secondly, compound **61** was reacted with triflic anhydride for four hours while slowly bringing the temperature from -78°C to room temperature. The product was purified by flash chromatography to give **53** in 40% yield, much lower than the reported value of 88% by Feichtinger *et al.*^{132,133}



Scheme 2.20

After isolation compound **53** was reacted with the alkyl diamine, **26d**, in the presence of triethylamine at room temperature (Scheme 2.21). After seven days the starting material was still observed by thin layer chromatography. After the removal of the excess solvent and column chromatography the aliphatic guanidine, **59a**, was isolated but only in a 36%

yield. Even raising the temperature to 50°C the yield of the reaction was only marginally increased to 38%.



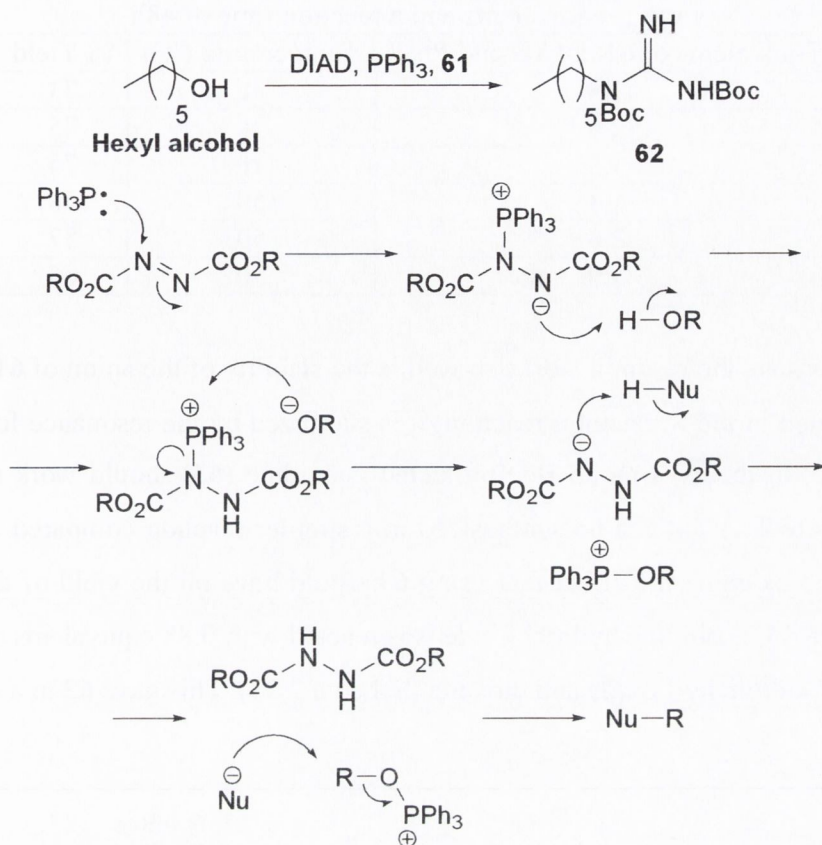
Scheme 2.21

Due to the poor yields obtained using this reaction scheme we did not prepare any other alkyl *bis*-guanidines using this route but decided to investigate other synthetic approaches.

(d) Route 4

In all the synthetic routes discussed so far the aliphatic *bis*-guanidines **19d-g** and **29a-c** were prepared from the alkyl dicarboxylic acids, **56a-d**. The major drawback with these commercial dicarboxylic acids is the limited number available. While the use of these carboxylic acids allowed us to complete the series of aliphatic *bis*-guanidines previously synthesized, we could neither prepare longer chain aliphatic *bis*-guanidines ($n > 14$) nor could we synthesize the aliphatic *bis*-guanidine where $n = 13$. Hence, it was necessary to further explore synthetic routes for longer chain aliphatic *bis*-guanidines. To prepare these compounds we decided to use the commercially available **hexyl alcohol**. The reason for using this compound as our starting material is that carboxylic acids and their derivatives could be easily converted to alcohols and vice versa.

The first synthesis we used was based on the procedure developed by Dodd *et al.* This synthesis was of interest because the guanidine could be prepared (without the need to synthesize the amine) by reaction, under Mitsunobu conditions, of an alcohol with **61**. Due to the uniqueness of the reaction we decided to experiment with different nucleophiles, temperature and equivalents of the reagents before attempting the reaction on the long chain aliphatic dicarboxylic acids.



Scheme 2.22

Initially, **hexyl alcohol** was reacted with 1.3 equivalents of **61**, DIAD and triphenylphosphine at room temperature in an inert atmosphere (Scheme 2.22). The reaction followed by tlc showed that the **hexyl alcohol** had completely reacted after 48 hours (44 hours longer than the reported reaction time). After purification by chromatography the yield of the aliphatic Boc protected guanidine, **62**, was calculated at 73%. Increasing the equivalents of the reagents (**61**, DIAD and triphenylphosphine) to 2.6 and 3.9 had little effect on the yield of the reaction (75% and 74%, respectively). Raising the temperature of the reaction to 50°C lowered the yield to 54% and 66% depending on the equivalents of the reagents used (Table 2.5).

Table 2.5.- Summary of the yields (%) of the reactions shown in Scheme 2.22 using various equivalents and a reaction time of 48h

Equivalents of 61 , DIAD and Ph ₃ P	Temperature (°C)	% Yield
1.3	rt	73
2.6	rt	75
3.9	rt	74
1.3	50	56
2.6	50	57
3.9	50	66

One of the reasons the reaction works so well is the stability of the anion of **61**. When the anion is formed in the Mitsunobu reaction, it is stabilized by the resonance forms shown in Figure 2.2. In theory a mono Boc protected guanidine (**63**) should work in a similar manner (Figure 2.2) and can be synthesized in a simpler reaction compared to **61**. Thus we decided to examine the effect that using **63** would have on the yield of the reaction. To synthesize **63**, guanidine hydrochloride was reacted with 0.88 equivalents of Boc₂O in a solution of sodium hydroxide and dioxane (Scheme 2.23). This gave **63** in a 49% yield.

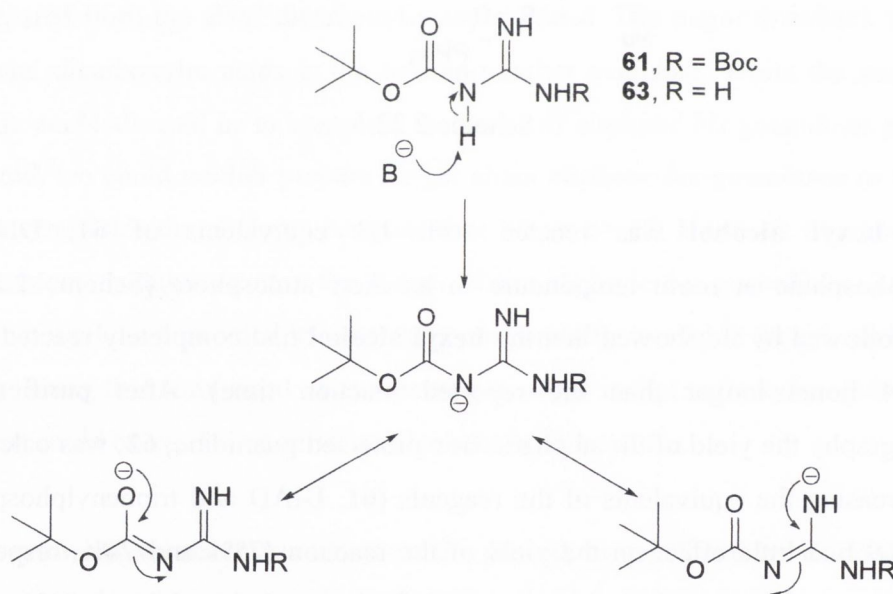
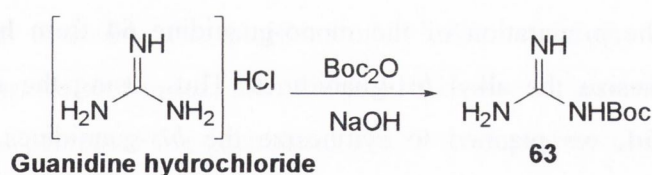
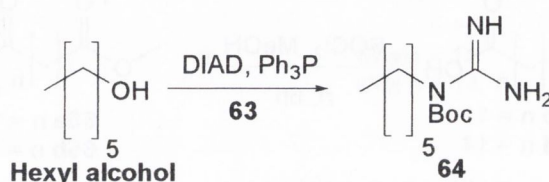


Figure 2.2.- Stability of **61** and **63**



Scheme 2.23

Replacing **61** with **63** and reacting the alcohol with 1.3 equivalents of the other reagents afforded the aliphatic mono-Boc protected guanidine, **64**, in 62% yield (Scheme 2.24).



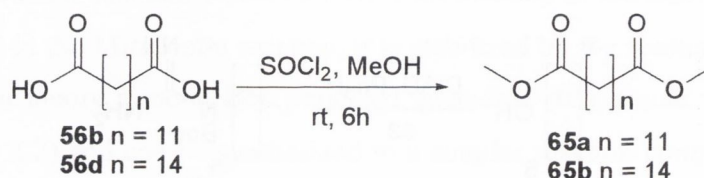
Scheme 2.24

The reaction of the alcohol with **63** at higher equivalents gives similar yields to those obtained for **61** (Table 2.6). When the reaction temperature was increased to 50°C the yields obtained remained similar to those obtained with **61** at room temperature but nearly 20% higher than those obtained with **61** at 50°C (Table 2.6). Based on these results there was no observable difference between using **61** or **63** at room temperature, and, thus, we decided to follow the original procedure and use **61** at 1.3 equivalents per functional group and at room temperature to synthesize the longer chain aliphatic *bis* guanidines.

Table 2.6.- Summary of the yields of the reactions shown in Scheme 2.24 using various equivalents and a reaction time of 48h

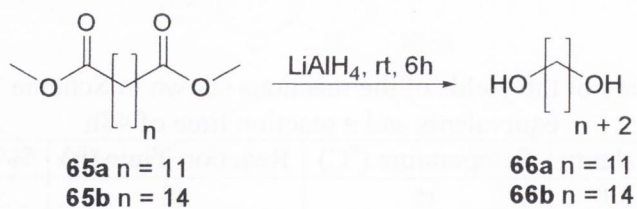
Equivalents	Temperature (°C)	Reaction Time (h)	% Yield
1.3	rt	48	62
2.6	rt	48	71
3.9	rt	48	73
1.3	50	48	77
2.6	50	48	75
3.9	50	48	56

After optimizing the preparation of the mono-guanidine **64** from **hexyl alcohol**, we proceeded to synthesize the alkyl *bis*-guanidines. Thus, using the alkyl dicarboxylic acids, **56b** and **56d**, we planned to synthesize the *bis*-guanidines with 13 and 16 methylene group linkers. In order to synthesize the aliphatic di-alcohols the carboxylic acids were first converted into the corresponding methyl esters, **65a-b**. This was accomplished by stirring the carboxylic acids, **56b** and **d**, in methanol at room temperature in the presence of thionyl chloride for six hours (Scheme 2.25).



Scheme 2.25

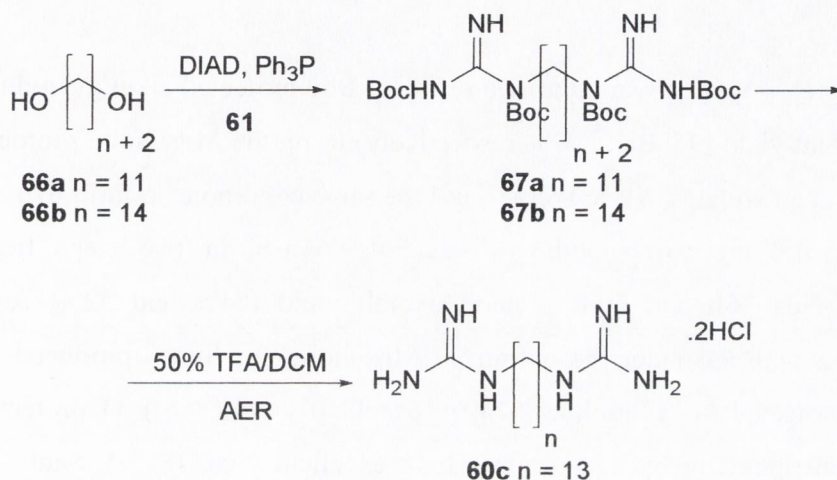
The alkyl *bis*-methyl esters, **65a-b**, were then reacted with lithium aluminium hydride at room temperature for six hours using tetrahydrofuran (THF) as solvent, producing the aliphatic di-alcohols, **66a-b**, in good yield (Scheme 2.26). Once the aliphatic di-alcohols, **66a-b**, were isolated and purified they were reacted with 2.6 equivalents of **61**, DIAD and PPh_3 at room temperature. The reaction, followed by tlc, showed complete disappearance of the aliphatic di-alcohol, **66a**, after eight days. The reaction work-up remained the same as for compound **62**.



Scheme 2.26

After purification by flash chromatography the corresponding alkyl bis-Boc protected guanidine, **67a**, was isolated in 75% yield. Unfortunately, the alkyl bis-Boc protected guanidine, **67b**, was obtained in a much lower yield and even after two weeks not all of

the di-alcohol had reacted. After purification by chromatography the alkyl bis-Boc-guanidine, **67b**, was isolated in less than 1% yield allowing for a partial characterization. The alkyl *bis*-Boc protected *bis*-guanidine, **67a**, was deprotected as discussed in the previous section giving the hydrochloride salt, **60c**, in an 85% yield. Based on this result the salt was isolated in an overall yield of 39% (Scheme 2.27).



Scheme 2.27

2.4 Summary and Conclusions

In order to synthesize the alkyl *bis*-guanidines, **19d-g**, and longer chain molecules of the same family, **60a-c**, we needed to find a long chain aliphatic series of compounds that could be used as precursors. The dicarboxylic acids, **56a-d**, satisfied this condition and were promptly converted into the primary aliphatic diamines, **26d-g**, in good yield (62 - 72%). Using the original procedure that was utilised to prepare the first alkyl *bis*-guanidines, **19a-d**, with these aliphatic diamines, **26d-g**, produced the corresponding alkyl *bis*-guanidines, **19d-g**, in low yield (11-17%).

Hence, we decided to investigate new potential routes. The first of these used a Boc protected thiourea, **37**, with mercury (II) chloride to produce two alkyl Boc protected *bis*-guanidines, **59a-b**, in good yield (65-83%), while the second route using a triflyl *bis*-Boc protected guanidine, **53**, was not as successful in synthesizing **59a** (36%) and so was not

used to synthesize other alkyl *bis*-guanidines. Deprotection of the alkyl Boc protected *bis*-guanidines, **59a-b**, was accomplished using TFA and an AER in good yield (70-75%). Neither of these two synthetic routes could be used to produce longer chain alkyl *bis*-guanidines due to the loss of two carbons in the synthesis of the diamines. To synthesize the longer chain alkyl *bis*-guanidines, **60a-c**, we first tested new procedures on hexyl alcohol.

The hexyl alcohol was converted to two different Boc protected alkyl guanidines, **62** and **64**, in excellent yield (75% and 77% respectively) using the Mitsunobu protocol and two Boc protected guanidines, **61** and **63**. To use the same conditions to form **67a** and **67b** we first synthesized the corresponding di-alcohols, **66a-b**, in two steps from the dicarboxylic acids **56b** and **56d** in good overall yield (54% and 52%, respectively). Reacting **66a** with **61** under the optimized Mitsunobu conditions produced the desired alkyl Boc protected *bis* guanidine, **67a**, in excellent yield (75%). Deprotection of **67a** gave the corresponding hydrochloride salt in excellent yield (85%). Sadly, **67b** could only be isolated in less than 1% yield.

In conclusion we have now synthesized four new alkyl *bis*-guanidines, **19e-f**, **29b-c**, using three separate syntheses. After the initial disappointment of using a well known S_N2 protocol with *S*-methylpseudothiourea we have optimized a procedure using mercury (II) chloride to synthesize long chain aliphatic Boc protected *bis*-guanidines, **59a-c**. We have also adapted a Mitsunobu protocol, previously used for small molecules, for the same purpose.

2.5 References

106. Wikberg, J. E. S.; Hudson, A. L. *Neurochem. Int.* **1996**, *30*, 1, 95.
110. Jakus, J.; Wolff, E. C.; Park, M. H.; Folk, J. E. *J. Biol. Chem.* **1993**, *268*, 13151.
111. Villarroya, M.; Gandia, L.; Lopez, M. G.; Garcia, A. G.; Cueto, S.; Garcia-Navio, J. L.; Alvarez-Builla, J. *Bioorg. Med. Chem.* **1996**, *8*, 1177.
112. Short, J. H.; Biermacher, U.; Dunnigan, D. A.; Leth, T. D. *J. Med. Chem.* **1963**, *6*, 275.
113. Katritzky, A. R., Rogovoy, B. V. *ARKIVOC*, **2005**, *iv*, 49.
114. Manimala, J. C., Anslyn, E. V. *Eur. J. Org. Chem.* **2002**, 3909.
115. Burgess, K., Chen, J. Solid Phase Synthesis of Guanidines, Solid Phase Organic Synthesis, Ed.; John Wiley & Sons, Inc., New York, 2000, p1-23.
116. Bosin, T. R.; Hanson, R. N.; Rodricks, J. V.; Simpson, R. A.; Rapoport, H. J. *Org. Chem.* **1973**, *38*, 1591.
117. Nagarajan, S.; Ho, T. L.; Du Bois, G. E. *Synth. Commun.* **1992**, *22*, 1191.
118. Stark, H.; Krause, M.; Arrang, J. M.; Ligneau, X. *Bioorg. Med. Chem. Lett.* **1994**, *4*, 2907.
119. Reddy, N. L.; Hu, L. Y.; Cotter, R. E.; Fischer, J. B.; Wong, W. J.; Mc Bumey, R. N.; Weber, E.; Holmes, D. L.; Wong, S. T.; Prasad, R.; Keana, J. F. W. *J. Med. Chem.* **1994**, *37*, 260.
120. Katritzky, A. R.; Parris, R. L.; Allin, S. M.; Steel, P. J. *Synth. Commun.* **1995**, *25*, 1173.
121. Ramadas, K., Srinivasan, N. *Tetrahedron Lett.* **1995**, *36*, 2841.
122. Yong, Y. F., Kowalski, J. A., Lipton, M. A. *J. Org. Chem.* **1997**, *62*, 1540.
123. Kim, K. S., Qian, L. *Tetrahedron Lett.* **1993**, *34*, 7677.
124. Levallet, C., Lerpiniere, J., Ko, S. Y. *Tetrahedron.* **1997**, *53*, 5291.
125. Dahmen, S., Brase, S. *Org. Lett.* **2000**, *2*, 3563.
126. Jirgensons, A., Kums, I., Kauss, V., Kalvins, I. *Synth. Commun.* **1997**, *27*, 315.
127. Kent, D. R., Cody, W. L., Doherty, A. M. *Tetrahedron Lett.* **1996**, *37*, 8711.

128. Rasmussen, C. R., Villani Jr., F. J., Reynolds, B. E., Plampin, J. N., Hood, A. R., Hecker, L. R., Nortey, S. O., Hanslin, A., Constanzo, M. J., Howse Jr., R. M., Molinari, A. J. *Synthesis*, **1988**, 460.
129. Chandrakumar, N. S. *Synth. Commun.* **1996**, *26*, 2613.
130. Molina, P.; Aller, E.; Lorenzo, A. *Synlett.* **2003**, 714.
131. Drewry, D. H.; Gerritz, S. W.; Linn, J. A.; *Tetrahedron Lett.* **1997**, *38*, 3377.
132. Feichtinger, K.; Zapf, C.; Sings, H. L.; Goodman, M. *J. Org. Chem.* **1998**, *63*, 3804 – 3905.
133. Feichtinger, K.; Sings, H. L.; Baker, T. J.; Matthews, K.; Goodman, M. *J. Org. Chem.* **1998**, *63*, 23, 8432.
134. Mackie R. K.; Smith, D. M.; Aitken, R. A. *Guidebook to Organic Synthesis*, Ed.; Pearson Education Ltd, Harlow, 1999, p22-23.
135. Zapf, C. W.; Creighton, C. J.; Tomioka, M.; Goodman, M. *Org. Lett.* **2001**, *3*, 1133.

Chapter 3

Synthesis of the alkyl bis-guanidino carbonyls

3.1 Introduction

After the synthesis of the alkyl *bis*-guanidines, **19e-f**, **60a-c**, the second family of ligands we planned to prepare were the alkyl *bis*-guanidino carbonyls, **23a-f**, (Figure 3.1). Just as the alkyl *bis*-guanidines, **19e-f**, **60a-c**, used a known I₂-IBS ligand as a prototype the alkyl *bis*-guanidino carbonyls, **23a-f**, are also based on a known I₂-IBS ligand. In this case the precursor was the ligand amiloride (Figure 3.1), which contains a modified guanidine functionality, the guanidino carbonyl group. Amiloride allows the two I₂-IBS subtypes, I_{2A}-IBS and I_{2B}-IBS, to be distinguished from one another. By incorporating the guanidino carbonyl moiety of amiloride onto the aliphatic linker chains of the alkyl *bis*-guanidines we had two aims. First, we wanted to investigate the effect of introducing the carbonyl moiety to the guanidine moiety on the affinity and selectivity of the ligands towards the I₂-IBS over the α_2 -ARs. Secondly, reduction of the carbonyl group could allow for the potential preparation of longer alkyl *bis*-guanidines.

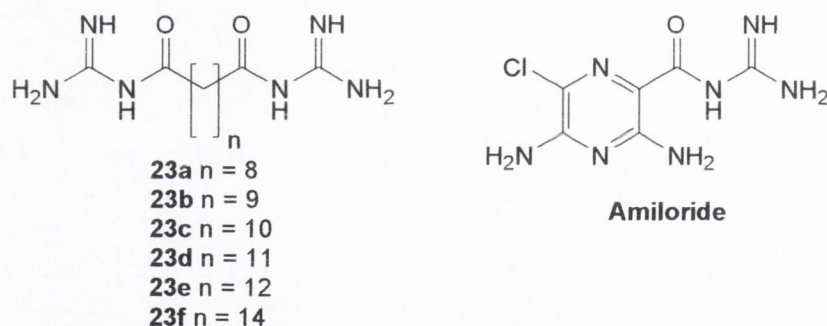


Figure 3.1.- The structures of the alkyl *bis*-guanidino carbonyls, **23a-f**, and amiloride

3.2 Existing synthetic routes for guanidino carbonyls

The guanidino carbonyl functional group consists of two separate moieties, the amide and amidine functionalities (Figure 3.2).

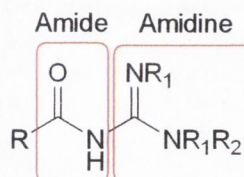
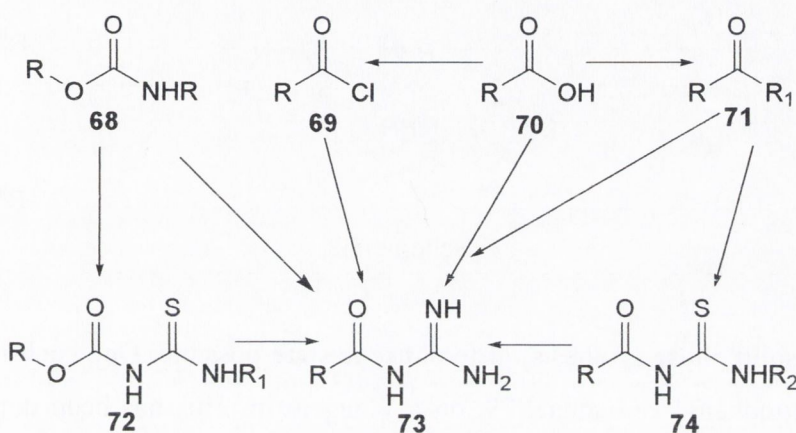


Figure 3.2.- The guanidino carbonyl functional group

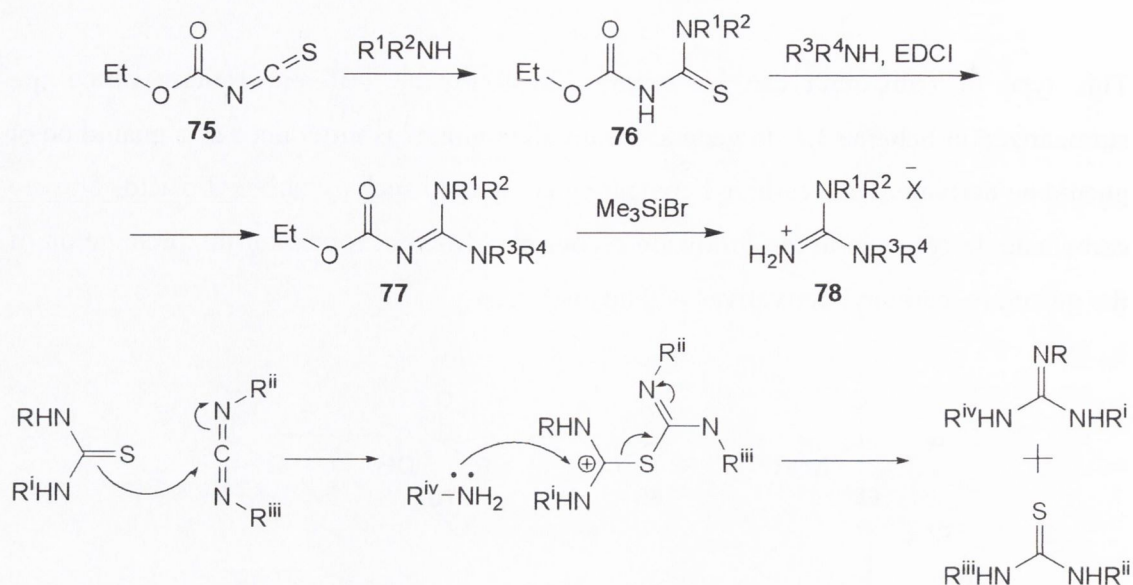
This type of compound can be synthesized following different routes, which are summarized in Scheme 3.1. In general the amidine moiety is introduced as a guanidine or guanidine derivative to a carbonyl containing compound such as carboxylic acids or even carbamate derivatives. In the following section the different routes for the preparation of the guanidino carbonyl derivatives will be discussed.



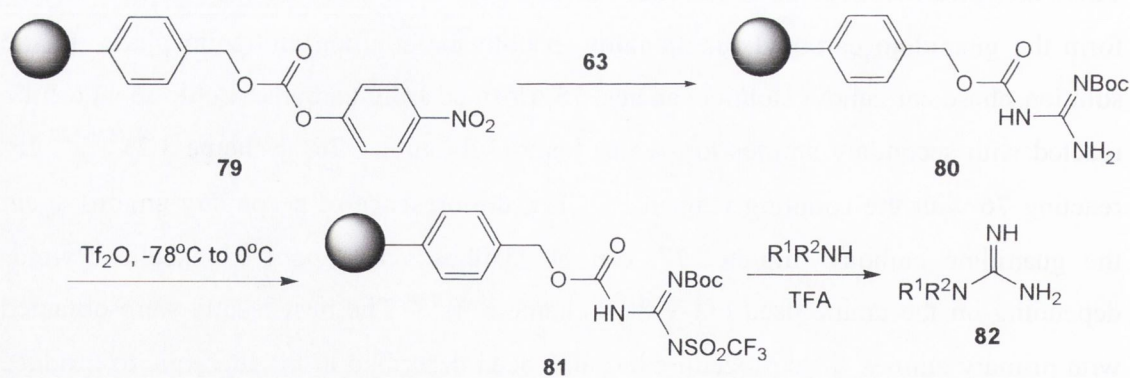
Scheme 3.1

(i) From carbamate derivatives

There are different methods to introduce the amidine moiety to carbamate derivatives to form the guanidino carbonyl functionality in both the solution and solid phase. In the solution phase carbamoyl isothiocyanates, **75**, (formed from carbamoyl chlorides) can be reacted with secondary amines to give carbamoyl thioureas, **76**, (Scheme 3.2).^{136,137} By reacting **76** with the coupling reagent EDCI in the presence of secondary amines again the guanidine carbonyl moiety, **77**, can be synthesized in poor to excellent yields depending on the amine used (34-99%, Scheme 3.2).¹³⁸ The best results were obtained with primary amines. This procedure has also been described in the literature to produce guanidines, **78**, in good yield (72-79%) by further reaction of **77** with Me_3SiBr (Scheme 3.2).¹³⁶⁻¹³⁸

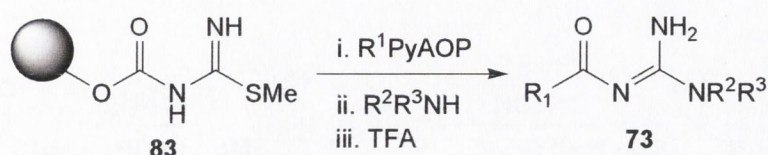


When using solid phase synthesis, different routes are possible. One such method is the use of a *p*-nitrophenyl carbamate, **79**, on a Wang resin. This has been demonstrated to react directly with **63** as shown in Scheme 3.3 to give a Boc protected guanidine containing the guanidino carbonyl moiety, **80**. The reaction of these compounds with triflate anhydride and further reaction with secondary amines gave the corresponding guanidines, **82**, with mixed results (33-100%, Scheme 3.3).¹³⁵



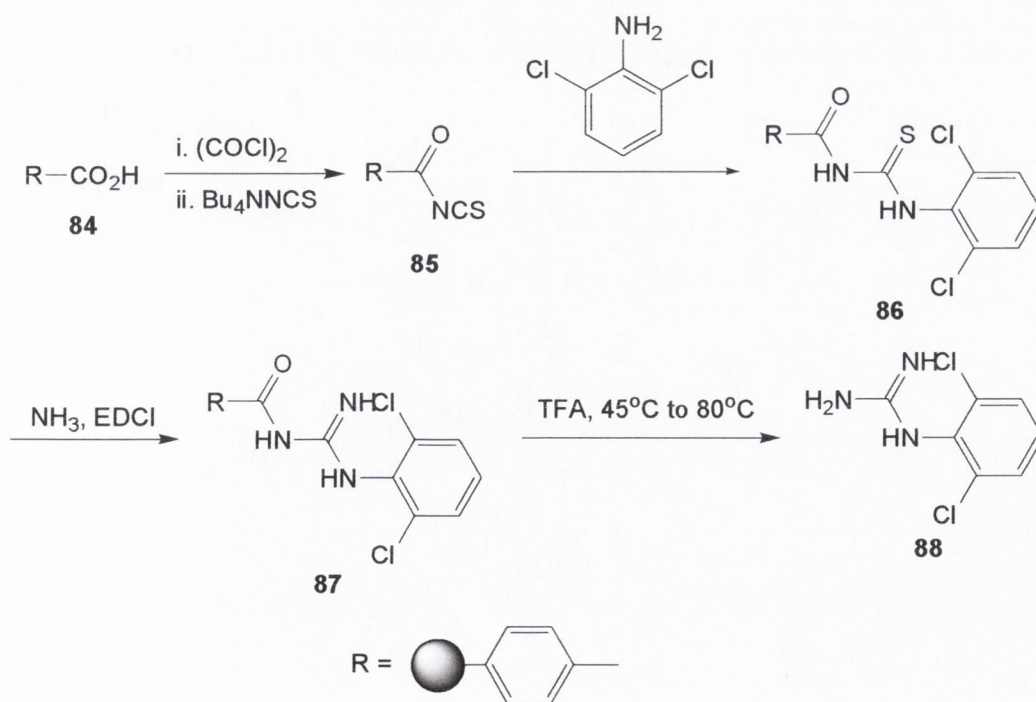
Carbamoyl pseudothioureas and coupling reagents have also been used in solid phase synthesis to produce guanidines containing the guanidino carbonyl moiety. The

carbamoyl pseudothiureas, **83**, can be reacted with a carboxylic acid, a coupling reagent, such as 7-axabenzotriazol-1-yloxytris(pyrrolidino)phosphonium hexafluorophosphate (PyAOP) or carbodiimide (CDI), and an amine to form the guanidino carbonyl compounds, **73** (Scheme 3.4).^{139,140}



Scheme 3.4

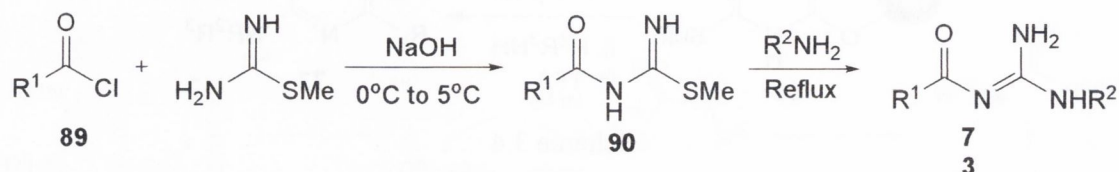
As well in solid phase and as stated previously carbamoyl isothiocyanates can be reacted to form carbamoyl thioureas, which can then be reacted to give guanidino carbonyl containing compounds. Recently Wilson *et al.*¹⁴¹ used acylisothiocyanates, **85**, to react with amines to give thioureas, **86**. Using EDCI as a coupling reagent they carried out the reaction of **86** with amines to give compounds containing the guanidino carbonyl group, **87**, which were further treated to yield the corresponding substituted guanidines, **88** (Scheme 3.5).



Scheme 3.5

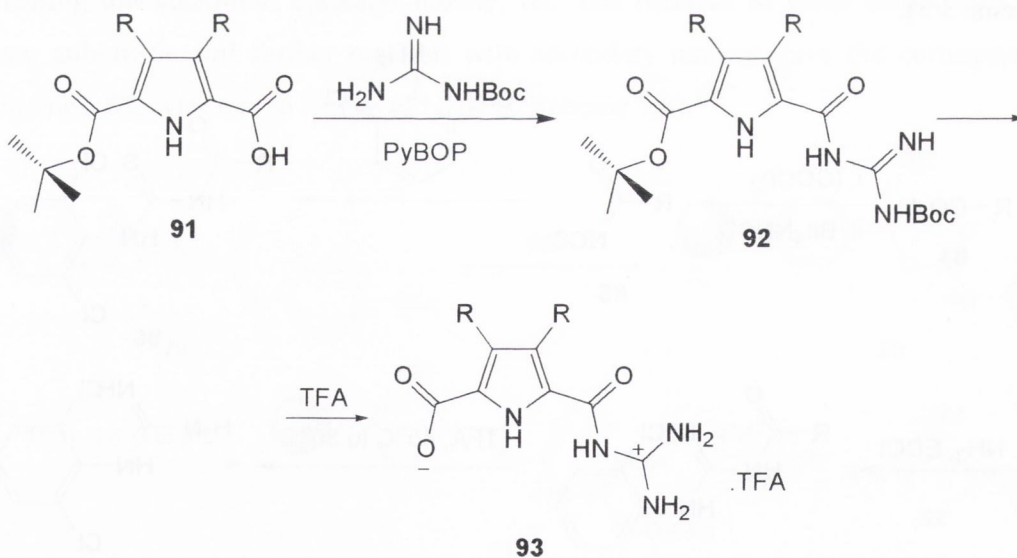
(ii) From carboxylic acid derivatives

Acyl chlorides, **89**, can react with S-methylisothiourea to give modified pseudothiureas, **90**. The pseudothiureas, as demonstrated in earlier sections, can be reacted with amines to give guanidino carbonyl compounds, **73** (Scheme 3.6).¹⁴²



Scheme 3.6

Carboxylic acids, **91**, have been used by Schmuck *et al.*^{143,144} to form guanidino carbonyl derivatives as pyrrole carboxylate zwitterions by using different coupling reagents. They performed the reaction of **91** with PyBOP to form an activated ester before further reaction of the ester with **63** to yield the guanidino carbonyl **92** (Scheme 3.7).

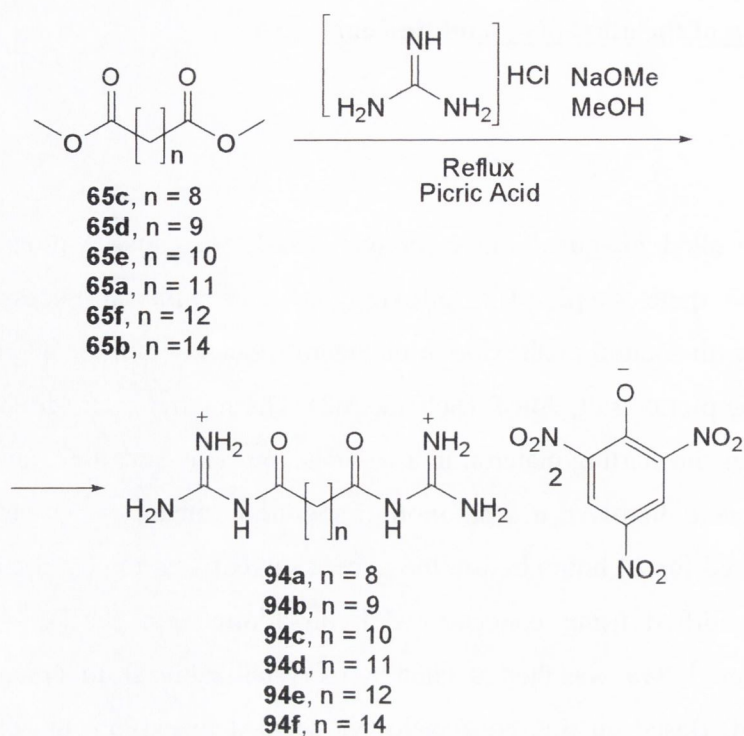


Scheme 3.7

3.3 Preparation of the alkyl *bis*-guanidino carbonyls

(a) Route 1

To prepare the alkyl *bis*-guanidino carbonyls, **23a-f**, we chose a procedure¹⁴⁵, which appeared to be quite simple. By refluxing an ester with an excess of guanidine hydrochloride with sodium methoxide in methanol we can obtain the alkyl *bis*-guanidino carbonyls as the picrate salt, **94a-f**, (Scheme 3.8). The methyl ester, dimethyl sebacate, **65c**, was used as the starting material in a test reaction. The ester, **65c**, and the guanidine hydrochloride were dissolved in a solution of sodium in methanol. The reaction mixture was then refluxed for 24 hours before the excess solvent was removed and the resulting residue was acidified using concentrated hydrochloric acid (HCl). The alkyl *bis*-guanidino carbonyl, **94a**, was then isolated by recrystallization from a picric acid solution in a 12% yield. Based on this poor yield we decided to explore the effect of adding different equivalents of HCl, with the results summarized in Table 3.1. It appears that a large excess of HCl should not affect the yield of the reaction, since the best yield (41%) was obtained when 75 equivalents of HCl were added. We then tried to improve the yield by varying the reflux time while using 75 equivalents of concentrated HCl. As can be seen from Table 3.1 the best result was obtained by refluxing for 72 hours. If the reaction was left to reflux for longer periods the yield was dramatically reduced. Once the reaction was optimized we attempted the preparation of longer chain derivatives.

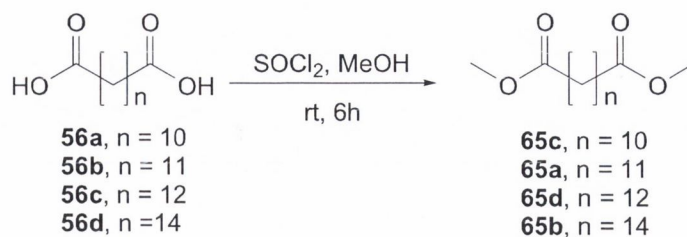


Scheme 3.8

Table 3.1.- Effect on Yield Based on Equivalents of HCl added in relation to the methyl ester and Reflux Time

Compound	Equivalents	Reflux Time	Yield (%)
94a	29	24	20
94a	44	24	30
94a	60	24	17
94a	75	24	41
94a	75	48	45
94a	75	72	80
94a	75	96	20
94a	75	120	12

Thus, we needed first to prepare the corresponding *bis*-methyl esters, **65a-f**, from their carboxylic acids. The carboxylic acids, **56a-d**, were converted into the *bis*-methyl esters in excellent yield by stirring in methanol at room temperature in the presence of thionyl chloride for six hours (Scheme 3.9, Table 3.2).



Scheme 3.9

Table 3.2.- Yield of Methyl Ester Formation from the Carboxylic Acids

Compound	Yield (%)
65a	86
65b	77
65e	91
65f	81

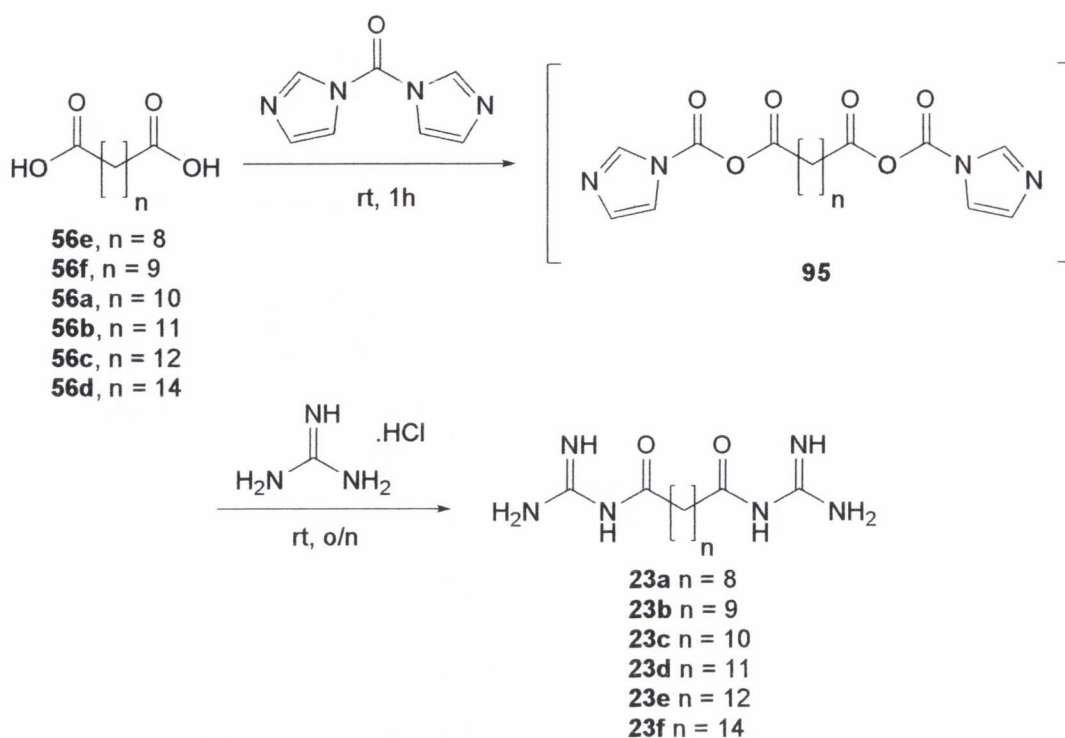
Once the methyl esters, **65a-f**, were synthesized we proceeded to prepare the guanidino carbonyl derivatives, **94a-f**, using the optimized conditions from Scheme 3.8. Regrettably, the yields obtained were very poor (Table 3.3). Due to these poor results we decided to explore other synthetic routes.

Table 3.3.- Yield for Compounds **94b-f** from Scheme 3.6

Compound	Percentage yield
94b	9
94c	17
94d	15
94e	11
94f	10

(b) Route 2

Hence, we decided to explore two separate routes in parallel. The first of these was originally used by Jansen *et al.*¹⁴⁶ when investigating structure activity relationships in sporangicin A. This reaction produces guanidino carbonyl derivatives in one step using the carboxylic acids as the starting material (Scheme 3.10).



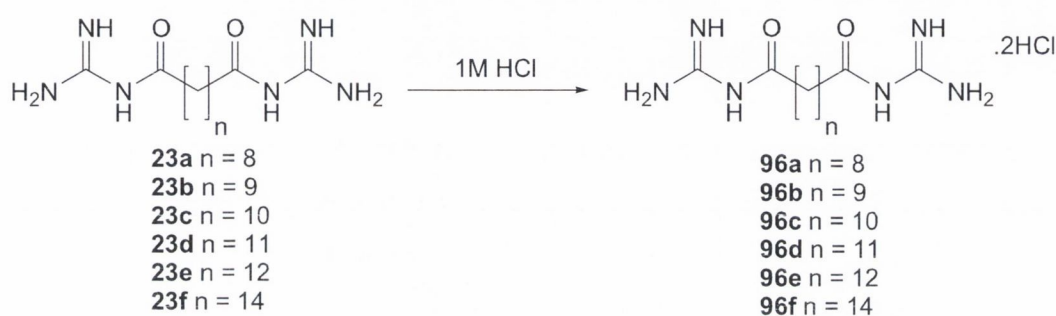
Scheme 3.10

The carboxylic acids, **56a-f**, are allowed to react with CDI for one hour at room temperature, forming the activated imidazolide. Using guanidine hydrochloride the guanidinylation takes place at room temperature overnight (Scheme 3.10). The reaction gave a moderate yield, firstly for **23a** and later for **23b-f** (Table 3.4).

Once we had isolated the alkyl *bis*-guanidino carbonyls, **23a-f**, the next step consisted in converting them into their corresponding salts, **96a-f**. In order to accomplish this we dissolved the alkyl *bis*-guanidino carbonyls, **23a-f**, in chloroform and washed it with 1M HCl (Scheme 3.12). The aqueous layer was separated and evaporated to dryness giving a white compound. ^1H NMR and Mass Spectrometry confirmed the presence of the HCl salt of the alkyl *bis*-guanidino carbonyl compounds, **96a-f**. Unfortunately this reaction did not produce the results we expected, with a large amount of the guanidino carbonyl still present in the organic layer. To deal with this, the guanidino carbonyl was re-dissolved in chloroform and washed several times with 1M HCl. The yields obtained were lower than expected and are summarized in Table 3.4.

Table 3.4.- Yield of reaction from Scheme 3.10 and Scheme 3.11

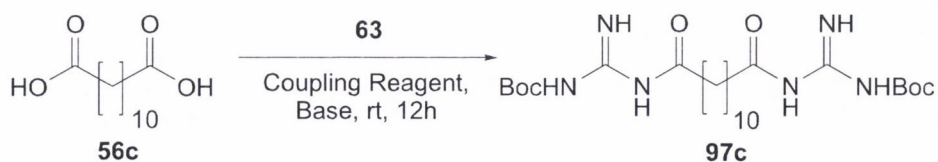
n =	Yield (%) of Formation of 23a-f	Yield (%) of Formation of the Hydrochloride Salts 96a-f	Overall Yield (%)
8	49	6	3
9	53	15	8
10	45	77	35
11	40	3	1
12	50	7	4
14	47	3	1



Scheme 3.11

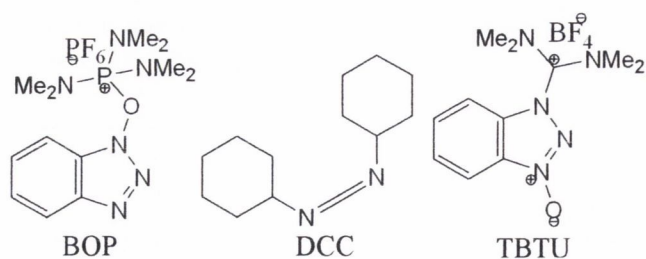
(c) Route 3

The other synthetic route, explored in parallel, was described by Schmcuk et al.^{143,144} who synthesized pyrrole carboxylate zwitterions. In this reaction the carboxylic acid is reacted with the mono Boc protected guanidine, **63**, and a coupling reagent, PyBOP, in the presence of a base to give the Boc protected guandino carbonyl, **97a-f**, at room temperature for 12 hours (Scheme 3.13).



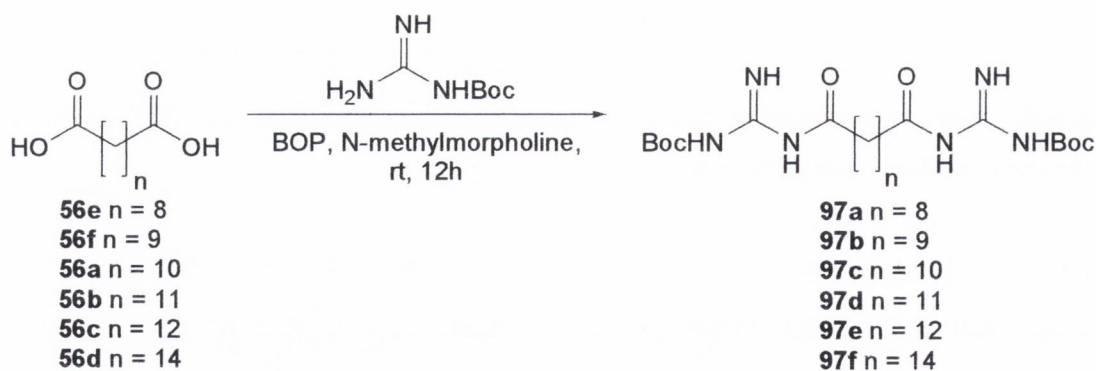
Scheme 3.12

Table 3.5.- Effect of Various Coupling Reagents and Bases on Scheme 3.13



Compounds	Coupling Reagent	Base	Percentage yield
97c	BOP	4-methylmorpholine	80
97c	DCC	Et ₃ N	-
97c	TBTU	Et ₃ N	77

The aliphatic dicarboxylic acids, **56a-f**, first react with the coupling reagent to form activated esters, which then undergo a substitution reaction with **63** to give the alkyl Boc protected *bis*-guanidino carbonyl derivatives, **97a-f**. We synthesized the compound, **97c**, initially using **63**, BOP, and N-methylmorpholine in an excellent yield of 80%. Using other coupling reagents such as DCC and TBTU did not improve the yield of the reaction (Table 3.5). Repeating the reaction using other carboxylic acids, BOP and N - methylmorpholine gave the alkyl Boc protected *bis*-guanidino carbonyls, **97a-f**, in good yield (Scheme 3.14, Table 3.6).

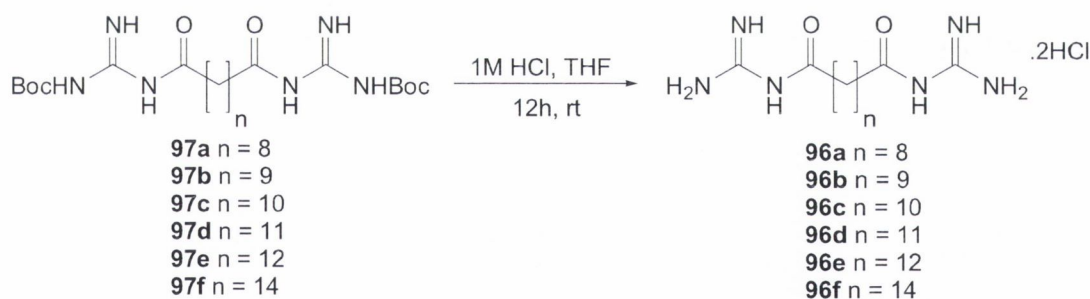


Scheme 3.13

Table 3.6.- Yield of Scheme 3.13 using BOP and 4-methylmorpholine

Compound	Yield (%)
97a	77
97b	62
97c	80
97d	85
97e	87
97f	63

Once the alkyl Boc protected *bis*-guanidino carbonyls, **97a-f**, were isolated we decided to explore different deprotection procedures to obtain the guanidino carbonyl salts directly. Firstly, to directly synthesize the hydrochloride salt we used 1M HCl, Scheme 3.14. The alkyl Boc protected *bis*-guanidino carbonyl derivative, **97c**, was left stirring in a mixture of THF and 1M HCl overnight. However, this only produced the hydrochloride salt, **96c**, in a low yield. In general, and for the rest of the compounds prepared, the overall yield from the alkyl dicarboxylic acids, **56a-f**, to the hydrochloride salts, **96a-f**, was very low (Table 3.7).

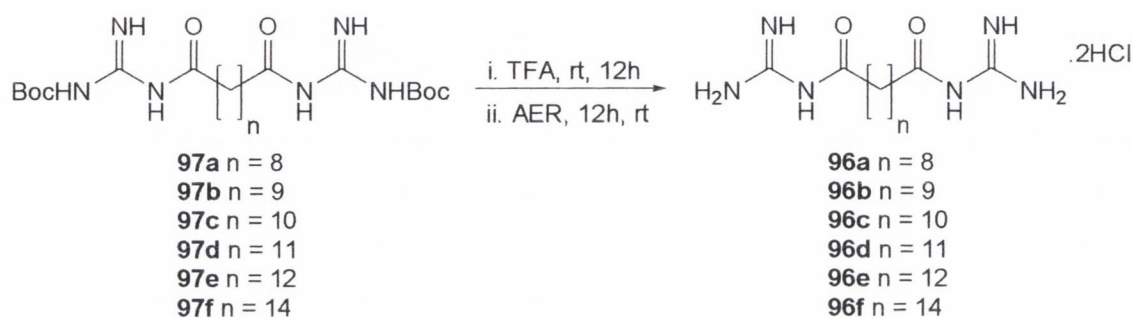


Scheme 3.14

Table 3.7.- Yield of Hydrochloride salts using Scheme 3.14 and overall yield of hydrochloride salts

Compounds	Yield (%) of Salt formation	Overall Yield (%)
96a	6	5
96b	15	9
96c	7	6
96d	3	3
96e	7	6
96f	3	2

The second synthesis used to form the alkyl *bis*-guanidino carbonyl salts, **96a-f**, involved deprotection with a 50% trifluoroacetic acid (TFA) solution in dichloromethane (DCM) followed by treatment of the salt with an anion exchange resin (AER, Scheme 3.15). The yields obtained for the hydrochloride salts prepared in this way were greatly improved compared to the previous deprotection method employed (Table 3.7 vs. Table 3.8). The overall yield of this synthesis from carboxylic acid to the hydrochloride salts proved to be quite high (Table 3.8).



Scheme 3.15

Table 3.8.- Yield of Hydrochloride salts using Scheme 3.15 and overall yield of Hydrochloride salts

Compounds	Yield (%) of Salt formation	Overall Yield (%)
96a	76	59
96b	65	40
96c	67	54
96d	71	60
96e	57	50
96f	63	40

3.4 Summary and conclusions

In summary, three separate methods were utilized to produce the alkyl *bis*-guanidino carbonyls, **23a-f**. The first procedure involved refluxing the alkyl *bis*-methyl esters, **65a-f**, with sodium methoxide and guanidine hydrochloride before isolation as the picrate salts, **94a-f**. This produced the alkyl *bis*-guanidino carbonyl picrate salts, **94a-f**, in very low yields with the exception of **94a**, which was isolated in 80%. Due to the poor results for this procedure new synthetic pathways were investigated.

In the next synthesis, the carboxylic acids, **56a-f**, were first reacted with CDI to form an activated ester intermediate that was not isolated. The intermediate was reacted *in situ* with guanidine hydrochloride to produce the alkyl *bis*-guanidines, **23a-f**, in moderate yield (40-53%). To form the alkyl *bis*-guanidino carbonyl salts, **96a-f**, the alkyl *bis*-guanidino carbonyls, **23a-f**, were washed with 1M HCl. The alkyl *bis*-guanidino carbonyl salts were isolated in poor yields (6-77%).

Finally, the carboxylic acids, **56a-f**, were reacted with the mono Boc protected guanidine, **63**, in the presence of a coupling reagent to produce the alkyl Boc-protected *bis*-guanidino carbonyls, **97a-f**, in excellent yield. Two methods were then employed to deprotect the alkyl *bis*-Boc-protected guanidino carbonyls, **97a-f**. First, the alkyl Boc-protected *bis*-guanidino carbonyls, **97a-f**, were washed with 1M HCl. This gave the alkyl *bis*-guanidino carbonyl salts, **96a-f**, in very low yield (3-15%). Second, the alkyl Boc-protected *bis*-guanidino carbonyls, **97a-f**, were deprotected with TFA before further treatment with an AER. This produced the alkyl *bis*-guanidino carbonyl salts, **96a-f**, in a good overall yield (40-60%).

We have now synthesized six new I₂-IBS Ligands. The conformational analysis and biological assays of the alkyl *bis*-guanidino carbonyls, **23a-f**, shall be discussed in chapters 5 and 6.

3.5 References

136. Poss, M. A.; Iwanowicz, E.; Reid, J. A.; Lin, J.; Gu, Z. *Tett. Lett.* **1992**, *33*, 5933.
137. Linton, B. R.; Carr, A. J.; Omer, B. P.; Hamilton, A. D. *J. Org. Chem.* **2000**, *65*, 1566.
138. Manimala, J. C.; Anslyn, E. V. *Tett. Lett.* **2002**, *43*, 565.
135. Zapf, C. W.; Creighton, C. J.; Tomioka, M.; Goodman, M. *Org. Lett.* **2001**, *3*, 1133.
139. Josey, J. A.; Tarlton, C. A.; Payne, C. E. *Tett. Lett.* **1998**, *39*, 5899.
140. Dodd, D. S.; Zhao, Y. *Tett. Lett.* **2001**, *42*, 1259.
141. Wilson, L. J.; Lin, M. *Tett. Lett.* **1999**, *40*, 3999.
142. Padmanabhan, S.; Lavin, R. C.; Thakker, P. M.; Durant, G. J. *Synth. Commun.* **2001**, *31*, 2491.
143. Schmuck, C. *Eur. J. Chem.* **2000**, *6*, 709.
144. Schmuck, C.; Weinard, W. *J. Am. Chem. Soc.* **2003**, *125*, 452.
145. Taylor, E. C.; Jacobi, P. A. *J. Am. Chem. Soc.* **1973**, *95*, 4455.
146. Jansen, R.; Schummer, D.; Holfe, G. *Liebigs. Ann. Chem.* **1990**, 975.

Chapter 4

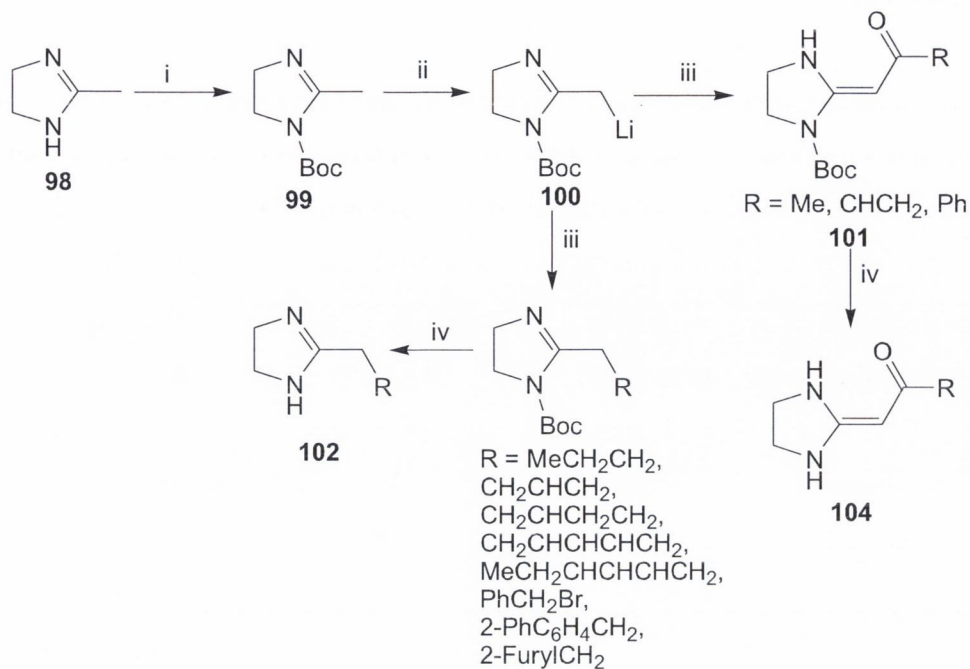
Synthesis of the alkyl bis-2- imidazolines and the alkyl bis- amidines

4.1 Introduction

In chapter one, the selectivity and affinity of two alkyl twin-type families was presented, the alkyl *bis*-guanidines, **19a-d**, and the alkyl *bis*-amino imidazolidines, **12a-d**. The alkyl *bis*-guanidines, **19a-d**, possessed higher affinity and better selectivity towards I₂-IBS over the α₂-ARs than the alkyl *bis*-amino imidazolidines, **12a-d**. The primary difference in the structure of the two families is the incorporation of two of the three nitrogen atoms into a five member ring. This difference in structure allowed us to begin to formulate a SAR, which, will be discussed in Chapter 6. To extend such a SAR we have to investigate the effect that the removal of the imine nitrogen of the 2-iminoimidazolidines, to give an alkyl *bis*-2-imidazoline would have on the I₂-IBS affinity and selectivity. Additionally, we have also examined the effect that the removal of the aliphatic five member rings of the alkyl *bis*-2-imidazolines, **24a-f**, yielding the alkyl *bis*-amidines, **25a-f**, would have on the I₂-IBS affinity and selectivity. These new ligands are based on the already known S14530, an aliphatic mono-2-imidazoline (pK_i I₂-IBS = 6.9, selectivity I₂-IBS/α₂-ARs = 110), and pentamidine, an aliphatic *bis*-amidine (pK_i I₂-IBS = 7.85). Before discussing our work on the synthesis of these families it is necessary to review existing synthetic routes towards imidazolines and then amidines.

4.2 General Synthesis of 2-Imidazolines

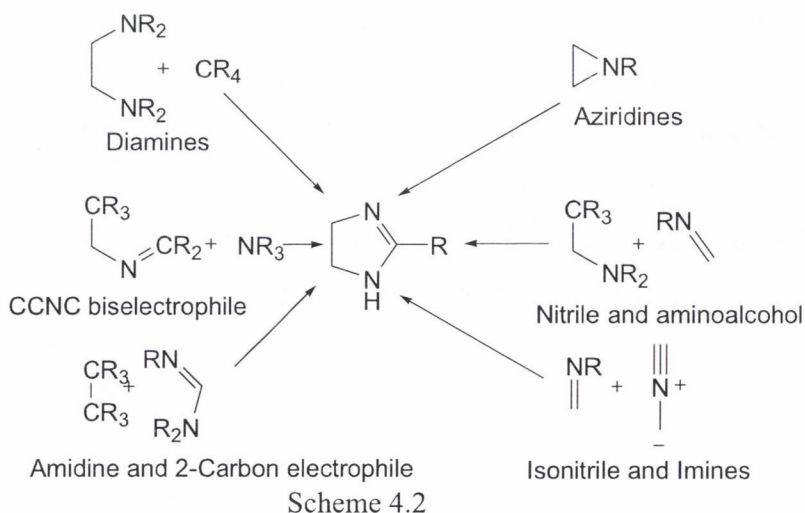
In general, incorporating a 2-imidazoline moiety into a compound can be accomplished two ways. The first method incorporates a complete imidazoline ring, **98**, onto a molecule and was devised by Jones *et al.*¹⁴⁷ They used *tert*-butoxycarbonyl as an N-1 protecting group before metallation of the α carbon, usually with Lithium, to give a lithio based imidazoline derivative, **100**. This derivative can then be reacted with a series of compounds to give 2-substituted imidazolines, **102**, **104** in good yield (67-87%, Scheme 4.1).



Regents: (i) Boc_2O , Et_3N , CH_2Cl_2 , 0 to 20°C ; (ii) sec-BuLi , THF, TMEDA, -78°C ; (iii) RHal , -78°C to 20°C ; (iv) TFA, 20°C

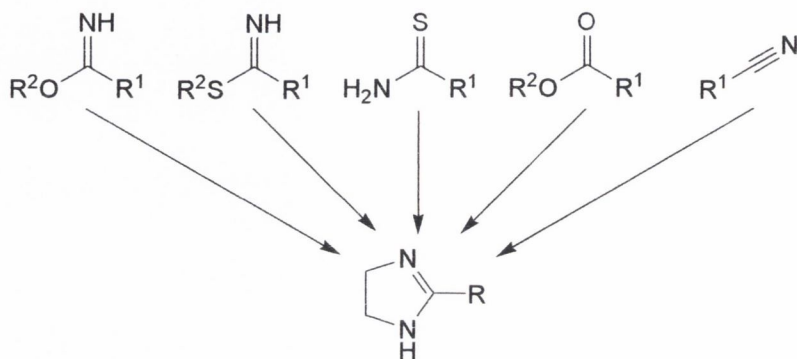
Scheme 4.1

The second method involves the synthesis of the imidazoline ring through a series of reactions between fragments, which provide specific parts of the ring (Scheme 4.2). For a more complete review of imidazoline synthesis one should consult the review of Grimmett *et al.*¹⁴⁸ In general there are eight methods to build the imidazoline ring and each is discussed briefly below.



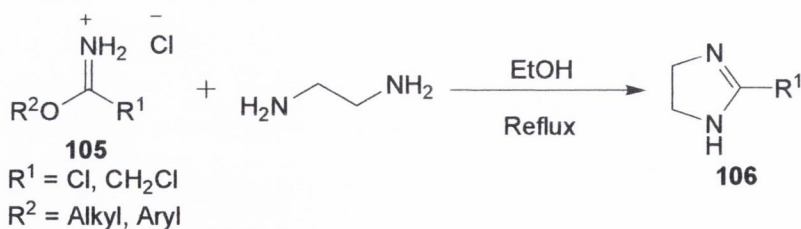
(i) Diamines and a one carbon fragment

There are several functional groups, which can be converted into 2-imidazolines using a diamine and a one carbon fragment these include imidic esters, thioimidates, carboxylic acid derivatives, thioester derivatives and nitriles (Scheme 4.3).



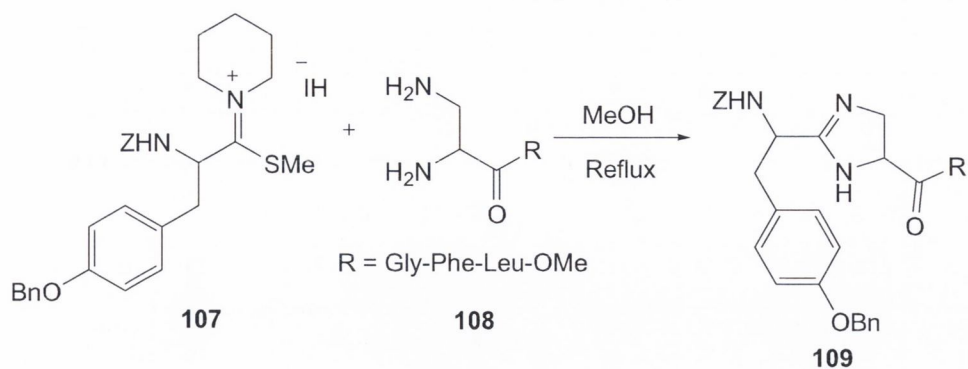
Scheme 4.3

Imidic esters were originally used by Pinner *et al.*¹⁴⁹, who reacted nitriles and alcohols in the presence of dry HCl to form imidate salts, **105**, which can then be reacted with ethylene diamine (EDA) to form the 2-imidazoline, **106** (Scheme 4.4). Other groups, including that of Klarer and Urech,¹⁵⁰ have used these syntheses to produce a 2-imidazoline moiety that can be introduced into other molecules similar to that of Jones *et al.*¹⁵¹



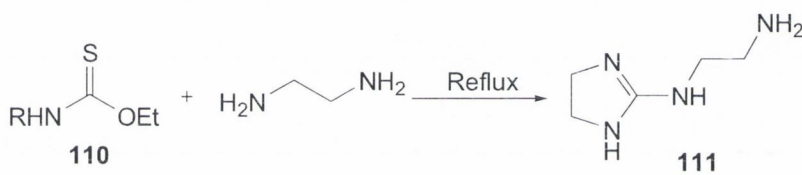
Scheme 4.4

Thioimidates, **107**, which can be easily prepared via *S*-alkylation of thioamides, can be condensed with diamines, **108**, to form imidazolines, **109** (Scheme 4.5).¹⁵²



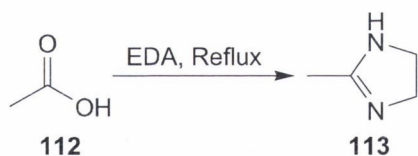
Scheme 4.5

The use of thioesters, **110**, as precursors for imidazolines, **111**, was a fortuitous discovery by Reynaud *et al.*¹⁵³ who was attempting to form iminoimidazolidines from EDA and *N*-substituted thiocarbamates (Scheme 4.6).



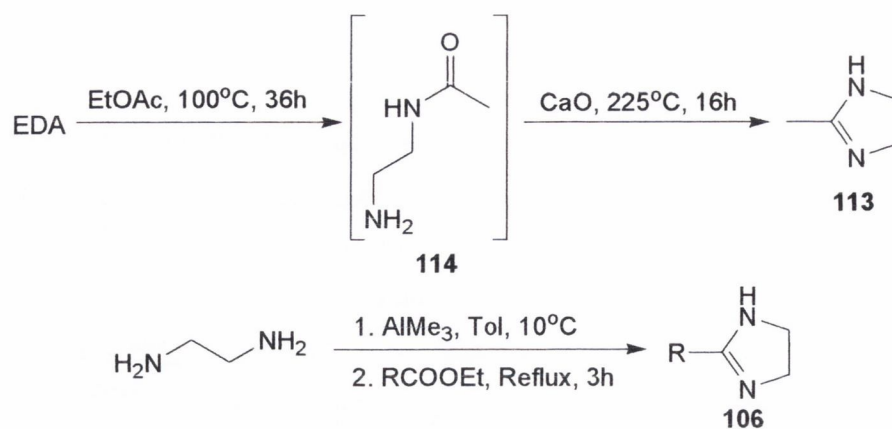
Scheme 4.6

Carboxylic acids, **112**, were first reacted with EDA by Chitwood and Reid to give 2-imidazolines, **113**, in a low yield (Scheme 4.7).¹⁵⁴



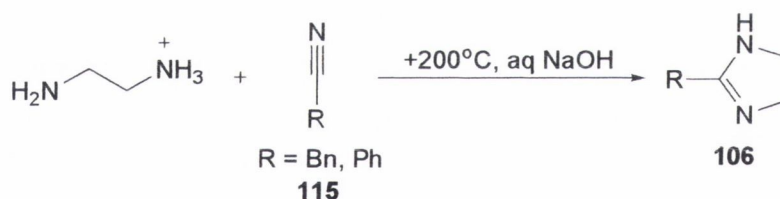
Scheme 4.7

Various ethyl esters have been reacted with different diamines in the presence of either calcium oxide or trimethylaluminium in order to form the imidazoline ring, **113**, as reported by Hill *et al.*¹⁵⁵ and Neef *et al.*¹⁵⁶, respectively (Scheme 4.8). Anastassiadou *et al.*⁹⁶ have also described the formation of 2-imidazolines, **106**, using trimethylaluminium.



Scheme 4.8

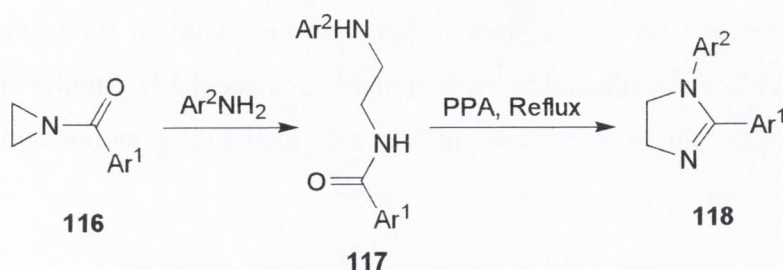
Nitriles, **115**, can be converted to imidazolines, **106**, in the presence of the sulphate of ethylenediamine as reported by Oxley *et al.*^{157,158} This reaction has provided the basis for several groups to repeat the process using a variety of methods to produce the amine salt, the most recent being Anastassiadou *et al.*⁹⁶ who used P_2S_5 to generate the amine salt (Scheme 4.9). In general moderate to good yields have been reported for this type of reaction (66-91%).



Scheme 4.9

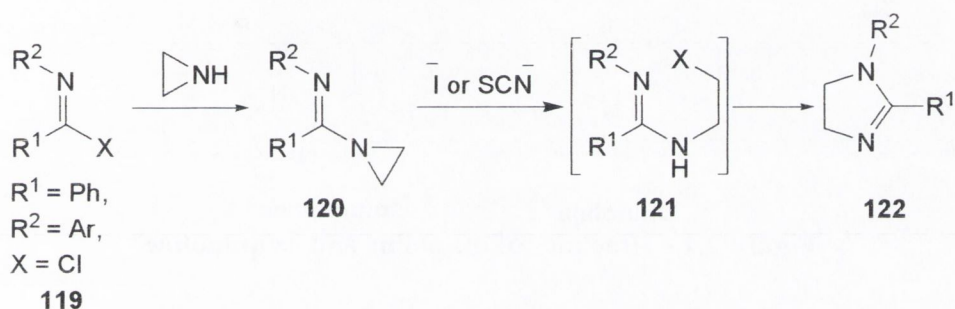
(ii) Aziridines

There are three distinct methods of synthesising 2-imidazolines from aziridines. In general the aziridine ring is opened and rearranges into the imidazoline and this can be accomplished in one of three methods. Wunsch *et al.*¹⁵⁹ reacted a series of *N*-acylaziridines, **116**, with anilines in the presence of polyphosphoric acid at high temperatures to obtain 2-imidazolines, **118**, in good yields (45-89%, Scheme 4.10).



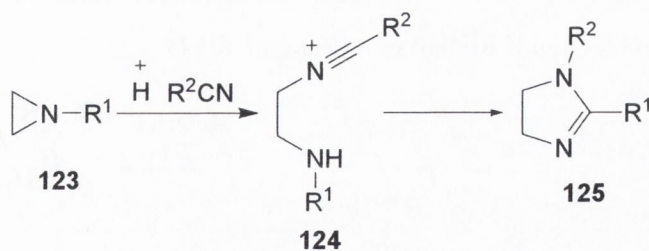
Scheme 4.10

Heine *et al.*¹⁶⁰ reacted aziridine with benzimidoyl chlorides, **119**, to form a substituted aziridine, **120**. This molecule then, when refluxed in the presence of iodine or thiocyanate ions rearranges into the imidazoline, **122** (Scheme 4.11).



Scheme 4.11

In a final method the aziridine ring is again opened to form a cation, which is trapped by a nitrile and undergoes subsequent cyclisation (Scheme 4.12).¹⁶¹



Scheme 4.12

(iii) Reaction of a Nitrile, Amide or Imidate with an Aminoalcohol Derivative

This reaction involves a cyclisation of an *N*-(2-haloethyl) amidine, **126**, which is formed via a 2,3-disconnection (Scheme 4.13). This type of reaction was first described by Stolle

*et al.*¹⁶² who reacted 2-bromoethylamine hydrobromide with an imidate ester, **127**, to obtain 2-phenyl-2-imidazoline, **125**, in low yield (Scheme 4.13). Similar style reactions have been used to synthesize various imidazolines, including quinoline and isoquinoline (Figure 4.1).^{163,164}

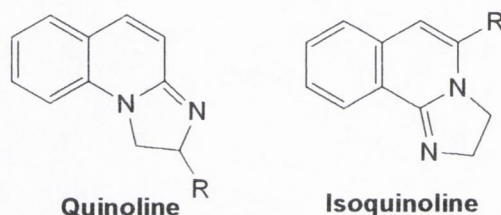
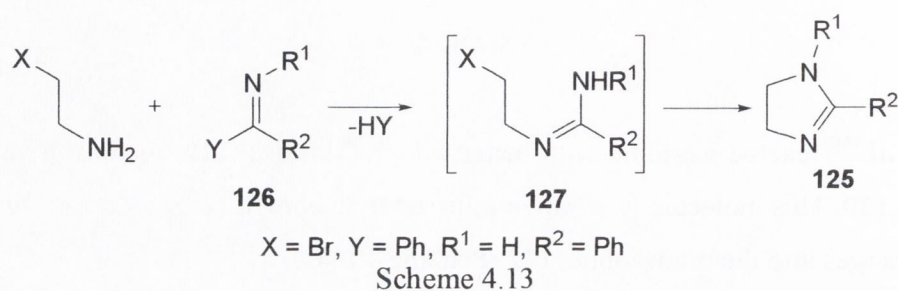
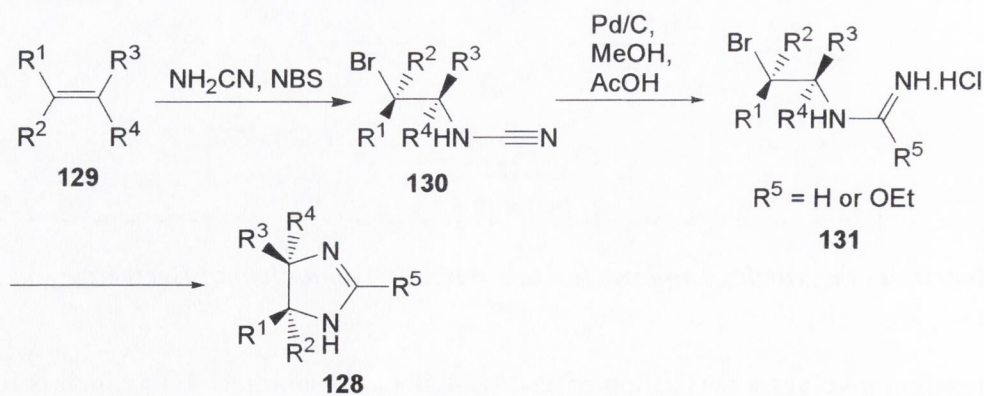


Figure 4.1.- Structures of **quinoline** and **isoquinoline**

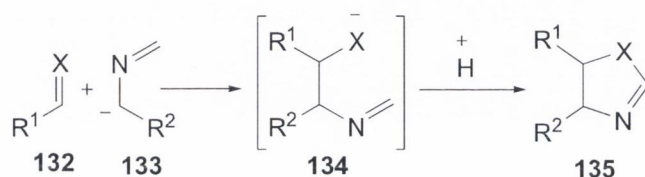
(iv) Amidines plus Two Carbon Electrophiles

Kohn *et al.*¹⁶⁵ prepared 4- and 5-substituted imidazolines, **128**, through the formation of nitriles from unactivated alkenes, **129**, cyanamide and *N*-bromosuccinimide (Scheme 4.14). Later work by Jung *et al.*¹⁶⁶ afforded the 2-imidazolines by reacting the *anti*-bromocyanamide adducts with weak bases (Scheme 4.14).



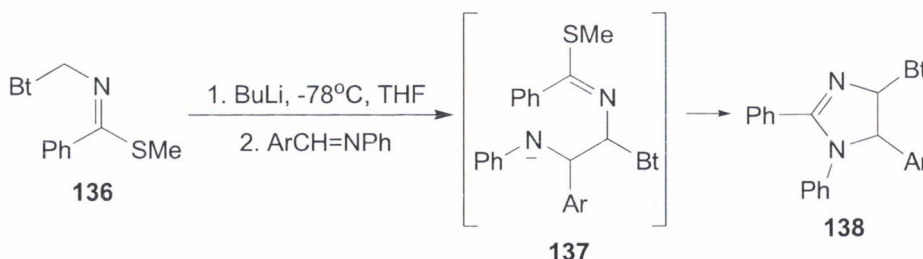
(v) Isonitriles and Imines

α -Methylated isocyanides, **132**, can react with polar double bonds, **133**, to form heterocycles as demonstrated by Schollkopf *et al.*¹⁶⁷ (Scheme 4.15). In general these reactions have been adapted to form 4- or 5-substituted imidazolines, **135**, with few 2-imidazolines formed following this method.¹⁶⁸⁻¹⁷⁰



Scheme 4.15

One of the few reactions to give 2-substituted imidazolines from imines, **136**, was reported by Katritzky *et al.*¹⁷⁰ who reacted diarylimines with benzotriazolyl methyl thioimidate (Scheme 4.16). Depending on the aromatic group used for the reaction the yield varies between 65% and 97%.

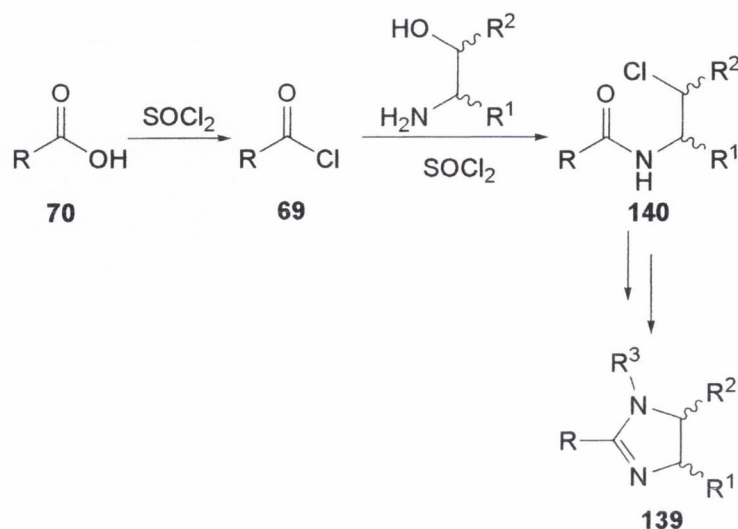


Scheme 4.16

(vi) CCNC biselectrophile

This method involves the formation of a CCNC fragment with two leaving groups. This fragment then undergoes a double substitution with an amine to give the desired 2-imidazoline (Scheme 4.17). This reaction was first described in 1949 by Partridge *et al.*¹⁷¹ as a one pot synthesis but had not been further developed until the group of Casey *et*

*al.*¹⁷² adopted the procedure and used it to synthesise chiral 2-, 4- and 5-substituted imidazolines, **139**, in moderate to good yield (47-90%, Scheme 4.17)



Scheme 4.17

4.3 Synthesis of the alkyl bis-2-imidazoline

(a) Route 1

Before synthesising the alkyl bis-imidazolines we decided to synthesize the imidazoline, **141**, (Figure 4.2) from the corresponding carboxylic acid, **142a**, or its corresponding acyl chloride, **142b** (Figure 4.2) using several different methods before optimizing the procedure for aliphatic compounds. The carboxylic acid structure possesses an aromatic group and is also partly aliphatic. The aromatic group would allow us to follow the reaction easily by tlc, thus, we believed that this molecule was an appropriate starting material for testing reaction conditions.

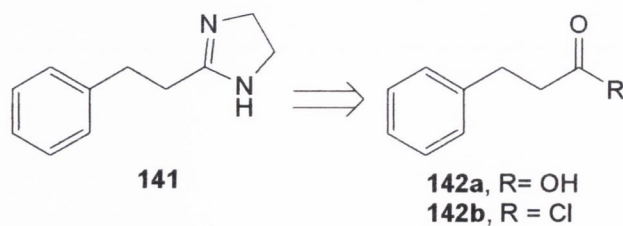
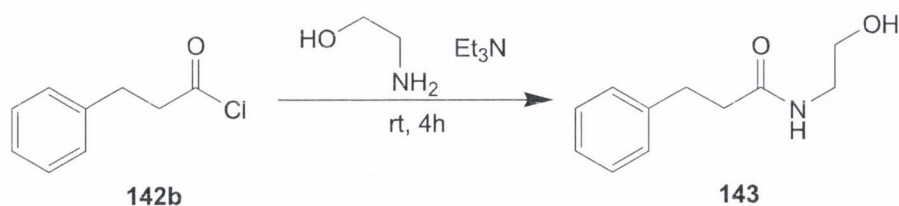


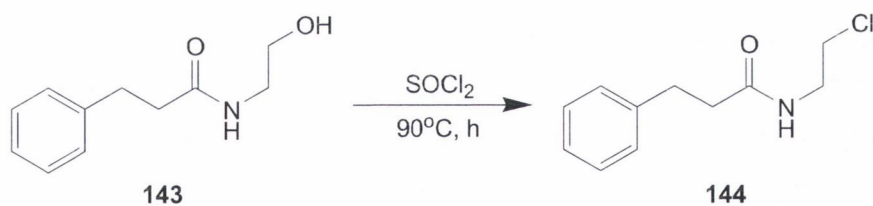
Figure 4.2.- Possible retrosynthetic analysis of **141**

The first attempt at synthesizing **141** utilised the method developed by Casey *et al.*¹⁷³ mentioned in the previous section. As can be seen from Scheme 4.17 the first step is the synthesis of an acyl chloride. The acyl chloride, **142b**, was commercially available and was purchased from Aldrich. **142b** then undergoes nucleophilic attack by ethanolamine in the presence of base to give the desired hydroxyethyl amide, **143**, (Scheme 4.18). The reaction takes place over four hours in good yield (63%) while leaving the reaction for longer times (12 hours) results in a lower yield (42%). One potential reason for this is the formation of the ester, which would require a longer reaction time than the amide reaction.



Scheme 4.18

Then, the hydroxyethylamide, **143**, is refluxed with thionyl chloride in DCM for six hours to produce the chloroethyl amide, **144**, (Scheme 4.19). **144** was isolated in moderate yield (52%).

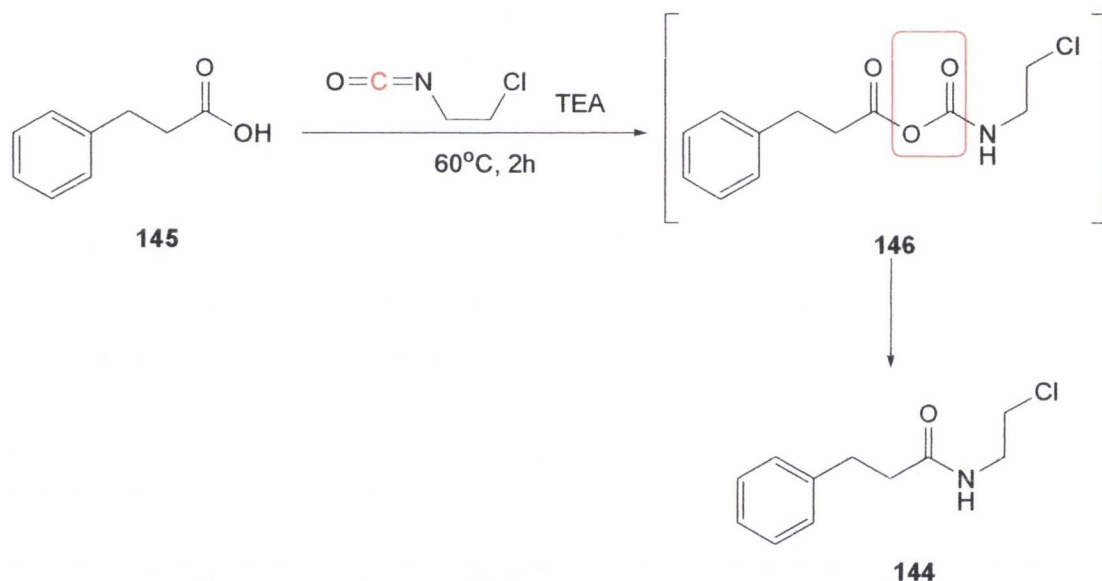


Scheme 4.19

This gave a yield of 32% over two steps, which is quite low. For this reason we decided to devise a different method to synthesize the chloroethyl amide.

While searching the literature for potential methods to synthesize the chloroethyl amide a novel procedure reported by Blagborough *et al.*¹⁷³ showed that carboxylic acids could be

reacted with isocyanates to give the corresponding amide. In fact Blagborough *et al.*¹⁷³ synthesized the chloroethyl amide, **144**, in good yield (73%). Due to this success we decided to attempt the same synthesis using their conditions. The carboxylic acid, **145**, 2-chloroethyl isocyanate and dry triethylamine in dry toluene were heated to 60°C for two hours. After the reaction mixture was cooled and excess solvent removed at reduced pressure, the chloroethyl amide, **144**, was isolated in a 95% yield (Scheme 4.20). Blagborough *et al.*¹⁷³ proposed the mixed anhydride as the intermediate, which undergoes decarboxylation to give the chloroethyl amide. The complete reaction mechanism has yet to be identified, although, it is known that the sp carbon of the isocyanate (marked in red, Scheme 4.20) is lost in the decarboxylation step.^{174,175}



Scheme 4.20

The final step in this reaction involves synthesizing an unstable chloroethyl imidoyl chloride intermediate, which then undergoes a double chlorine displacement to yield the 2-imidazoline. According to the original paper the formation of the chloroethyl imidoyl chloride, **147**, can be monitored by ¹H NMR and indeed this was the case with the N-H peak of the chloroethyl amide usually disappearing within ten minutes. Attempts to isolate **147** proved unsuccessful with only **144** isolated after the solvent was evaporated. In spite of this setback we decided to carry out the reaction between **147** *in situ* with the sources of nitrogen shown in Figure 4.3.

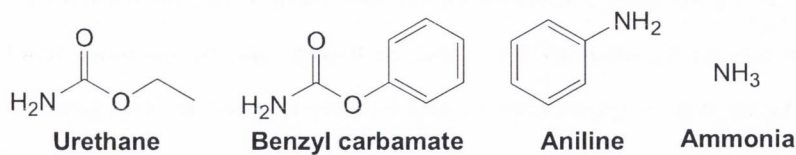
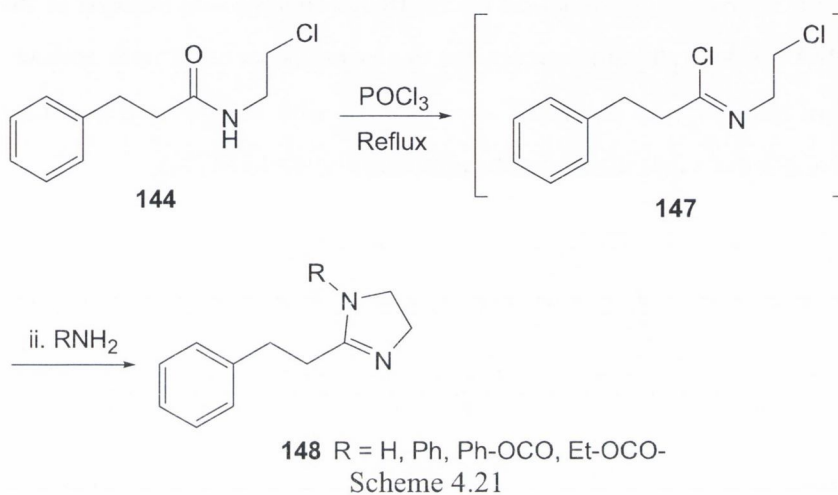


Figure 4.3.- Sources of nitrogen for Scheme 4.21



We first attempted to react both benzyl carbamate and urethane with the chloroethyl imidoyl chloride, **147** (intermediate formed in Scheme 4.21). We believed that the reaction if successful, would yield the imidazoline salts directly from cleavage of the carbamate bond using hydrochloric acid according to the procedure developed by Wijtmans *et al.*¹⁷⁶ Unfortunately, this reaction did not produce the expected results with no observable products being formed. This result is hardly surprising when one considers the stability of the amide bond in the molecule. This stability is due to the delocalisation of the lone pair of electrons on the nitrogen atom forming a partial double bond with the carbonyl carbon and putting a negative charge on the oxygen (Figure 4.4). This resonance means that the carbamates have low pK_a values of around 23 - 25.¹⁷⁷

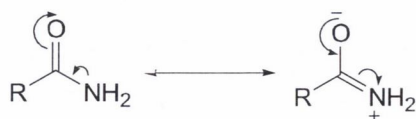


Figure 4.4.- Resonance forms of an amide

In light of these results we decided to use a more basic nitrogen containing compound in aniline, which has a pK_a value of 28¹⁷⁷ and, in theory, should be more reactive than both carbamates. Again the disappearance of the chloroethyl amide N-H peak in the ¹H NMR indicated the formation of **147**, after which a solution of the amine in chloroform was added dropwise. After the addition of the amine, the solution was refluxed for several hours. Through following the reaction by NMR no change was noticed in the spectra of the chloroethyl imidoyl chloride except for the peaks associated with aniline. This result was surprising based on the work of Casey *et al.*¹⁷² who synthesized a similar compound (Figure 4.5) using the same method although in a low yield (47%).

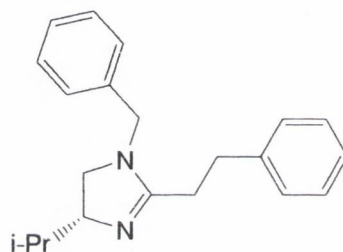


Figure 4.5.- Compound synthesized by Casey *et al.*¹⁷²

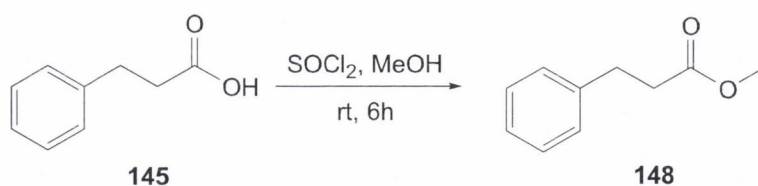
Finally, we decided to use ammonia as the source of nitrogen. Ammonia is the most basic of the four compounds shown in Figure 4.2 with a pK_a of 38.¹⁷⁷ Following the exact procedure used by Casey *et al.*¹⁷³, adding the chloroethyl imidoyl chloride dropwise to a solution of dry NH_3 in chloroform and using a basic workup after refluxing for several hours, failed to produce the desired imidazoline (Table 4.1). Repeated attempts to synthesize the imidazoline also resulted in disappointment, encouraging the exploration of alternative routes.

Table 4.1.- Effects of Various Chlorine Sources and Amine Sources on Imidazoline
Scheme 4.22

Chlorine Source	Temperature	Time	Amine	Temperature	Time
POCl ₃	Reflux	1h	Ph-NH ₂	0°C	12h
POCl ₃	Reflux	1h	Ph-NH ₂	rt	12h
POCl ₃	Reflux	1h	Ph-NH ₂	50 °C	12h
PCl ₅	Reflux	12h	Ph-NH ₂	rt	12h
PCl ₅	Reflux	10m	NH ₃	Reflux	12h
PCl ₅	Reflux	10m	NH ₃	Reflux	12h
PCl ₅	Reflux	10m	EtOCONH ₂	Reflux	12h
PCl ₅	Reflux	10m	EtOCONH ₂	Reflux	12h
PCl ₅	Reflux	10m	PhCH ₂ OCONH ₂	Reflux	12h

(b) Route 2

Anastassiadou *et al.*⁹⁶ reported the synthesis of aromatic 2-imidazolines from the corresponding ester using trimethylaluminium. We decided to test this method again using the carboxylic acid, **145**, as the starting point. This meant that the carboxylic acid would have to be converted into its corresponding ester, **148**. This was accomplished by reacting **145** with thionyl chloride in alcohol and stirring at room temperature for six hours (Scheme 4.22). **148** was synthesized good yield (90%).



Scheme 4.22

The second step in this synthetic route consists of forming a complex between the trimethylaluminium and ethylenediamine as shown in Figure 4.6. This complex can then be reacted with an ester to give the required 2-imidazoline (Scheme 4.23). Trimethylaluminium (2M solution in hexane) and ethylenediamine (1.5 equivalents of each) were added to a solution of dry toluene under an argon atmosphere at 0°C and allowed to stir at room temperature for 30 minutes. After this, **148** was added dropwise

before the reaction mixture was heated to 80°C for 12 hours. After the reaction was quenched by addition of methanol, water and chloroform the organic layers were separated dried and evaporated to give the 2-imidazoline as a white solid in good yield (50%).

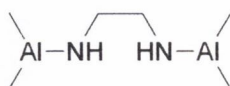
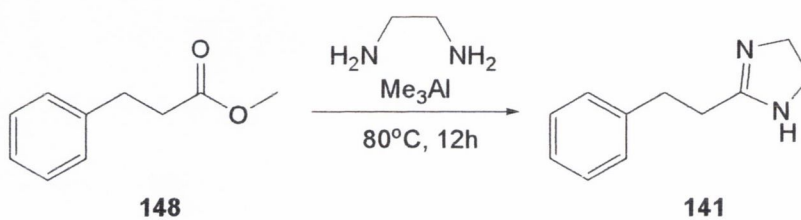


Figure 4.6.- Complex formed by trimethylaluminium and ethylene diamine



Scheme 4.23

Based on the initial success of this method we attempted to adapt the procedure for the synthesis of the alkyl bis-imidazolines, **25a-f**, using dimethyl sebacate, **65c**, (Figure 4.7) a commercially available aliphatic methyl ester.

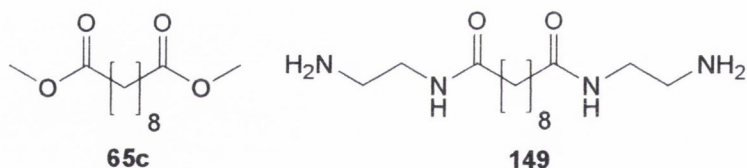


Figure 4.7.- Structure of **65c** and the amide intermediate, **149**, from Scheme 4.24

Initial results using three equivalents of trimethylaluminium and ethylene diamine and refluxing for 12 hours at 120°C gave the starting methyl ester (S.M. in Table 4.2). Based on this result we refluxed the reaction for longer periods but always with similar results except where the reaction was refluxed for 60h, where a second compound was identified from the ¹H NMR (Table 4.2). We believed this second compound was the open chain amide, **149**, shown in Figure 4.7 (A in Table 4.2). Since refluxing the reaction for longer periods of time did not improve the results of the reaction we began to experiment with

the equivalents of the trimethylaluminium and ethylenediamine and the temperature. Refluxing the reaction at 120°C for 40 hours using six equivalents of trimethylaluminium and three equivalents of ethylenediamine primarily gave **149** as the product. Heating the reaction at a lower temperature (90°C) for only one hour using the same equivalents (1:3:6, ester: EDA: Me₃Al) gave a mixture of the alkyl bis-imidazoline, **24a**, (I in Table 4.2) and starting methyl ester, **65c**. We then decided to further increase the equivalents of the EDA and Me₃Al to five and ten, respectively and to reflux the reaction for 20 hours. The result of this reaction yielded both the amide, **149**, and the alkyl *bis*-2-imidazoline, **24a**, as products. This indicated that the formation of the amide, **149**, was based on reflux time and equivalents. Heating the reaction for two and a half hours at 90°C with a ratio of 1:3:6 (ester: EDA: Me₃Al) again gave a mixture of the starting methyl ester, **65c**, and alkyl bis-imidazoline, **24a**. However, using the same conditions with a ratio of 1:5:10 (ester: EDA: Me₃Al) gave the alkyl *bis*-2-imidazoline, **24a**, exclusively in a high yield of 77%.

Table 4.2.- Summary of the effects of reflux time, temperature, equivalents of reagents and the products observed from ¹H NMR using dimethyl sebacate as the ester*

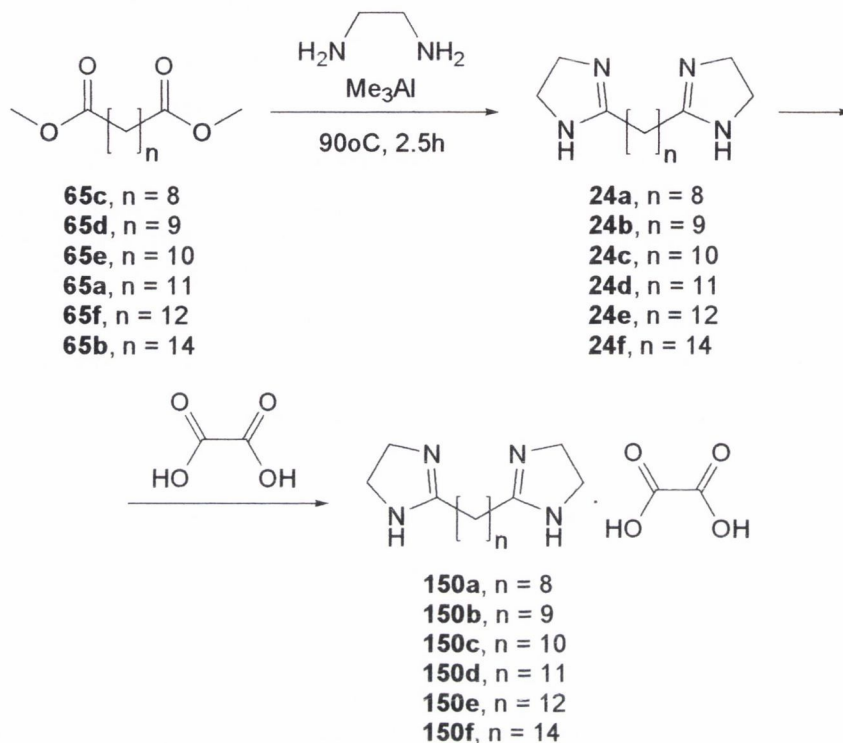
Equivalents of Ester	Equivalents of EDA	Equivalents of Me ₃ Al	Temperature °C	Time (h)	Products Identified [§]
1	3	3	120	44	S.M
1	3	3	120	60	S.M/A
1	3	6	120	40	A
1	3	6	90	1	I/S.M
1	5	10	90	20	I/A
1	3	6	90	2.5	I/S.M
1	5	10	90	2.5	I

* Reactions performed in conjunction with Grainne Gallwey

[§] S.M. = Starting Material, A = Amide, I = Alkyl *bis*-2-imidazoline

Based on the success of this reaction, we reacted different alkyl bis-methyl esters, **65a-b,d-f**, using the same conditions as the optimised reaction with **65c** (Scheme 4.24). The alkyl *bis*-2-imidazolines, **24b-f**, were again obtained in good yield (Table 4.3). However, the yield decreased as the length of the methylene chain increased. To synthesize the salts for biological testing the alkyl *bis*-2-imidazolines, **24a-f**, was dissolved in small amount of an oxalic acid solution (0.875M), after which the solution was evaporated down to

dryness to give the alkyl bis-2-imidazoline salts, **150a-f**, as white compounds in excellent yield (Table 4.3, Scheme 4.24).



Scheme 4.24

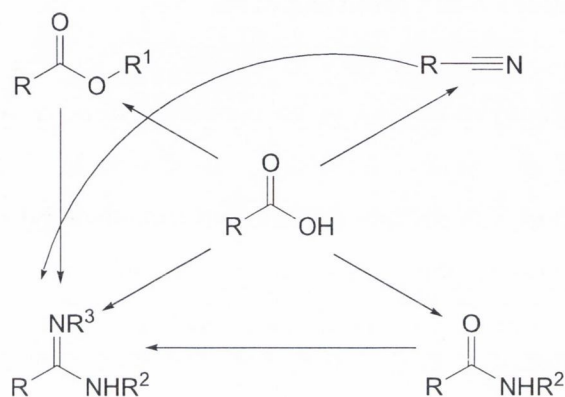
Table 4.3.- Average Percentage Yield of the conversion of esters into the corresponding *bis*-imidazolines and subsequent conversion to their corresponding salts.

n	Yield (%) of alkyl <i>bis</i> -2-imidazoline Formation 24a-f	Yield (%) of the alkyl <i>bis</i> -2-imidazoline Salt Formation 150a-f
8	77	91
9	26	78
10	64	83
11	39	93
12	45	86
14	45	91

4.4 General Synthesis of Amidines

As stated at the beginning of this chapter we wished to examine the effect that removal of the five member ring would have on the affinity towards the I₂-IBS. Before we began to

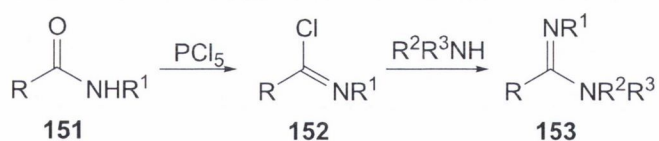
synthesis the alkyl bis-amidines we investigated potential synthetic routes to be found in the literature. We found that amidines are generally synthesized in multistep reactions from a variety of starting materials including amides, carboxylic acids, esters and nitriles (Scheme 4.25).



Scheme 4.25

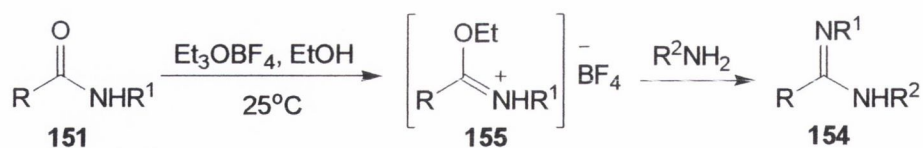
(i) Amidines Synthesised From Amides

Secondary amides, **151**, when converted into imidoyl chlorides, **152**, can be reacted with amines to give the corresponding amidine, **153**, although this reaction works poorly to produce unsubstituted amidines (Scheme 4.26).¹⁷⁸



Scheme 4.26

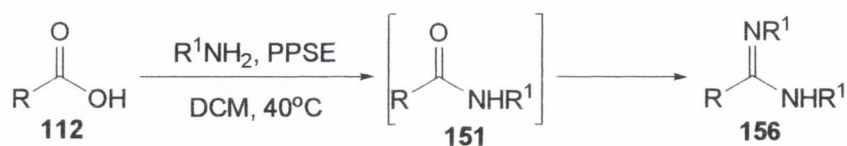
Secondary amides can also be converted into the corresponding amidine, **154**, via formation of an imidic ester fluoroborate, **155** (Scheme 4.27).¹⁷⁹



Scheme 4.27

(ii) Amidines Synthesized From Carboxylic Acids

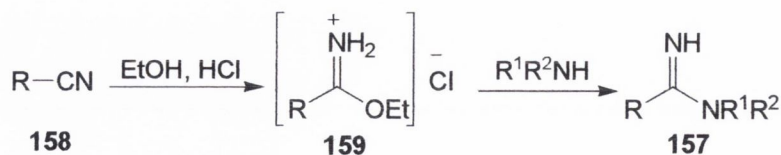
Aliphatic and aryl carboxylic acids can be converted directly into the corresponding amidines by forming an amide intermediate as shown by Kakimoto *et al.*¹⁸⁰ The carboxylic acid is reacted with polyphosphoric acid trimethylsilyl ester (PPSE, formed *in situ* by the reaction between phosphorous pentoxide and hexamethyldisiloxane) before reacting with an aryl amine to give the desired amidine in good yield (65-88%, Scheme 4.28)



Scheme 4.28

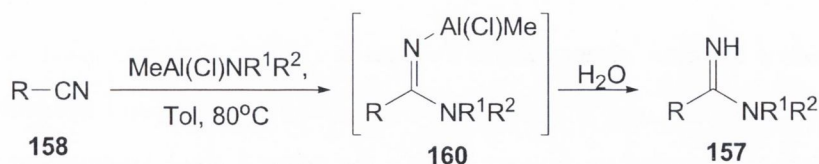
(iii) Amidine Synthesized from Nitriles

The synthesis of unsubstituted amidines, **157**, from nitriles, **158**, as performed by Pinner, and its derivatives remains the most common preparation of amidines.¹⁸¹ The reaction proceeds through the formation of an imidic ester, **159**, which then can be reacted with amines to give the desired amidine (Scheme 4.29).



Scheme 4.29

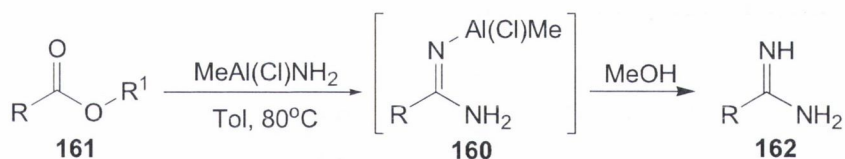
More recently, work by Garigipati converted nitriles, **158**, to amidines, **157**, in a one step reaction involving alkylchloroaluminium amides, **160** (Scheme 4.30).¹⁸² This procedure had originally been used by Weinreb *et al.*¹⁸³ to convert esters to amides.



Scheme 4.30

(iv) Amidines Synthesized From Esters

As mentioned earlier carboxylic acids, **112**, can be converted into the corresponding amidine, **156**, through an amide intermediate, **151** (Scheme 4.28). Recent work by Gielen *et al.*¹⁸⁴, based on the original work of both Garigipati *et al.*¹⁸² and Weinreb *et al.*¹⁸³ converted esters, **161**, into the corresponding amidine, **162**, in a one step reaction and in good yield (Scheme 4.31). The methylchloroaluminium amide, **160**, was again formed *in situ* and was hydrolysed to give the desired product (Scheme 4.31).

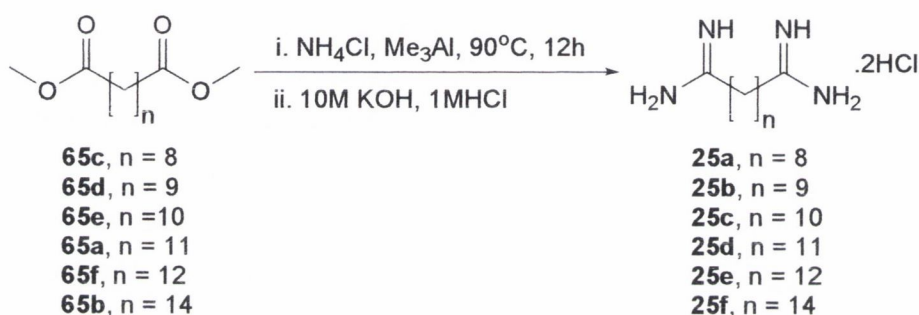


Scheme 4.31

4.5 Amidine Synthesis

As stated earlier in Chapter 1, one of the aims of this thesis was to synthesize a series of aliphatic *bis*-amidines, **25a-f**, based on both pentamidine and agmatine in order to do this we decided to adopt the procedure of Gielen *et al.*¹⁸² because of the ease of the method and our experience using trimethylaluminium in synthesizing the alkyl *bis*-2-imidazolines, **24a-f**. Similar to the preparation of the alkyl *bis*-2-imidazolines, **24a-f**, the

reaction uses a 1:10:5 (ester: ammonium hydrochloride: Me_3Al) to synthesize the amidines. Despite the similarity in the use of equivalents, the reaction requires longer reflux time (12h) and the alkyl *bis*-amidine is isolated as the hydrochloride salt. After quenching the reaction (using the same method as the alkyl *bis*-2-imidazolines) the alkyl *bis*-amidines are purified by firstly creating the free base of the crude product (dissolved in water) with a solution of potassium hydroxide (10M). The free alkyl *bis*-amidine is precipitated out, filtered and then redissolved in a hydrochloric acid solution (1M). This solution is then evaporated to dryness to give the desired alkyl *bis*-amidine salt in good yield (Scheme 4.32, Table 4.4).



Scheme 4.32

Table 4.4.- Yield of Formation of the Amidine Salts from Scheme 4.34

Compound	Yield (%)
25a	75
25b	73
25c	80
25d	80
25e	77
25f	74

4.6 Summary and conclusions

To synthesize the alkyl *bis*-imidazolines, **24a-f**, we have utilized the aliphatic dicarboxylic acids, **56a-f**, as precursors. Before attempting any reactions with the aliphatic dicarboxylic acids we tested reaction conditions using the aromatic carboxylic acid **145**. Using **145** we first attempted to synthesize the corresponding imidazoline, **141**, using a procedure developed by Casey *et al.*¹⁷² However, the final step of the reaction, an

intramolecular ring closure, was unsuccessful despite the use of nucleophiles of different strengths.

After this setback a second procedure using trimethylaluminium and ethylene diamine and the aromatic ester, **148**, was investigated. Using the aromatic methyl ester, **148**, produced the aromatic imidazoline, **141**, in moderate yield (50%). Initially using this procedure to produce the alkyl bis-imidazolines, **24a-f**, produced mixed results. Examining the equivalents of the reagents used resulted in optimized reaction conditions. The best results for producing the alkyl bis-imidazolines, **24a-f**, are obtained when ten equivalents of trimethylaluminium and five equivalents of ethylene diamine in relation to the alkyl bis-methyl ester are used and the reaction was heated at reflux for two and a half hours. Using these reaction conditions produced the alkyl bis-imidazolines, **24a-f**, in good yield (26 – 77%). The corresponding alkyl bis-imidazoline salts, **150a-f**, were obtained by washing with a 0.875M solution of oxalic salt in good yield (78 – 93%).

To synthesize the alkyl bis-amidines, **25a-f**, we followed the procedure of Gielen *et al.*¹⁸⁴ This procedure used five equivalents of trimethylaluminium in relation to the methyl ester and rather than use ethylenediamine as the source of nitrogen Gielen *et al.*¹⁸⁴ used ammonium hydrochloride. Following this procedure and using ten equivalents of both the trimethylaluminium and ammonium hydrochloride produced the alkyl bis-amidines, **25a-f**, as their hydrochloride salts in good yield (73 – 80%).

We have now synthesized 12 new I₂-IBS ligands and two new families of aliphatic *bis* ligands. The conformational analysis and biological assay results of both the alkyl bis-imidazolines and the alkyl bis-amidines will be discussed in Chapters 5 and 6.

4.7 References

96. Anastassiadou, M., Danoun, S., Crane, L., Baziard-Mouysset, G., Payard, M., Caignard, M., Rettori, M., Renard, P. *Bioorg. Med. Chem.* **2001**, *9*, 585.
147. Jones, R. C. F., Dimopoulos, P. *Tetrahedron.* **2000**, *56*, 2061.
148. Grimmett, M. R.; Meth-Cohn, O.; Katritsky, A. R. *Imidazole and Benzimidazole Synthesis*. Academic Press.
149. Pinner, A. Verlag R. Oppenheim. Berlin. **1892**.
150. Klarer, W., Urech, E. *Helv. Chim. Acta.* **1944**, *27*, 1762.
151. Jones, R. C. F., Dimopoulos, P. *Tetrahedron.* **2000**, *56*, 2061 – 2074.
152. Jones, R. C. F., Ward, G. J. *Tetrahedron. Lett.* **1988**, *29*, 3853.
153. Reynaud, P., Brion, J. D., Davirinche, C., Dao, P. C. *J. Heterocycl. Chem.* **1980**, *17*, 1789.
154. Chotwood, H. C., Reid, E. E. *J. Am. Chem. Soc.* **1935**, *57*, 2424.
155. Hill, A. J., Aspinall, S. R. *J. Am. Chem. Soc.* **1939**, *61*, 822.
156. Neef, G., Eder, U., Sauer, G. *J. Org. Chem.* **1981**, *46*, 2824.
157. Oxley, P., Short, W. F. *J. Chem. Soc.* **1947**, 1085.
158. Oxley, P., Short, W. F. *J. Chem. Soc.* **1946**, 147.
159. Wunsch, K. H., Dettmann, H., Schonberg, S. *Chem. Ber.* **1969**, *102*, 3891.
160. Heine, H. W., Bender, H. S. *J. Org. Chem.* **1963**, *28*, 1496.
161. Letgers, J., Willems, J. G. H., Thijs, L. Zwanenburg, B. *Rec. Trav. Chim. Pays-Bas.* **1992**, *111*, 59.
162. Stolle, R., Merkle, M., Hanusch, F. *J. Prakt. Chem.* **1934**, *140*, 59.
163. Yoshikawa, Y., Kiyota, R., Urabe, Y. *Yakugaku Zasshi.* **1969**, *89*, 767.
164. Nair, M. D., Mehta, S. R. *Indian J. Chem.* **1967**, *5*, 403.
165. Jung, S. H., Kohn, H. *Tetrahedron. Lett.* **1984**, *24*, 399.
166. Jung, S. H., Kohn, H. *J. Am. Chem. Soc.* **1985**, *107*, 2931.
167. Schollkopf, U. *Angew. Chem. Int. Ed. Engl.* **1977**, *16*, 339.
168. Van Leusen, A. M., Wildeman, J., Oldenziel, O. H. *J. Org. Chem.* **1977**, *42*, 1153.

169. Hayashi, T. Kishi, E., Soloshonok, V. A., Uozomi, Y. *Tetrahedron. Lett.* **1996**, 37, 4969.
170. Katritzky, A. R., Zhu, L., Lang, H., Denisko, O., Wang, Z. *Tetrahedron.* **1995**, 51, 13271.
171. Partridge, M. W., Turner, H. A. *J. Chem. Soc.* **1949**, 1308.
172. Boland, N. A.; Casey, M.; Hynes, S. J.; Matthews, J. W.; Smyth, M. P. *J. Org. Chem.* **2002**, 67, 3919.
173. Blagborough, I. S.; Mac Kenzie, N. E.; Ortiz, C.; Scott, A. I. *Tetrahedron. Lett.* **1985**, 27, 11, 1251.
174. Fry, A. *J. Am. Chem. Soc.* **1953**, 75, 2686.
175. Ram, R. N.; Ashare, R.; Mukerjee, A. K. *Chem. Ind.* **1983**, 569.
176. Wijnmans, M.; Pratt, D. A.; Brinkhorst, J.; Serwa, R.; Valgimigli, L.; Pedulli, G. F.; Porter, N. A. *J. Org. Chem.* **2004**, 69, 9215.
177. www.chem.wisc.edu/areas/reich/pkatable/kacont.htm
178. Partridge, M. W., Smith, A. *J. Chem. Soc. Perkin Trans. I* **1973**, 453.
179. Weintraub, L., Oles, S. R., Kalish, N. *J. Org. Chem.* **1968**, 33, 1679.
180. Kakimoto, M., Ogata, S., Mochizuki, A., Imai, Y. *Chem. Lett.* **1984**, 821.
181. Pinner, A. Die Iminather und ihre Derivate, *Verlag, R. Oppenheim: Berlin*, **1892**.
182. Garigapati, R. S. *Tetrahedron. Lett.* **1990**, 31, 1969.
183. Levin, J. I., Turos, E., Weinrab, S. M. *Synth. Commun.* **1982**, 12, 989.
184. Gielen, H., Alonso-Alija, C., Hendrix, M., Niewohner, U., Schauss, D. *Tetrahedron. Lett.* **2002**, 43, 419 – 421.

Chapter 5

Conformation analysis of the alkyl bis-guanidines, alkyl bis-guanidino carbonyls, alkyl bis-2-imidazolines and alkyl bis-amidines

5.1 Introduction

Considering the number of I₂-IBS ligands that had been synthesized we decided to investigate the potential Structure Activity Relationships (SAR) between the members of each family (for example **19b** versus **19c**, Figure 5.1) and between the families themselves (e.g. the alkyl *bis*-guanidines versus the alkyl *bis*-guanidino carbonyls). As stated earlier in Chapter one, the full three dimensional (3-D) structure of the I₂-IBS remains unknown, and therefore we do not know the structural requirements needed to interact with the binding site and no receptor-based design of I₂-IBS ligands can be carried out. Moreover, the only attempts to develop an I₂-IBS pharmacophore have been based on aromatic ligands and this knowledge cannot be properly applied to aliphatic ligand design.¹⁸⁵⁻¹⁸⁷ In order to overcome this problem we decided to model the conformation by, which each molecule may act in a physiological environment to determine if any ligand or any family posses a particular shape or characteristic in common using conformational analysis techniques in a solvent model environment.

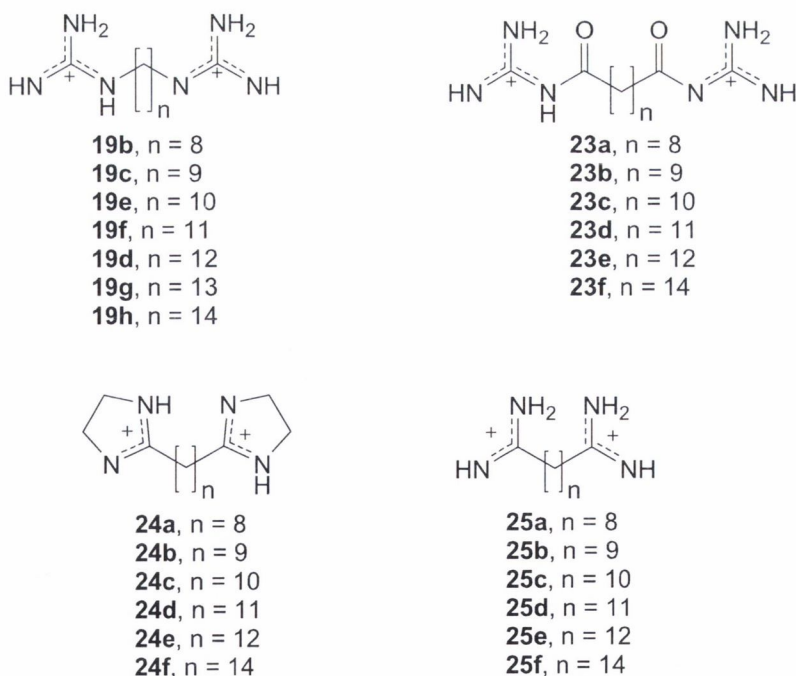


Figure 5.1.- Structure of the ligand families synthesized

Conformational analysis is the study of the three dimensional structures, called conformations, that a molecule can adopt and their effect on the physical, chemical and biological properties of that molecule. An important aspect of conformational analysis is the conformational search. The conformational search identifies the more stable or preferred conformations of a molecule. To accomplish this, the potential energy surface is examined to find not only the global minimum energy conformation (GMEC) but also other minimum energy conformations. The GMEC can be difficult to find due to the existence of multiple local minima. There are many different methods to search for the minimum energy conformations, but we will comment on those most generally used.

(i) Systematic Searches

A systematic conformational search is an exploration where all the rotatable bonds of a molecule are identified and rotated through 360° using a fixed increment. Once a conformation has been generated all the atoms in the molecule are examined to investigate the possibility of steric conflict. If a conformation is found to have steric conflict, it is discarded.¹⁸⁸ Conformations are also subject to structural optimizations, thus higher energy conformations are eliminated. The search is ended when all possible torsion angles have been rotated and the conformation thus, generated have been minimized.

The problem with this type of search is a phenomenon known as combinatorial explosion. This is due to the extremely large number of conformations generated in a systematic search when many bonds are rotated. The formula for calculating the number of conformations that can be generated in this manner is given by:

$$V = (360/A)^T$$

V = number of conformations

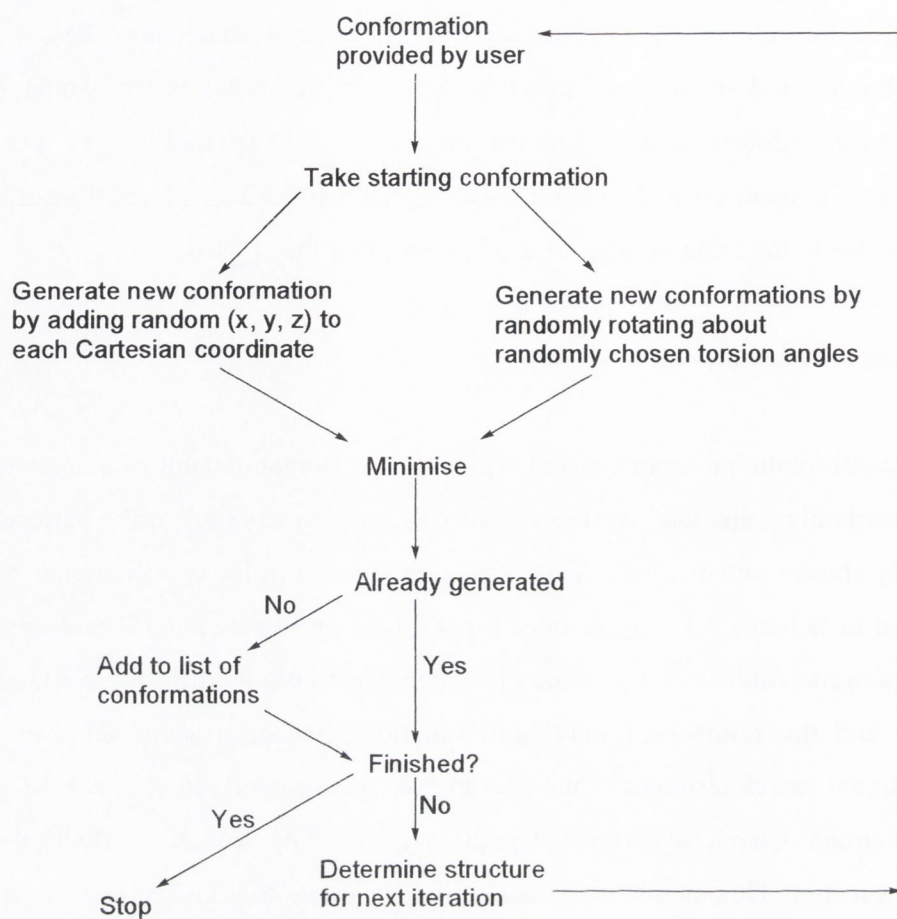
T = number of rotatable bonds

A = torsion angle increment

Applying this formula to the smallest of our synthesized molecules, **19a**, with nine rotatable bonds, and by rotating these bonds in 30° increments we would generate 61,917,364,224 conformations! This is obviously an extremely large number of conformations to examine and so this type of search was not considered for our aliphatic derivatives due to the large number of single bonds that they possess.

(ii) Random Conformational Searches

Random conformational searches (RCS), unlike systematic conformational searches, work by randomly generating conformations by changing any part of the molecule about a randomly chosen torsion angle. This random generation follows an iteration pattern as represented in Scheme 5.1. Again, once a conformation is generated it undergoes steric and energy optimizations.¹⁸⁹ The search is ended when no new different conformation is generated and the number of maximum iterations has been achieved. The random conformational search also allows the user to take solvation effects into consideration. If a conformational search is performed without considering solvation effects the search occurs in vacuum. This causes the charges of a molecule to either attract or repel from one another, and is not representative of the conformations that occur under physiological conditions. By changing the dielectric constant we take into consideration solvation effects, thus, the conformational analysis can mimic the polar physiological environment. This will affect the conformations generated and will produce conformations more likely to be the Biological Active Conformation (BAC). Once the search has been completed several parameters of the conformation can be calculated, these include (but are not limited to); Energy, Distance between atoms, Total Dipole moment, Polar Surface Area (PSA), Molecular Volume and Molecular Area.



Scheme 5.1

5.2 Methodology of the Random search analysis

The RCS was performed using Random Search tool implemented in Sybyl (versions 6.9 and 7.1).¹⁹⁰ Before the RCS began all the molecules were built protonated using the Sybyl program. The search was performed like this in order to mimic the way the molecules would perform in physiological conditions.^{186,187} The following conditions were established in the conformational analyses performed in all of the compounds **19b-h**, **23a-f**, **24a-f** and **25a-f** all the single bonds of the linker chain were rotated. All the atomic charges were evaluated with the Gasteiger–Huückel method. Each generated conformer was minimized over 300 cycles using the Conjugate Gradient method and the maximum number of cycles in the search was set to 6000 with an energy cut-off of 5 kcal/mol⁻¹, following the procedure previously used by our group.¹⁹¹

When the RCS was performed we used the dielectric constant of water ($\epsilon = 80.0$) to mimic physiological conditions. Once the RCS was completed several parameters for each conformation were evaluated. These were:

- 1) the Energy of the conformation,
- 2) the Distances between the cationic centres,
- 3) the Total Dipole of each conformation,
- 4) the Polar Surface Area (PSA)
- 5) the Molecular Volume of space occupied by each conformation and finally
- 6) the total Molecular Area of each conformation.

The energy of the conformation was calculated to find the GMEC. Once the GMEC was identified the conformations with energy values greater than 5 kcal/mol^{-1} over the GMEC energy were discarded. These conformations were discarded because when a molecule forms a ligand-receptor complex the maximum energy change that the ligand can undergo (induced by the interaction with the receptor) will be within 5 kcal/mol^{-1} of the energy of the original conformation.

The distances between the cationic centres were calculated based on the delocalisation of the functional groups of each family. As can be seen in Figure 5.1, the cationic centres of all families have been chosen as the carbon atoms marked by a positive sign in Figure 5.1. Using the Sybyl¹⁹⁰ program the distance between these C atoms were measured. This distance between cationic centres would give an indication, for a certain compound, of the shape of the conformation and, thus, an indication of potentially how the ligand may bind to the I₂-IBS. Thus, Figure 5.2a shows a pronounced U shape conformation of **19b** (short distance between cations), while Figure 5.2b shows a straight line shape conformation of the same molecule (large distance between cations). As can be seen from these figures there would be a large range of distances between the cationic centres. This is indeed the case, the distance for Figure 5.2a is 7 Å and for Figure 5.2b is 13 Å.

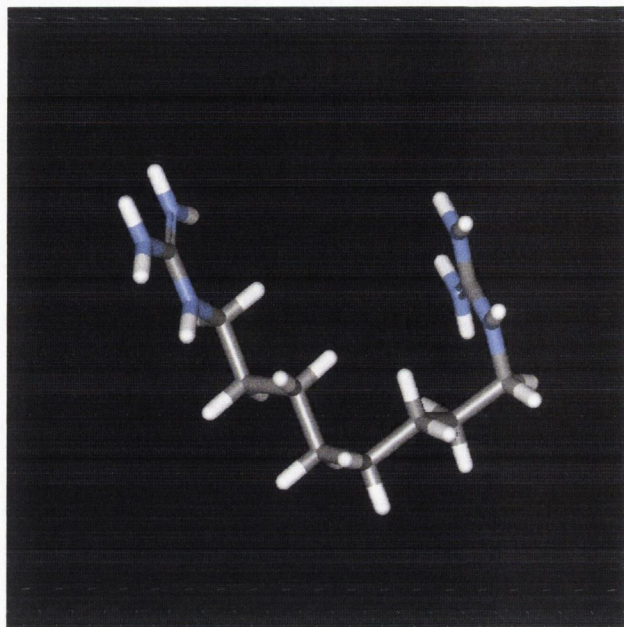


Figure 5.2a.- 19b conformation 515

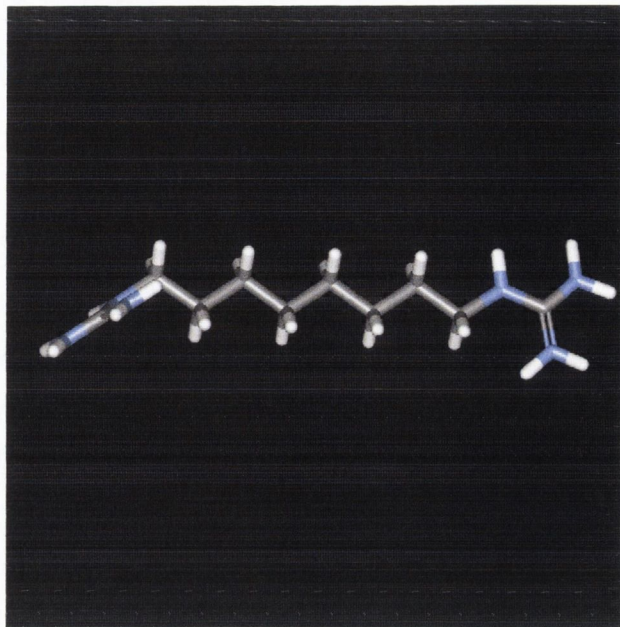


Figure 5.2b.- 19b conformation 510

The Total Molecular Dipole of each conformer was measured as a vector in Debyes (Db). The dipole of a molecule is calculated based on the electronegativity of the atoms in the molecule. Due to the large number of nitrogen atoms in each family of ligands a dipole is created in the molecule between those points where the functional groups are located. The Total Dipole of the ligands may give an indication of the direction of the ligand within the ligand-receptor complex.

The Polar Surface Area (PSA) of each conformation is formed by the polar atoms of a molecule and is defined as the sum of the surface contributions of the polar atoms to the total molecular surface. The PSA of a molecule is a very important factor in determining if a molecule can cross the Blood Brain Barrier (BBB) and it has been demonstrated to correlate well with drug transport properties because it is a measure of the lipophilicity of the molecule.^{192,193} In general, it is accepted that for intestinal absorption a molecule that possesses a PSA greater than 140 \AA^2 will encounter difficulty, while the ideal PSA for intestinal absorption is 50 \AA^2 .¹⁹⁴ For the BBB there are two main computational formulas

proposed for calculating the probable penetration of a molecule into the brain. Both of these formulas rely on the PSA of the molecule:

$$1) \text{ Log BB} = 0.4275 - 0.3873(\text{Nacc/solv}) + 0.1092\text{Log P} - 0.0017\text{PSA}$$

Nacc/solv = the number of hydrogen bond acceptors in aqueous media

Log P = the partition coefficient of the molecule (a measure of the lipophilicity of the molecule).¹⁹⁵

$$2) \text{ Log PS} = -2.19 + 0.262\text{Log D} + 0.0583\text{vas_base} - 0.00897\text{PSA}$$

Log PS = BBB permeability surface area product,

Log D = distribution coefficient

vas_base = van der Waals surface area of the basic atoms (i.e. N, O etc) of the molecule.¹⁹⁶

The Molecular Volume and Area of the conformations were calculated because, similar to the distance, they would be good indicators of the shape of each conformation. We assume that the larger the Molecular Volume the straighter the molecule as can be seen in Figures 5.3a and 5.3b, where conformations 907 and 623 of **19b** have volumes of 782 \AA^3 and 877 \AA^3 , respectively.

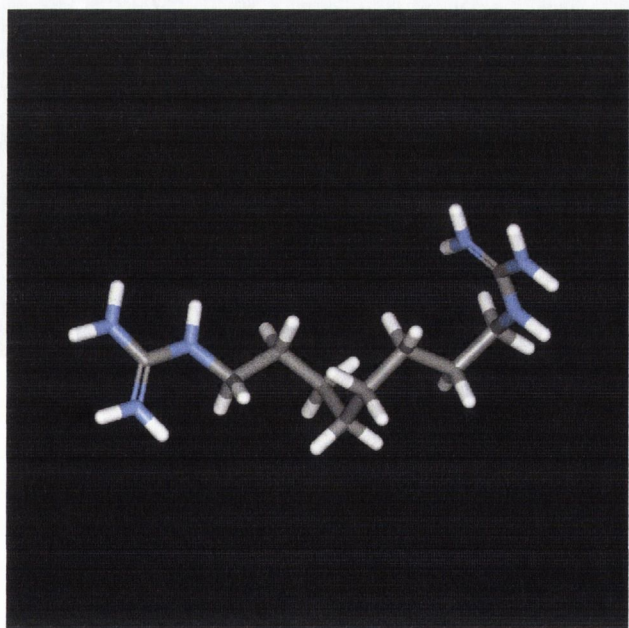


Figure 5.3.a.- **19b** conformation 907

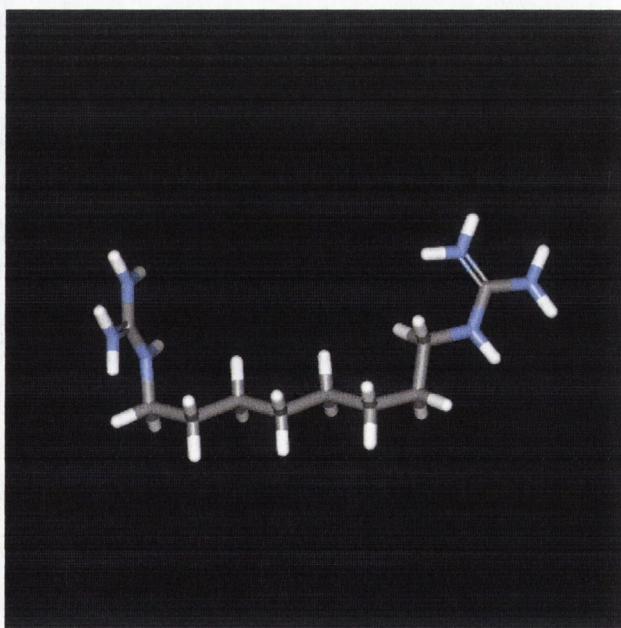


Figure 5.3b.- **19b** conformation 623

Similarly, with the Molecular Area of the conformations we assume that a large area indicates how straight the conformation would be. An example can be seen in Figures 5.4a and 5.4b, where conformations 654 and 365 of molecule **19b** have areas of 478 Å² and 602 Å², respectively.

Once the six parameters were calculated for each conformation of each molecule synthesized, the most populated range for each parameter was identified. In doing this we hoped to find the potential Biological Active Conformations (BAC) of each molecule. The BAC is the conformation that the molecule adopts when interacting with the receptor. To find the BAC, the conformations with parameter values within the most populated range of each parameter were identified since these represent the most likely conformation to exist and interact with the receptor.

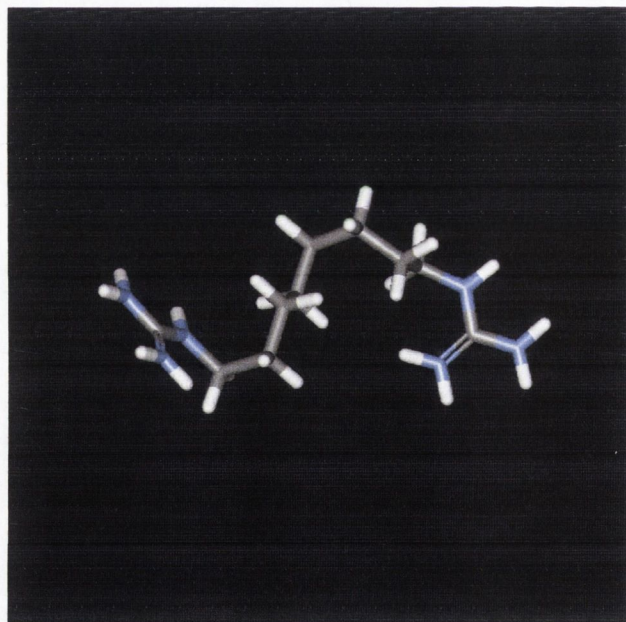


Figure 5.4a.- 19b conformation 654

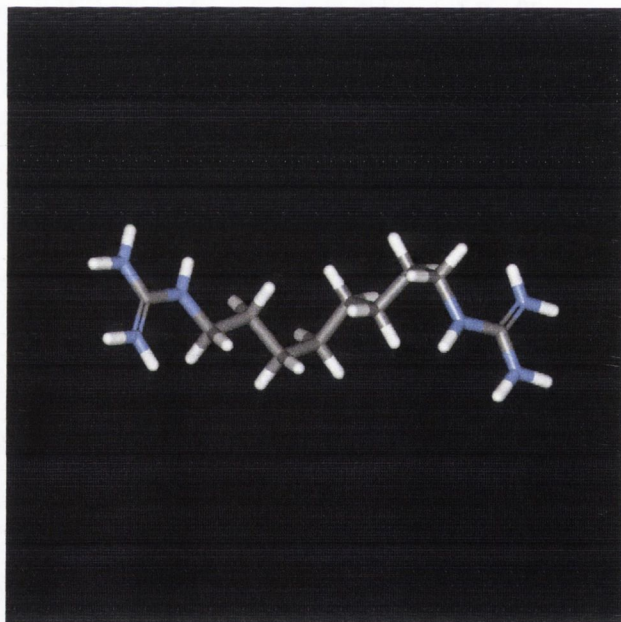


Figure 5.4b.- 19b conformation 363

We followed the general procedure outlined in Scheme 5.2 to find these BACs. We identified the conformations within the most populated range of energy values. From these conformations those within the most populated range of distance values were identified. This identified the conformations within the most populated range for energy

and distance between the cationic centres. From these conformations those within the most populated range of Total Dipole values were identified. This gave the conformations within the most populated range for energy, distance between the cationic centres and Total Dipole. From these conformations those within the most populated range of PSA values were identified. This gave the conformations within the most populated range for energy, distance between the cationic centres, total dipole and PSA. From these conformations those within the most populated range of molecular volume values were identified. This gave the conformations within the most populated range for energy, distance between the cationic centres, total dipole, PSA and molecular volume. Finally, from these conformations those within the most populated range of molecular area values were identified. This gave the conformations within the most populated range for all six parameters and the most likely candidates for the BAC (Table 5.1).

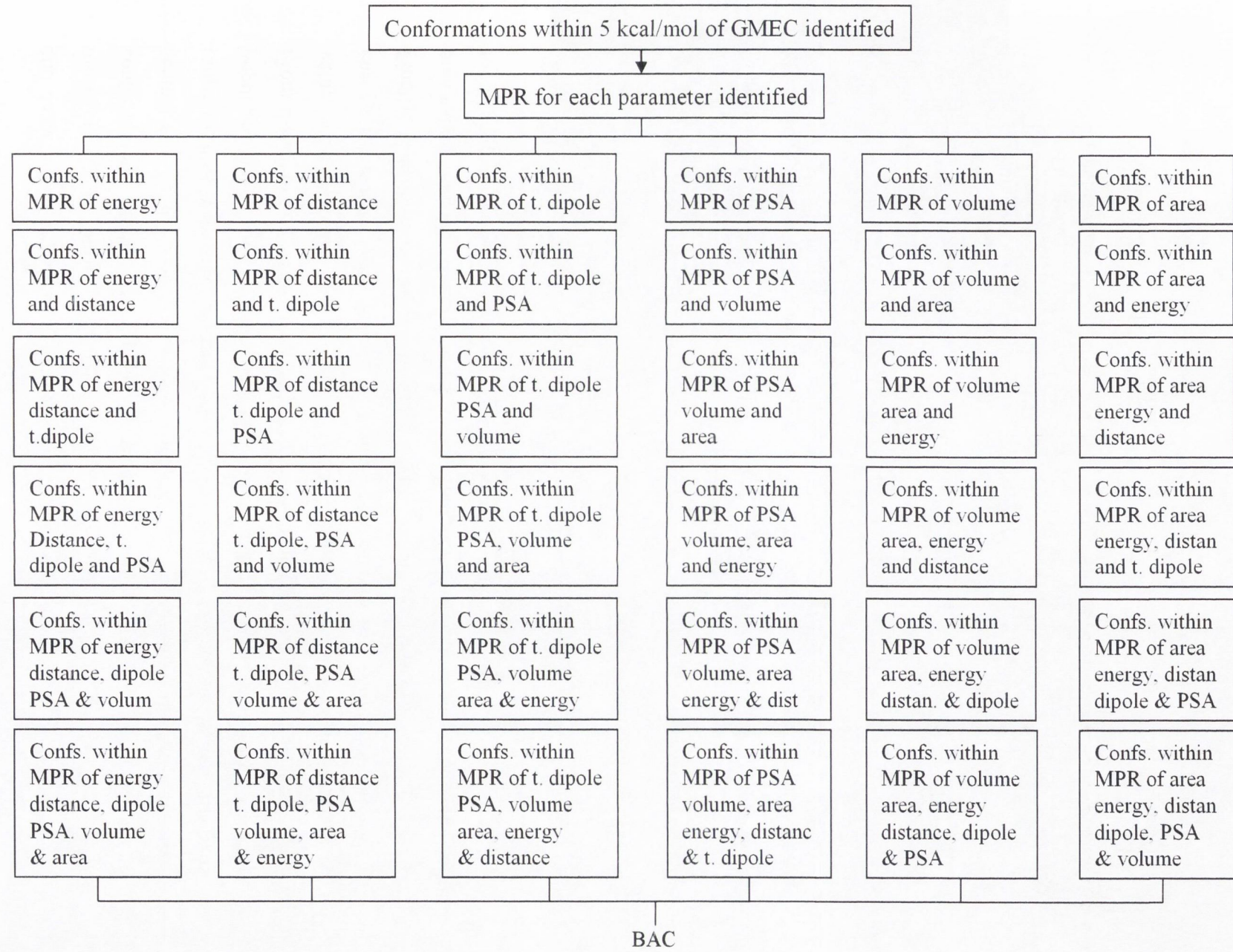
Table 5.1.- The conformations identified for each step in the search for the BAC for **19b**

Function	Energy	Distance	Total Dipole	PSA	Volume	Area
Energy	X	102	56	21	3	1

To ensure the veracity of this method this procedure was repeated using different starting points but following the same order (energy, distance between cationic centres, total dipole, PSA, molecular volume and molecular area). Table 5.2 shows the number of conformations identified in each step for **19b**, where X denotes the starting point for each search for the potential BAC. The corresponding tables for all other ligands can be seen in the appendix.

Table 5.2.- The conformations identified for each step at different starting points in the search for the BAC for **19b**

Function	Energy	Distance	Total Dipole	PSA	Volume	Area
Energy	X	102	56	21	3	1
Distance	1	X	115	48	11	5
Total Dipole	2	1	X	110	31	9
PSA	4	1	1	X	57	18
Volume	14	8	5	1	X	36
Area	51	29	16	6	1	X

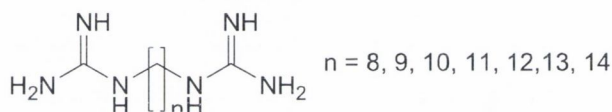


Scheme 5.2

5.3 Conformational Analysis of the alkyl *bis*-guanidines, 19b-h

The first family of compounds to undergo random conformational analysis were the guanidines **19b-h**. The most populated range for each ligand can be seen in Table 3, as the length of the methylene chain linking the two guanidine groups increases the most populated ranges of the area and volume increase too. This is an expected result due to the addition of extra atoms to the linker. However, as can be seen from Table 5.3 there is no clear pattern for the increase in area and volume as the ligands increase in length.

Table 5.3.- Summary of the Conformational Analysis results obtained for the alkyl *bis*-guanidines, **19b-h**



Function	19b	19c	19e	19f	19d	19g	19h
Energy (kcal/mol)	15 – 16	18 – 19	15 – 16	19 – 20	19 – 20	20 – 21	20 – 21
Distance (Å)	10 – 11	11 – 12	12 – 13	12 – 14	12 – 15	13 – 15	14 – 18
Total Dipole (Db)	145 – 150	60 – 70	170 – 175	140 – 150	75 – 80	75 – 80	40 – 45
PSA (Å ²)	260 – 270	260 – 280	260 – 270	260 – 270	260 – 270	260 – 280	270- 280
Volume (Å ³)	830 – 840	860 – 870	940 – 950	1000 – 1010	1020 – 1050	1080 – 1110	1090 – 1110
Area (Å ²)	530 – 540	560 – 570	580 – 590	610 – 620	650 – 670	690 – 700	710 – 750

Another parameter that also increases with the length of the molecule is the distance between the cationic centres. In this case as the chain length increases the distance between the cationic centres increases by 1 Å. This is particularly the case for the ligands **19b, c, e** and **f**. From this data we may hypothesize that these four molecules share a similar bent or U shape. However, for the molecules **19d, g** and **h** we see a widening of the distance between the cationic centres.

As stated earlier in this chapter the energy of each conformation is dependent on the number of atoms in the molecule and their relationship to each other. Bearing this in mind the fact that **19b** and **19c** possess the same most populated range in energy is interesting. This may indicate that **19c** is taking a slightly energetically disfavoured shape similar to **19b**. In the case of the dipole moment there is no definable trend, with **19h** having the smallest dipole moment and **19e** the largest values, while the other molecules share dipole moments in between the two ranges.

Finally, with the PSA all seven molecules having the same range of 260 to 270 Å², this result is not surprising considering that all the molecules have six nitrogen atoms. Due to the way the PSA is calculated this indicates that all the molecules within this family share a similar functional group orientation.

Table 5.4.- Number of potential BAC identified for each molecule

Compound	Number of Conformations
19b	1
19c	4
19e	2
19f	1
19d	8
19g	3
19h	3

Table 5.4 shows the number of BAC identified for each alkyl *bis*-guandine following the procedure outlined earlier in this chapter. From Table 5.4 we can see that following this procedure, the compounds **19b** and **19f** generated one potential BAC each, while **19c** and **19e** generated four and two BACs, respectively. **19g** and **19h** generated three each and **19d** generated eight BACs.

Regarding the conformations of **19b** and **19c** we can see that both structures show a broad U shape (Figure 5.5a and 5.5b, respectively). Similarly, when we look at the BACs of **19e** and **19f** we can see the U shape being repeated (Figure 5.6a and 5.6b, respectively). However, when we look at the conformations of **19d** we can see that when

the conformations are overlapped over one another (Figure 5.7a) a general shape cannot be seen. In fact the broad U shape is repeated for **19g** (Figure 5.7b) but not for **19h**. For **19h** we start to see a flattening of the broad U shape, although the molecule does still possess a slight curve (Figure 5.8a).

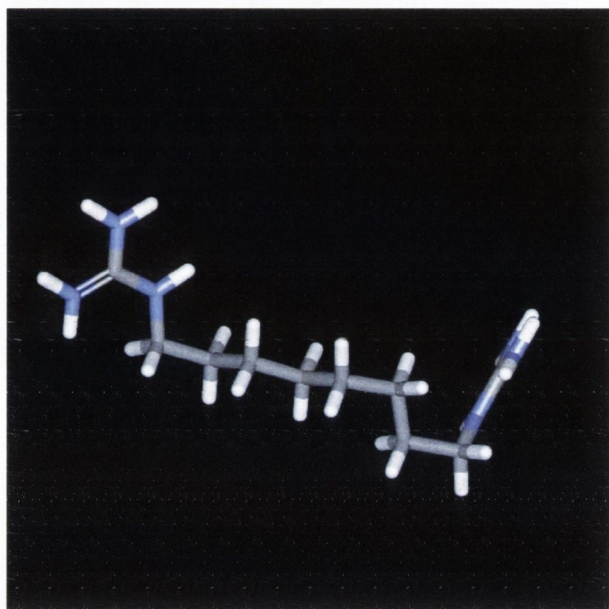


Figure 5.5a.- BAC of **19b**

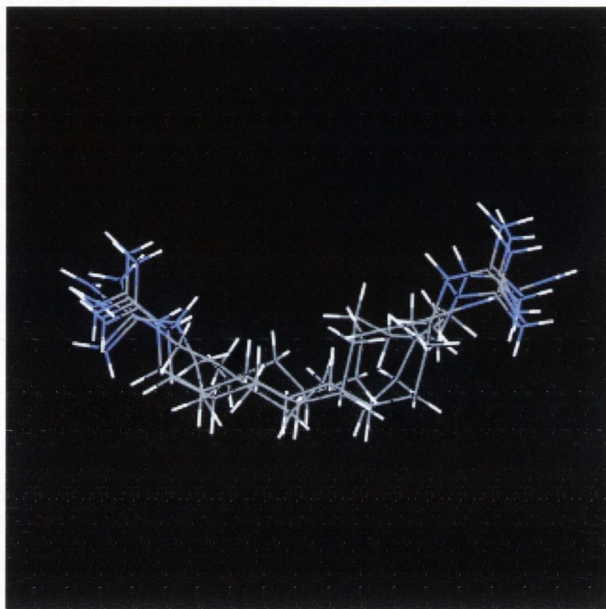


Figure 5.5b.- BAC of **19c**

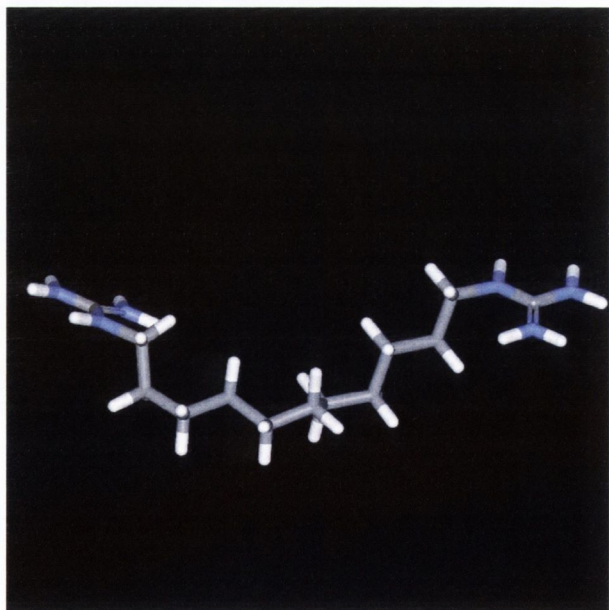


Figure 5.6a.- Overlap of the BAC of **19e**

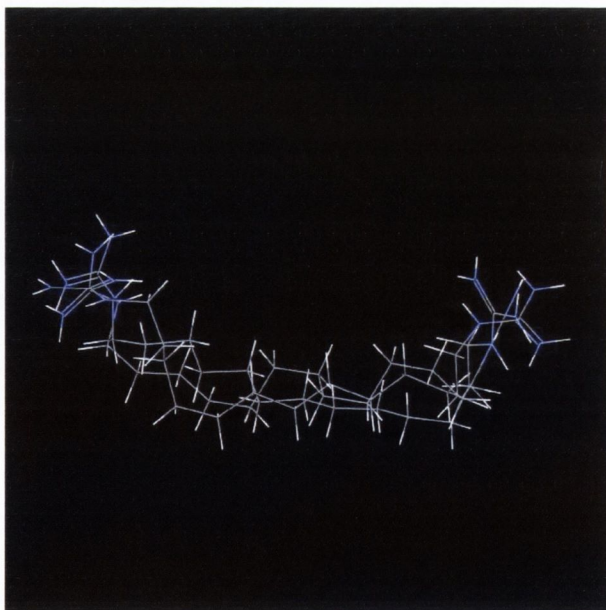


Figure 5.6b.- BAC overlap for **19f**

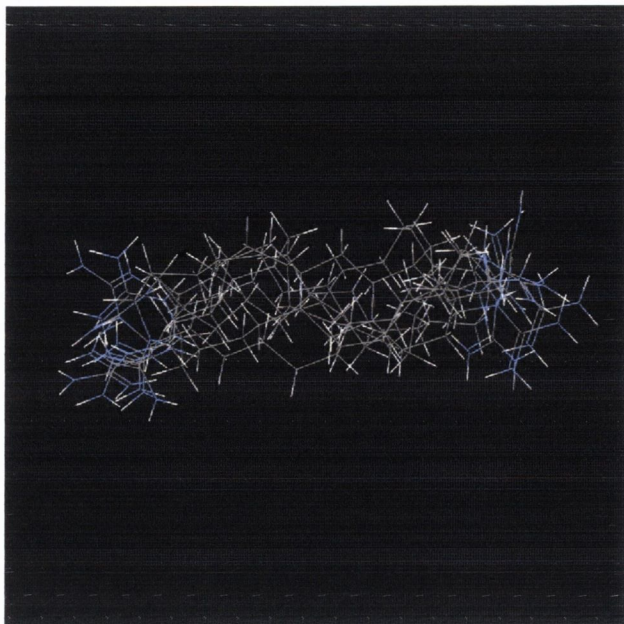


Figure 5.7a.- BAC overlap for 19d

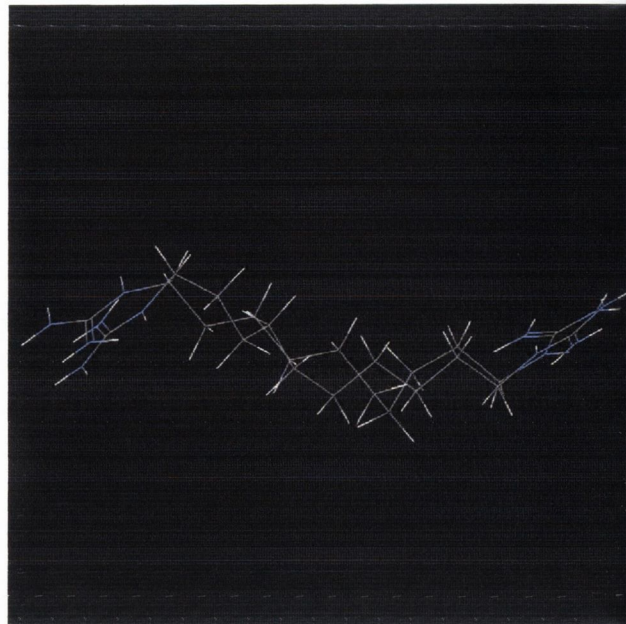


Figure 5.7b.- BAC overlap for 19g

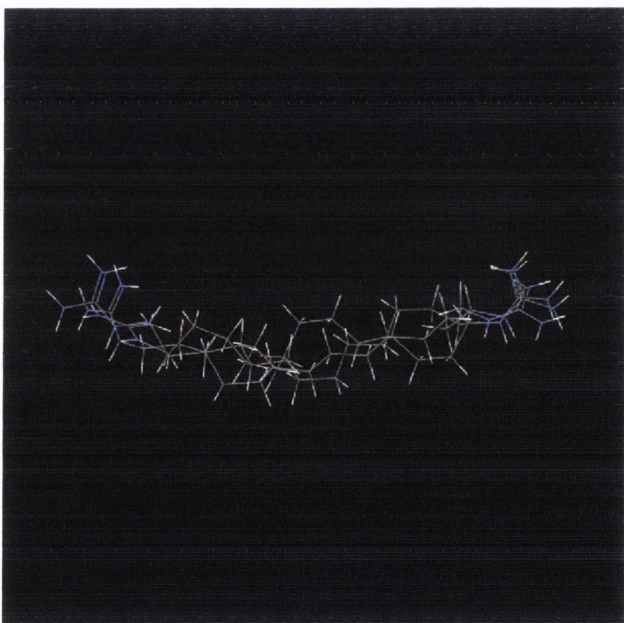


Figure 5.8a.- BAC overlap for 19h

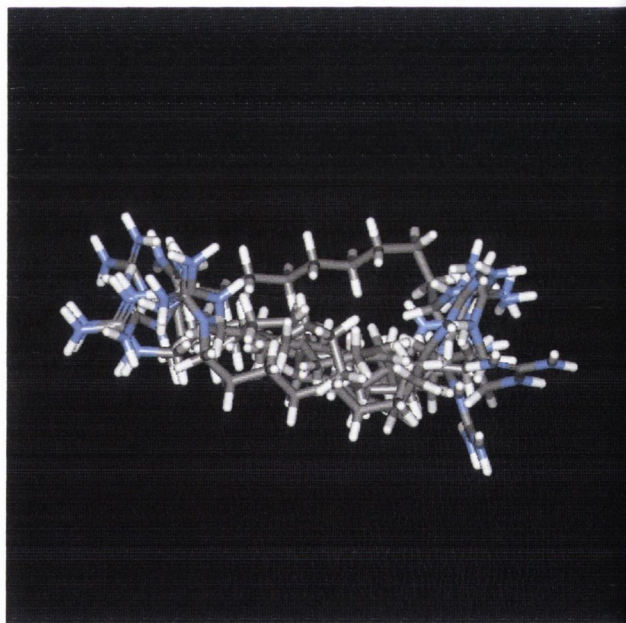


Figure 5.8b.- overlap BAC 19b-h

Due to the general U shape of the potential BAC generated for each molecule we then overlapped one conformation from each of the molecules over one another to generate Figure 5.8b. From this Figure 5.8b we can see that indeed six out of the seven molecules

boast a similar shape, the BAC for **19d** proving to be the exception. This would indicate that the distance and the PSA parameters can be used to determine if the structures of molecules would be similar or not.

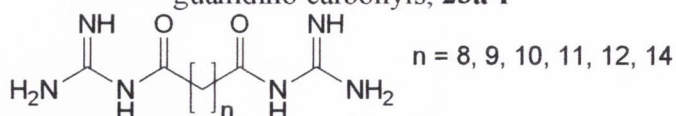
5.4 Conformational Analysis of the alkyl *bis*-guanidino carbonyls

The most populated ranges for the six parameters for the six alkyl *bis*-guanidino carbonyls synthesized are shown in Table 5.5. The area and volume increase as the length of the linker increases. This result is similar to that obtained for the alkyl *bis*-guanidine series. Similarly, there is no discernable pattern in the increase of the area and volume. The distance between the cationic centres also increases as the length of the chain length increases. This result is expected in linear conformations when the chain length increases. The trend in the changes in distance as the linker chain increases witnessed for the guanidines **19b-h** is also observed for the guanidino carbonyls **23a-f**. For the alkyl *bis*-guanidino carbonyls **23a-f** we again see a widening in the most populated range of distances, which spans 11 and 18 Å. Finally, in general the three parameters of Distance, Volume and Area for the alkyl *bis*-guanidino carbonyl series are much larger across the six molecules compared to the alkyl *bis*-guanidines. This result is to be expected due to the presence of the two extra carbonyl groups.

The range of energy values obtained for the alkyl *bis*-guanidino carbonyl family (between -8 and -9.9 kcal/mol) are much narrower than the ranges obtained for the alkyl *bis*-guanidines. The most populated energy ranges for each *bis*-guanidino carbonyl derivative are similar to one another, except for **23f**. Similarly, to the alkyl *bis*-guanidines this could indicate that all the alkyl *bis*-guanidino carbonyls share a similar conformation. The most populated range for the dipole moments of the alkyl *bis*-guanidino carbonyls **23a-c**, is the same (145 – 155 Db). This result is quite interesting and could indicate that the polar extremities of the three molecules are orientated in a similar direction. Compounds **23d** and **23e** also have the same most populated dipole moment (110 – 125 Db) range although lower than that of **23a-c**, and **23e**. Compound **23f**, on the contrary, has a higher

most populated range for the dipole moment than the other compounds including all of the alkyl *bis*-guanidine molecules.

Table 5.5.- Summary of the Conformational Analysis results obtained for the alkyl *bis*-guanidino carbonyls, **23a-f**



Function	23a	23b	23c	23d	23e	23f
Energy (kcal/mol)	-9.9 – -8.0	-9.9 – -8.0	-9.9 – -8.0	-9.9 – -9.0	-9.9 – -9.0	-8.9 – -8.0
Distance (Å)	11 – 12	12 – 14	13 – 14	13 – 16	13 – 17	14 – 18
Total Dipole (Db)	145 – 150	145 – 155	145 – 155	110 – 125	115 – 125	170 – 185
PSA (Å ²)	300 – 310	300 – 320	300 – 320	300 – 320	300 – 310	300 – 310
Volume (Å ³)	920 – 930	960 – 970	1000 – 1010	1060 – 1100	1090 – 1140	1240 – 1270
Area (Å ²)	580 – 590	610 – 620	640 – 650	670 – 680	680 – 730	750 – 760

The PSA ranges are again identical to one another (300 to 310 Å²) but larger than those of the alkyl *bis*-guanidines (260 to 270 Å²). This result is to be expected because of the presence of the two extra carbonyl groups. Again this information supports the belief that all the alkyl *bis*-guanidino carbonyl molecules share a similar structural conformation.

Following the same procedure used for the guanidines the potential BACs of the alkyl *bis*-guanidino carbonyls were identified (Table 5.5). Multiple BACs were identified for **23b**, **23d** and **23e** while single BACs were identified for **23a**, **23c** and **23f**. For the multiple conformations of **23d-e** we can see a general U shape trend (Figure 5.9a and 5.9b). For **23b** however, there is a kink in three out of the four BACs thus giving it a W shape (Figure 5.10). Again this result is quite interesting considering that all other molecules share a curved structure (Figures 5.11a and Figure 5.11b).

Table 5.6.- Number of potential BAC identified for each molecule

Compound	Number of Conformations
23a	1
23b	4
23c	1
23d	9
23e	7
23f	1

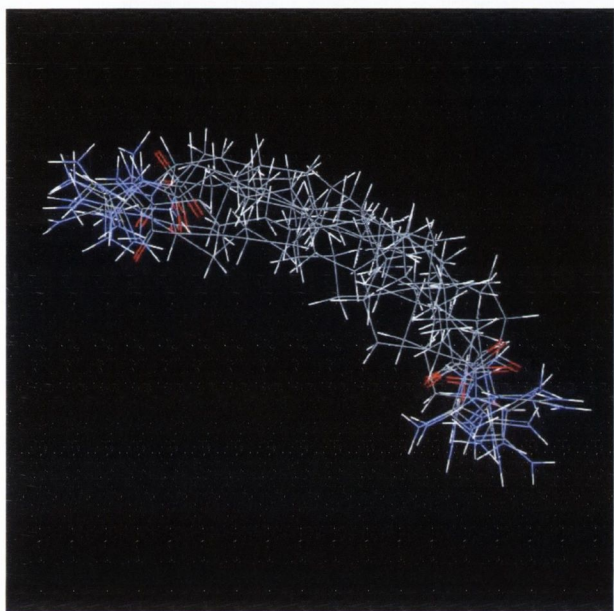


Figure 5.9a.- Overlap of the BACs of 23d

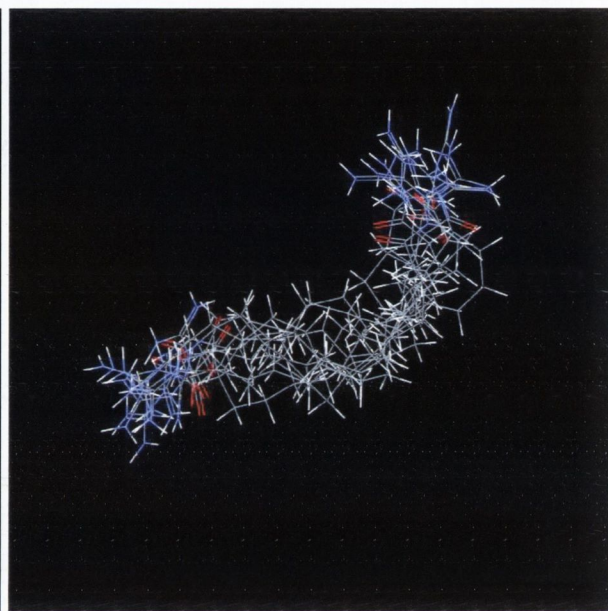


Figure 5.9b.- Overlap of the BACs of 23e

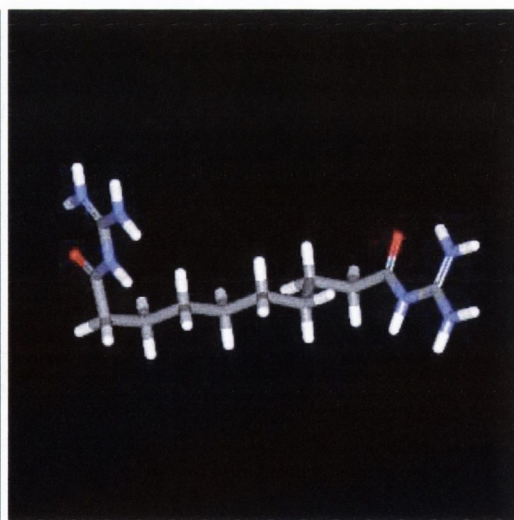
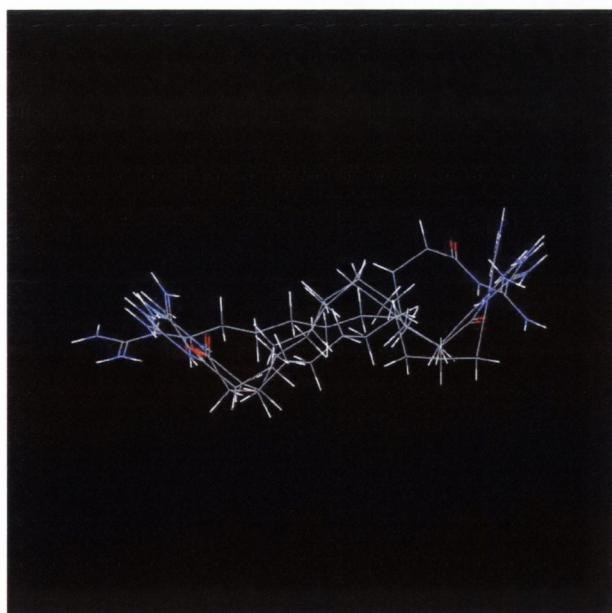


Figure 5.10.- Overlap of the BACs of 23b (left) and BAC of 23a

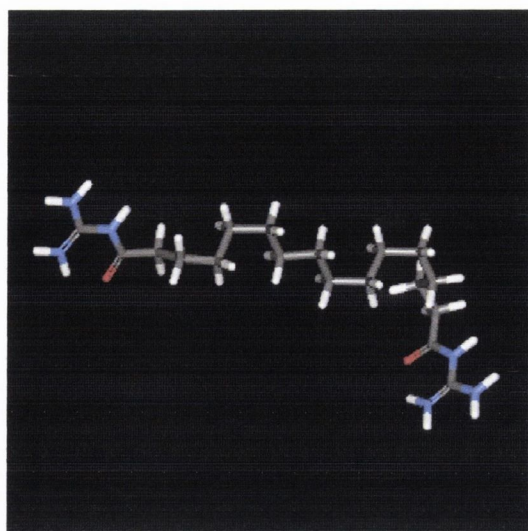
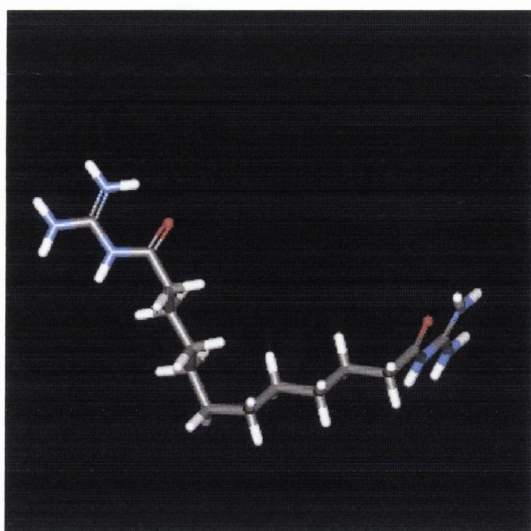


Figure 5.11a.- Overlap of the BAC of **23c** **Figure 5.11b.-** Overlap of the BAC of **23f**

The overlapping of one of conformations of each molecule gives a general U shape for this family of compounds (Figure 5.12). This general shape is similar to the overall shape obtained for the alkyl *bis*-guanidines.

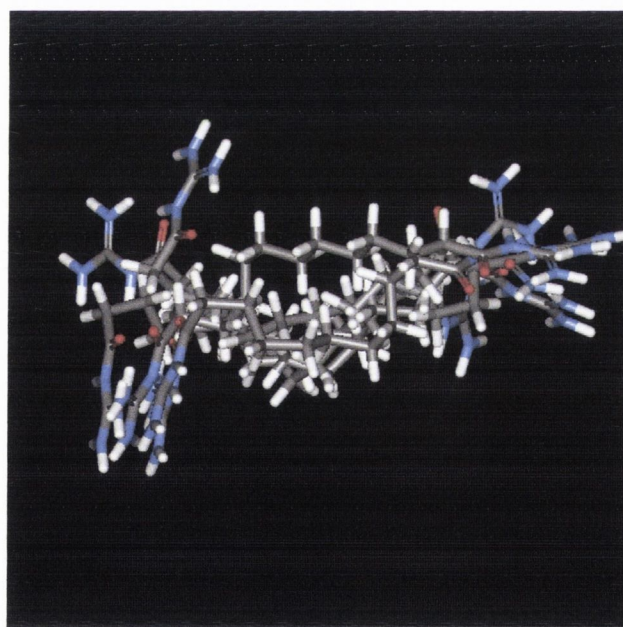


Figure 5.12.- Overlap of the BAC of the alkyl *bis*-guanidino carbonyls **23a-f**

5.5 Conformational Analysis of the alkyl *bis*-2-imidazolines, 24a-f

In Table 5.7 the most populated ranges for the same six parameters for all six *bis*-2-imidazolines synthesized and for S15430 are presented. This compound, S15430, has been included in the study because it is considered the lead compound of the series. The area and volume ranges increase as the length of the linker increases. The result is similar to those obtained for both the alkyl *bis*-guanidines and the alkyl *bis*-guanidino carbonyl series and once again there is no clear pattern in the increase in area and volume. The distance between the cationic centres also increases as the length of the chain length increases. This result is expected in linear conformations when the chain length increases. The trend witnessed for the alkyl *bis*-guanidines **19b-h** and the alkyl *bis*-guanidino carbonyls **23a-f** is again found for the alkyl *bis*-2-imidazolines **24a-f**. The only difference is a widening of the most populated range for the distance parameter in the case of **24f**. What is interesting to note is that the distances between the cationic centres of the alkyl *bis*-2-imidazolines are smaller than those of the alkyl *bis*-guanidines and the alkyl *bis*-guanidino carbonyls. This can be rationalised by the removal of the secondary amine of the guanidines and the amide bond of the ketoguanidine, thus shortening the distance between the centres of the positive charges as expected (Figure 5.13). For S15430 (Table 5.7), the area and volume values are approximately half of those of **24f**. Similarly, the distance between the imidazoline sp^2 carbon and the terminal carbon atom is also approximately half the value for **24f**.

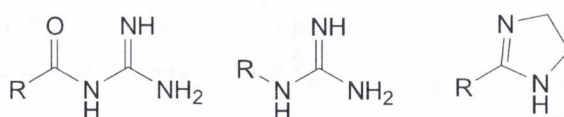
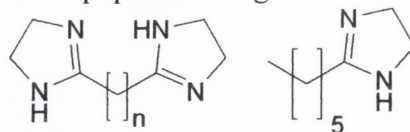


Figure 5.13.- Functional groups; guanidino carbonyl, guanidine and imidazoline

The energy values are the largest values obtained yet and, similarly, to the alkyl *bis*-guanidino carbonyl series, are identical to one another (48 – 49 kcal/mol). Based on the results obtained for the alkyl *bis*-guanidines and the alkyl *bis*-guanidino carbonyls, we would expect that the general shapes of the alkyl *bis*-2-imidazoline conformations will be

similar to each other. The dipole moment ranges again show no clear pattern. In the case of S15430 the energy range is smaller than those of the alkyl *bis*-2-imidazolines and the dipole range is again approximately half of those for **24f**.

Table 5.7.- Summary of most populated ranges for the Alkyl *bis*-2-imidazolines



n = 8, 9, 10, 11, 12, 14 S15430

Function	24a	24b	24c	24d	24e	24f	S15430
Energy (kcal/mol)	48 – 50	48 – 49	47 – 49	47 – 49	48 – 49	48 – 49	14 – 15
Distance (Å)	8 – 9	9 – 10	10 – 12	10 – 12	12 – 13	12 – 15	6 – 7
Total Dipole (Db)	60 – 65	75 – 80	60 – 65	95 – 105	150 – 160	110 – 120	70 – 75
PSA (Å ²)	100 – 110	100 – 110	100 – 110	100 – 110	100 – 110	100 – 110	40 – 50
Volume (Å ³)	890 – 900	940 – 950	1020 – 1030	1040 – 1090	1070 – 1080	1220 – 1260	670 – 680
Area (Å ²)	580 – 600	600 – 610	630 – 650	640 – 690	680 – 690	740 – 760	430 – 440

The PSA ranges of the alkyl *bis*-2-imidazolines are identical to each other, a result that is expected based on the results for the previous two families. Due to the absence of the amide bond of the guanidino carbonyl and the secondary amine of the guanidine the PSA values of the alkyl *bis*-2-imidazolines are three times and two and half times smaller, respectively. While the values may be smaller, the fact that the alkyl *bis*-2-imidazoline molecules possess the same PSA ranges indicates that the conformations should be similar. For S15430, again the PSA value is half that of **24f**. This result for the PSA value for S15430 can be easily explained through the absence of a second imidazoline group. The trend in values for S15430 can also be explained in a similar way. The molecule S15430 is structurally around a half of the molecules **24f** and **24e** when compared in structure.

Table 5.8.- Number of potential BAC identified for each molecule

Compound	Number of Conformations
24a	5
24b	2
24c	1
24d	1
24e	5
24f	2
S15430	4

As can be seen from Table 5.8 multiple potential BACs were identified for **24a**, **24b**, **24e** and **24f**. The conformations generated for **24e** and **24a** show an S shape (Figure 5.14). This makes a change compared to the general shapes of the previous two families of compounds (both broad U shapes). For the other four compounds with either one or two potential BACs the S shape is found as well (Figures 5.15 and 5.16).

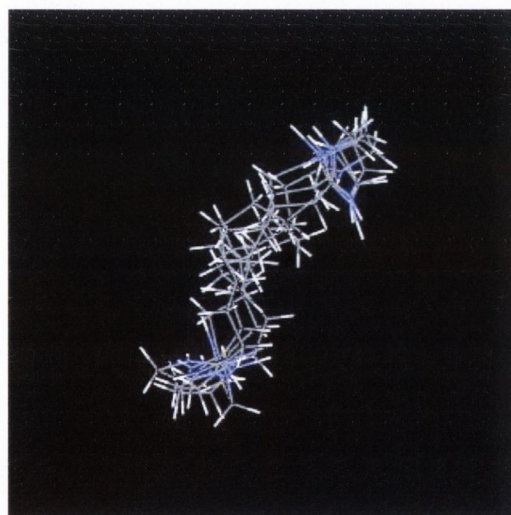
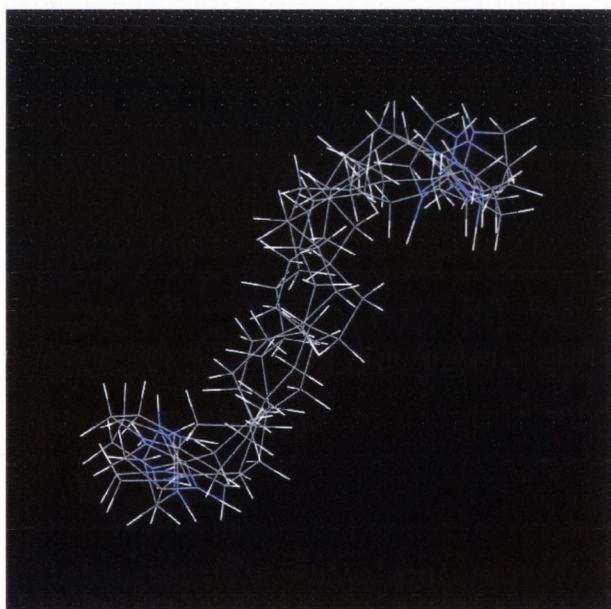


Figure 5.14.- Overlap of the BACs of **24e** (left) and **24a** (above)

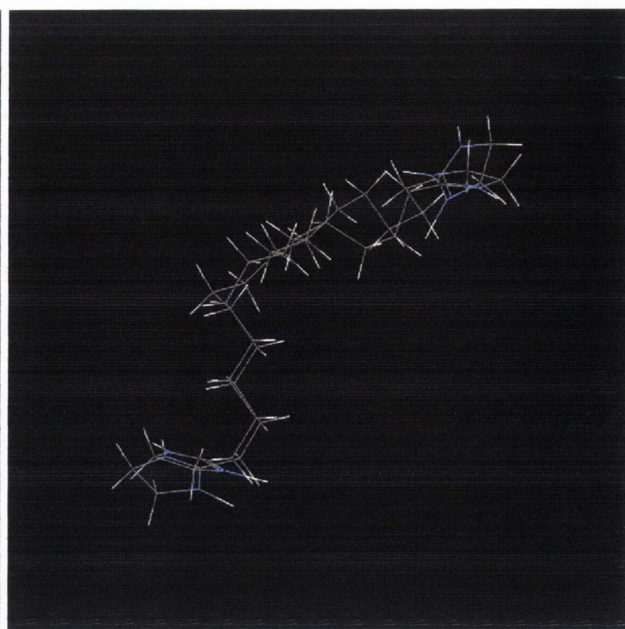
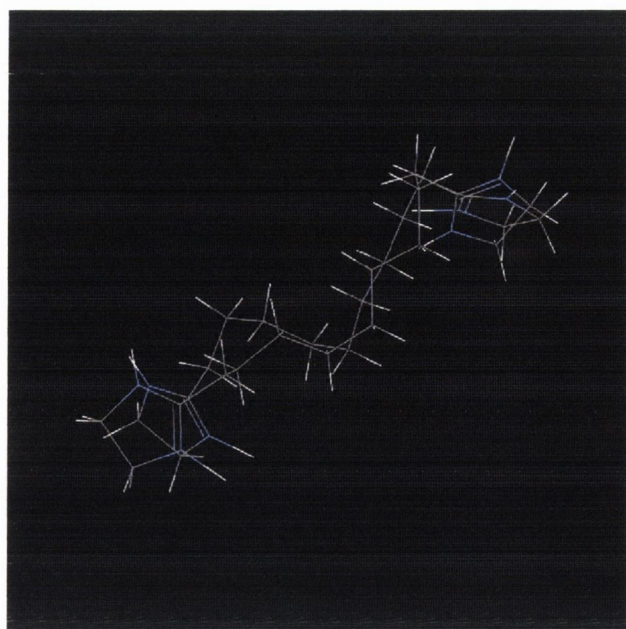


Figure 5.15a.- Overlap of the BACs of **24b** **Figure 5.15b.-** Overlap of the BACs of **24f**

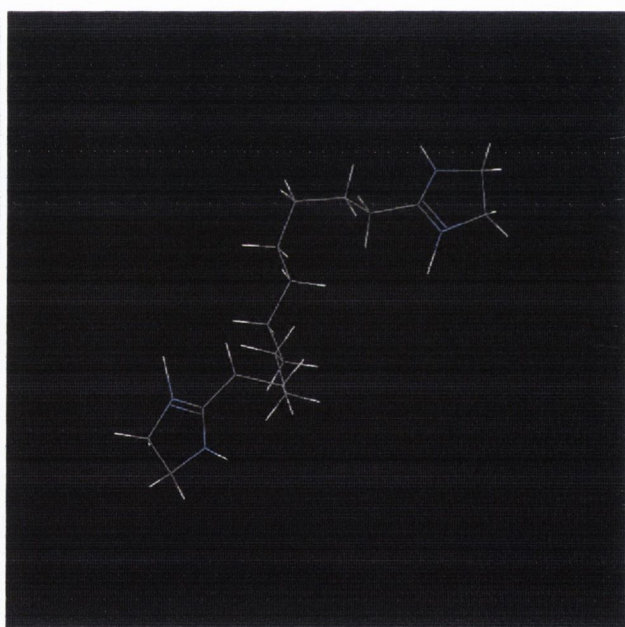
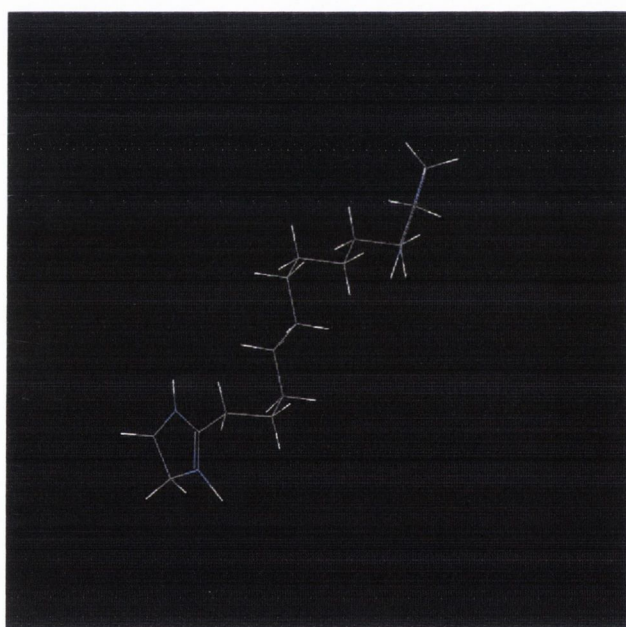


Figure 5.16a.- Overlap of the BACs of **24c** **Figure 5.16b.-** Overlap of the BACs of **24d**

By overlapping one potential BAC of each molecule the S shape can be observed (Figure 5.17a). The conformational analysis of S15430 revealed four potential BACs and from this we can see that there is a preference towards an L shape (Figure 5.17b). This L shape

can be overlapped quite easily with the S shape adopted by the alkyl *bis*-2-imidazolines (Figure 5.18).



Figure 5.17b.- BAC overlap of 24a-f

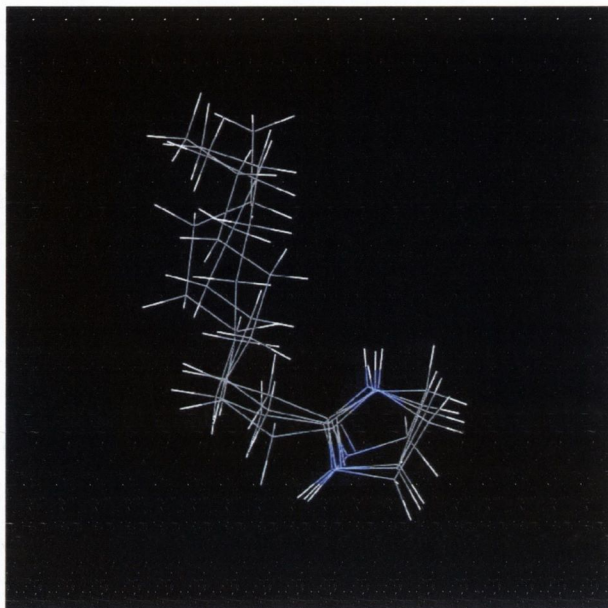


Figure 5.17b.- BAC overlap for S15430

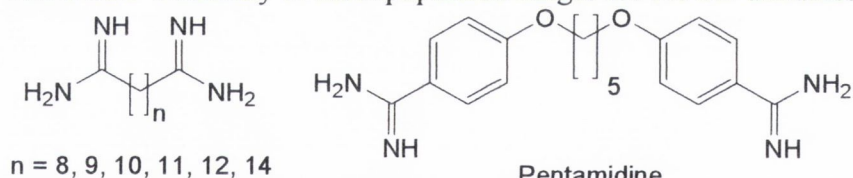


Figure 5.18.- BAC overlap 24a-f and S15430

5.6 Conformational Analysis of the alkyl bis-amidines, 25a-f

The area, volume and distance ranges, as expected, increase as the length of the methylene linker chain between the two amidine groups increases. Again there is no obvious trend in the increase of the volume and area as each CH₂ is added to the molecule (Table 5.9). The distance between the positive charges again increase by 1 Å per addition of each CH₂ (Table 5.9). These values are identical to those obtained for the alkyl bis-2-imidazolines. This result is not surprising because of the similarity in the structure of the two families, the only difference being the amidine moiety contained in a five member ring (Figure 5.19). Table 5.9 also shows the conformational analysis for the lead compound pentamidine discussed in Chapter 4. The area values for pentamidine are similar to those obtained for **25c**, while the volume values are similar to those obtained for **25e**. This was an unexpected result but looking at the value for the distance we can deduce that the molecule has an extremely curved shape. This hypothesis can also be rationalised due to the presence of the two aromatic groups in the molecule. These aromatic moieties can potentially lead to stacking.

Table 5.9.- Summary of most populated ranges for the Bis-amidines



Function	25A	25B	25C	25D	25E	25F	Pentamidine
Energy (kcal/mol)	17 – 18	16 – 17	16 – 17	16 – 18	16 – 17	16 – 17	11 – 13
Distance (Å)	8 – 10	9 – 10	10 – 11	11 – 12	12 – 13	13 – 15	4 – 5
Total Dipole (Db)	110 – 115	100 – 110	110 – 115	115 – 130	135 – 140	65 – 75	65 – 70
PSA (Å ²)	250 – 260	250 – 260	250 – 260	250 – 260	250 – 260	250 – 260	200 – 210
Volume (Å ³)	779 – 780	820 – 830	880 – 890	930 – 950	980 – 990	1120 – 1140	960 – 970
Area (Å ²)	510 – 520	520 – 540	550 – 560	580 – 590	600 – 630	670 – 680	550 – 560

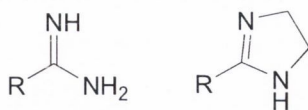


Figure 5.19.- Structure of the amidine and imidazoline functional groups

The restriction of the amidine moiety in the alkyl *bis*-2-imidazolines would also explain why the energy values of the amidines are much lower than those of the alkyl *bis*-2-imidazolines (nearly three times smaller for each molecule). The dipole moments of the alkyl *bis*-amidines are higher than those of the alkyl *bis*-2-imidazolines. This is not surprising because the free amidine moiety would be more polarised than the restricted amidine moiety of the alkyl *bis*-2-imidazolines. Thus, nitrogen atoms would exert a greater pull on the electrons of the sp^2 carbon creating a greater positive charge and thus a larger dipole moment. The energy values for pentamidine are similar to those obtained for the alkyl *bis*-2-imidazolines. Although these values are slightly lower than the alkyl *bis*-2-imidazolines they do not rule out the possibility of stacking in the molecule.

The PSA values are, again, equal across the alkyl *bis*-amidine family and are two times larger than those values obtained for the alkyl *bis*-2-imidazolines. This result can be rationalised by the unrestricted nature of the amidine moiety meaning that less of the nitrogen orbitals are involved in bonding to other atoms and are more dispersed. This in turn leads to a greater PSA. The PSA of pentamidine is similar to the PSA values for the *bis*-amidines.

Table 5.10.- Number of potential BAC identified for each molecule

Compound	Number of Conformations
25a	1
25b	10
25c	2
25d	7
25e	2
25f	1
Pentamidine	1

As can be seen from Table 5.10, **25b** to **25e** produced multiple BACs. Compounds **25b** and **25d**, the two molecules with the largest numbers of potential BACs, share the broad U shaped structure previously seen in both the alkyl *bis*-guanidines and the alkyl *bis*-guanidino carbonyl series (Figure 5.20). Similarly, compound **25c** also shows this same U structure (Figure 5.21a). Compound **25e** however, possesses the S shape structure seen for the alkyl *bis*-2-imidazolines (Figure 5.21b). Compounds, **25a** and **25f**, also share the broad U shape of **25b** and **25d** (Figure 5.22a and 5.26b, respectively).

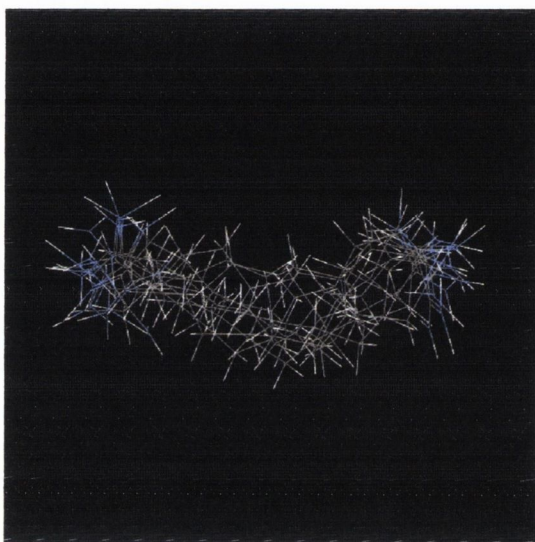


Figure 5.20a.- Overlap of the BACs of **25b**

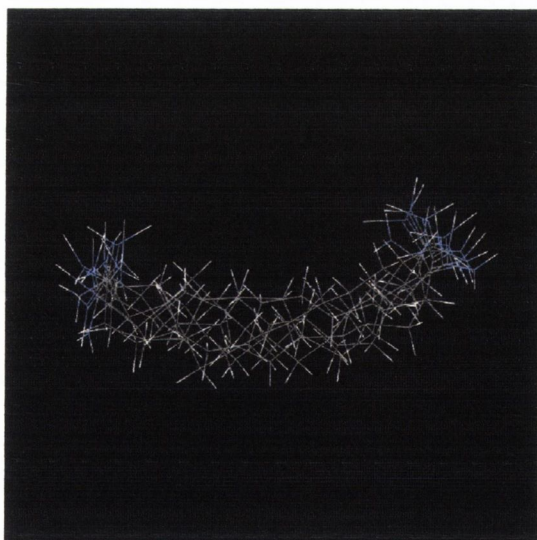


Figure 5.20b.- BACs overlap for **25d**

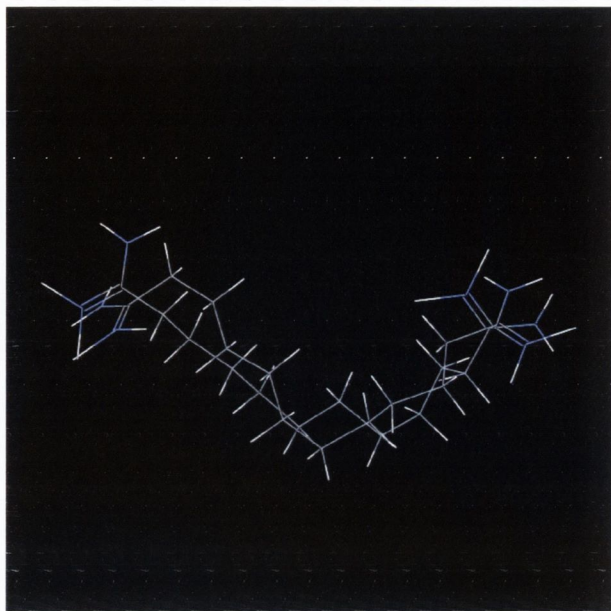


Figure 5.21a.- Overlap of the BACs of **25c**

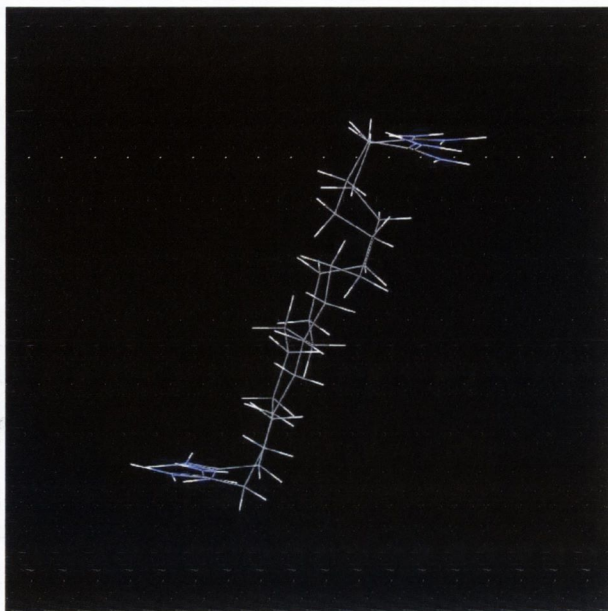


Figure 5.21b.- BACs overlap for **25e**

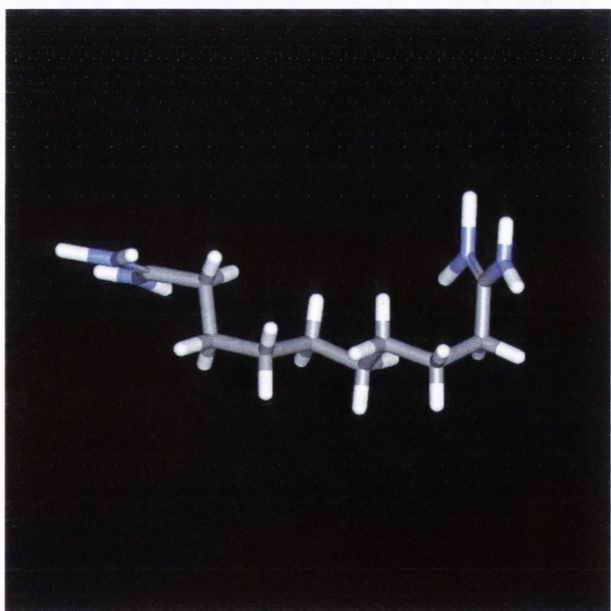


Figure 5.22a.- Overlap of the BACs of **25a**

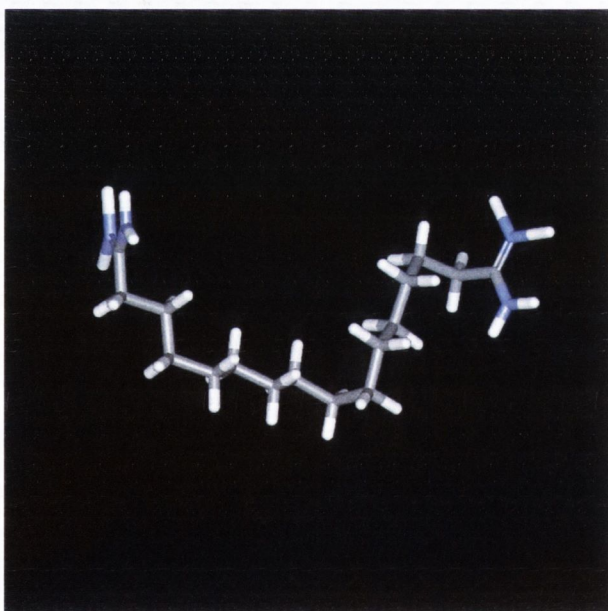


Figure 5.22b.- BACs overlap for **25f**

When overlapping a selected BAC of each molecule, the general U shape can be seen, with the exception of **25e** (Figure 5.23a). Pentamidine also exhibits a U shape, however this U shape is far more pronounced and shows the possibility of aromatic stacking in the molecule (Figure 5.23b). However, this meant that the overlap of pentamidine with the

amidine family results in a different picture to that of the alkyl *bis*-2-imidazolines and S15430.

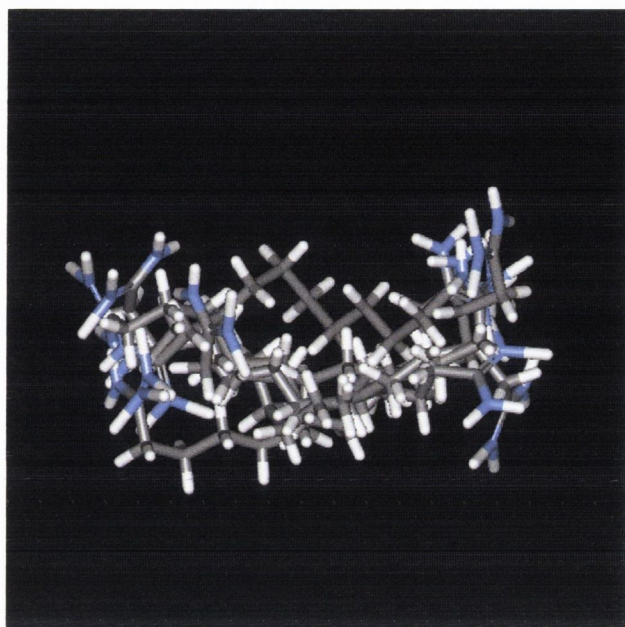


Figure 5.23a.- BAC overlap of 25a-f

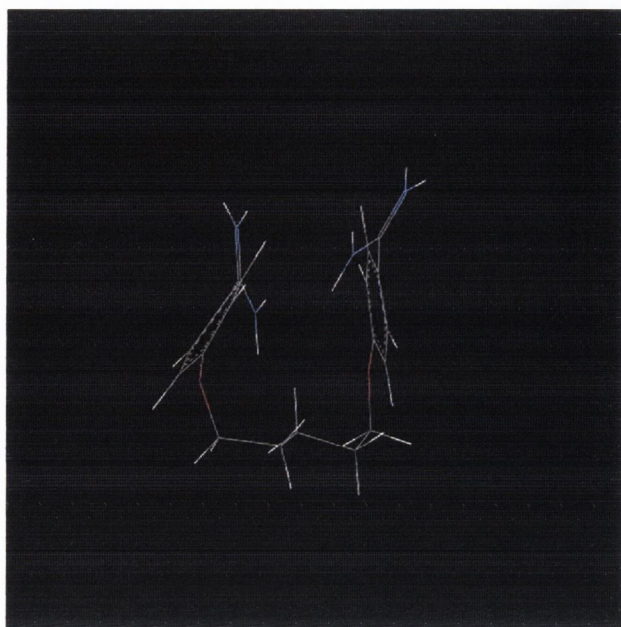


Figure 5.23b.- BAC pentamidine

5.7 Summary and Conclusions

The data obtained from the most populated ranges of parameters of each family of ligands presents several clear trends. Firstly, there is no trend to be seen in the Total Dipole of any of the molecules. Secondly, as the length of the methylene linker between the two functional groups increases, the area, volume and distance values increase as well. In the majority of cases as a CH₂ moiety is added to the linker the distance between the cationic centres increase by 1 Å. Thirdly, both the PSA and Energy cannot be used as an indicator of affinity towards I₂-IBS based on the results for pentamidine and S15430 (pK_i I₂-IBS = 7.85 and 6.9 respectively, PSA = 200 – 210 Å² and 40 – 50 Å², respectively, Energy = 11 – 13 kcal/mol and 14 – 15 kcal/mol, respectively). However, the PSA can be used as an indication of whether the ligands within a family share a similar shape.

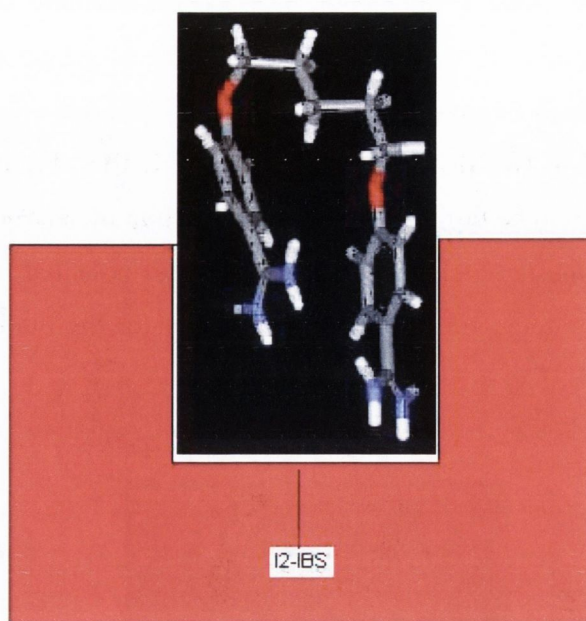


Figure 5.24.- Possible interaction of pentamidine with the I₂-IBS

From the BACs of each compound four distinctive shapes are apparent. These are U, S, W and L. The U shape is the most prevalent shape and can be found in all four families. The U shape can also be found in pentamidine. In the case of pentamidine binding to the I₂-IBS, it is likely that both amidine moieties are involved in the actual binding to the receptor. Due to the close proximity of both moieties to one another it is also likely they are binding to the same site (Figure 5.24).

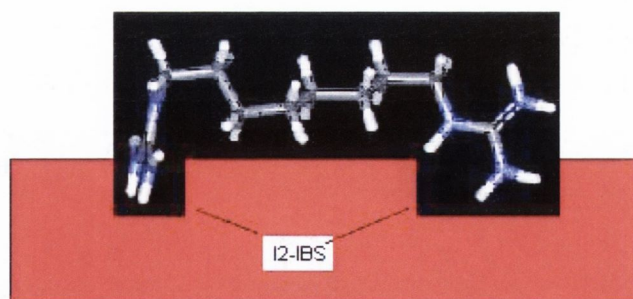


Figure 5.25.- Possible interaction of **19b** with the I₂-IBS

Based on this possible mode of interaction between Pentamidine and the I₂-IBS we can propose two possible modes of interaction between the four ligand families and the I₂-IBS. These can be seen in Figures 5.25 and 5.26. The first mode of interaction may be the binding of the ligand to two distinct sites within the I₂-IBS (Figure 5.25). The second mode of interaction could be through one functional group moiety bound to an I₂-IBS and the rest of the molecule is blocking the site from other potential ligands (Figure 5.26). The second mode of interaction offers an explanation for the binding of the molecules possessing a W, S or L shape.

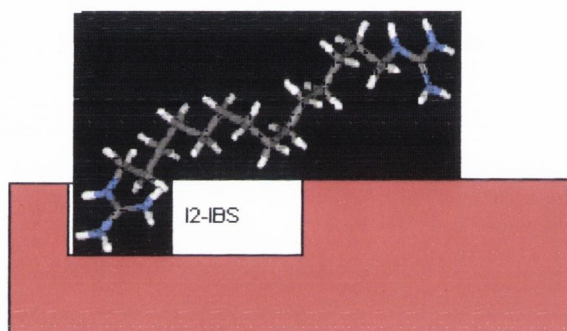


Figure 5.26.- Possible interaction of **19h** with the I₂-IBS

To confirm either of these two modes of interactions we needed to examine the biological competitive binding assays. The results of these assays shall be discussed in the next chapter.

5.8 References

185. Pigni, M.; Bousquet, P.; Brasili, L.; Carrieri, A.; Cavagna, R.; Dontenwill, M.; Gentili, F.; Giannella, M.; Leonetti, F.; Piergentili, A.; Quaglia, W.; Carotti, A. *Bioorg. Med. Chem.* **1998**, *6*, 2245.
186. Carrieri, A.; Brasili, L.; Leonetti, F.; Pigni, M.; Gianella, M.; Bousquet, P.; Carotti, A. *Bioorg. Med. Chem.* **1997**, *5*, 843.
187. Baurin, N.; Vangrevelinghe, E.; Morin-Allory, L.; Merour, J-Y.; Renard, P.; Payard, M.; Guillaumet, G.; Marot, C. *J. Med. Chem.* **2000**, *43*, 1109.
188. Beusen, D. D.; Berkley Shands, E. F.; Karasek, S. F.; Marshall, G. R.; Dammkoehler, R. A. *J. Mol. Struct.* **1996**, *370*, 157.
189. Dardonville, C.; Goya, P.; Rozas, I.; Aleusa, A.; Martin, I.; Borrego, J. *Bioorg. Med. Chem.* **2000**, *8*, 1567.
190. Sybyl 6.9 and 7.2 Molecular Modelling System, Tripos associates: St. Louis. MO.
191. Kinsella, G. K.; Watson, G.; Rozas, I. *Bioorg. Med. Chem.* **2006**, *14*, 1580.
192. Palm, K.; Luthman, K.; Ungell, A. L.; Strandlund, G.; Beigi, F.; Lundahl, P.; Artursson, P. *J. Med. Chem.* **1998**, *41*, 5382.
193. Ertl, P.; Rohde, B.; Selzer, P. *J. Med. Chem.* **2000**, *43*, 3714.
194. Web ref
195. Feher, M.; Sourial, E.; Schmidt, J. M. *Int. J. Pharmaceutics.* **2000**, *201*, 239.
196. Liu, X.; Tu, M.; Kelly, R. S.; Chen, C.; Smith, B. J. *Drug Metabolism Disposition.* **2003**, *32*, 132.

Chapter 6

Biological assay results for the alkyl bis-guanidines, alkyl bis-guanidino carbonyls, alkyl bis-2-imidazolines and alkyl bis-amidines

6.1 Introduction

As stated in Chapter 1 the objective of this thesis was three fold. Firstly, the synthesis of four new families of ligands we hoped would prove to be selective for I₂-IBS over α₂-ARs. These ligands were the alkyl *bis*-guanidines, the alkyl *bis*-guanidino carbonyls, the alkyl *bis*-imidazolines and the alkyl *bis*-amidines. Second the examination of the conformations and potential pharmacophoric elements that the ligands may have using conformational analysis. Using the results generated by the conformational analysis we then wanted to examine possible characteristics and/or shapes that the ligands may share in common to generate a SAR. Finally, the biological evaluation of the compounds synthesized as potential I₂-IBS ligands. This would allow us to further develop the SAR and possible interaction pattern of the compounds with the I₂-IBS.

To evaluate the compounds as potential I₂-IBS ligands competitive binding assays against either the selective I₂-IBS radioligand [3H]-2-BFI or against the α₂-AR radioligand [3H]-RX821002 (Figure 6.1). The tests were performed using the frontal cortex of *post mortem* human brain tissue because this tissue is rich in I₂-IBS.¹⁹⁷⁻¹⁹⁹ From these tests the inhibition constant (K_i) was obtained and are expressed as the corresponding pK_i in the tables throughout this chapter. In all cases Idazoxan (pK_i I₂-IBS = 8.37, pK_i α₂-ARs = 7.72 I₂-IBS/α₂-AR selectivity = 1.35, Figure 6.1) was used as a reference value. The compounds with a high affinity towards I₂-IBS ($pK_i \geq 6$) were also tested for their I₂-IBS/α₂-AR selectivity. The I₂-IBS/α₂-AR selectivity was calculated using the antilog of the difference between the pK_i I₂-IBS and the pK_i α₂-ARs (i.e. $\text{antilog}(pK_i \text{ I}_2\text{-IBS} - pK_i \text{ } \alpha_2\text{-ARs})$).

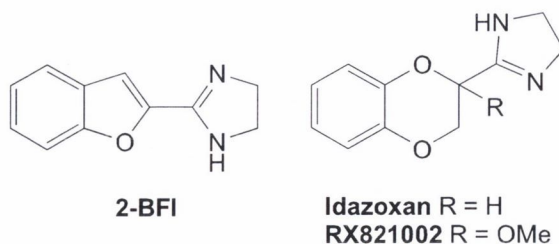


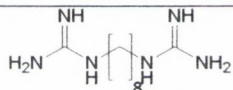
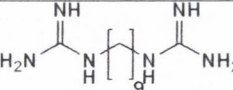
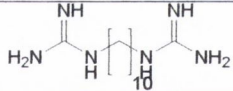
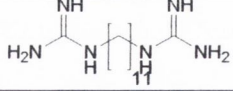
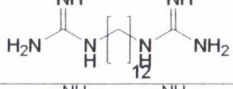
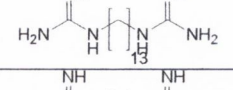
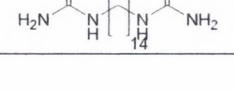
Figure 6.1.- Structures of 2-BFI, Idazoxan and RX821002

The results of these competitive binding assays and their impact on the possible mode of interaction with the I₂-IBS will be discussed in the following sections. A SAR will also be proposed.

6.2 Biological results for the alkyl *bis*-guanidines series of compounds, 19a-h

The competitive binding assay results for the alkyl *bis*-guanidines are summarized in Table 6.1. The alkyl *bis*-guanidines previously synthesized by our group are marked with an asterisk (*). From the trend seen in the original alkyl *bis*-guanidines synthesized we would like to verify if by increasing the length of the methylene linker the affinity towards the I₂-IBS would increase. The values presented in Table 6.1 show that this trend is indeed observed for all the alkyl *bis*-guanidines with the exception of 19h. This data indicates that there may be an optimum chain length of 13 methylene moieties.

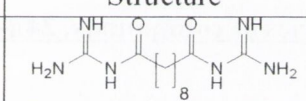
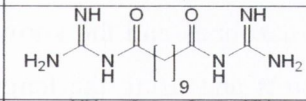
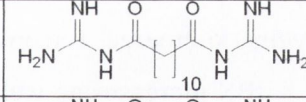
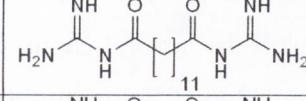
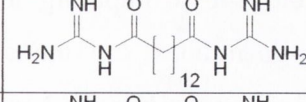
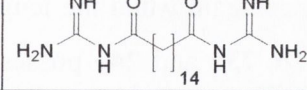
Table 6.1.- Summary of the competitive binding assays for the alkyl *bis*-guanidines

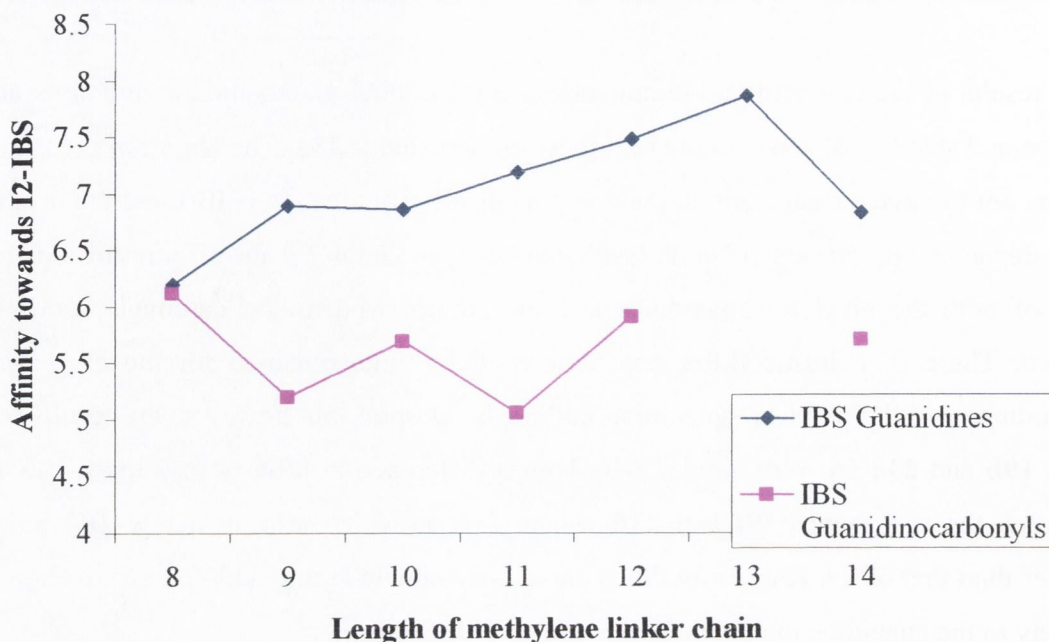
Name	Structure	pK _i I ₂ -IBS	pK _i α ₂ -ARs	Selectivity I ₂ -IBS/α ₂ -ARs
19b		6.20*	6.26*	0.87*
19c		6.89*	6.07*	6.61*
19e		6.86		
19f		7.19		
19d		7.48*	6.29*	15.49*
19g		7.86		
19h		6.82		

6.3 Biological results for the alkyl *bis*-guanidino carbonyl series of compounds, 23a-f

The results of the competitive binding assays for the alkyl *bis*-guanidino carbonyls are shown in Table 6.2. The most potent of these compounds is **23a**. The length of the chain seems not to have a clear trend in the compounds affinity towards I₂-IBS and the results vary depending on this chain length (see Graph 6.1). In Graph 6.1 the affinity towards I₂-IBS of both the alkyl *bis*-guanidines and the alkyl *bis*-guanidino carbonyls series is shown. There is a drastic difference between the results obtained for the alkyl *bis*-guanidines and the alkyl *bis*-guanidino carbonyls. Despite this however, the results for both **19b** and **23a** are very similar. The largest difference in affinity towards I₂-IBS is between the compounds **19f** and **23d**, where **19f** shows an affinity nearly 100 times higher than that of the **23d**. From this data we may conclude that addition of a carbonyl moiety to the guanidine moiety is detrimental to I₂-IBS affinity.

Table 6.2.- Summary of the competitive binding assays for the alkyl *bis*-guanidino carbonyls

Name	Structure	pK _i I ₂ -IBS	pK _i α ₂ -ARs	Selectivity I ₂ -IBS/α ₂ -ARs
23a		6.11	5.12	10
23b		5.20	nt	nt
23c		5.69	nt	nt
23d		5.06	nt	nt
23e		5.91	nt	nt
23f		5.70	nt	nt

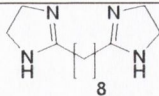
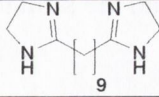
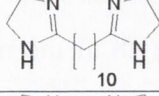
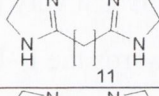
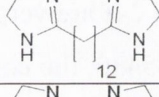
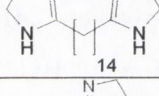
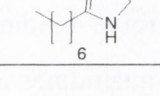


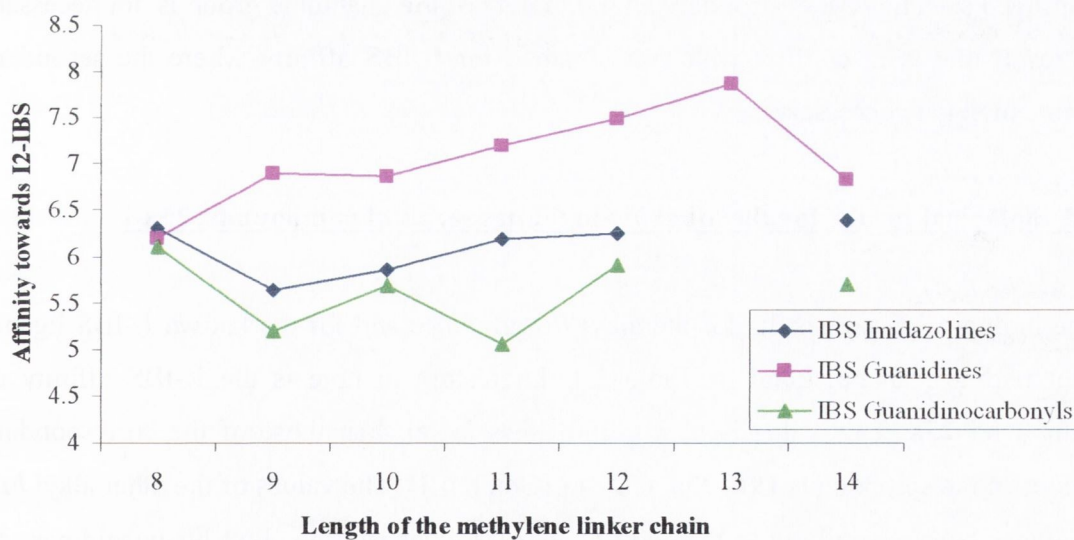
Graph 6.1.- Affinity of both the alkyl *bis*-guanidines and the alkyl *bis*-guanidino carbonyls towards I₂-IBS

6.4 Biological results for the alkyl *bis*-imidazolines series of compounds, 24a-f

The results of the biological testing of the alkyl *bis*-imidazolines and the known I₂-IBS ligand S15430 are shown in Table 6.3. From these results and using the length of the methylene linker chain as an indicator a general trend seems to emerge. Except for **24a**, as the length of the chain increases the affinity towards I₂-IBS increases as well. Unlike the alkyl *bis*-guanidine series however, the compound with the longest chain, **24f**, does not show lower affinity towards I₂-IBS than compound **24e**. Comparing the I₂-IBS affinities of the alkyl *bis*-imidazolines, the alkyl *bis*-guanidines and the alkyl *bis*-guanidino carbonyls (see Graph 6.2), we can see that once again when the length of the methylene linker chain is eight all three compounds **19b**, **23a** and **24a** possess similar affinity. The other alkyl *bis*-imidazolines show higher affinity values than those of the corresponding alkyl *bis*-guanidino carbonyls but these values are nearly 10 times lower than those of the alkyl *bis*-guanidines. This may indicate the importance of the secondary amine moiety of the guanidine molecule to I₂-IBS affinity (Figure 6.2).

Table 6.3.- Summary of the competitive binding assays for the alkyl *bis*-imidazolines

Name	Structure	pK_i I ₂ -IBS	pK_i α_2 -ARs	Selectivity I ₂ -IBS/ α_2 -ARs
24a		6.30	4.23	117
24b		5.64	nt	nt
24c		5.86	nt	nt
24d		6.19	4.60	39
24e		6.25	4.22	107
24f		6.38	3.56	661
S15430		6.90	<4	794



Graph 6.2.- Affinity of the alkyl *bis*-guanidines, the alkyl *bis*-guanidino carbonyls and the alkyl *bis*-imidazolines towards I₂-IBS

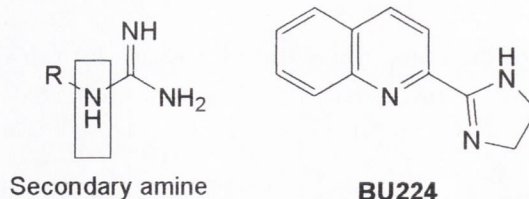


Figure 6.2.- The secondary amine moiety of a guanidine and the structure of BU224

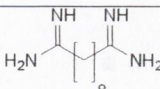
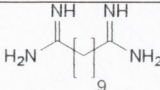
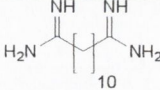
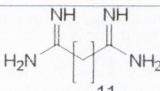
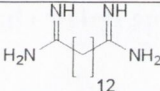
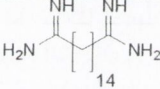
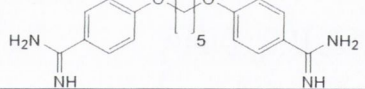
The affinity of the alkyl *bis*-imidazolines towards the α_2 -ARs is also shown in Table 6.3. The results show that, with the exception of **24a**, as the length of the methylene linker chain increases the affinity towards the α_2 -ARs decreases. This is a very promising result because when the selectivity of the alkyl *bis*-imidazolines towards the I_2 -IBS over the α_2 -ARs is calculated (see Table 6.3) they show that **24a**, **24e** and **24f** are very selective. Both **24a** and **24e** possess a similar selectivity to that shown by S15430, the compound used as a basis for the synthesis of the alkyl *bis*-imidazolines. However, **24f** possesses near identical selectivity as shown by S15430 and close to that of BU224 (Figure 6.2, selectivity $I_2/\alpha_2 = 832$, the compound used in the competitive binding assays). This result, when compared to the available data for the alkyl *bis*-guanidines indicates that for improved selectivity the secondary amine moiety of the guanidine group is not necessary (a result that is in conflict with that obtained for I_2 -IBS affinity where the secondary amine moiety is necessary).

6.5 Biological results for the alkyl *bis*-amidines series of compounds, 25a-f

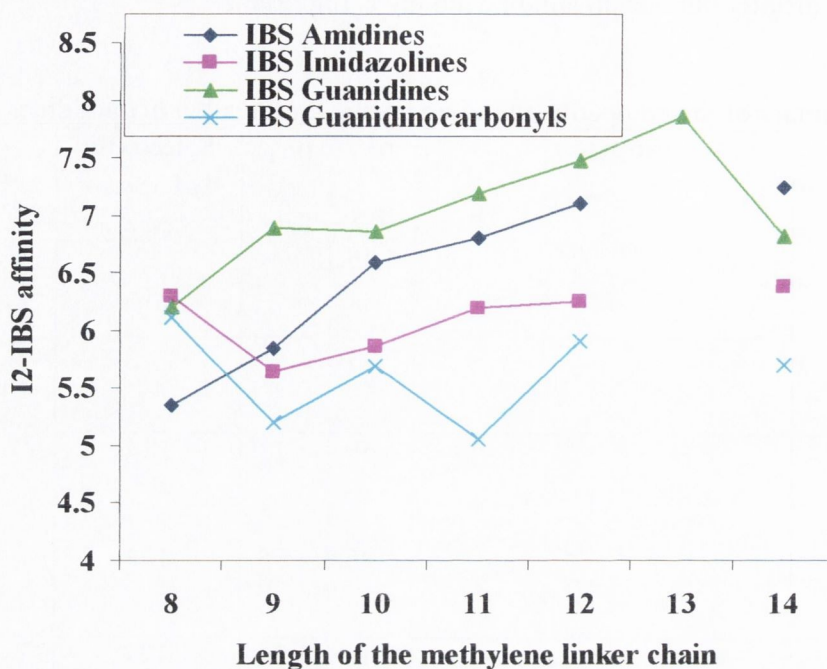
The biological assay results for the alkyl *bis*-amidines and for the known I_2 -IBS ligand, pentamidine, can be found in Table 6.4. Interesting to note is the I_2 -IBS affinity of compound **25a**. This value is nearly 200 times lower than those of the corresponding values of the compounds **19b**, **23a** and **24a** (Graph 6.3). The values of the other alkyl *bis*-amidines behave similarly to the alkyl *bis*-imidazolines and the alkyl *bis*-guanidines. As the length of the methylene linker chain increases the affinity towards I_2 -IBS also increases (see Graph 6.3). However, unlike the alkyl *bis*-imidazolines (whose I_2 -IBS affinity values are 10 times lower than those of the alkyl *bis*-guanidines) the I_2 -IBS affinity values of the alkyl *bis*-amidines are similar to those of the alkyl *bis*-guanidines.

This result shows that the secondary amine moiety of the guanidine group is not important for I₂-IBS affinity but that an amidine moiety is important.

Table 6.4.- Summary of the competitive binding assays for the alkyl *bis*-amidines

Name	Structure	p <i>K</i> _i I ₂ - IBS	p <i>K</i> _i α ₂ - ARs	Selectivity I ₂ -IBS/α ₂ - ARs
25a		5.35		
25b		5.84		
25c		6.59	4.22	234
25d		6.80	4.55	178
25e		7.10	4.56	347
25f		7.24	4.14	1259
Pentamidine		7.85		

Unlike the alkyl *bis*-imidazolines as the length of the methylene linker chain increases in length the affinity towards α₂-ARs does not decrease, rather there appears to be no clear trend. Both **25d** and **25e** possess higher affinities towards α₂-ARs than **25c** and **25f**. This result is reflected in the I₂-IBS/α₂-AR selectivity values of these molecules. Compound **25d** has a lower selectivity value than both **25c** and **25e**. Compared to any of the aliphatic twin derivatives synthesized, **25f** shows an unprecedented selectivity value of 1259. This value is nearly twice of that of the alkyl *bis*-imidazoline **24f**. The other alkyl *bis*-amidines show higher selectivity values compared to their corresponding alkyl *bis*-imidazolines. From this data we may conclude that an unrestricted free amidine moiety is important for I₂-IBS/α₂-AR selectivity compared to the restricted amidine moiety of the imidazoline group.



Graph 6.3.- Affinity of the alkyl *bis*-guanidines, the alkyl *bis*-guanidino carbonyls, the alkyl *bis*-imidazolines and the alkyl *bis*-amidines towards I₂-IBS

6.6 Structure Activity Relationships I₂-IBS affinity

To further pursue a SAR between the four families of ligands and to support the hypotheses suggested at the conclusion of the previous section we combined the data from Tables 6.1 – 6.4 into a new table (Table 6.5) based on the ranges of I₂-IBS and of α_2 -AR affinities.

Table 6.5.- Ligands used to create SAR for I₂-IBS/ α_2 -ARs selectivity

I ₂ -IBS affinity ranges	α_2 -AR affinity ranges	Ligand name	Total number of ligands
5 – 6	-	23b-f, 25a-b, 24b-c	9
6 – 7	-	19b-c, 19h, 23a, 24a, 24d-f, 25c-d	11
7 +	-	19f-g, 25e-f	5
-	3 – 4	24f	1
-	4 – 5	24a, 24d-e, 25c-f	7
-	5 – 6	23a	1
-	6 – 7	19b-c, d	3

I₂-IBS pKi range between 5 – 6

From Table 6.5 we can propose two SARs, first, for I₂-IBS affinity and, second, for I₂-IBS/ α_2 -ARs selectivity. Regarding I₂-IBS affinity, a general trend can be observed. The presence of a carbonyl moiety added to a guanidine group lowers the I₂-IBS affinity no matter the length of the aliphatic chain linking the two groups. If we look at all the BACs of the guanidino carbonyls overlapped we can see that, there are is very little conformational similarities between the conformations (Figure 6.3). This would support the hypothesis that the guanidino carbonyl functional group is not a suitable functional group for I₂-IBS binding. However, short chain molecules bearing an imidazoline group or an amidine group at both ends also display low affinity towards I₂-IBS. This may indicate that there is an optimum aliphatic chain length for both families.

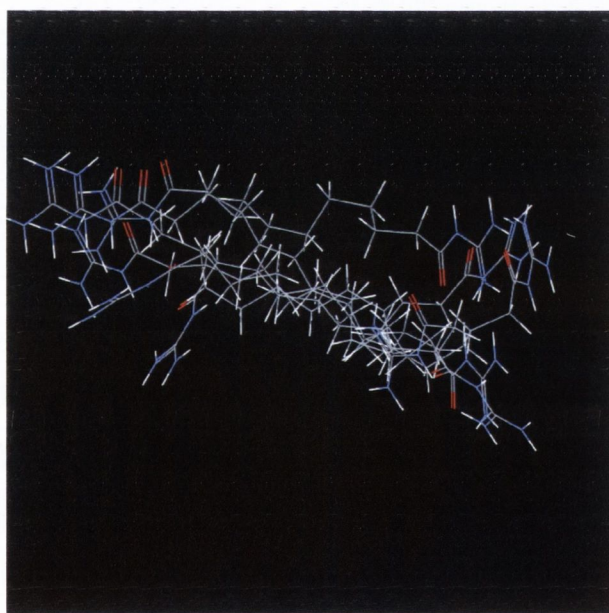


Figure 6.3.- BAC overlap of 23a-f

I₂-IBS pK_i range between 6 – 7

The presence of an imidazoline group at the end of long aliphatic chains increases the affinity towards I₂-IBS. It also appears that the chain length reaches an optimum length of either 12 or 13 methylene groups for I₂-IBS affinity (Table 6.3). For the alkyl *bis*-amidines prepared here, however, an optimum chain length has not yet been reached. In the case of the guanidine ligands an optimum chain length for I₂-IBS affinity has been achieved and it lies within the ligands **19f-g**, since the affinity towards I₂-IBS of **19h** is lower than all three. Overlapping the BAC of ligands **19a-b**, **24a**, **24c-f**, **25c-d** we can see that all six molecules adapt a similar disposition for the alkyl chain but the orientation of the functional groups differ.

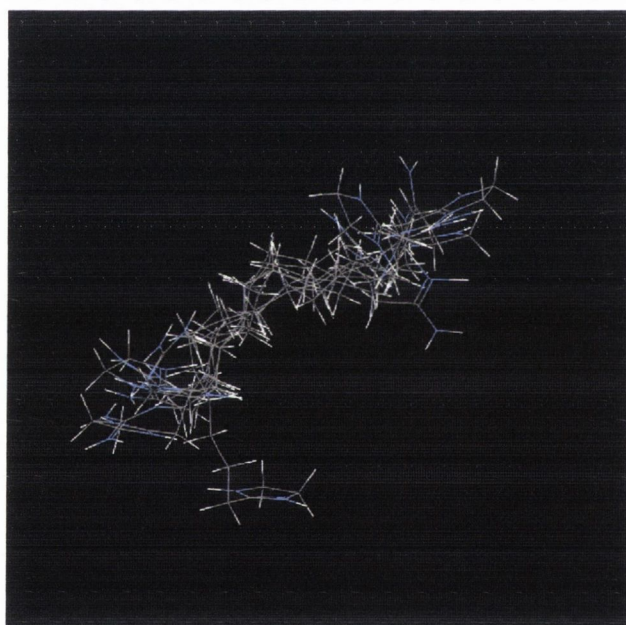


Figure 6.4.- BAC overlap of 19a-b, 24a, 24c-f, 25c-d

I₂-IBS pK_i range of 7+

For the best I₂-IBS affinity either an amidine or guanidine moiety seems to be required at both ends of long aliphatic chains. The fact that the guanidine functional group includes an amidine moiety confirms this observation (Figure 6.5). Also, the overlapping of the

BACs of the compounds within this range, once again reveals conformational similarities between the ligands at least in the linker sections (Figure 6.6).

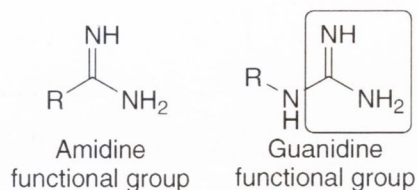


Figure 6.5.- The guanidine and amidine functional groups

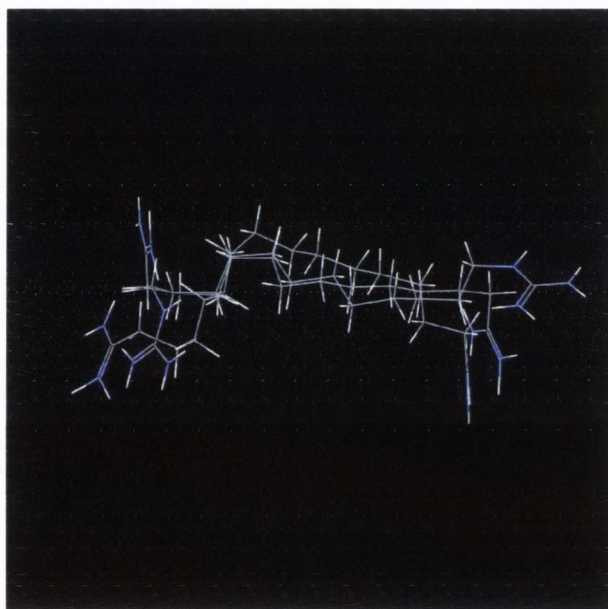


Figure 6.6.- BAC overlap of **19f-g** and **25e-f**

From this data we may conclude the following:

- 1) In general the order for increasing affinity towards I₂-IBS for ligand functional groups is the following guanidino carbonyl < imidazolines < guanidines = amidines.
- 2) Using length and functional groups as an indicator of I₂-IBS affinity the following increasing order is observed guanidino carbonyl of any length = amidine with a chain length of 8 or 9 methylene chain = imidazoline with a 9 or 10 methylene chain < imidazoline with a 11 to 14 methylene chain = amidine with a 10 or 11

chain = guanidine with a 8 or 9 or 14 chain < guanidines with a 11 to 13 chain = amidine with a 12 to 14 chain.

6.7 Structure Activity Relationship I₂-IBS/ α_2 -ARs selectivity

Since only ligands with an I₂-IBS pK_i affinity greater than six were tested for their affinity towards α_2 -ARs, this narrowed the set of ligands that could be used to produce a SAR for I₂-IBS selectivity over α_2 -ARs (Table 6.6).

Table 6.6.- ligands used to create SAR for I₂-IBS/ α_2 -ARs selectivity

Ligand name	I ₂ -IBS pK _i ranges	α_2 -AR pK _i ranges	I ₂ -IBS/ α_2 -ARs selectivity
23a	6 – 7	5 – 6	10
19b	6 – 7	6 – 7	0.87
19c	6 – 7	6 – 7	6.61
19d	7 – 8	6 – 7	15.49
24a	6 – 7	4 – 5	117
24d	6 – 7	4 – 5	39
24e	6 – 7	4 – 5	107
24f	6 – 7	3 – 5	661
25c	6 – 7	4 – 5	234
25d	6 – 7	4 – 5	178
25e	7 – 8	4 – 5	347
25f	7 – 8	4 – 5	1259

From Table 6.6 a general trend for selectivity regarding functional groups is observed. This data indicates that both the guanidine and guanidino carbonyl functional groups possess medium affinity towards α_2 -ARs. Both the imidazoline and amidine functional groups, however, show low affinity towards α_2 -ARs. The general trend appears to be in order of decreasing affinity towards α_2 -ARs guanidine < guanidino carbonyl < imidazolines = amidines. This may indicate the importance of the secondary amine moiety of both the guanidino carbonyl and the guanidine functional groups (Figure 6.7) to α_2 -AR binding.

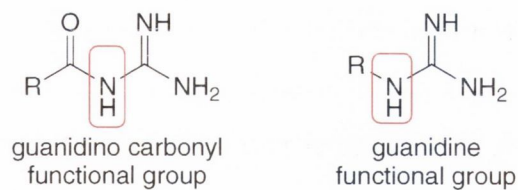


Figure 6.7.- The secondary amine of both the guanidine and guanidino carbonyl functional groups

What is clear is that the absence of this secondary amine lowers the affinity towards α_2 -ARs, thus increasing the selectivity of the ligands towards I₂-IBS over α_2 -ARs. In particular if we examine **24e** and **25e** we can see that, as stated in the previous section, while the affinity towards α_2 -ARs remains similar, the affinity towards I₂-IBS increases upon the removal of the ethylene moiety of the imidazoline ring. Also, if we examine the BACs of these ligands we observe that both possess nearly identical shapes (Figure 6.8). This data further supports the theory that the secondary amine (Figure 6.7) is important for α_2 -AR binding but not for I₂-IBS binding.

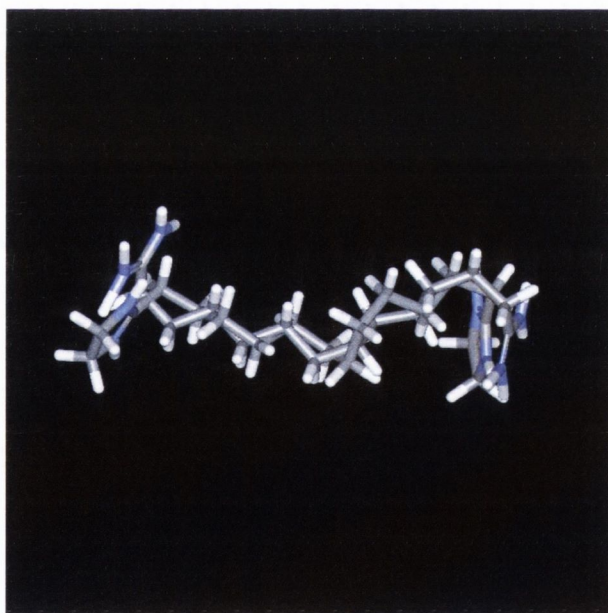


Figure 6.8.- BAC overlap of **24e** and **25e**

Another trend regarding the length of the alkyl chain linking the two functional groups can be seen. In general, as the length of this linker increases the I₂-IBS/ α_2 -ARs selectivity also increases. The rise in selectivity is due to an increase in the affinity towards I₂-IBS rather than a reduction in the affinity towards α_2 -ARs. The affinity towards the α_2 -ARs remains within the same range according to the ligand family despite any increment in the length of the alkyl linker chain. This may indicate that length is a factor involved in the binding of the ligand to the I₂-IBS but not for α_2 -ARs binding. Further evidence linking the length of the alkyl chain and binding to the I₂-IBS can be seen in the increase of the selectivity of both the imidazolines and amidines as the length of the linker increases (Table 6.7).

Table 6.7.- Imidazoline vs Amidine biological results based on chain length

Chain length (CH ₂) _n n =	Amidine I ₂ -IBS pK _i	Imidazoline I ₂ -IBS pK _i	Amidine α_2 -ARs pK _i	Imidazoline α_2 -ARs pK _i	Amidine I ₂ -IBS/ α_2 -ARs Selectivity	Imidazoline I ₂ -IBS/ α_2 -ARs Selectivity
8	5.35	6.30		4.23		117
9	5.84	5.64				
10	6.59	5.86	4.22		234	
11	6.80	6.19	4.55	4.60	178	39
12	7.10	6.25	4.56	4.22	347	107
14	7.24	6.38	4.14	3.56	1259	661

From this table we clearly see an increase in the selectivity as the length of the alkyl chain increases. It would also appear that further increases to the alkyl chain may be tolerated with the exception of the alkyl *bis*-guanidines. Of this family **19g** showed the best affinity and **19d** the best selectivity. This data supports both modes of interaction proposed in the previous chapter. The ligands may bind to one I₂-IBS or they may be binding to two I₂-IBS. For the ligand to bind to one I₂-IBS we may envisage one functional group bound to the receptor while the remaining part of the ligand blocks the unbound part of the receptor from other ligands (Figure 6.9b). For the ligand to bind to two separate I₂-IBS we may picture each functional group bound to two different receptor sites (Figure 6.9a). However, it may also be possible that when a ligand binds to the I₂-IBS both modes of interaction are presented depending on the length of the ligand. If this is the case, it may explain the large jump in the selectivity for I₂-IBS over α_2 -ARs for the

ligands **24f** and **25f** compared to **24e** and **25e**, respectively. Due to the absence of alkyl *bis*-imidazoline and alkyl *bis*-amidine with 13 methylene linkers we cannot confirm this hypothesis.

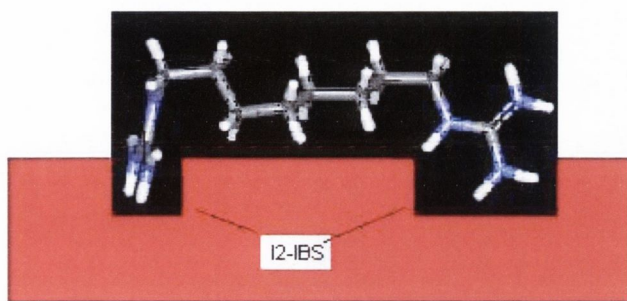


Figure 6.9a.- Mode of Interaction 1

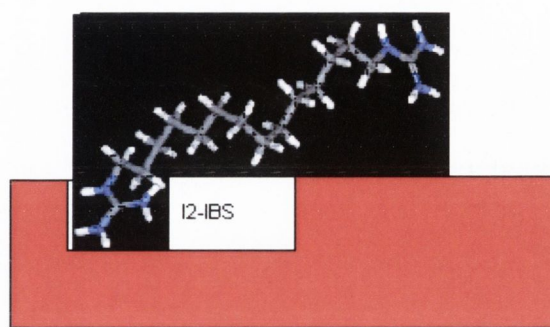


Figure 6.9b.- Mode of Interaction 2

6.8 Summary and conclusions

In summary, for I₂-IBS affinity the best results were produced by the alkyl *bis*-amidines and the alkyl *bis*-guanidines followed by the alkyl *bis*-imidazolines and then the alkyl *bis*-guanidino carbonyl series. This trend could be further separated into the following order: all alkyl *bis*-guanidino carbonyls = short linker alkyl *bis*-amidines = short linker alkyl *bis*-imidazoline < medium sized linker alkyl *bis*-imidazolines = medium sized linker alkyl *bis*-amidine = short linker alkyl *bis*-guanidines and longer linker alkyl *bis*-guanidines < medium linker alkyl *bis*-guanidines = long linker alkyl *bis*-amidines.

The best results for I₂-IBS/ α_2 -ARs selectivity were obtained for the long chain alkyl *bis*-amidines and *bis*-imidazolines. These results indicated that the secondary amine moiety of the alkyl *bis*-guanidines and the amide moiety of the alkyl *bis*-guanidino carbonyls were unnecessary for I₂-IBS binding and that their absence increased selectivity over the α_2 -ARs. The results also showed that the free amidine functional group produced higher affinity and better selectivity for the I₂-IBS over the restricted amidine within the imidazoline functional group.

Finally, the biological data of all the Ligands synthesized did not support one mode of interaction with the I₂-IBS over another. Rather, it may suggest that both modes of interaction are possible depending on the alkyl linker length.

6.9 References

197. Garcia-Sevilla, J. A.; Escriba, P. V.; Sastre, M.; Walzer, C.; Busquets, X.; Jaquet, G.; Reis, D. J.; Guimon, X. J. *Arch. Gen. Psychiatry* **1996**, *53*, 803.
198. Ruiz, J.; Martin, I.; Callado, L. F.; Meana, J. J.; Barturen, F.; Garcia-Sevilla, J. *A. Neurosci. Lett.* **1993**, *160*, 109.
199. Miralles, A.; Olmos, G.; Sastre, M.; Barturen, F.; Martin, I.; Garcia-Sevilla, J. *A. J. Pharmacol. Exp. Ther.* **1993**, *264*, 1187.

Chapter 7

Thesis Summary and Future Work

7.1 Synthesis of the ligands in Chapters 2-4

The I₂-IBS is a binding site that is widely distributed throughout both animal and human bodies. They have been located in the lung,¹⁷ adipocytes,¹⁸ placenta,¹⁹ pancreatic islet,²⁰ adrenal chromaffin cells,¹⁵ as well as the CNS.²¹ The highest density of I₂-IBS can be found in the adipocytes,¹⁸ liver, kidney and brain.¹⁹ Previous research by our group reported the synthesis of four alkyl *bis*-guanidines, **19a-d**.¹⁰¹ When the I₂-IBS / α_2 -ARs selectivity of these four ligands was represented the results indicated that as the length of the linker chain increases the I₂-IBS / α_2 -ARs selectivity increases as well.

The first aim of this thesis was the synthesis of longer alkyl *bis*-guanidines, **19e-g** and **29c**, to investigate if this trend between affinity and selectivity continued. Using synthetic routes previously developed by Rozas' group the alkyl *bis*-guanidines **19e-g** were prepared but only moderate yields were obtained. To synthesize **29c** a reaction using the Mitsunobu protocol was used. This produced the Boc protected guanidine in 75% yield and after deprotection using TFA the hydrochloride salt **29c** was isolated in an overall yield of 39% after four steps. Attempts to prepare longer chain alkyl *bis*-guanidines were unsuccessful.

After the synthesis of the of the alkyl *bis*-guanidines a new family of ligands, the alkyl *bis*-guanidino carbonyls, was prepared. The first attempt at the synthesis of these ligands only produced the desired compounds in low yield using sodium methoxide and guanidine hydrochloride (9-17%). Reacting a carboxylic acid with guanidine hydrochloride in the presence of a coupling reagent (CDI) produced the desired derivatives in a much higher yield (47-53%). Converting the alkyl *bis*-guanidino carbonyls into their corresponding salts produced mixed yields (3-77%). The final approach to the synthesis of the alkyl *bis*-guanidino carbonyls was the reaction of the carboxylic acids with a Boc protected guanidine, **33**, again in the presence of a coupling reagent (BOP). This produced the Boc protected alkyl *bis*-guanidino carbonyls, **43a-f**, in good yield (62-87%). Deprotection of these compounds produced the hydrochloride salts in a good overall yield (57-76%).

Before attempting to prepare the alkyl *bis*-imidazolines we decided to use an aromatic carboxylic acid as a precursor to test possible reaction pathways. The first reaction scheme was based on the work of Casey *et al.*¹⁷³ and we attempted to synthesize the alkyl *bis*-imidazolines by means of an intramolecular substitution reaction. Unfortunately, this reaction was unsuccessful. The aromatic imidazoline, **44**, was prepared by reacting the aromatic ester, **49**, with ethylene diamine and trimethylaluminium (50%). Adaptation of this procedure for the case of alkyl *bis*-methyl esters, **35a-f**, resulted in the alkyl *bis*-2-imidazolines, **24a-f**, in moderate yields (26-77%). Washing the compounds with oxalic acid yielded the corresponding salts, **51a-f** (78-93%). The final family of ligands, the alkyl *bis*-amidines **25a-f**, were synthesized using the same procedure as the alkyl *bis*-2-imidazolines, replacing ethylene diamine with ammonium hydrochloride. This reaction produced the salts in excellent yields (73-80%).

7.2 Conformational analysis, biological assay results and subsequent SAR

The random conformational analyses performed showed that, within each family of ligands, as the length of the methylene linker increases the area, volume and distance values increase as well. It also revealed that neither the PSA nor the energy values of the conformations can be used as indicators of potential affinity towards I₂-IBS. Examination of the results of the random conformational analysis showed that four distinct shapes (U, S, W and L shapes) were prevalent. The U shape is the most common form and can be found in all four families. Based on the results obtained for pentamidine binding to the I₂-IBS, it is likely that both amidine moieties are involved in the actual binding to one receptor. Based on this hypothesis we proposed two possible modes of interaction between the four ligand families and the I₂-IBS. The first mode of interaction may be the binding of the ligand to two distinct sites within the I₂-IBS. The second mode of interaction could occur through the binding of only one functional group to an I₂-IBS while the rest of the molecule would be blocking the site from other potential ligands.

The biological results of the four ligand families could not rule out either possible mode of interaction. It did, however, produce some excellent results. The alkyl *bis*-2-imidazolines **24a,e-f** and the alkyl *bis*-amidine **25e** proved to be highly selective towards the I₂-IBS over the α_2 -ARs. The results for these ligands matched and improved those of S15430 and pentamidine the precursor ligands for both families. The best result was obtained by the ligand **25f** which proved to be 1259 times more selective for the I₂-IBS than for the α_2 -ARs.

The overall biological assay results for the four ligand families indicated that:

- 1) the best results were produced by the alkyl *bis*-amidines and the alkyl *bis*-guanidines followed by the alkyl *bis*-imidazolines and then the alkyl *bis*-guanidino carbonyls.
- 2) this trend could be further separated into the following order: all alkyl *bis*-guanidino carbonyls = short chain alkyl *bis*-amidines = short chain alkyl *bis*-imidazoline < medium sized chain alkyl *bis*-imidazolines = medium sized chain alkyl *bis*-amidine = short chain alkyl *bis*-guanidines = longer chain alkyl *bis*-guanidines < medium chain alkyl *bis*-guanidines = long chain alkyl *bis*-amidines.

7.3 Future work

One of the aims of this thesis was the synthesis and biological evaluation of a series of alkyl *bis*-guanidines. Thus, the alkyl *bis*-guanidines **19e-g** and **29b** were prepared and their affinity towards I₂-IBS measured. However, their affinity towards the α_2 -AR has yet to be determined. Therefore, a clear continuation of this research should be the evaluation of their affinity towards α_2 -ARs, to determine their selectivity, moreover, to be able to complete the SAR developed in this thesis.

In terms of biological assays, another possible new route could consist in a collaboration with Prof. Roth who, is the principal contractor of the Psychoactive Drug Screening Program (PDSP), at the Western Case University in USA. This PDSP program, supported by the NIMH, is designed to identify and characterise novel psychoactive compounds of

potential therapeutic activity at a large number of cloned neurotransmitter receptors. The I₂-IBS as well as the I₁-IBS are amongst these cloned receptors and therefore the 25 synthesized ligands, **19b-g**, **29b**, **24a-f**, **25a-f** and **51a-f** could be tested for their affinity towards these cloned receptors. This also could reveal affinities for the I₁-IBS that could be of interest, and more importantly the I₂-IBS/I₁-IBS selectivity of these four families of compounds in the human receptors.

Another future development of the present thesis could include the synthesis of longer chain alkyl *bis*-amidines (where n > 14). By lengthening this family of ligands we can investigate if the very good trend in I₂-IBS/α₂-ARs selectivity observed up until now will continue.

Due to the two possible modes of interaction for the alkyl twin compounds proposed in this thesis a new project could be undertaken to investigate the effect of restricting the movement of the linker chain. Thus, compounds analogous to the four families could be prepared using as linkers aliphatic cycles such as those described in Figure 7.1. These new ligands could provide further insight into ligand-receptor interaction for aliphatic compounds and more importantly could bring some light to the actual structure of the binding pocket of I₂-IBS.

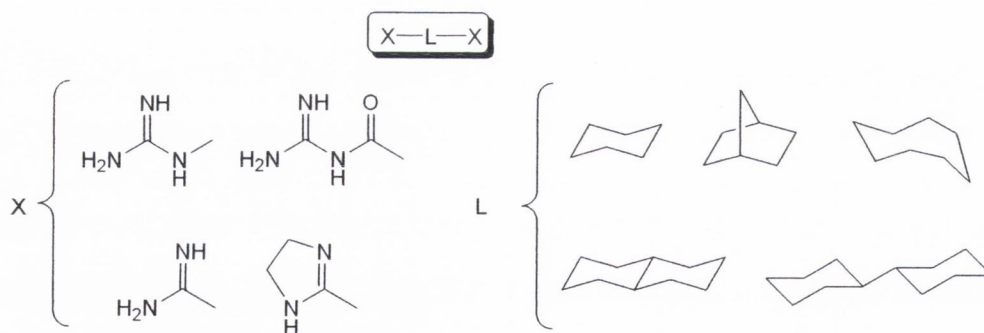


Figure 7.1.- Potential future I₂-IBS aliphatic cyclic ligands

7.4 References

15. Regunathan, S.; Meeley, M. P.; Reis, D. *J. Biochem. Pharmacol.* **1993**, *45*, 1667.
17. Tesson, F.; Limon, I. Parini, A. *Eur. J. Pharmacol.* **1992**, *219*, 335.
18. Langin, D.; Paris, H.; Lafontan, M. *Mol. Pharmacol.* **1990**, *37*, 876.
19. Diamant, S.; Eldar-Geva, T. Atlas, D. *Br. J. Pharmacol.* **1992**, *106*, 101.
20. Lacombe, C.; Viillard, V.; Paris, H. *Let. J. Biochem.* **1993**, *25*, 1077.
21. Escriba, P. V. *Neurosci. Lett.* **1994**, *178*, 81.
101. Dardonville, C.; Rozas, I.; Callado, L. F.; Meana, J. J. *Bioorg. Med. Chem.* **2002**, *10*, 5, 1525.
173. Boland, N. A.; Casey, M.; Hynes, S. J.; Matthews, J. W.; Smyth, M. P. *J. Org. Chem.* **2002**, *67*, 3919 – 3922.

Chapter 8

Experimental

8.1 General Conditions

NMR spectra were recorded on a Bruker DPX 400 spectrometer. Proton and Carbon chemical shifts are reported in part per million (ppm) downfield and are measured relative to tetramethylsilane (TMS) as an internal standard. Coupling constants (J) are expressed in Hertz (Hz). Multiplicities are abbreviated as follows: singlet (s), doublet (d), triplet (t), quartet (q) and multiplet (m). Mass spectra were recorded on a Micromass LCT electrospray TOF instrument with a WATERS 2690 autosampler. Accurate mass was determined relative to a standard of leucine enkephaline (Tyr-Gly-Gly-Phe-Lu) and all accurate mass calculated to ≥ 5 ppm. IR spectra were measured on a Perkin Elmer Paragon 1000 infrared spectrometer in Nujol. Melting points were measured in an unsealed capillary tube using a Stuart Scientific Melting Point SMP1. Thin layer chromatography (tlc) was carried out with silica gel plates (60 F254), or on aluminium oxide plates (N/UV254). The plates were visualised by 253 nm ultraviolet light or by staining with phosphomolybdic acid. Column chromatography was run using Silica gel 600 (230-400 mesh ASTM) or aluminium oxide (neutral STD grade 150 mesh). Evaporation was carried out under reduced pressure in a Buchi rotary evaporator. All starting materials were obtained from Sigma-Aldrich Ireland unless specified. Solvents were purified and dried using standard laboratory procedures.

8.2 General synthetic procedures

8.2.1 Procedure 1; synthesis of the alkyl diamines

To a solution of dicarboxylic acid (1 equivalent) in chloroform (50 ml) and concentrated sulphuric acid (10 ml), was added sodium azide (4 eq) over a period of 1 hour at 50°C. The reaction mixture was heated at reflux for 2 hours, allowed to cool and diluted with ice. The resulting slush was basified to pH 13 with potassium hydroxide (10M solution). A white solid precipitated and was removed by filtration. The filtrate was extracted with chloroform (3 times with 50 ml) and the organic layers dried over magnesium sulfate. The excess solvent was evaporated under reduced pressure to yield the aliphatic diamine.

8.2.2 Procedure 2; synthesis of the alkyl bis-guanidines

The aliphatic diamine (1 eq) and 2-methylpseudothiuronium sulfate (2.2 eq) were heated at reflux in distilled water (20 ml) for 20 hrs. A white solid precipitated upon cooling and was filtered. The solid was washed with water, acetone and recrystallised from water.

8.2.3 Procedure 3; synthesis of the alkyl *bis*-Boc protected *bis*-guanidines

To a solution of aliphatic diamine (1 eq), **27** (2.2 eq) and triethylamine (7 eq) in dry DCM (10 ml) under an atmosphere of argon at 0°C was treated with HgCl₂ (2.2 eq). The reaction warmed to room temperature over two hours. The reaction was stirred at room temperature for a further 20 hours. The solution was diluted with ethyl acetate (20 ml) and filtered through a bed of celite. The solution was washed with water (20 ml) followed by brine (20 ml) and finally dried over magnesium sulphate. The solvent was removed under reduced pressure to give the crude product. The product was further purified by flash chromatography on a alumina column in an ethyl acetate/hexane mixture (4:1).

8.2.4 Procedure 4; Removal of the Boc group

The Boc protected compound (1 mmol) was dissolved in 50% TFA/DCM (10 ml) and allowed to stir at room temperature overnight. The solvent was removed under reduced pressure to give a brown residue. This residue was dissolved in THF (10 ml) and water (10 ml). Previously prepared anion interchange amberlite resin was added and the mixture left stirring at room temperature overnight. Excess solvent was evaporated under reduced pressure and the solid washed with water (5 ml) and acetone (5 ml).

8.2.5a Procedure 5a; synthesis of the alkyl Boc protected guanidines using the Mitsunobu protocol A

To a solution of alcohol (1 eq), triphenylphosphine (1.3 eq) and the protected guanidine, **31** or **33** (1.3 eq), in dry THF (5 ml) under an atmosphere of argon diisopropylazodicarboxylate (DIAD, 1.3 eq) was added at 0°C. The reaction warmed to room temperature over one hour. The reaction was left to stir at room temperature for a further 48 hours. The solvent was removed under reduced pressure to give a residue. The product was isolated after flash chromatography on a alumina column in an ethyl acetate/hexane mixture.

8.2.5b Procedure 5b; synthesis of the alkyl Boc protected guanidines using the Mitsunobu protocol B

To a solution of alcohol (1 eq), triphenylphosphine (1.3 eq) and the protected guanidine, **31** or **33** (1.3 eq), in dry THF (5 ml) under an atmosphere of argon diisopropylazodicarboxylate (DIAD, 1.3 eq) was added at 0°C. The reaction left warmed to room temperature over one hour. The reaction was stirred at 50°C for a further 48 hours. The solvent was removed under reduced pressure to give a residue. The product was isolated after flash chromatography on an alumina column in an ethyl acetate/hexane mixture.

8.2.6 Procedure 6; synthesis of alkyl bis-methyl esters

To a solution of carboxylic acid (1 eq) in methanol (20 ml) thionyl chloride (2.2 eq) was added dropwise at 0°C. The mixture was then left to stir at room temperature overnight. The solvent was removed under reduced pressure to give the desired product.

8.2.7 Procedure 7; synthesis of the alkyl di-alcohols

Lithium aluminium hydride (2 eq) was suspended in THF (15 ml) and cooled to 0°C. A solution of alkyl bis-methyl ester (1 eq) in THF (5 ml) was added dropwise. The reaction was left to stir at room temperature overnight. The reaction was quenched with water (1 ml per gram of lithium aluminium hydride), sodium hydroxide (1M, 1 ml per gram of lithium aluminium hydride) and water again (1 ml per gram of lithium aluminium hydride). The reaction was filtered through a bed of celite and washed with ether (20 ml). The organic layers were dried over sodium sulphate, which was removed by filtration. The solvent was removed to give the desired alkyl dialcohol.

8.2.8 Procedure 8; synthesis of the alkyl bis-guanidinylamides picrate salts

The ester (1 eq) and the guanidinium hydrochloride (10 eq) were dissolved in a solution of sodium methoxide (sodium -10 eq- in methanol -25 ml-). The reaction mixture was heated at reflux for 72 hours. The solvent was evaporated and the residue gathered up with distilled water (50 ml). The resulting solution was acidified using concentrated hydrochloric acid (75 eq). A white solid precipitated and was removed by filtration. The solid was dissolved in a hot picric acid solution (0.2M, 10 ml) filtered and allowed to precipitate overnight. The yellow precipitate was filtered.

8.2.9 Procedure 9; synthesis of the alkyl bis-guanidinylamides

A solution of carboxylic acid (1 eq) and CDI (2 eq) in DCM (10 ml) was stirred at room temperature for one hour. Solvent was evaporated and the resulting residue dissolved in DMF (10 ml). Guanidine hydrochloride (10 eq) and drierite (2 eq) in DMF (2 ml) were added to the solution. The reaction mixture was left to stir at room temperature for a further 20 hours. The solvent was evaporated and the residue dissolved in chloroform (10ml) and washed with water (6 times with 10 ml). The organic layer was dried over magnesium sulphate, which was removed by filtration, and the solvent was removed under reduced pressure to give the desired product.

8.2.10 Procedure 10; synthesis of the alkyl bis-guanidino carbonyl hydrochloride salts

The alkyl bis-guanidinylamide (1 mmol) was dissolved in DCM (15 ml) and was washed with 1M HCl (2 x 10ml). The aqueous layer was removed under reduced pressure to yield the desired guanidino salt.

8.2.11 Procedure 11; synthesis of the Boc protected alkyl bis-guanidino carbonyls

Under an atmosphere of argon the carboxylic acid (1 eq) was dissolved in DMF (20 ml). Then, the Boc-guanidine **33** (4 eq), BOP (2.4 eq) and *N*-methylmorpholine (6 eq) were added and the solution left to stir at room temperature overnight. Brine (70 ml) was added and a white solid precipitated. This solid was removed by filtration and redissolved in chloroform (20 ml) and washed with water (6 times with 20 ml). The organic layer was dried over magnesium sulfate and the solvent was removed under reduced pressure to give the desired product.

8.2.12 Procedure 12; Synthesis the alkyl bisguanido carbonyl hydrochloride salts

To a solution of the Boc protected alkyl bis-guanidinylamide (1 mmol) in THF (5 ml), a solution of hydrochloric acid (1M, 5 ml) was added. The reaction mixture was stirred at room temperature for 24 hours. The excess solvent was removed under reduced pressure to give a white solid.

8.2.13 Procedure 13; Synthesis of the alkyl bis-2-imidazolines

Trimethylaluminium in toluene (2M, 10 ml) was added dropwise to a solution of ethylene diamine (5 eq) and stirred at 0°C for 20 minutes. The ester (1 eq) in dry toluene (20 ml) was added dropwise. The solution was then heated at 90°C for two and a half hours. The

reaction was cooled to 0°C, water (12 ml), methanol (12 ml) and DCM (12 ml) were then added dropwise sequentially. The solution was filtered and the aqueous layer extracted with DCM (2 x 20 ml). The organic layers were dried over magnesium sulfate and solvent removed under reduced pressure.

8.2.14 Procedure 14; Synthesis of the alkyl *bis*-2-imidazoline oxalate salts

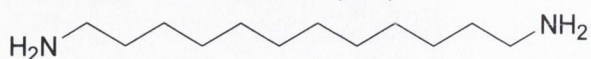
The alkyl *bis*-2-imidazoline (1 eq) was dissolved in an oxalic acid solution (0.875M, 2 eq), after which the solution was evaporated down to dryness to give the imidazoline salts as a white solid. The alkyl *bis*-2-imidazoline was further purified by recrystallisation from water.

8.2.15 Procedure 15; Synthesis of the alkyl *bis*-amidines

Trimethylaluminium in toluene (2M, 10 ml) was added dropwise to a solution of ammonium hydrochloride (20 mmol) and stirred at 0°C for 20 minutes. The ester (2 mmol) in dry toluene (20 ml) was added dropwise. The reaction was then heated at 90°C for 12 hours. The reaction was cooled to 0°C, water (12 ml), methanol (12 ml) and DCM (12 ml) were then added dropwise sequentially. The solution was filtered and the aqueous layer extracted with DCM (2 x 20 ml). The organic layers were dried over magnesium sulfate and excess solvent removed under reduced pressure under reduced pressure. The solid isolated was dissolved in 10M KOH (10 ml) and the white solid that precipitated was filtered. The solid was then dissolved in 1M HCl (5 ml) and removed under reduced pressure.

8.3 Synthesis and characterisation of compounds in Chapter 2

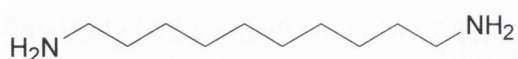
Dodecane-1,12-diamine (26a)



Compound **26a** was prepared following **Procedure 1**, using the carboxylic acid **27c** (2.58 g, 10 mmol) and sodium azide (2.60 g, 40 mmol). A white solid was isolated (1.37 g, 69

%). δ_{H} (400.1MHz; CDCl_3)/ppm: 2.62 (4H, m), 1.37 (4H, m), 1.15 (16H, bs). $\nu_{\text{max}}/\text{cm}^{-1}$: 3328, 1597. $\text{mp}/^\circ\text{C}$: 132 – 136. m/z found: 201.2348 calculated for: $[\text{C}_{12}\text{H}_{28}\text{N}_2+\text{H}]^+$: 201.2331.

Decane-1,10-diamine (26e)



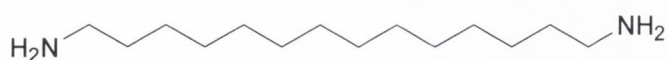
Compound **26e** was prepared following **Procedure 1**, using the carboxylic acid **27a** (2.30 g, 10 mmol) and sodium azide (2.60 g, 40 mmol). A white solid was isolated (1.23 g, 71 %). δ_{H} (400.1MHz; d_6 -DMSO)/ppm: 2.50 (4H, m), 1.32 (4H, m), 1.25 (12H, bs). δ_{C} (100.1MHz; d_6 -DMSO)/ppm: 26.4, 29.0, 29.1, 33.4, 41.8. $\nu_{\text{max}}/\text{cm}^{-1}$: 3323, 1596. $\text{mp}/^\circ\text{C}$: 132 – 136. m/z found: 173.2030 calculated for: $[\text{C}_{10}\text{H}_{24}\text{N}_2+\text{H}]^+$: 173.2018.

Undecane-1,11-diamine (26f)



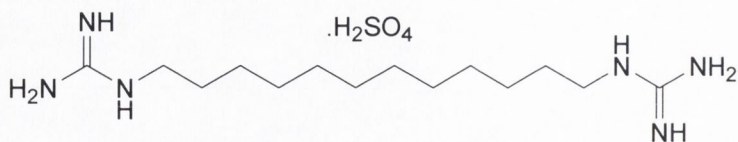
Compound **26f** was prepared following **Procedure 1**, using the carboxylic acid **27b** (2.44 g, 10 mmol) and sodium azide (2.60 g, 40 mmol). A white solid was isolated (1.13 g, 62 %). δ_{H} (400.1MHz; d_6 -DMSO)/ppm: 2.50 (4H, m), 1.31 (4H, m), 1.24 (14H, bs). $\nu_{\text{max}}/\text{cm}^{-1}$: 3328, 1594. $\text{mp}/^\circ\text{C}$: 132 – 138. m/z found: 187.2173 calculated for: $[\text{C}_{11}\text{H}_{26}\text{N}_2+\text{H}]^+$: 187.2174.

Tetradecane-1,14-diamine (26g)



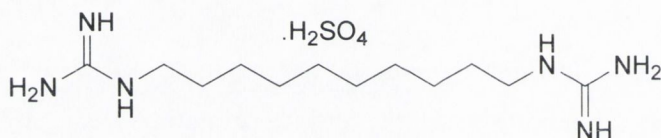
Compound **26g** was prepared following **Procedure 1**, using the carboxylic acid **27d** (2.86 g, 10 mmol) and sodium azide (2.60 g, 40 mmol). A white solid was isolated (1.65 g, 72 %). δ_{H} (400.1MHz; d_6 -DMSO)/ppm: 2.50 (4H, m), 1.31 (4H, m), 1.24 (20H, bs). $\nu_{\text{max}}/\text{cm}^{-1}$: 3329, 1594. $\text{mp}/^\circ\text{C}$: 128 – 132. m/z found: 229.2642 calculated for: $[\text{C}_{14}\text{H}_{32}\text{N}_2+\text{H}]^+$: 229.4319.

1,12-Dodecanediguandinium sulphate (19d)



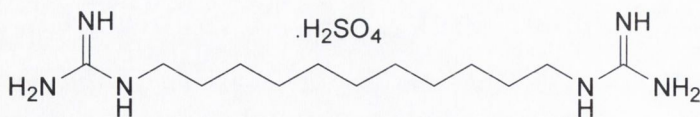
Compound **19d** was prepared according to **Procedure 2**, using the diamine **26d** (1.00 g, 5 mmol) and 2-methylpseudothiuronium sulphate (2.24 g, 12 mmol). A white solid was isolated (153 mg, 8 %). δ_{H} (400.1MHz; D₂O)/ppm: 3.03 (4H, m), 1.44 (4H, m), 1.15 (16H, bs). $\nu_{\text{max}}/\text{cm}^{-1}$: 3346, 3261, 1631. mp/°C: decomposes above 250 (lit⁴⁴ 250 - 254 °C). Anal. Calcd for C₁₄H₃₄N₆O₄S: C, 43.96; H, 8.96; N, 21.97. Found: C, 43.67; H, 9.09; N, 21.78.

1,10-Decanediguandinium sulphate (19e)



Compound **19e** was prepared according to **Procedure 2**, using the diamine **26e** (0.86 g, 5 mmol) and 2-methylpseudothiuronium sulphate (2.24 g, 12 mmol). A white solid was isolated (336 mg, 19 %). δ_{H} (400.1MHz; D₂O)/ppm: 3.03 (4H, t, J = 6.8 Hz), 1.44 (4H, m), 1.17 (12H, bs). $\nu_{\text{max}}/\text{cm}^{-1}$: 3467, 3291, 3060, 1625. mp/°C: decomposes above 250. Anal. Calcd for C₁₂H₃₀N₆O₄S: C, 40.66; H, 8.53; N, 23.71. Found: C, 40.68; H, 8.45; N, 23.22.

1,11-Undecanediguandinium sulphate (19f)



Procedure A:

Compound **19f** was prepared according to **Procedure 2**, using the diamine **26f** (0.47 g, 2.5 mmol) and 2-methylpseudothiuronium sulphate (1.12 g, 6 mmol) and refluxing the reaction for 12 hours. A white solid was isolated (64 mg, 7 %)

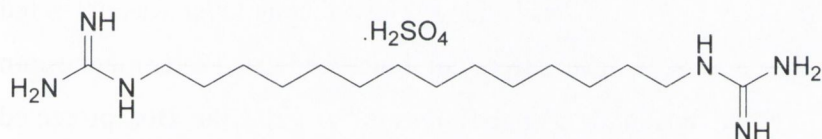
Procedure B:

Compound **19f** was prepared according to **Procedure 2**, using the diamine **26f** (0.93 g, 5 mmol) and 2-methylpseudothiuronium sulphate (2.24 g, 12 mmol). A white solid was isolated (239 mg, 13 %)

Procedure C:

Compound **19f** was prepared according to **Procedure 2**, using the diamine **26f** (0.47 g, 2.5 mmol) and 2-methylpseudothiuronium sulphate (1.12 g, 6 mmol) and refluxing the reaction for 48 hours. A white solid was isolated (101 mg, 11 %). δ_{H} (400.1MHz; D₂O)/ppm: 3.03 (4H, t, J = 6.1 Hz), 1.4 (4H, m), 1.16 (14H, bs). $\nu_{\text{max}}/\text{cm}^{-1}$: 3349, 3261, 1625. mp/^oC: decomposes above 250. Anal. Calcd for C₁₃H₃₂N₆O₄S: C, 42.37; H, 8.75; N, 22.81. Found: C, 42.39; H, 8.37; N, 22.32.

1,14-Tetradecanediguanidinium sulphate (19g)



Procedure A:

Compound **19g** was prepared according to **Procedure 2**, using the diamine **26g** (0.57 g, 2.5 mmol) and 2-methylpseudothiuronium sulphate (2.34 g, 12.5 mmol). A white solid was isolated (174 mg, 17 %)

Procedure B:

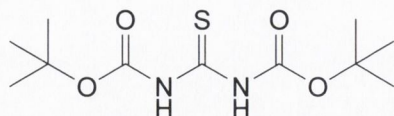
Compound **19g** was prepared according to **Procedure 2**, using the diamine **26g** (0.57 g, 2.5 mmol) and 2-methylpseudothiuronium sulphate (4.70 g, 25 mmol). A white solid was isolated (123 mg, 12 %)

Procedure C:

Compound **19g** was prepared according to **Procedure 2**, using the diamine **26g** (0.57 g, 2.5 mmol) and 2-methylpseudothiuronium sulphate (10.28 g, 55 mmol). A white solid was isolated (143 mg, 14 %). δ_{H} (400.1MHz; D₂O)/ppm: 3.04 (4H, t, J = 6.8 Hz), 1.45

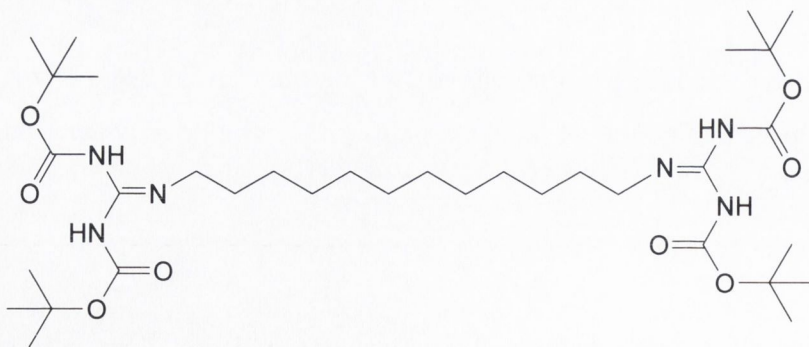
(4H, m), 1.65 (20H, bs). δ_C (400.1MHz; D₂O)/ppm: 7.7, 17.7, 25.2, 27.3, 27.7, 28.1, 28.2, 40.1, 156.2. $\nu_{\max}/\text{cm}^{-1}$: 3316, 3260, 3105, 1631. mp/°C: decomposes above 250.

Boc protected thiourea (37)



Under an atmosphere of argon, thiourea (0.61 g, 8 mmol) was dissolved in dry THF (200 ml) at 0°C. To this stirred solution sodium hydride (0.86 g, 36 mmol) was added and stirring continued at 0°C for five minutes, after warming to room temperature the reaction mixture was stirred for a further ten minutes then recooled to 0°C when di-*tert*-butoxycarbonyl anhydride (3.84 g, 17.6 mmol) was added. The reaction was allowed to warm to room temperature and stirred overnight. The reaction was terminated by the dropwise addition of a saturated solution of sodium hydrogencarbonate (10 ml) to remove any excess sodium hydride, water (250 ml) was added. The aqueous layer was extracted by ethyl acetate (3 x 70 ml), the organic layers were combined and dried over magnesium sulphate. The solvent was removed under reduced pressure to yield the Boc protected thiourea as yellow crystals (1.55 g, 70 %). δ_H (400.1MHz; CDCl₃)/ppm: 1.54 (18H, s). δ_C (100.1MHz; CDCl₃)/ppm: 27.5, 83.8, 156.4. $\nu_{\max}/\text{cm}^{-1}$: 1130, 3169, 3362. mp/°C: 122 – 124°C. m/z found: 299.1031 calculated for: [C₁₁H₂₀N₂O₄+Na]⁺: 299.1041

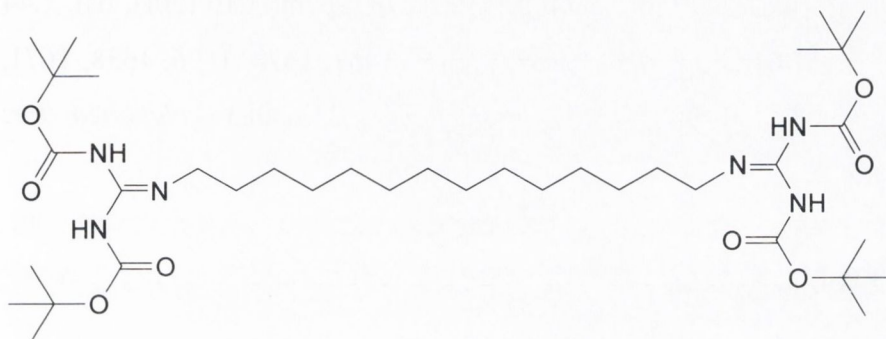
1, 12-Bis[*N, N'*- di(*tert*-butoxycarbonyl) guanidino] Dodecanediamine (59a)



Compound **59a** was prepared according to **Procedure 3**, using the diamine **26d** (1.00 g, 5 mmol), **27** (3.04 g, 11 mmol), HgCl₂ (2.99 g, 11 mmol) and Et₃N (4.84 ml, 35 mmol). A

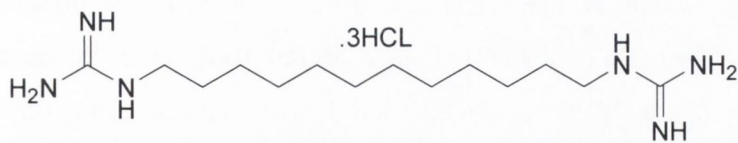
yellow solid was isolated (2.33 g, 68 %). δ_{H} (400.1MHz; CDCl_3)/ppm: 1.27 (16H, bs), 1.54 (36H, bs), 1.70 (4H, m), 3.41 (4H, m). $\nu_{\text{max}}/\text{cm}^{-1}$: 1414, 1473, 1451, 1737, 3004, 3128, 3332. mp/°C: 76 – 80°C. m/z found: 685.4872 calculated for: $[\text{C}_{34}\text{H}_{64}\text{N}_6\text{O}_8+\text{H}]^+$: 685.4864.

1, 14-Bis[*N, N'*- di(*tert*-butoxycarbonyl) guanidino] Tetradecanediamine (59b)



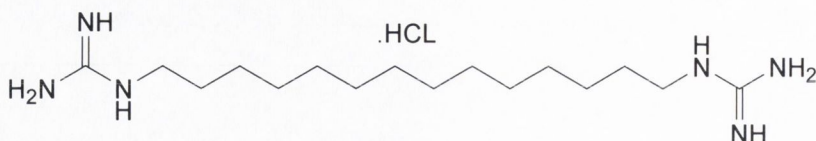
Compound **59b** was prepared according to **Procedure 3**, using the diamine **26g** (1.14 g, 5 mmol), **37** (3.04 g, 11 mmol), HgCl_2 (2.99 g, 11 mmol) and Et_3N (4.84 ml, 35 mmol). A yellow solid was isolated (2.95 g, 83 %). δ_{H} (400.1MHz; CDCl_3)/ppm: 1.25 (20H, bs), 1.54 (36H, bs), 1.56 (4H, m), 3.39 (4H, m). δ_{C} (100.1MHz; CDCl_3)/ppm: 17.2, 26.4, 29.1, 40.5, 48.9, 76.3, 82.5, 155.6, 163.2. $\nu_{\text{max}}/\text{cm}^{-1}$: 1415, 1454, 1471, 1624, 1652, 1736, 3007, 3112, 3333. mp/°C: 104 – 106°C. m/z found: 313.3027 calculated for: $[\text{C}_{16}\text{H}_{32}\text{N}_6+\text{H}]^+$: 309.4769

1,12-Dodecanediguanidinium hydrochloride (60a)



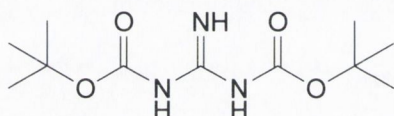
Compound **60a** was prepared according to **Procedure 4**, using **59a** (1.50 g, 2.2 mmol). A white solid was isolated (0.59 g, 75 %). δ_{H} (400.1MHz; D_2O)/ppm: 1.15 (16H, bs), 1.45 (4H, m), 3.04 (4H, t, $J = 6.5$ Hz). $\nu_{\text{max}}/\text{cm}^{-1}$: 1469, 1478, 1605, 1639, 1671, 3135, 3308, 3387. mp/°C: 140 – 146°C. m/z found: 285.2756 calculated for: $[\text{C}_{14}\text{H}_{33}\text{N}_6+\text{H}]^+$: 285.2767. Anal. Calcd for $\text{C}_{14.5}\text{H}_{35}\text{N}_6\text{Cl}_3$: C, 43.56; H, 8.82; N, 21.02. Found: C, 43.57; H, 8.63; N, 21.28.

1,14-Tetradecanediguanidinium hydrochloride (60b)



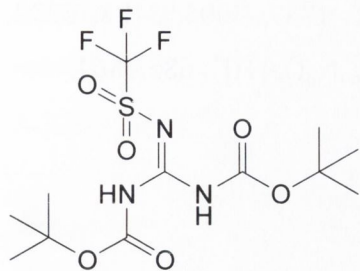
Compound **60b** was prepared according to **Procedure 4**, using **59b** (1.57 g, 2.2 mmol). A white solid was isolated (0.62 g, 73 %). δ_{H} (400.1MHz; D₂O)/ppm: 1.16 (20H, bs), 1.44 (4H, t, J = 7.0 Hz), 3.03 (4H, t, J = 6.5 Hz). ν_{max} /cm⁻¹: 1467, 1478, 1606, 1638, 1671, 3133, 3307, 3391. mp/°C: 140 – 146°C. m/z *found*: 313.3083 *calculated for*: [C₁₆H₃₆N₆+H]⁺: 313.3080.

bis-Boc protected guanidine (61)



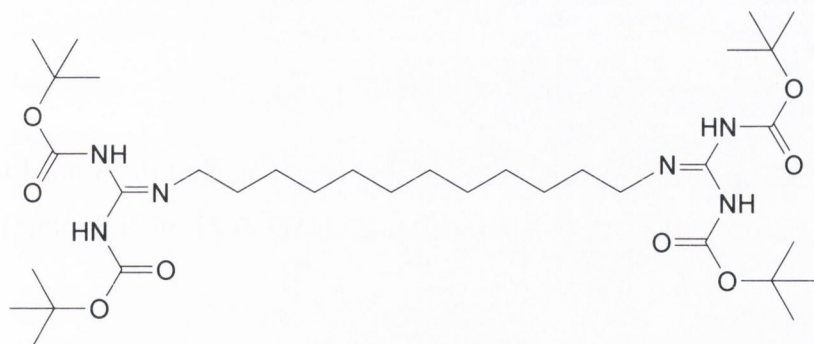
Guanidine hydrochloride (2.36 g, 25 mmol) was dissolved in a sodium hydroxide solution (4M, 40 ml) and cooled to 0°C. Di-*tert*-butyldicarbonate (12.00 g, 55 mmol) was dissolved in dioxane (80 ml) and added dropwise with stirring. The reaction was left to warm to room temperature over two hours after which, it was left stirring at room temperature overnight. Solvent was removed under reduced pressure to give a white residue. The white residue was suspended in water (50 ml) and the aqueous layer was extracted with ethyl acetate (3 x 50ml). The organic layers were combined and washed with citric acid (10 % solution, 50 ml), water (50 ml), and brine (50 ml). The organic layer was dried over magnesium sulphate and the solvent removed under reduced pressure to give the crude product. The pure white solid was isolated after flash chromatography in 100 % DCM. A white solid was isolated (4.41 g, 60 %). δ_{H} (400.1MHz; CDCl₃)/ppm: 1.50 (18H, s). δ_{C} (100.1MHz; CDCl₃)/ppm: 27.6, 80.2, 157.8. ν_{max} /cm⁻¹: 3401, 3310, 3114, 1663, 1601. mp/°C: 132 – 134°C. m/z *found*: 282.1204 *calculated for*: [C₁₁H₂₁N₃O₄+Na]⁺: 282.2946.

Triflic bis-Boc protected guanidine (53)



A solution of **61** (0.65 g, 2 mmol) and DIPEA (0.75 ml, 4.4 mmol) in dry DCM (30 ml) was cooled to -78°C . The reaction was kept at -78°C and triflic anhydride (0.31 g, 1.1 mmol) was added slowly. The reaction was left to warm to room temperature over four hours. The solution was washed with sodium bisulfate (2M, 15 ml), followed by water (15 ml). The organic layer was dried over sodium sulphate and solvent removed under reduced pressure to give the crude product as a yellow solid. The pure product was isolated after flash chromatography on a silica column in 100 % DCM as a white solid, 376 mg (40 %). $\nu_{\text{max}}/\text{cm}^{-1}$: 1101, 1128, 1186, 1325, 1374, 1553, 1626, 1731, 1784, 3144, 3301, 3374. $\text{mp}/^{\circ}\text{C}$: 86 – 88 $^{\circ}\text{C}$.

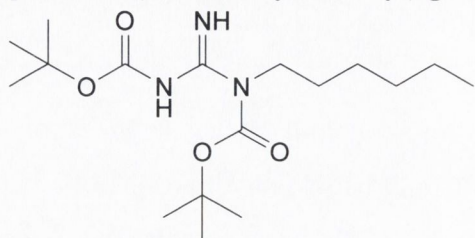
1, 12-Bis[*N*, *N'*- di(*tert*-butoxycarbonyl) guanidino] Dodecanediamine (59a)



The aliphatic diamine (1.0 eq), the triflic protected guanidine (2.2 eq) and triethylamine (7.0 eq) were dissolved in dry DCM (10 ml) under an atmosphere of argon and left to stir at room temperature for 20 hours. The solution was washed with water (20 ml) followed by brine (20 ml) and finally dried over magnesium sulphate. The excess solvent was removed under reduced pressure to give the crude product. The product was further

purified by flash chromatography in an ethyl acetate/hexane mixture (4:1) and isolated as a white solid, 67 mg (19 %). δ_{H} (400.1MHz; CDCl_3)/ppm: 1.27 (16H, bs), 1.54 (36H, bs), 1.70 (4H, m), 3.41 (4H, m). $\nu_{\text{max}}/\text{cm}^{-1}$: 1414, 1473, 1451, 1737, 3004, 3128, 3332. $\text{mp}/^\circ\text{C}$: 76 – 80 $^\circ\text{C}$. m/z found: 685.4872 calculated for: $[\text{C}_{34}\text{H}_{64}\text{N}_6\text{O}_8+\text{H}]^+$: 685.4864.

[N, N'- di(*tert*-butoxycarbonyl) guanidino] hexylamine (62)



Procedure A:

Compound **62** was prepared following **Procedure 5a**, using Hexyl alcohol (0.13 ml, 1.0 mmol), Ph_3P (0.34 g, 1.3 mmol), **61** (0.38 g, 1.3 mmol) and DIAD (0.26 ml, 1.3 mmol). A white crystalline solid was isolated (250 mg, 73 %).

Procedure B:

Compound **62** was prepared following **Procedure 5a**, using Hexyl alcohol (0.13 ml, 1.0 mmol), Ph_3P (0.68 g, 2.6 mmol), **61** (0.77 g, 2.6 mmol) and DIAD (0.51 ml, 2.6 mmol). A white crystalline solid was isolated (257 mg, 75 %).

Procedure C:

Compound **62** was prepared following **Procedure 5a**, using Hexyl alcohol (0.13 ml, 1.0 mmol), Ph_3P (0.10 g, 3.9 mmol), **61** (1.15 g, 3.9 mmol) and DIAD (0.77 ml, 3.9 mmol). A white crystalline solid was isolated (254 mg, 74 %).

Procedure D:

Compound **62** was prepared following **Procedure 5b**, using Hexyl alcohol (0.13 ml, 1.0 mmol), Ph_3P (0.34 g, 1.3 mmol), **61** (0.38 g, 1.3 mmol) and DIAD (0.26 ml, 1.3 mmol). A white crystalline solid was isolated (192 mg, 56 %).

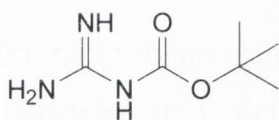
Procedure E:

Compound **62** was prepared following **Procedure 5b**, using Hexyl alcohol (0.13 ml, 1.0 mmol), Ph_3P (0.68 g, 2.6 mmol), **61** (0.77 g, 2.6 mmol) and DIAD (0.51 ml, 2.6 mmol). A white crystalline solid was isolated (195 mg, 57 %).

Procedure F:

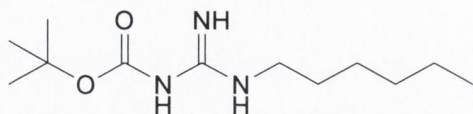
Compound **62** was prepared following **Procedure 5b**, using Hexyl alcohol (0.13 ml, 1.0 mmol), Ph_3P (0.10 g, 3.9 mmol), **61** (1.15 g, 3.9 mmol) and DIAD (0.77 ml, 3.9 mmol). A white crystalline solid was isolated (226 mg, 66 %). δ_{H} (400.1MHz; CDCl_3)/ppm: 0.84 (3H, t, $J = 7.0$ Hz), 1.29 (6H, bs), 1.42 (18H, bs), 1.45 (2H, m), 3.56 (2H, t, $J = 7.0$ Hz). δ_{C} (400.1MHz; m/z found: 366.2364 calculated for: $[\text{C}_{17}\text{H}_{32}\text{N}_3\text{O}_4+\text{H}]^+$: 366.2369.

Mono-Boc protected guanidine (**63**)



Guanidine hydrochloride (7.42 g, 78.5 mmol) was dissolved in a sodium hydroxide solution (4M, 40 ml) and cooled to 0°C. Ditertbutyldicarbonate (13.7 g, 62.8 mmol) was dissolved in dioxane (80 ml) and added dropwise with stirring. The reaction was left stirring at room temperature overnight. Excess solvent was removed under reduced pressure. The white solid produced was suspended in water (50 ml) and sonicated for 10 minutes. The solid was filtered and resuspended in ether and sonicated for a further 10 minutes. Finally the white solid was filtered and dried in a desiccator overnight. A white solid was isolated (6.11 g, 49 %). δ_{H} (400.1MHz; CDCl_3)/ppm: 1.52 (9H, s). δ_{C} (100.1MHz; CDCl_3)/ppm: 27.9, 78.3, 161.7, 265.9. $\nu_{\text{max}}/\text{cm}^{-1}$: 3401, 3310, 3114, 1663, 1601.

[N, N']-(*tert*-butoxycarbonyl) guanidino] hexylamine (64**)**



Procedure A:

Compound **64** was prepared following **Procedure 5a**, using Hexyl alcohol (0.13 ml, 1.0 mmol), Ph₃P (0.34 g, 1.3 mmol), **63** (0.21 g, 1.3 mmol) and DIAD (0.26 ml, 1.3 mmol). A white crystalline solid was isolated (151 mg, 62 %).

Procedure B:

Compound **64** was prepared following **Procedure 5a**, using Hexyl alcohol (0.13 ml, 1.0 mmol), Ph₃P (0.68 g, 2.6 mmol), **63** (0.41 g, 2.6 mmol) and DIAD (0.51 ml, 2.6 mmol). A white crystalline solid was isolated (172 mg, 71 %).

Procedure C:

Compound **64** was prepared following **Procedure 5a**, using Hexyl alcohol (0.13 ml, 1.0 mmol), Ph₃P (0.10 g, 3.9 mmol), **63** (0.62 g, 3.9 mmol) and DIAD (0.77 ml, 3.9 mmol). A white crystalline solid was isolated (177 mg, 73 %).

Procedure D:

Compound **64** was prepared following **Procedure 5b**, using Hexyl alcohol (0.13 ml, 1.0 mmol), Ph₃P (0.34 g, 1.3 mmol), **63** (0.21 g, 1.3 mmol) and DIAD (0.26 ml, 1.3 mmol). A white crystalline solid was isolated (187 mg, 77 %).

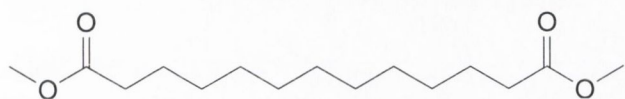
Procedure E:

Compound **64** was prepared following **Procedure 5b**, using Hexyl alcohol (0.13 ml, 1.0 mmol), Ph₃P (0.68 g, 2.6 mmol), **63** (0.41 g, 2.6 mmol) and DIAD (0.51 ml, 2.6 mmol). A white crystalline solid was isolated (182 mg, 75 %).

Procedure F:

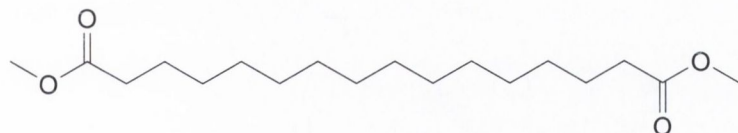
Compound **64** was prepared following **Procedure 5b**, using Hexyl alcohol (0.13 ml, 1.0 mmol), Ph_3P (0.10 g, 3.9 mmol), **63** (0.62 g, 3.9 mmol) and DIAD (0.77 ml, 3.9 mmol). A white crystalline solid was isolated (136 mg, 56 %). δ_{H} (400.1MHz; CDCl_3)/ppm: 1.29 (3H, m), 1.47 (15H, bm), 1.86 (2H, q, $J = 3.5$ Hz), 3.75 (2H, m). $\nu_{\text{max}}/\text{cm}^{-1}$: 1365, 1457, 1479, 1628, 1698, 3313. $\text{mp}/^\circ\text{C}$: 115 – 117. m/z found: 228.2379 calculated for: $[\text{C}_{12}\text{H}_{24}\text{N}_2\text{O}_2+\text{H}]^+$: 228.3338.

1,11-Undecanedimethyl ester (65a)



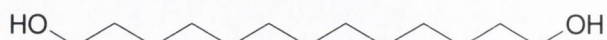
Compound **65a** was prepared according to **Procedure 6**, using **56b** (2.44 g, 10 mmol) and thionyl chloride (1.61 ml, 22 mmol). A yellow crystalline solid was isolated (2.46 g, 86 %). δ_{H} (400.1MHz; CDCl_3)/ppm: 3.69 (6H, s), 2.32 (4H, t, $J = 7.5$ Hz), 1.63 (4H, m), 1.28 (16H, bs). δ_{C} (100.1MHz; CDCl_3)/ppm: 24.5, 28.8, 28.9, 33.7, 51.0, 173.9. $\nu_{\text{max}}/\text{cm}^{-1}$: 1747, 1169. $\text{mp}/^\circ\text{C}$: 48 – 51. m/z found: 295.1876 calculated for: $[\text{C}_{15}\text{H}_{28}\text{O}_4+\text{Na}]^+$: 295.1885.

1,14-Tetradecanedimethyl ester (65b)



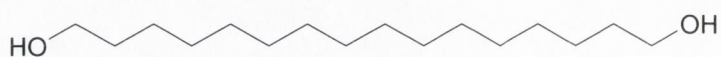
Compound **65b** was prepared according to **Procedure 6**, using **56d** (2.86 g, 10 mmol) and thionyl chloride (1.61 ml, 22 mmol). A yellow crystalline solid was isolated (2.52 g, 77 %). δ_{H} (400.1MHz; CDCl_3)/ppm: 3.68 (6H, s), 2.32 (4H, t, $J = 7.5$ Hz), 1.63 (4H, m), 1.30 (20H, bs). δ_{C} (100.1MHz; CDCl_3)/ppm: 24.5, 29.1, 33.7, 51.0, 173.9. $\nu_{\text{max}}/\text{cm}^{-1}$: 1747, 1170. $\text{mp}/^\circ\text{C}$: 39 – 41. m/z found: 337.2368 calculated for: $[\text{C}_{18}\text{H}_{34}\text{O}_4+\text{Na}]^+$: 337.2355.

Tridecane-1,13-diol (66a)



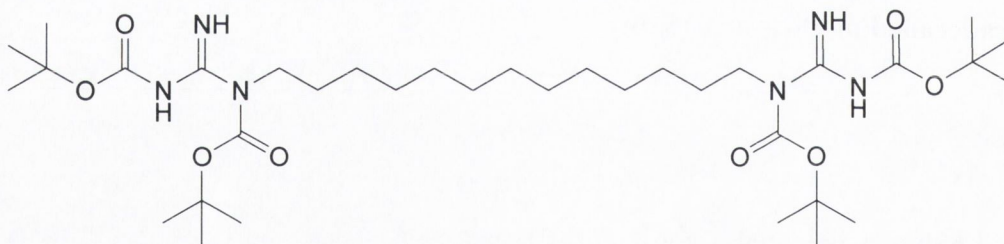
Compound **66a** was prepared following **Procedure 7**, using **65a** (0.57 g, 2 mmol) and lithium aluminium hydride (0.15 g, 4 mmol). A white waxy solid was isolated (307 mg, 71 %). δ_{H} (400.1MHz; CDCl_3)/ppm: 3.51 (4H, m), 1.47 (4H, m), 1.19 (18H, bs). $\nu_{\text{max}}/\text{cm}^{-1}$: 1324, 1344, 1462, 1472, 3243. mp/ $^{\circ}\text{C}$: 66 – 68.²⁰⁰ m/z *found*: 239.1996 calculated for: $[\text{C}_{13}\text{H}_{28}\text{O}_2+\text{Na}]^+$: 239.1987.

Hexadecane-1,16-diol (66b)



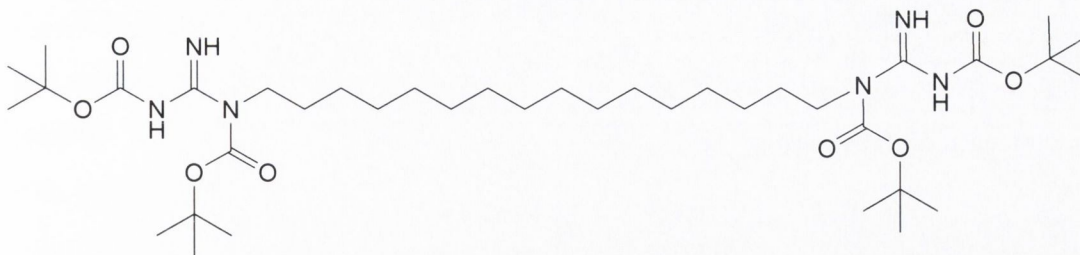
Compound **66b** was prepared following **Procedure 7**, using **65b** (0.66 g, 2 mmol) and lithium aluminium hydride (0.15 g, 4 mmol). A white waxy solid was isolated (361 mg, 70 %). δ_{H} (400.1MHz; CDCl_3)/ppm: 3.65 (4H, t, $J = 6.8$ Hz), 1.58 (4H, m), 1.29 (24H, bs). $\nu_{\text{max}}/\text{cm}^{-1}$: 3327. mp/ $^{\circ}\text{C}$: 39 – 41.²⁰¹ m/z *found*: 281.2444 calculated for: $[\text{C}_{16}\text{H}_{34}\text{O}_2+\text{Na}]^+$: 281.2457.

[Bis-(*tert*-butoxycarbonyl) guanidino] Tridecane-1,13-diamine (67a)



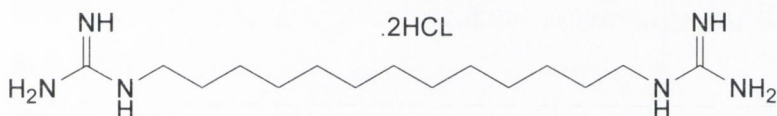
Compound **67a** was prepared following **Procedure 5a**, using **66a** (216 mg, 1.0 mmol), Ph_3P (680 mg, 2.6 mmol), **33** (414 mg, 2.6 mmol) and DIAD (0.51 ml, 2.6 mmol). A white crystalline solid was isolated (523 mg, 75%). δ_{H} (400.1MHz; CDCl_3)/ppm: 1.23 (18H, bs), 1.43 (36H, s), 1.59 (4H, m), 3.71 (4H, m). $\nu_{\text{max}}/\text{cm}^{-1}$: 1256, 1686, 1739, 2850, 2923, 3370, 3430.

[Bis-(*tert*-butoxycarbonyl) guanidino] Hexadecane-1,16-diamine (**67b**)



Compound **67b** was prepared following **Procedure 5a**, using **66a** (258 mg, 1.0 mmol), Ph_3P (68 mg, 2.6 mmol), **61** (414 mg, 2.6 mmol) and DIAD (0.51 ml, 2.6 mmol). A white crystalline solid was isolated (7 mg, 19 %). δ_{H} (400.1MHz; CDCl_3)/ppm: 1.26 (24H, bs), 1.51 (36H, bs), 1.77 (4H, q, $J = 6.5\text{Hz}$), 4.24 (4H, t, $J = 6.5\text{Hz}$). $\nu_{\text{max}}/\text{cm}^{-1}$: 1245, 1521, 1686, 1736, 2850, 2917, 3371, 3428.

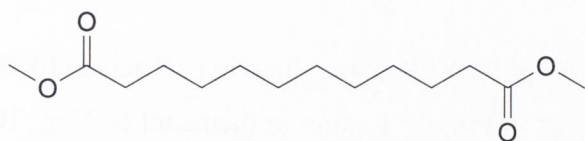
1,13-tridecanediguanidinium hydrochloride (**60c**)



Compound **60c** was prepared according to **Procedure 4**, using **67a** (1.54 g, 2.2 mmol). A white solid was isolated (0.70 g, 85%). δ_{H} (400.1MHz; D_2O)/ppm: 1.18 (18H, bs), 1.44 (4H, m), 3.03 (4H, t, $J = 7.0\text{ Hz}$) m/z found: 299.2915 calculated for: $[\text{C}_{14}\text{H}_{33}\text{N}_6+\text{H}]^+$: 299.2923 Anal. Calcd for $\text{C}_{18}\text{H}_{47}\text{N}_6\text{O}_{3.5}\text{Cl}_2$: C, 45.56; H, 9.98; N, 17.70. Found: C, 46.10; H, 8.90; N, 16.97.

8.4 Synthesis and characterisation of compounds in Chapter 3

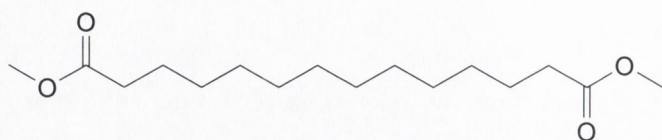
1,10-Decanedimethyl ester (**65e**)



Compound **65e** was prepared according to **Procedure 6**, using **56a** (2.30 g, 10 mmol) and thionyl chloride (1.61 ml, 22 mmol). A white crystalline solid was isolated (2.35 g, 91 %). δ_{H} (400.1MHz; CDCl_3)/ppm: 3.68 (6H, s), 2.32 (4H, t, $J = 7.5\text{ Hz}$), 1.62 (4H, m), 1.29

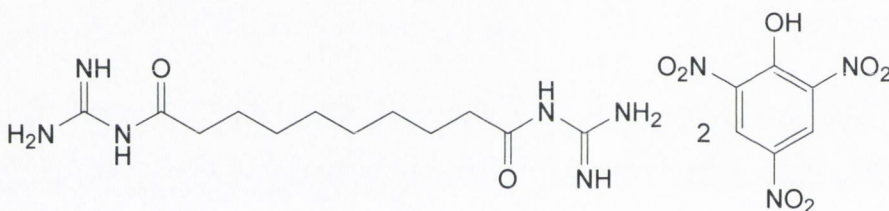
(12H, bs). $\nu_{\max}/\text{cm}^{-1}$: 1747, 1170. $\text{mp}/^{\circ}\text{C}$: 39 – 41. m/z found: 281.1753 calculated for: $[\text{C}_{14}\text{H}_{26}\text{O}_4+\text{Na}]^+$: 281.1729.

1,12-Dodecanedimethyl ester (65f)



Compound **65e** was prepared according to **Procedure 6**, using **56c** (2.58 g, 10 mmol) and thionyl chloride (1.61 ml, 22 mmol). A white crystalline solid was isolated (2.43 g, 81 %). δ_{H} (400.1MHz; CDCl_3)/ppm: 3.69 (6H, s), 2.32 (4H, t, $J = 7.6$ Hz), 1.60 (4H, m), 1.28 (16H, bs). $\nu_{\max}/\text{cm}^{-1}$: 1747, 1170. $\text{mp}/^{\circ}\text{C}$: 39 – 41. m/z found: 309.2054 calculated for: $[\text{C}_{16}\text{H}_{30}\text{O}_4+\text{Na}]^+$: 309.2042.

1, 8 - Octane bis-guanidinylamide picrate salt (94a)



Procedure A:

Compound **94a** was prepared according to **Procedure 8**, using dimethyl sebacate (0.23 g, 1 mmol), guanidine hydrochloride (0.95 g, 10 mmol), sodium in methanol (0.23 g, 10 mmol). The reaction was refluxed for 24 h and concentrated hydrochloric acid (29 eq) was used. A yellow solid was isolated (146 mg, 20 %)

Procedure B:

Compound **94a** was prepared according to **Procedure 8**, using dimethyl sebacate (0.23 g, 1 mmol), guanidine hydrochloride (0.95 g, 10 mmol), sodium in methanol (0.23 g, 10 mmol). The reaction was refluxed for 24 h and concentrated hydrochloric acid (45 eq) was used. A yellow solid was isolated (219 mg, 30 %).

Procedure C:

Compound **94a** was prepared according to **Procedure 8**, using dimethyl sebacate (0.23 g, 1 mmol), guanidine hydrochloride (0.95 g, 10 mmol), sodium in methanol (0.23 g, 10 mmol). The reaction was refluxed for 24 h and concentrated hydrochloric acid (60 eq) was used. A yellow solid was isolated (121 mg, 16.6 %).

Procedure D:

Compound **94a** was prepared according to **Procedure 8**, using dimethyl sebacate (0.23 g, 1 mmol), guanidine hydrochloride (0.95 g, 10 mmol), sodium in methanol (0.23 g, 10 mmol). The reaction was refluxed for 24 h and concentrated hydrochloric acid (75 eq) was used. Yellow Solid, (300 mg, 41 %)

Procedure E:

Compound **94a** was prepared according to **Procedure 8**, using dimethyl sebacate (0.23 g, 1 mmol), guanidine hydrochloride (0.95 g, 10 mmol), sodium in methanol (0.23 g, 10 mmol). The reaction was refluxed for 48 h and a yellow solid was isolated (329 mg, 45 %).

Procedure F:

Compound **94a** was prepared according to **Procedure 8**, using dimethyl sebacate (0.23 g, 1 mmol), guanidine hydrochloride (0.95 g, 10 mmol), sodium in methanol (0.23 g, 10 mmol). The reaction refluxed for 72 h. A yellow solid was isolated (585 mg, 80 %).

Procedure G:

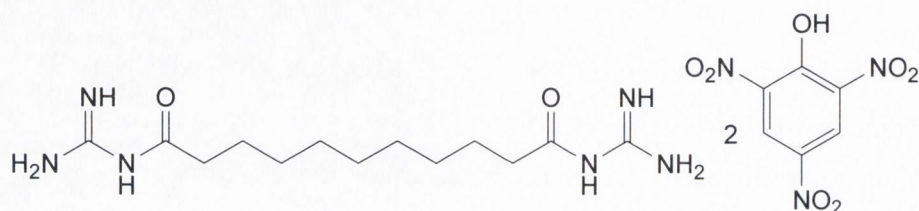
Compound **94a** was prepared according to **Procedure 8**, using dimethyl sebacate (0.23 g, 1 mmol), guanidine hydrochloride (0.95 g, 10 mmol), sodium in methanol (0.23 g, 10 mmol). The reaction refluxed for 96 h. A yellow solid was isolated (146 mg, 20 %)

Procedure H:

Compound **94a** was prepared according to **Procedure 8**, using dimethyl sebacate (0.23 g, 1 mmol), guanidine hydrochloride (0.95 g, 10 mmol), sodium in methanol (0.23 g, 10

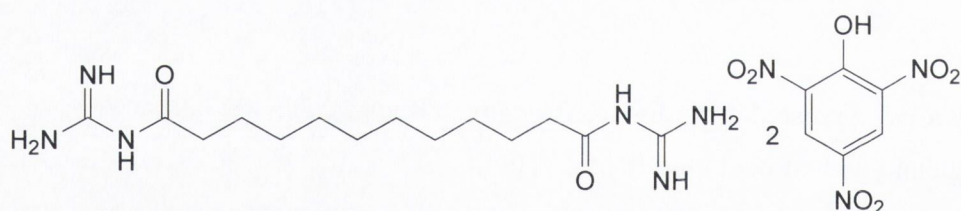
mmol). The reaction refluxed for 120 h. A yellow solid was isolated (87 mg, 12 %). δ_{H} (400.1MHz; D₂O)/ppm: 7.40 (s, 4H), 2.23 (4H, t, J = 7.5 Hz), 1.47 (4H, m), 1.19 (8H, bs). δ_{C} (100.1MHz; D₂O)/ppm: 23.7, 27.5, 27.6, 33.3, 128.3, 140.7, 173.7, 190.7. $\nu_{\text{max}}/\text{cm}^{-1}$: 3390, 1690, 1601. mp/°C: 138 – 140.

1, 9-Nonane bis-guanidinylamide picrate salt (94b)



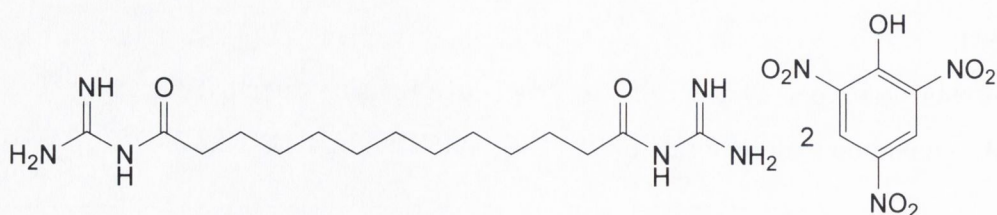
Compound **94b** was prepared according to **Procedure 8**, using dimethyl nonane (0.24 g, 1 mmol), guanidine hydrochloride (0.95 g, 10 mmol), sodium in methanol (0.23 g, 10 mmol). A yellow solid was isolated (67 mg, 9 %). δ_{H} (400.1MHz; D₂O)/ppm: 7.41 (s, 4H), 2.24 (4H, t, J = 7.5 Hz), 1.46 (4H, m), 1.16 (10H, bs). $\nu_{\text{max}}/\text{cm}^{-1}$: 3393, 1686, 1603. mp/°C: 128 – 133.

1, 10-Decane bis-guanidinylamide picrate salt (94c)



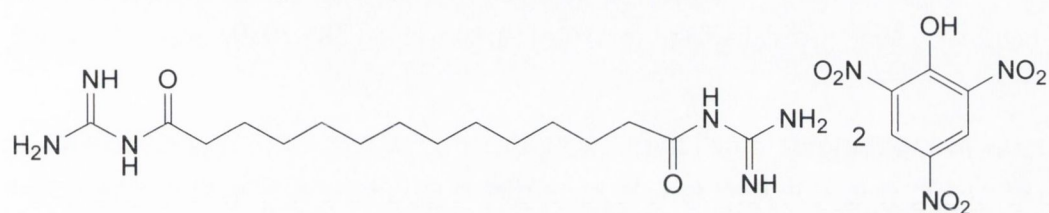
Compound **94b** was prepared according to **Procedure 8**, using **65e** (0.26 g, 1 mmol), guanidine hydrochloride (0.95 g, 10 mmol), sodium in methanol (0.23 g, 10 mmol). A yellow solid was isolated (131 mg, 17.2 %). δ_{H} (400.1MHz; D₂O)/ppm: 7.40 (s, 4H), 2.23 (4H, m), 1.44 (4H, m), 1.17 (12H, bs). $\nu_{\text{max}}/\text{cm}^{-1}$: 3393, 1686, 1605. mp/°C: 121 – 124.

1, 11-Undecane bis-guanidinylamide picrate salt (94d)



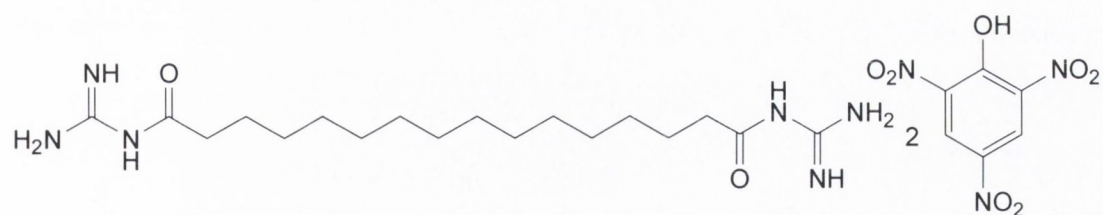
Compound **94b** was prepared according to **Procedure 8**, using **65a** (0.29 g, 1 mmol), guanidine hydrochloride (0.95 g, 10 mmol), sodium in methanol (0.23 g, 10 mmol). A yellow solid was isolated (116 mg, 15 %). δ_{H} (400.1MHz; D₂O)/ppm: 7.44 (s, 4H), 2.25 (4H, m), 1.44 (4H, m), 1.18 (14H, bs). $\nu_{\text{max}}/\text{cm}^{-1}$: 3420, 1687, 1606. mp/°C: 122 – 124.

1, 12-Dodecane bis-guanidinylamide picrate salt (41e)



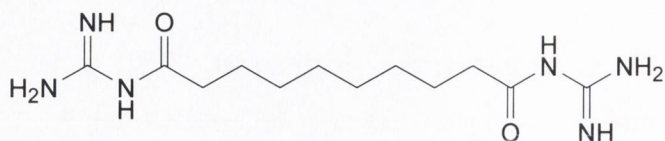
Compound **94b** was prepared according to **Procedure 8**, using **65f** (0.3 g, 1 mmol), guanidine hydrochloride (0.95 g, 10 mmol), sodium in methanol (0.23 g, 10 mmol). A yellow solid was isolated (87 mg, 11 %). δ_{H} (400.1MHz; D₂O)/ppm: 7.41 (s, 4H), 2.23 (4H, t, J = 7.5 Hz), 1.47 (4H, m), 1.19 (16H, bs). $\nu_{\text{max}}/\text{cm}^{-1}$: 3400, 1680, 1605. mp/°C: 121 – 124.

1, 14-Tetradecane bis-guanidinylamide, picrate salt (94f)



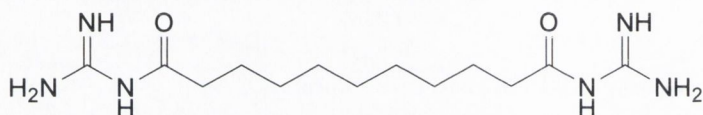
Compound **94b** was prepared according to **Procedure 8**, using **65b** (0.33 g, 1 mmol), guanidine hydrochloride (0.95 g, 10 mmol), sodium in methanol (0.23 g, 10 mmol). A yellow solid was isolated (82 mg, 10 %). δ_{H} (400.1MHz; D₂O)/ppm: 7.42 (s, 4H), 2.23 (4H, t, J = 7.5 Hz), 1.47 (4H, m), 1.19 (20H, bs). $\nu_{\text{max}}/\text{cm}^{-1}$: 3413, 1670, 1606. mp/°C: 118 – 122.

1,8-Octane bisguanidinylamide (23a)



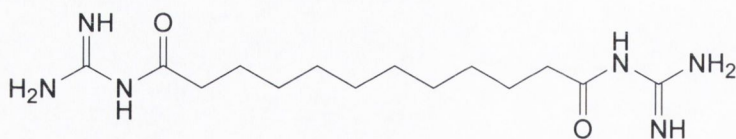
Compound **23a** was prepared according to **Procedure 9**, using **56e** (202 mg, 1 mmol), CDI (324 mg, 2 mmol), guanidine hydrochloride (945 mg, 10 mmol) and drierite (272 mg, 2 mmol). A white solid was isolated (116 mg, 49 %). δ_{H} (400.1MHz; CDCl_3)/ppm: 2.81 (4H, m) 1.78 (4H, m), 1.19 (8H, bs). $\nu_{\text{max}}/\text{cm}^{-1}$: 3459, 3326, 1736, 1596. $\text{mp}^{\circ}\text{C}$: 150 – 154. m/z found: 285.2031 calculated for: $[\text{C}_{12}\text{H}_{24}\text{N}_6\text{O}_2+\text{H}]^+$: 285.2039.

1,9-Nonane bisguanidinylamide (23b)



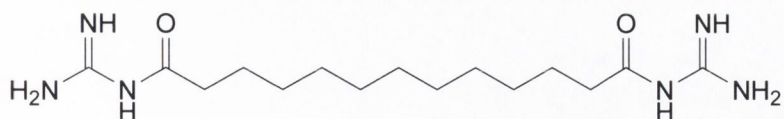
Compound **23b** was prepared according to **Procedure 9**, using **56f** (220 mg, 1 mmol), CDI (324 mg, 2 mmol), guanidine hydrochloride (945 mg, 10 mmol) and drierite (272 mg, 2 mmol). A white solid was isolated (133 mg, 53 %). δ_{H} (400.1MHz; CDCl_3)/ppm: 2.86 (4H, m) 1.81 (4H, m), 1.27 (10H, bs). $\nu_{\text{max}}/\text{cm}^{-1}$: 3459, 3326, 1736, 1596. $\text{mp}^{\circ}\text{C}$: 146 – 150.

1,10-Decane bisguanidinylamide (23c)



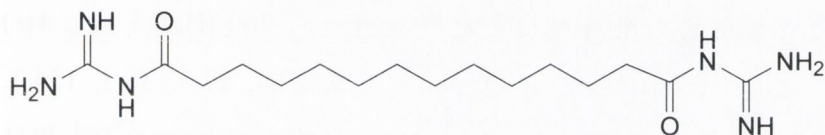
Compound **23c** was prepared according to **Procedure 9**, using **56a** (230 mg, 1 mmol), CDI (324 mg, 2 mmol), guanidine hydrochloride (945 mg, 10 mmol) and drierite (272 mg, 2 mmol). A white solid was isolated (119 mg, 45 %). δ_{H} (400.1MHz; CDCl_3)/ppm: 2.86 (4H, m) 1.83 (4H, m), 1.33 (12H, bs). $\nu_{\text{max}}/\text{cm}^{-1}$: 3460, 3328, 1736, 1597. m/z found: 167.2989 calculated for: $[\text{C}_{14}\text{H}_{28}\text{N}_6\text{O}_2+\text{H}+\text{Na}]^{2+}$: 168.2061.

1,11-Undecane bisguanidinylamide (23d)



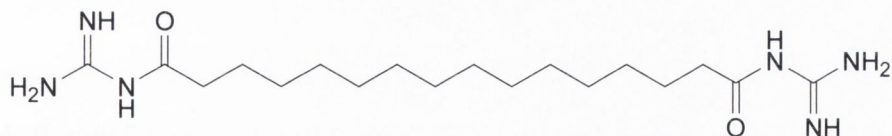
Compound **23d** was prepared according to **Procedure 9**, using **56b** (244 mg, 1 mmol), CDI (324 mg, 2 mmol), guanidine hydrochloride (945 mg, 10 mmol) and drierite (272 mg, 2 mmol). A white solid was isolated (111 mg, 40 %). δ_{H} (400.1MHz; CDCl_3)/ppm: 2.84 (4H, m) 1.83 (4H, m), 1.29 (14H, bs). $\nu_{\text{max}}/\text{cm}^{-1}$: 3430, 3380, 1774, 1656. m/z *found*: 327.2514 calculated for: $[\text{C}_{15}\text{H}_{30}\text{N}_6\text{O}_2+\text{H}]^+$: 327.2508.

1,12-Dodecane bisguanidinylamide (23e)



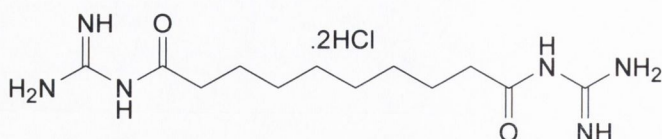
Compound **23e** was prepared according to **Procedure 9**, using **56c** (258 mg, 1 mmol), CDI (324 mg, 2 mmol), guanidine hydrochloride (945 mg, 10 mmol) and drierite (272 mg, 2 mmol). A white solid was isolated (146 mg, 50 %). δ_{H} (400.1MHz; CDCl_3)/ppm: 2.87 (4H, t, $J = 7.52$ Hz) 1.82 (4H, q, $J = 7.52$ Hz), 1.30 (16H, bs). $\nu_{\text{max}}/\text{cm}^{-1}$: 3459, 3306, 1736, 1597. $\text{mp}/^\circ\text{C}$: 136 – 138. m/z *found*: 341.2680 *calculated for*: $[\text{C}_{16}\text{H}_{32}\text{N}_6\text{O}_2+\text{H}]^+$: 341.2665.

1,14-Tetradecane bisguanidinylamide (23f)



Compound **23f** was prepared according to **Procedure 9**, using **56d** (286 mg, 1 mmol), CDI (324 mg, 2 mmol), guanidine hydrochloride (945 mg, 10 mmol) and drierite (272 mg, 2 mmol). A white solid was isolated (150 mg, 47 %). δ_{H} (400.1MHz; CDCl_3)/ppm: 2.79 (4H, m) 1.87 (4H, m), 1.31 (20H, bs). $\nu_{\text{max}}/\text{cm}^{-1}$: 3420, 3326, 1736, 1639. $\text{mp}/^\circ\text{C}$: 136 – 140.

1,8-Octane bisguanidinylamide, hydrochloride salt (96a)

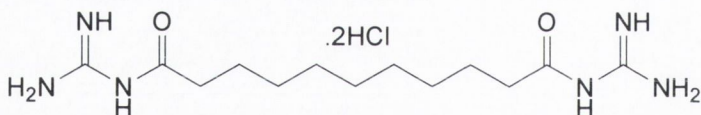


Compound **96a** was prepared following **Procedure 4**, using **97a** (339 mg, 0.7 mmol). A white solid was isolated (190 mg, 76 %).

Compound **96a** was prepared following **Procedure 10**, using **23a** (200 mg, 0.7 mmol). A white solid was isolated (15 mg, 6 %).

Compound **96a** was prepared following **Procedure 12**, using **97a** (339 mg, 0.7 mmol). A white solid was isolated (15 mg, 6 %). δ_{H} (400.1MHz; D₂O)/ppm: 2.36 (4H, t, J = 6.5 Hz) 1.51 (4H, m), 1.19 (8H, bs). δ_{C} (100.1MHz; D₂O)/ppm: 23.8, 27.4, 27.5, 36.3, 154.1, 177.2. ν_{max} /cm⁻¹: 3418, 1730, 1600. mp/°C: decomposes above 250. m/z found: 285.2031 calculated for: [C₁₂H₂₅N₆O₂+H]⁺: 285.2039. Anal. Calcd for C₁₂H₂₆N₆O₂Cl₂: C, 38.51; H, 7.27; N, 22.45. Found: C, 39.09; H, 7.26; N, 22.51.

1,9-Nonane bisguanidinylamide, hydrochloride salt (96b)



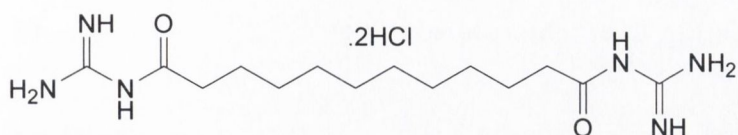
Compound **96b** was prepared following **Procedure 4**, using **97b** (349 mg, 0.7 mmol). A white solid was isolated (169 mg, 65 %).

Compound **96b** was prepared following **Procedure 10**, using **23b** (200 mg, 0.7 mmol). A white solid was isolated (39 mg, 15 %).

Compound **96b** was prepared following **Procedure 12**, using **97b** (349 mg, 0.7 mmol). A white solid was isolated (39 mg, 15%). δ_{H} (400.1MHz; D₂O)/ppm: 2.33 (4H, m) 1.50 (4H, m), 1.18 (10H, bs). δ_{C} (100.1MHz; D₂O)/ppm: 23.3, 27.5, 27.6, 27.7, 36.3, 154.2, 177.4. ν

$\nu_{\max}/\text{cm}^{-1}$: 3440, 1723, 1599. $\text{mp}/^{\circ}\text{C}$: decomposes above 250. m/z found: 299.2209
calculated for: $[\text{C}_{13}\text{H}_{27}\text{N}_6\text{O}_2+\text{H}]^+$: 299.2195.

1, 10-octane bisguanidinylamide, hydrochloride salt (96c)

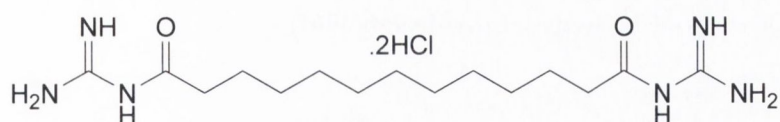


Compound **96c** was prepared following **Procedure 4**, using **97c** (358 mg, 0.7 mmol). A white solid was isolated (181 mg, 67 %).

Compound **96c** was prepared following **Procedure 10**, using **23c** (200 mg, 0.7 mmol). A white solid was isolated (207 mg, 77 %).

Compound **96c** was prepared following **Procedure 12**, using **97c** (358 mg, 0.7 mmol). A white solid was isolated (19 mg, 7 %). δ_{H} (400.1MHz; D₂O)/ppm: 2.36 (4H, t, $J = 7.5$ Hz) 1.52 (4H, m), 1.16 (12H, bs). δ_{C} (100.1MHz; D₂O)/ppm: 23.4 27.5, 27.7, 27.9, 36.3, 154.2, 177.4. $\text{mp}/^{\circ}\text{C}$: decomposes above 250. $\nu_{\max}/\text{cm}^{-1}$: 3422, 1719, 1600. $\text{mp}/^{\circ}\text{C}$: 126 – 130.

1,11-Undecane bisguanidinylamide, hydrochloride salt (96d)



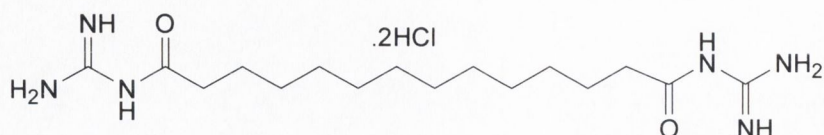
Compound **96d** was prepared following **Procedure 4**, using **97d** (368 mg, 0.7 mmol). A white solid was isolated (198 mg, 71 %).

Compound **96d** was prepared following **Procedure 10**, using **23d** (200 mg, 0.7 mmol). A white solid was isolated (8 mg, 3 %).

Compound **96d** was prepared following **Procedure 12**, using **97d** (368 mg, 0.7 mmol). A white solid was isolated (8 mg, 3 %). δ_{H} (400.1MHz; D₂O)/ppm: 2.37 (4H, m) 1.52 (4H,

m), 1.16 (14H, bs). $\nu_{\max}/\text{cm}^{-1}$: 3425, 1714, 1606. $\text{mp}/^{\circ}\text{C}$: decomposes above 250. m/z found: 327.2494 calculated for: $[\text{C}_{15}\text{H}_{30}\text{N}_6\text{O}_2+\text{H}]^+$: 327.2508. Anal. Calcd for $\text{C}_{15}\text{H}_{32}\text{N}_6\text{O}_4\text{Cl}_2$: C, 43.27; H, 7.99; N, 20.18. Found: C, 44.09; H, 7.93; N, 20.13.

1,12-Dodecane bisguanidinylamide, hydrochloride salt (96e)

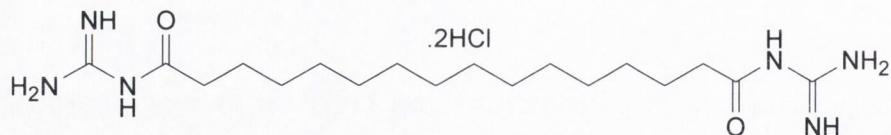


Compound **96d** was prepared following **Procedure 4**, using **97d** (378 mg, 0.7 mmol). A white solid was isolated (165 mg, 57 %).

Compound **96d** was prepared following **Procedure 10**, using **23d** (200 mg, 0.7 mmol). A white solid was isolated (20 mg, 7 %).

Compound **96e** was prepared following **Procedure 12**, using **97e** (378 mg, 0.7 mmol). A white solid was isolated (20 mg, 7 %). δ_{H} (400.1MHz; D₂O)/ppm: 2.37 (4H, t, $J = 7.5$ Hz) 1.52 (4H, m), 1.19 (16H, bs). $\text{mp}/^{\circ}\text{C}$: decomposes above 250. $\nu_{\max}/\text{cm}^{-1}$: 3420, 1718, 1599. m/z found: 341.2680 calculated for: $[\text{C}_{16}\text{H}_{32}\text{N}_6\text{O}_2+\text{H}]^+$: 341.2665.

1,14-Tetradecane bisguanidinylamide, hydrochloride salt (96f)

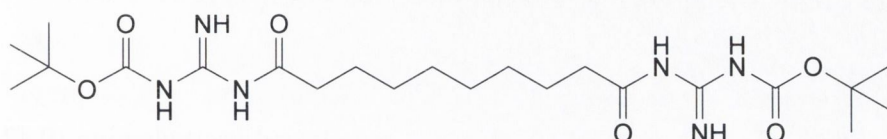


Compound **96d** was prepared following **Procedure 4**, using **97d** (398 mg, 0.7 mmol). A white solid was isolated (195 mg, 63 %).

Compound **96d** was prepared following **Procedure 10**, using **23d** (200 mg, 0.7 mmol). A white solid was isolated (93mg, 3 %).

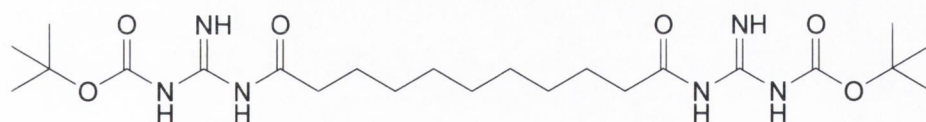
Compound **96f** was prepared following **Procedure 12**, using **97f** (398 mg, 0.7 mmol). A white solid was isolated (9 mg, 3 %). δ_{H} (400.1MHz; D₂O)/ppm: 2.36 (4H, m) 1.52 (4H, m), 1.18 (20H, bs). mp/°C: decomposes above 250. $\nu_{\text{max}}/\text{cm}^{-1}$: 3425, 1723, 1608. Anal. Calcd for C₁₈H₄₁N₉O_{3.5}Cl₂: C, 45.37; H, 8.67; N, 17.64. Found: C, 46.32; H, 8.21; N, 17.31.

1,8-Octane bis-*N*-bocguanidinylamide (**97a**)



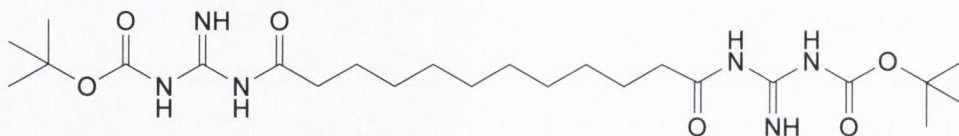
Compound **97a** was prepared according to **Procedure 11**, using **56e** (0.20 g, 1.0 mmol), **63** (0.64 g, 4.0 mmol), BOP (1.6 g, 2.4 mmol) and *N*-methyl morpholine (0.66 ml, 6.0 mmol). A white solid was isolated (373 mg, 77 %). δ_{H} (400.1MHz; CDCl₃)/ppm: 2.45 (4H, t, *J* = 7.5 Hz) 1.68 (4H, m), 1.52 (18H, s), 1.33 (8H, bs). δ_{C} (100.1MHz; CDCl₃)/ppm: 24.3, 27.7, 28.2, 28.4, 37.4, 79.6, 158.1, 161.2, 176.6. $\nu_{\text{max}}/\text{cm}^{-1}$: 3371, 3278, 3104, 1704, 1620. mp/°C: 50 – 52. *m/z* found: 485.3064 calculated for: [C₂₂H₄₀N₆O₆+H]⁺: 485.3088. Anal. Calcd for C₂₂H₄₂N₆O₇: C, 52.57; H, 8.02; N, 16.72. Found: C, 52.83; H, 8.19; N, 16.46.

1,9-Nonane bis-*N*-bocguanidinylamide (**97b**)



Compound **97b** was prepared according to **Procedure 11**, using **56f** (0.22 g, 1.0 mmol), **63** (0.64 g, 4.0 mmol), BOP (1.6 g, 2.4 mmol) and *N*-methyl morpholine (0.66 ml, 6.0 mmol). A white solid was isolated (309 mg, 62 %). δ_{H} (400.1MHz; CDCl₃)/ppm: 2.40 (4H, m) 1.65 (4H, m), 1.52 (18H, s), 1.33 (10H, bs). δ_{C} (100.1MHz; CDCl₃)/ppm: 24.4, 27.7, 28.2, 28.3, 28.4, 37.3, 79.4, 158.4, 161.4. $\nu_{\text{max}}/\text{cm}^{-1}$: 3373, 3277, 3111, 1702, 1622. mp/°C: 50 – 54. *m/z* found: 499.3260 calculated for: [C₂₃H₄₂N₆O₆+H]⁺: 499.3244.

1,10-Decane bis-*N*-bocguanidinylamide (97c)



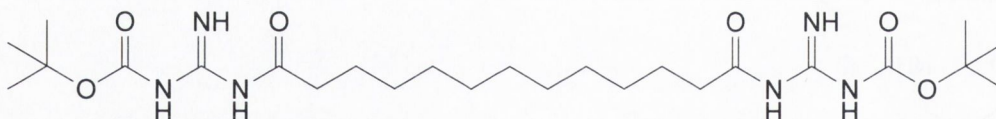
Procedure A:

Compound **97c** was prepared according to **Procedure 11**, using **56a** (0.23 g, 1.0 mmol), **63** (0.64 g, 4.0 mmol), BOP (1.6 g, 2.4 mmol) and *N*-methyl morpholine (0.66 ml, 6.0 mmol). A white solid was isolated (394 mg, 77 %).

Procedure B:

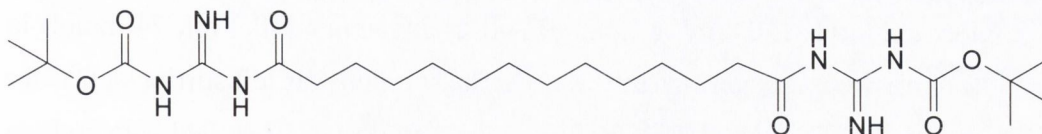
The carboxylic acid (0.23 g, 1.0 mmol), **63** (0.64 g, 4.0 mmol) and triethylamine (0.42 ml, 3.0 mmol) were dissolved in dry acetonitrile (20 ml). TBTU (0.77 g, 2.4 mmol) was added at 0°C and the solution left at room temperature overnight. Work up remained the same as for **Procedure 11**. A white solid was isolated (409 mg, 80 %). δ_{H} (400.1MHz; CDCl₃)/ppm: 2.39 (4H, t, J = 7.5 Hz) 1.65 (4H, m), 1.48 (18H, s), 1.27 (12H, bs). δ_{C} (100.1MHz; CDCl₃)/ppm: 24.4, 27.6, 27.7, 28.0, 28.2, 28.3, 37.5, 79.6, 158.3, 162.1, 179.9. ν_{max} /cm⁻¹: 3369, 3269, 3100, 1705, 1661. mp/°C: 48 – 52. m/z found: 513.3409 calculated for: [C₂₄H₄₄N₆O₆+H]⁺: 513.3401.

1,11-Undecane bis-*N*-bocguanidinylamide (97d)



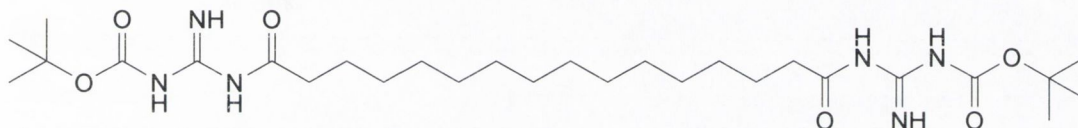
Compound **97d** was prepared according to **Procedure 11**, using **56b** (0.24 g, 1.0 mmol), **63** (0.64 g, 4.0 mmol), BOP (1.6 g, 2.4 mmol) and *N*-methyl morpholine (0.66 ml, 6.0 mmol). A white solid was isolated (447 mg, 85 %). δ_{H} (400.1MHz; CDCl₃)/ppm: 2.38 (4H, t, J = 6.8 Hz) 1.65 (4H, m), 1.49 (18H, s), 1.26 (14H, bs). δ_{C} (100.1MHz; CDCl₃)/ppm: 24.4, 27.7, 28.4, 28.6, 28.7, 37.4, 79.4, 158.4, 162.1, 191.3. ν_{max} /cm⁻¹: 3359, 3103, 1693, 1605. mp/°C 48 – 52. m/z found: 549.3373 calculated for: [C₂₅H₄₆N₆O₆+Na]⁺: 549.3377. Anal. Calcd for C₂₅H₅₁N₆O_{8.5}: C, 52.52; H, 8.11; N, 14.70. Found: C, 52.50; H, 8.19; N, 14.39.

1,12-Dodecane bis-*N*-bocguanidinylamide (97e)



Compound **97e** was prepared according to **Procedure 11**, using **56c** (0.26 g, 1.0 mmol), **63** (0.64 g, 4.0 mmol), BOP (1.6 g, 2.4 mmol) and *N*-methyl morpholine (0.66 ml, 6.0 mmol). A white solid was isolated (469 mg, 87 %). δ_{H} (400.1MHz; CDCl_3)/ppm: 2.39 (4H, t, $J = 7.5$ Hz) 1.65 (4H, m), 1.48 (18H, s), 1.26 (16H, bs). δ_{C} (100.1MHz; CDCl_3)/ppm: 24.4, 27.7, 28.2, 28.5, 28.6, 37.4, 79.5, 158.2, 191.4. $\nu_{\text{max}}/\text{cm}^{-1}$: 3340, 3270, 3103, 1691, 1618. mp/ $^{\circ}\text{C}$: 46 – 50. Anal. Calcd for $\text{C}_{26}\text{H}_{51}\text{N}_6\text{O}_7$: C, 56.81; H, 8.80; N, 15.29. Found: C, 56.73; H, 8.91; N, 15.06.

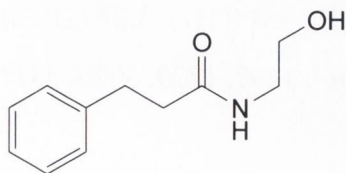
1,14-Tetradecane bis-*N*-bocguanidinylamide (97f)



Compound **97f** was prepared according to **Procedure 11**, using **56d** (0.29 g, 1.0 mmol), **63** (0.64 g, 4.0 mmol), BOP (1.6 g, 2.4 mmol) and *N*-methyl morpholine (0.66 ml, 6.0 mmol). A white solid was isolated (358 mg, 63 %). δ_{H} (400.1MHz; CDCl_3)/ppm: 2.39 (4H, t, $J = 7.52$ Hz) 1.66 (4H, m), 1.49 (18H, s), 1.26 (20H, bs). δ_{C} (100.1MHz; CDCl_3)/ppm: 24.4, 27.7, 28.4, 28.7, 28.8, 28.9, 37.4, 79.4, 158.3, 162.1, 176.5. $\nu_{\text{max}}/\text{cm}^{-1}$: 3350, 3104, 1710, 1668. mp/ $^{\circ}\text{C}$: 47 – 50. Anal. Calcd for $\text{C}_{28}\text{H}_{54}\text{N}_6\text{O}_7$: C, 57.31; H, 8.93; N, 14.32. Found: C, 57.38; H, 9.27; N, 14.81.

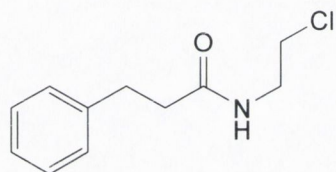
8.5 Synthesis and characterisation of compounds in Chapter 4

N-(2-Hydroxy-ethyl)-3-phenyl-propionamide (143)



To a solution of ethanolamine (4.1 ml, 67 mmol) in dry DCM (20 ml) was added the 3-Phenyl-propionyl chloride (10.0 ml, 67 mmol) and triethylamine (10.3 ml, 74 mmol) in dry DCM (10.0 ml) dropwise concurrently at 0°C. The solution was left stirring at 0°C for one hour and at room temperature for two hours. The solution was basified with sodium hydroxide solution (10 % w/v, 20 ml). The organic layer was separated and dried over sodium sulphate. The excess solvent was removed under reduced pressure. A white solid was isolated (5.43 g, 42 %). δ_{H} (400.1MHz; CDCl_3)/ppm: 2.43 (2H, t, $J = 7.5$ Hz), 2.89 (2H, t, $J = 7.5$ Hz), 3.28 (2H, quartet, $J = 5.0$ Hz), 3.55 (2H, t, $J = 5.0$ Hz), 7.19 (5H, m). δ_{C} (100.1MHz; CDCl_3)/ppm: $\nu_{\text{max}}/\text{cm}^{-1}$: 1443, 1453, 1644, 3063, 3086, 3290. mp/°C: 72 – 74. m/z found: 216.1008 calculated for: $[\text{C}_{11}\text{H}_{15}\text{NO}_2 + \text{Na}]^+$: 216.1000

***N*-(2-Chloro-ethyl)-3-phenyl-propionamide (144)**



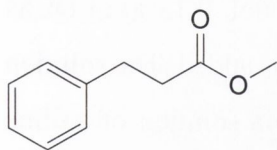
Procedure A:

A mixture of the *N*-(2-Hydroxy-ethyl)-3-phenyl-propionamide (2.1 mmol, 0.4 g), thionyl chloride (3 mmol, 0.23 ml) dissolved in DCM (5.00 ml) and refluxed for four hours. The solvent was removed under reduced pressure to give the desired product (231 mg, 52 %).

Procedure B:

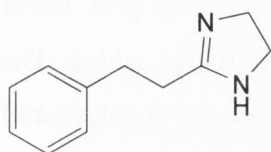
The carboxylic acid (2.1 mmol, 0.32g) was dissolved in dry toluene (2.0 ml) under an atmosphere of argon. Dry triethylamine (0.1 mmol, 14 μl) and 2-chloroethyl isocyanate (4.2 mmol, 1.8 ml) was added. The solution was heated to 60°C for three hours. The solvent was removed under reduced pressure to give a white solid (422 mg, 95 %). δ_{H} (400.1MHz; CDCl_3)/ppm: 2.74 (2H, t, $J = 8.0\text{Hz}$), 2.94 (2H, $J = 8.0$ Hz), 3.27 (2H, s), 4.39 (2H, s), 7.19 (5H, m). δ_{C} (400.1MHz; D_2O)/ppm: $\nu_{\text{max}}/\text{cm}^{-1}$: 1497, 1729, 3026, 3377. mp/°C: 100 – 102.

3-Phenyl-propionic acid methyl ester (148)



Compound **148** was prepared following **Procedure 6**, using **142a** (1.49 g, 10 mmol) and thionyl chloride (0.8 ml, 11 mmol). A clear colourless liquid was isolated (1.47 g, 90 %). δ_{H} (400.1MHz; CDCl_3)/ppm: 2.45 (2H, m), 2.79 (2H, m), 3.51 (3H,s), 7.19 (5H, m).

2-Phenethyl-4,5-dihydro-1H-imidazole (141)



Procedure A:

To a solution of *N*-(2-Chloro-ethyl)-3-phenyl-propionamide (0.6 mmol, 0.13 g) in DCM (10 ml) under argon, phosphorous oxychloride (0.7 mmol, 63 μl) was added. The solution was left to stir for one hour. This solution was added dropwise to a solution of aniline (2.0 mmol, 186 mg) in DCM (10 ml) and left to stir at 0°C for 12 hours. The organic layer was washed with water (2 x 30 ml). The organic layer was dried over magnesium sulphate and removed under reduced pressure.

Procedure B:

To a solution of *N*-(2-Chloro-ethyl)-3-phenyl-propionamide (0.6 mmol, 0.13g) in DCM (10 ml) under argon, phosphorous oxychloride (0.7 mmol, 63 μl) was added. The solution was left to stir for one hour. This solution was added dropwise to a solution of aniline (2.0 mmol, 186 mg) in DCM (10 ml) and left to stir at room temperature for 12 hours. The organic layer was washed with water (2 x 30 ml). The organic layer was dried over magnesium sulphate and removed under reduced pressure.

Procedure C:

To a solution of *N*-(2-Chloro-ethyl)-3-phenyl-propionamide (0.6 mmol, 0.13 g) in DCM (10 ml) under argon, phosphorous oxychloride (0.7 mmol, 63 μ l) was added. The solution was left to stir for one hour. This solution was added dropwise to a solution of aniline (2.0 mmol, 186 mg) in DCM (10 ml) left to stir at 50°C for 12 hours. The organic layer was washed with water (2 x 30 ml). The organic layer was dried over magnesium sulphate and removed under reduced pressure.

Procedure D:

To a solution of *N*-(2-Chloro-ethyl)-3-phenyl-propionamide (0.6 mmol, 0.13 g) in DCM (10 ml) under argon, phosphorous pentachloride (0.7 mmol, 146 mg) was added. The solution was left to stir for 12 hours. This solution was added dropwise to a solution of aniline (2.0 mmol, 186 mg) in DCM (10 ml) and left to stir at room temperature for 12 hours. The organic layer was washed with water (2 x 30 ml). The organic layer was dried over magnesium sulphate and removed under reduced pressure.

Procedure E:

To a solution of *N*-(2-Chloro-ethyl)-3-phenyl-propionamide (0.6 mmol, 0.13 g) in DCM (10 ml) under argon, phosphorous pentachloride (0.7 mmol, 146 mg) was added. The solution was left to stir for 10 min. This solution was added dropwise to a saturated solution of ammonia in DCM (50 ml) and refluxed for 12 hours. The organic layer was washed with water (2 x 30 ml). The organic layer was dried over magnesium sulphate and removed under reduced pressure.

Procedure F:

To a solution of *N*-(2-Chloro-ethyl)-3-phenyl-propionamide (0.6 mmol, 0.13 g) in DCM (10 ml) under argon, phosphorous pentachloride (0.7 mmol, 146 mg) was added. The solution was left to stir for 10 min. This solution was added dropwise to a solution of urethane (2.0 mmol, 154 mg) in DCM (10 ml) and refluxed for 12 hours. The organic layer was washed with water (2 x 30 ml). The organic layer was dried over magnesium sulphate and removed under reduced pressure.

Procedure G:

To a solution of *N*-(2-Chloro-ethyl)-3-phenyl-propionamide (0.6 mmol, 0.13 g) in DCM (10 ml) under argon, phosphorous pentachloride (0.7 mmol, 146 mg) was added. The solution was left to stir for 10 min. This solution was added dropwise to a solution of urethane (2.0 mmol, 154 mg) in DCM (10 ml) and refluxed for 12 hours. The organic layer was washed with water (2 x 30 ml). The organic layer was dried over magnesium sulphate and removed under reduced pressure.

Procedure H:

To a solution of *N*-(2-Chloro-ethyl)-3-phenyl-propionamide (0.6 mmol, 0.13 g) in DCM (10 ml) under argon, phosphorous pentachloride (0.7 mmol, 146 mg) was added. The solution was left to stir for 10 min. This solution was added dropwise to a solution of urethane (2.0 mmol, 154 mg) in DCM (10 ml) and refluxed for 12 hours. The organic layer was washed with water (2 x 30 ml). The organic layer was dried over magnesium sulphate and removed under reduced pressure.

Procedure I:

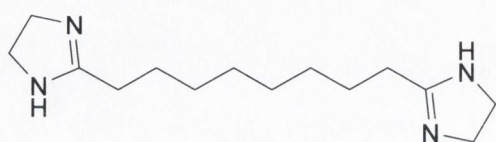
To a solution of *N*-(2-Chloro-ethyl)-3-phenyl-propionamide (0.6 mmol, 0.13 g) in DCM (10 ml) under argon, phosphorous pentachloride (0.7 mmol, 146 mg) was added. The solution was left to stir for 10 min. This solution was added dropwise to a solution of benzyl carbamate (2.0 mmol, 250 mg) in DCM (10 ml) and refluxed for 12 hours. The organic layer was washed with water (2 x 30 ml). The organic layer was dried over magnesium sulphate and removed under reduced pressure.

Procedure J:

Methyl hydrocinnamate (328 mg, 2 mmol) in distilled hexane (20 ml) was added dropwise to a rapidly stirred solution of trimethylaluminium in hexane (7.5 ml, 2M) at 0°C. After addition was complete ethylene diamine (1.2 g, 20 mmol) was added and the solution heated to 80°C overnight. The solution was cooled on an ice bath and water (30 ml) added dropwise. The solution was filtered and the aqueous layer extracted with hexane (2 times with 20 ml). The organic layers were dried over magnesium sulfate and

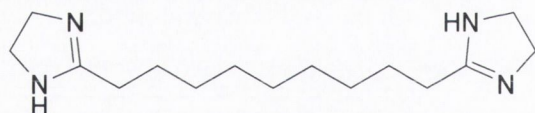
excess solvent removed under reduced pressure under reduced pressure. The resulting residue was dissolved in methanol (30 ml) and hydrochloric acid (0.2M, 50 ml) added. A yellowy solid precipitated. Yellow solid, 31.5 mg (7.5 %). δ_{H} (400.1MHz; D₂O)/ppm; 2.43 (2H, m), 2.95 (2H, m), 3.49 (4H, s), 7.23 (5H, m). $\nu_{\text{max}}/\text{cm}^{-1}$: 3102, 1602. mp/°C: 124 – 126. $\nu_{\text{max}}/\text{cm}^{-1}$: 1451, 1643, 3030, 3063, 3298. m/z *found*: 175.0873 calculated for: [C₁₁H₁₄N₂+H]⁺: 175.2529.

1,8-octane bis(-4,5-dihydro-1H-imidazole) (24a)



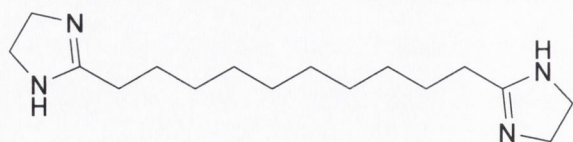
Compound **24a** was prepared following **Procedure 13**, using **65e** (230 mg, 1 mmol) and ethylene diamine (0.33 ml, 5 mmol). A white solid was isolated (199 mg, 77 %). δ_{H} (400.1MHz; CDCl₃)/ppm: 1.33 (8H, bs), 1.63 (4H, m), 2.26 (4H, t, J = 7.5 Hz), 3.61 (8H, s). $\nu_{\text{max}}/\text{cm}^{-1}$: 1458, 1469, 1494, 1611, 1643, 3171, 3306. mp/°C: 155 – 157 m/z *found*: 251.2240 calculated for: [C₁₄H₂₆N₄+H]⁺: 251.2236.

1,9-nonane bis(-4,5-dihydro-1H-imidazole) (24b)



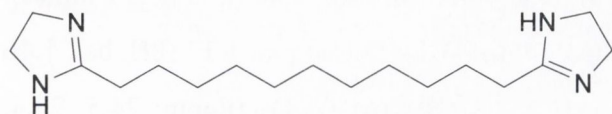
Compound **24b** was prepared following **Procedure 13**, using **65f** (244 mg, 1 mmol) and ethylene diamine (0.33 ml, 5 mmol). A white solid was isolated (71 mg, 26 %). δ_{H} (400.1MHz; CDCl₃)/ppm: 1.31 (10H, bs), 1.62 (4H, m), 2.25 (4H, t, 8.04Hz), 3.60 (8H, s). $\nu_{\text{max}}/\text{cm}^{-1}$: 1423, 1471, 1496, 1611, 1643, 3199, 3298. mp/°C: 118 – 120. m/z *found*: 265.2384 calculated for: [C₁₅H₂₈N₄+H]⁺: 265.2392.

1,10-decane bis(-4,5-dihydro-1H-imidazole) (24c)



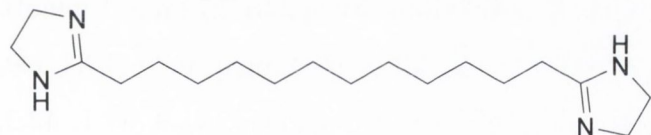
Compound **24c** was prepared following **Procedure 13**, using **65c** (258 mg, 1 mmol) and ethylene diamine (0.33 ml, 5 mmol). A white solid was isolated (183 mg, 64 %). δ_{H} (400.1MHz; CDCl_3)/ppm: 1.29 (12H, bs), 1.63 (4H, q, $J = 7.5$ Hz), 2.32 (4H, quartet, $J = 7.5$ Hz), 3.64 (8H, s). $\nu_{\text{max}}/\text{cm}^{-1}$: 1420, 1435, 1458, 1469, 1493, 1611, 1645, 3175, 3305. $\text{mp}/^\circ\text{C}$: 157 – 159. m/z found: 279.2556 calculated for: $[\text{C}_{16}\text{H}_{30}\text{N}_4+\text{H}]^+$: 279.2549.

1,11-undecane bis(-4,5-dihydro-1H-imidazole) (**24d**)



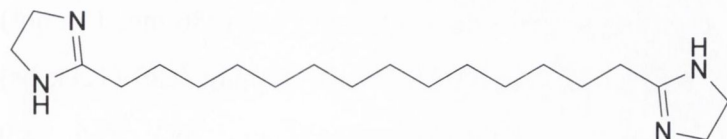
Compound **24d** was prepared following **Procedure 13**, using **65a** (272 mg, 1 mmol) and ethylene diamine (0.33 ml, 5 mmol). A white solid was isolated (117 mg, 39 %). δ_{H} (400.1MHz; CDCl_3)/ppm: 0.87 (14H, bs), 1.28 (4H, m), 2.14 (4H, m), 3.50 (8H, s). $\nu_{\text{max}}/\text{cm}^{-1}$: 1461, 1472, 1496, 1611, 1643, 3203, 3300. $\text{mp}/^\circ\text{C}$: 114 – 116. m/z found: 293.2704 calculated for: $[\text{C}_{17}\text{H}_{32}\text{N}_4+\text{H}]^+$: 293.2705.

1,12-dodecane bis(-4,5-dihydro-1H-imidazole) (**24e**)



Compound **24e** was prepared following **Procedure 13**, using **65d** (300 mg, 1 mmol) and ethylene diamine (0.33 ml, 5 mmol). A white solid was isolated (141 mg, 45 %). δ_{H} (400.1MHz; CDCl_3)/ppm: 1.26 (16H, bs), 1.63 (4H, m), 2.31 (4H, m), 3.64 (8H, s). $\nu_{\text{max}}/\text{cm}^{-1}$: 1421, 1470, 1612, 1642, 3087, 3178, 3304. $\text{mp}/^\circ\text{C}$: 115 – 117. m/z found: 154.1530 $[\text{C}_{18}\text{H}_{34}\text{N}_4+2\text{H}]^{2+}$: 154.2546.

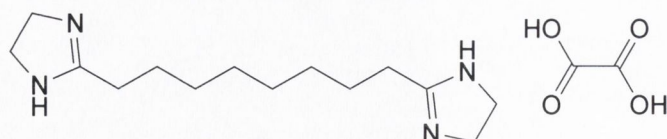
1,14-tetradecane bis(-4,5-dihydro-1H-imidazole) (**24f**)



Compound **24f** was prepared following **Procedure 13**, using **65b** (328 mg, 1 mmol) and ethylene diamine (0.33 ml, 5 mmol). A white solid was isolated (154 mg, 45 %).

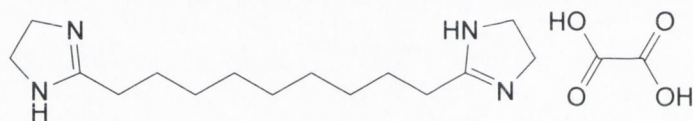
δ_{H} (400.1MHz; CDCl_3)/ppm: 1.23 (20H, bs), 1.64 (4H, m), 2.38 (4H, m), 3.70 (8H, s). $\nu_{\text{max}}/\text{cm}^{-1}$: 1467, 1734, 3294. mp/ $^{\circ}\text{C}$: 78 – 80.

1,8-octane bis(-4,5-dihydro-1H-imidazole) oxalate salt (150a)



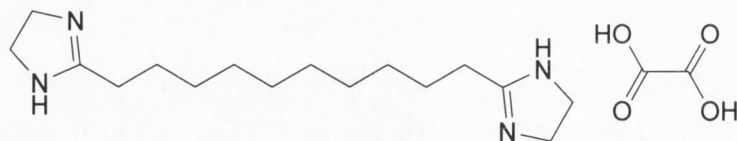
Compound **150a** was prepared according to **Procedure 14**, using **24a** (258 mg, 1 mmol). A white solid was isolated (317 mg, 91 %). δ_{H} (400.1MHz; D_2O)/ppm: 1.13 (8H, bs), 1.46 (4H, m), 2.34 (4H, t, $J = 7.5$ Hz), 3.71 (8H, s). δ_{C} (100.1MHz; D_2O)/ppm: 24.5, 25.4, 27.3, 29.7, 35.1, 38.6, 171.3. $\nu_{\text{max}}/\text{cm}^{-1}$: 1382, 1394, 1406, 1451, 3675. mp/ $^{\circ}\text{C}$: 158 – 160.

1,9-nonane bis(-4,5-dihydro-1H-imidazole) oxalate salt (150b)



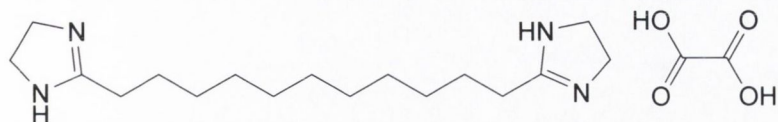
Compound **150b** was prepared according to **Procedure 14**, using **24b** (272 mg, 1 mmol). A white solid was isolated (282 mg, 78 %). δ_{H} (400.1MHz; D_2O)/ppm: 0.90 (10H, bs), 1.31 (4H, m), 2.19 (4H, m), 3.52 (8H, s). δ_{C} (100.1MHz; D_2O)/ppm: 41.9, 42.1, 42.3, 42.5, 42.7, 80.1, 80.2, 163.3. $\nu_{\text{max}}/\text{cm}^{-1}$: 1402, 1435, 1466, 1482, 1601, 1711, 3126, 3262. mp/ $^{\circ}\text{C}$: 138 – 140. m/z found: 265.2400 calculated for: $[\text{C}_{15}\text{H}_{28}\text{N}_4+\text{H}]^+$: 265.2392.

1,10-decane bis(-4,5-dihydro-1H-imidazole) oxalate salt (150c)



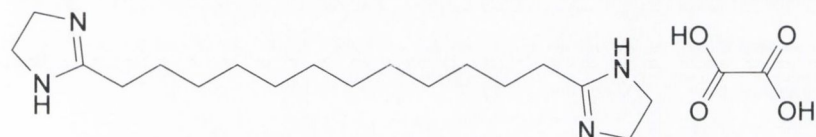
Compound **150c** was prepared according to **Procedure 14**, using **24c** (286 mg, 1 mmol). A white solid was isolated (312 mg, 83 %). δ_{H} (400.1MHz; D_2O)/ppm: 0.89 (12H, bs), 1.29 (4H, m), 2.17 (4H, m), 3.52 (8H, s). δ_{C} (100.1MHz; D_2O)/ppm: 26.1, 25.5, 28.0, 28.1, 28.3, 28.4, 30.7, 160.7. $\nu_{\text{max}}/\text{cm}^{-1}$: 1394, 1468, 1593, 1692, 3105. mp/ $^{\circ}\text{C}$: 136 – 138. m/z found: 279.2554 calculated for: $[\text{C}_{16}\text{H}_{30}\text{N}_4+\text{H}]^+$: 279.2549.

1,11-undecane bis(-4,5-dihydro-1H-imidazole) oxalate salt (150d)



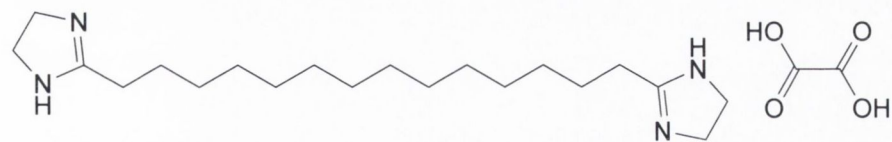
Compound **150d** was prepared according to **Procedure 14**, using **24d** (300 mg, 1 mmol). A white solid was isolated (363 mg, 93 %). δ_{H} (400.1MHz; D₂O)/ppm: 1.09 (14H, bs), 1.46 (4H, m), 2.34 (4H, t, J = 7.5 Hz), 3.71 (8H, s). δ_{C} (100.1MHz; D₂O)/ppm: 24.5, 25.4, 27.4, 27.7, 27.9, 29.2, 35.1, 43.6, 171.4. $\nu_{\text{max}}/\text{cm}^{-1}$: 1440, 1610, 1686, 3416. mp/°C: 98 – 100.

1,12-dodecane bis(-4,5-dihydro-1H-imidazole) oxalate salt (150e)



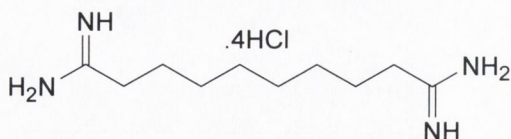
Compound **150e** was prepared according to **Procedure 14**, using **24e** (314 mg, 1 mmol). A white solid was isolated (347 mg, 86 %). δ_{H} (400.1MHz; D₂O)/ppm: 1.17 (16H, bs), 1.55 (4H, q, J = 5.0 Hz), 2.43 (4H, t, J = 5.0 Hz), 3.80 (8H, s). δ_{C} (100.1MHz; D₂O)/ppm: 24.8, 25.8, 27.7, 27.9, 28.2, 28.4, 35.4, 35.5, 43.9, 171.8. $\nu_{\text{max}}/\text{cm}^{-1}$: 1421, 1438, 1469, 1612, 1643, 3179, 3307. m/z found: 307.2867 calculated for: [C₁₈H₃₄N₄+H]⁺: 307.2862.

1,14-tetradecane bis(-4,5-dihydro-1H-imidazole) oxalate salt (150f)



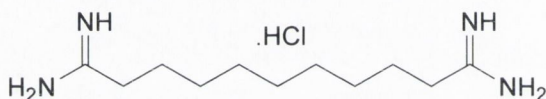
Compound **150f** was prepared according to **Procedure 14**, using **24f** (342 mg, 1 mmol). A white solid was isolated (393 mg, 91 %). δ_{H} (400.1MHz; D₂O)/ppm: 1.19 (20H, bs), 1.57 (4H, q, J = 5.0 Hz), 2.45 (4H, t, J = 5.0 Hz), 3.81 (8H, s). δ_{C} (100.1MHz; D₂O)/ppm: 24.8, 25.8, 27.7, 28.3, 28.6, 35.5, 36.6, 39.0, 44.0, 171.8. $\nu_{\text{max}}/\text{cm}^{-1}$: 1401, 1483, 1715, 3389.

1,8-octane bis-amidine (25a)



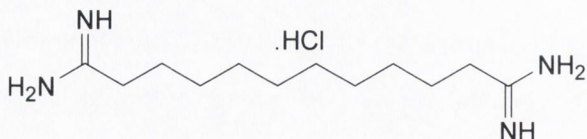
Compound **25a** was prepared by following **Procedure 15**, using **65a** (230 mg, 1 mmol), ammonium hydrochloride (535 mg, 10 mmol). A yellow solid was isolated (203 mg, 75%). δ_{H} (400.1MHz; D₂O)/ppm: 1.31 (8H, bs), 1.66 (4H, q, J = 5.2 Hz), 2.45 (4H, t, J = 5.2 Hz). δ_{C} (100.1MHz; D₂O)/ppm: 25.9, 27.6, 27.8, 31.9, 171.5. $\nu_{\text{max}}/\text{cm}^{-1}$: 1434, 1451, 1470, 1688, 3080, 3239. mp/°C: decomposes above 250. m/z found: 199.1924 calculated for: [C₁₀H₂₂N₄+H]⁺: 199.1923. Anal. Calcd for C₁₀H₂₇N₄Cl₄: C, 31.56; H, 7.15; N, 14.72. Found: C, 31.67; H, 6.37; N, 14.59.

1,9-nonane bis-amidine (25b)



Compound **25b** was prepared by following **Procedure 15**, using **65b** (244 mg, 1 mmol), ammonium hydrochloride (535 mg, 10 mmol). A yellow solid was isolated (208 mg, 73 %). δ_{H} (400.1MHz; D₂O)/ppm: 1.21 (10H, bs), 1.57 (4H, m), 2.36 (4H, t, J = 7.5 Hz). δ_{C} (100.1MHz; D₂O)/ppm: 25.6, 27.3, 27.6, 27.7, 31.6, 171.2. $\nu_{\text{max}}/\text{cm}^{-1}$: 1407, 1688, 3081, 3244. mp/°C: decomposes above 250. m/z found: 213.2069 calculated for: [C₁₁H₂₅N₄+H]⁺: 213.2079.

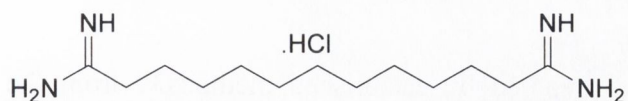
1,10-decane bis-amidine (25c)



Compound **25c** was prepared by following **Procedure 15**, using **65c** (258 mg, 1 mmol), ammonium hydrochloride (535 mg, 10 mmol). A yellow solid was isolated (239 mg, 80 %). δ_{H} (400.1MHz; D₂O)/ppm: 1.26 (12H, bs), 1.64 (4H, q, J = 5.3 Hz), 2.43 (4H, t, J = 5.3 Hz). δ_{C} (100.1MHz; D₂O)/ppm: 25.9, 27.7, 28.0, 28.2, 31.9, 171.6. $\nu_{\text{max}}/\text{cm}^{-1}$: 1435,

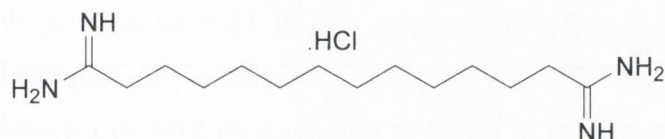
1471, 1690, 3077, 3245. mp/°C: decomposes above 250. m/z *found*: 227.2227 calculated for: [C₁₂H₂₆N₄+H]⁺: 227.2230.

1,11-undecane *bis*-amidine (25d)



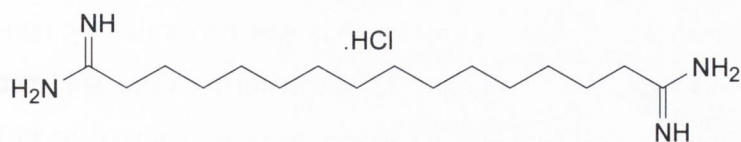
Compound **25d** was prepared by following **Procedure 15**, using **65d** (272 mg, 1 mmol), ammonium hydrochloride (535 mg, 10 mmol). A yellow solid was isolated (250 mg, 80 %). δ_{H} (400.1MHz; D₂O)/ppm: 1.18 (14H, bs), 1.57 (4H, m), 2.36 (4H, t, J = 7.5 Hz). δ_{C} (100.1MHz; D₂O)/ppm: 25.6, 27.3, 27.7, 27.9, 28.0, 31.6, 171.2. ν_{max} /cm⁻¹: 1408, 1431, 1471, 1688, 3078, 3245. mp/°C: decomposes above 250. m/z *found*: 241.2383 calculated for: [C₁₃H₂₈N₄+H]⁺: 241.2392.

1,12-dodecane *bis*-amidine (25e)



Compound **25e** was prepared by following **Procedure 15**, using **65d** (286 mg, 1 mmol), ammonium hydrochloride (535 mg, 10 mmol). A yellow solid was isolated (252 mg, 77 %). δ_{H} (400.1MHz; D₂O)/ppm: 1.26 (16H, bs), 1.65 (4H, m), 2.45 (4H, t, J = 5.0Hz). δ_{C} (100.1MHz; D₂O)/ppm: ν_{max} /cm⁻¹: 1435, 1471, 1688, 3081, 3246. mp/°C: decomposes above 250. m/z *found*: 255.2558 calculated for: [C₁₄H₃₀N₄+H]⁺: 255.2549.

1,14-tetradecane *bis*-amidine (25f)



Compound **25f** was prepared by following **Procedure 15**, using **65f** (314 mg, 1 mmol), ammonium hydrochloride (535 mg, 10 mmol). A yellow solid was isolated (263 mg, 74 %). δ_{H} (400.1MHz; D₂O)/ppm: 1.16 (20H, bs), 1.56 (4H, m), 2.35 (4H, t, J = 7.5 Hz). δ_{C} (100.1MHz; D₂O)/ppm: 25.6, 27.9, 28.1, 28.2, 29.7, 31.6, 171.2. ν_{max} /cm⁻¹: 1413,

1435, 1471, 1688, 3081, 3244. mp/°C: decomposes above 250. m/z *found*: 283.2859
calculated for: [C₁₆H₃₄N₄+H]⁺: 283.2862.

8.6 Biological Assays

Neural membranes (P2 fractions) were prepared by established methods³⁴ from the prefrontal cortex of human brains obtained at autopsy in the Instituto Vasco de Medicina Legal, Bilbao, Spain. Briefly, the tissue samples were homogenised in 5 mL of ice-cold Tris sucrose buffer (5 mM Tris-HCl, 250mM sucrose, pH 7.4). The homogenates were centrifuged at 1100g for 10min, and the supernatants were then recentrifuged at 40,000g for 10min. The resulting pellet was washed twice and resuspended in 50mM Tris-HCl buffer (pH 7.5) to a final protein content of 0.83_0.14 mg mL⁻¹. [3H]2-BFI binding assay. Total [3H]2-BFI binding was measured in 0.55 mL aliquots (50 mM Tris-HCl, pH 7.5) of the neural membranes that were incubated with [3H]2-BFI (1 nM) for 45 min at 25 °C in the absence or presence of the competing compounds (10⁻¹² M to 10⁻³ M, 10 concentrations). Total binding was determined and plotted as a function of the compound concentration. Incubations were terminated by diluting the samples with 5 mL of ice-cold Tris incubation buffer (4 °C). Membrane bound [3H]2-BFI was separated by vacuum filtration through Whatman GF/C glass fibre filters. The filters were then rinsed twice with 5 mL of incubation buffer and transferred to minivials containing 3 mL of OptiPhase 'HiSafe' II cocktail and counted for radioactivity by liquid scintillation spectrometry. [3H]RX821002 binding assay. The binding of [3H]RX821002 (1 nM) to brain cortical membranes was performed as described for the [3H]2-BFI binding except in the incubation conditions (30min at 25 °C). Analysis of binding data. Analysis of competition experiments to obtain the inhibition constant (K_i) was performed by non-linear regression using the EBDALIGAND program. All experiments were analysed assuming a one-site model of radioligand binding. K_i values were normalized to pK_i values and expressed as mean_ standard error of the means. Drugs. [3H]2-BFI (specific affinity 70Ci/mmol) was purchased from Amersham International, UK. [3H]RX821002 (specific affinity 59 Ci/mmol) was obtained from Amersham International, UK. Idazoxan

HCl was synthesised by Dr. F. Geijo at S.A. Lasa Laboratories, Barcelona, Spain. Other reagents were obtained from Sigma Chemical Co. (St. Louis, MO, USA).

8.7 References

44. Meana, J. J.; Barturen, F.; Martin, I.; Garcia-Sevilla, J. A. *Biol Psych.* 1993, 34, 498.
200. Nakamura, N.; Takayama, T. *Acta Cryst.* **1997**, C53, 253.
201. Nakamura, N.; Yamamoto, T. *Acta Cryst.* **1994**, C50, 946.

Appendix

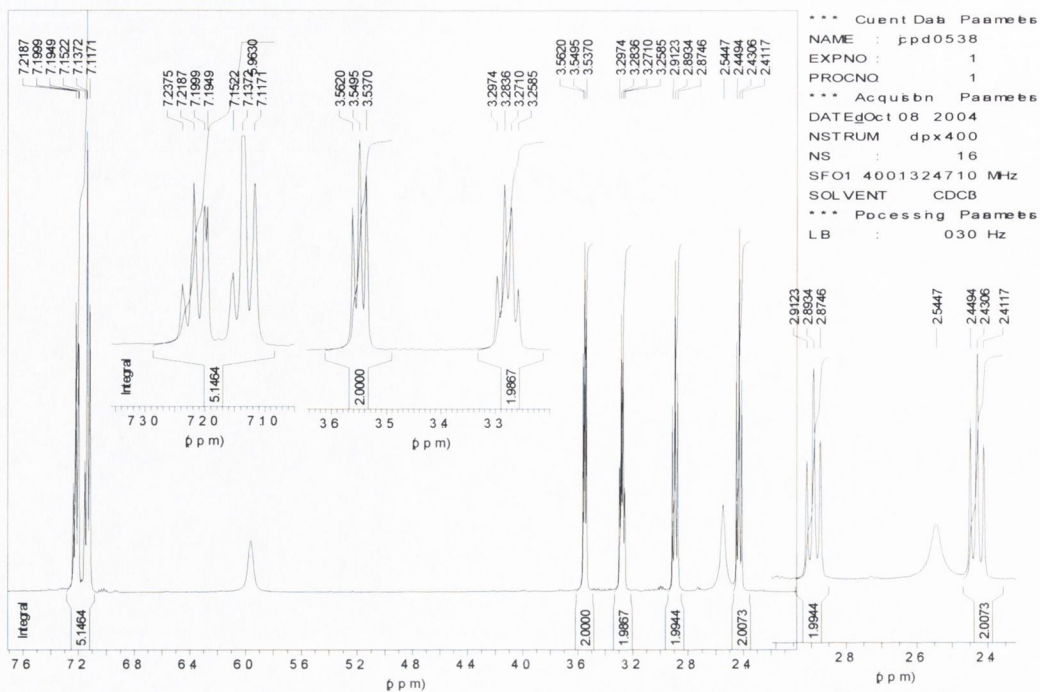


Figure A1.- ¹H NMR of the *N*-(2-Chloro-ethyl)-3-phenyl-propionamide

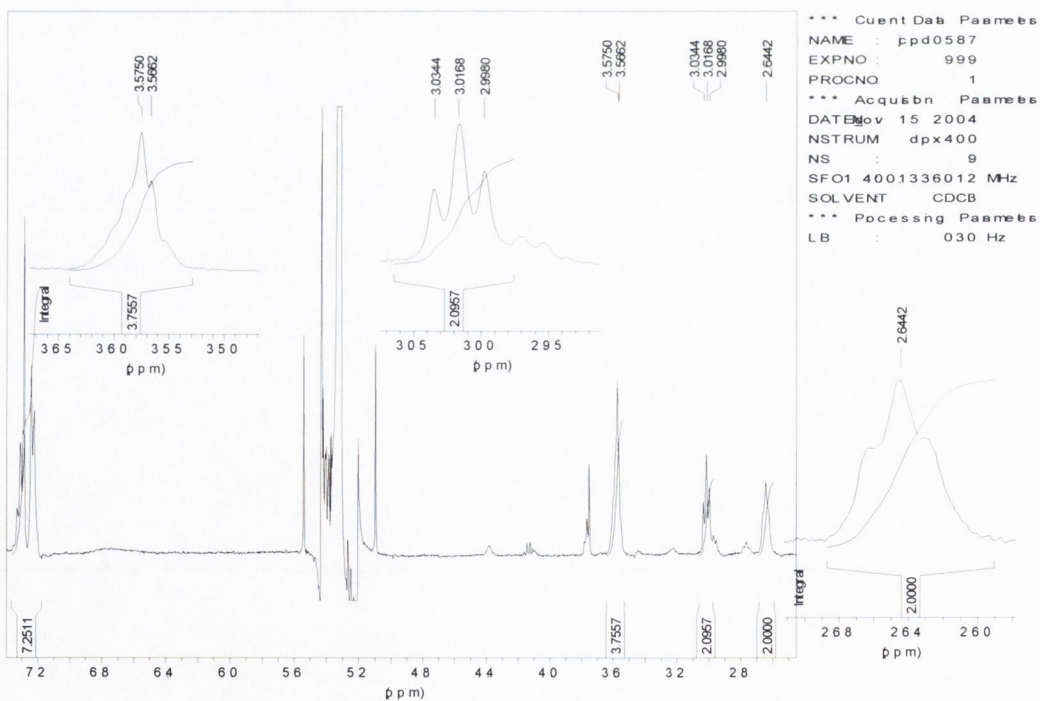


Figure A1.- ¹H NMR of the *N*-(2-Chloro-ethyl)-3-phenyl-propionimidoyl chloride

Table A.1.- The conformations identified for each step at different starting points in the search for the BAC for **19b**

Function	Energy	Distance	Total Dipole	PSA	Volume	Area
Energy	X	102	56	21	3	1
Distance	1	X	115	48	11	5
Total Dipole	2	1	X	110	31	9
PSA	4	1	1	X	57	18
Volume	14	8	5	1	X	36
Area	51	29	16	6	1	X

Table A.2.- The conformations identified for each step at different starting points in the search for the BAC for **19c**

Function	Energy	Distance	Total Dipole	PSA	Volume	Area
Energy	X	84	46	39	11	4
Distance	4	X	95	81	22	4
Total Dipole	5	4	X	216	60	14
PSA	10	4	4	X	105	34
Volume	14	4	4	4	X	41
Area	69	24	15	13	4	X

Table A.3.- The conformations identified for each step at different starting points in the search for the BAC for **19e**

Function	Energy	Distance	Total Dipole	PSA	Volume	Area
Energy	X	62	21	10	4	2
Distance	2	X	51	24	8	2
Total Dipole	3	2	X	60	11	3
PSA	9	4	2	X	44	15
Volume	15	7	3	2	X	27
Area	48	20	9	4	2	X

Table A.4.- The conformations identified for each step at different starting points in the search for the BAC for **19f**

Function	Energy	Distance	Total Dipole	PSA	Volume	Area
Energy	X	85	55	28	7	1
Distance	1	X	119	52	8	1
Total Dipole	2	2	X	100	17	2
PSA	7	1	1	X	42	15
Volume	14	6	2	2	X	30
Area	54	26	17	9	1	X

Table A.5.- The conformations identified for each step at different starting points in the search for the BAC for **19d**

Function	Energy	Distance	Total Dipole	PSA	Volume	Area
Energy	X	103	55	24	13	8
Distance	8	X	117	46	19	12
Total Dipole	8	8	X	69	30	14
PSA	21	16	8	X	79	42
Volume	37	28	14	8	X	80
Area	69	49	27	14	8	X

Table A.6.- The conformations identified for each step at different starting points in the search for the BAC for **29c**

Function	Energy	Distance	Total Dipole	PSA	Volume	Area
Energy	X	54	17	17	10	3
Distance	3	X	37	35	20	8
Total Dipole	3	3	X	95	43	9
PSA	11	8	3	X	111	26
Volume	12	8	3	3	X	33
Area	28	13	5	5	3	X

Table A.7.- The conformations identified for each step at different starting points in the search for the BAC for **19g**

Function	Energy	Distance	Total Dipole	PSA	Volume	Area
Energy	X	101	20	8	3	3
Distance	3	X	42	18	6	6
Total Dipole	3	3	X	26	7	6
PSA	15	10	3	X	47	38
Volume	31	19	4	3	X	73
Area	104	72	15	7	0	X

Table A.8.- The conformations identified for each step at different starting points in the search for the BAC for **42a**

Function	Energy	Distance	Total Dipole	PSA	Volume	Area
Energy	X	90	22	8	2	1
Distance	1	X	37	17	4	3
Total Dipole	4	1	X	55	11	9
PSA	21	6	1	X	42	33
Volume	38	11	1	1	X	60
Area	187	55	12	5	1	X

Table A.9.- The conformations identified for each step at different starting points in the search for the BAC for **42b**

Function	Energy	Distance	Total Dipole	PSA	Volume	Area
Energy	X	95	43	32	7	4
Distance	4	X	104	75	17	9
Total Dipole	4	4	X	164	34	12
PSA	9	7	4	X	76	25
Volume	9	7	4	4	X	25
Area	41	21	10	8	4	X

Table A.10.- The conformations identified for each step at different starting points in the search for the BAC for **42c**

Function	Energy	Distance	Total Dipole	PSA	Volume	Area
Energy	X	139	23	11	1	1
Distance	1	X	39	22	2	2
Total Dipole	2	1	X	97	13	4
PSA	12	5	1	X	87	33
Volume	15	7	1	1	X	42
Area	21	17	1	1	1	X

Table A.11.- The conformations identified for each step at different starting points in the search for the BAC for **42d**

Function	Energy	Distance	Total Dipole	PSA	Volume	Area
Energy	X	103	68	42	22	9
Distance	9	X	114	70	35	11
Total Dipole	19	9	X	139	66	27
PSA	26	12	9	X	99	38
Volume	30	15	10	9	X	43
Area	54	27	21	16	9	X

Table A.12.- The conformations identified for each step at different starting points in the search for the BAC for **42e**

Function	Energy	Distance	Total Dipole	PSA	Volume	Area
Energy	X	193	84	47	20	3
Distance	7	X	134	81	32	8
Total Dipole	8	7	X	92	40	11
PSA	18	15	6	X	114	34
Volume	27	23	8	6	X	47
Area	69	60	24	16	6	X

Table A.13.- The conformations identified for each step at different starting points in the search for the BAC for **42f**

Function	Energy	Distance	Total Dipole	PSA	Volume	Area
Energy	X	68	18	13	2	1
Distance	1	X	42	25	6	3
Total Dipole	2	1	X	48	12	6
PSA	15	9	1	X	69	45
Volume	22	14	1	1	X	64
Area	66	34	8	8	1	X

Table A.14.- The conformations identified for each step at different starting points in the search for the BAC for **52a**

Function	Energy	Distance	Total Dipole	PSA	Volume	Area
Energy	X	130	89	55	8	5
Distance	5	X	117	71	13	11
Total Dipole	10	5	X	178	37	25
PSA	18	13	5	X	64	40
Volume	26	17	6	5	X	56
Area	113	70	46	32	5	X

Table A.14.- The conformations identified for each step at different starting points in the search for the BAC for **52b**

Function	Energy	Distance	Total Dipole	PSA	Volume	Area
Energy	X	116	69	47	5	2
Distance	2	X	140	92	13	6
Total Dipole	3	2	X	201	30	9
PSA	9	3	2	X	72	18
Volume	8	5	3	2	X	24
Area	40	28	21	18	2	X

Table A.15.- The conformations identified for each step at different starting points in the search for the BAC for **52c**

Function	Energy	Distance	Total Dipole	PSA	Volume	Area
Energy	X	55	19	15	1	1
Distance	1	X	49	27	6	3
Total Dipole	2	1	X	99	13	6
PSA	7	3	1	X	46	20
Volume	15	4	1	1	X	35
Area	59	21	8	6	1	X

Table A.16.- The conformations identified for each step at different starting points in the search for the BAC for **52d**

Function	Energy	Distance	Total Dipole	PSA	Volume	Area
Energy	X	38	13	8	2	1
Distance	1	X	45	29	7	5
Total Dipole	2	1	X	81	20	14
PSA	21	6	1	X	59	47
Volume	35	1	1	1	X	78
Area	95	30	11	7	1	X

Table A.17.- The conformations identified for each step at different starting points in the search for the BAC for **52e**

Function	Energy	Distance	Total Dipole	PSA	Volume	Area
Energy	X	81	4	38	8	5
Distance	5	X	83	52	10	6
Total Dipole	11	5	X	189	36	14
PSA	14	6	5	X	48	19
Volume	17	7	6	5	X	22
Area	100	37	30	19	5	X

Table A.18.- The conformations identified for each step at different starting points in the search for the BAC for **52f**

Function	Energy	Distance	Total Dipole	PSA	Volume	Area
Energy	X	45	20	11	4	2
Distance	2	X	50	25	6	3
Total Dipole	3	2	X	61	20	9
PSA	12	2	2	X	48	25
Volume	15	9	2	2	X	41
Area	26	14	3	2	2	X

Table A.19.- The conformations identified for each step at different starting points in the search for the BAC for **S15430**

Function	Energy	Distance	Total Dipole	PSA	Volume	Area
Energy	X	17	17	15	13	4
Distance	4	X	103	77	70	27
Total Dipole	16	4	X	211	145	59
PSA	17	4	4	X	148	61
Volume	21	4	4	4	X	78
Area	22	4	4	4	4	X

Table A.20.- The conformations identified for each step at different starting points in the search for the BAC for **25a**

Function	Energy	Distance	Total Dipole	PSA	Volume	Area
Energy	X	52	45	21	10	1
Distance	1	X	167	70	19	6
Total Dipole	7	1	X	76	21	8
PSA	13	11	1	X	55	22
Volume	19	17	6	1	X	42
Area	52	45	21	10	1	X

Table A.21.- The conformations identified for each step at different starting points in the search for the BAC for **25b**

Function	Energy	Distance	Total Dipole	PSA	Volume	Area
Energy	X	89	48	22	10	7
Distance	7	X	128	51	18	12
Total Dipole	19	10	X	147	80	49
PSA	17	10	7	X	70	43
Volume	31	17	11	7	X	81
Area	94	47	28	15	7	X

Table A.22.- The conformations identified for each step at different starting points in the search for the BAC for **25c**

Function	Energy	Distance	Total Dipole	PSA	Volume	Area
Energy	X	30	6	3	1	0
Distance	2	X	54	24	6	3
Total Dipole	3	2	X	74	14	7
PSA	3	2	2	X	51	19
Volume	10	8	3	2	X	44
Area	59	29	12	6	2	X

Table A.23.- The conformations identified for each step at different starting points in the search for the BAC for **25d**

Function	Energy	Distance	Total Dipole	PSA	Volume	Area
Energy	X	115	90	28	14	6
Distance	6	X	129	44	21	7
Total Dipole	15	6	X	135	57	20
PSA	26	10	7	X	89	34
Volume	53	20	11	6	X	66
Area	98	33	24	11	6	X

Table A.24.- The conformations identified for each step at different starting points in the search for the BAC for **25e**

Function	Energy	Distance	Total Dipole	PSA	Volume	Area
Energy	X	55	16	10	3	2
Distance	2	X	45	27	8	5
Total Dipole	5	2	X	60	15	10
PSA	13	5	2	X	45	21
Volume	25	9	3	2	X	55
Area	79	25	11	6	2	X

Table A.25.- The conformations identified for each step at different starting points in the search for the BAC for **25f**

Function	Energy	Distance	Total Dipole	PSA	Volume	Area
Energy	X	61	22	4	0	0
Distance	1	X	60	15	6	1
Total Dipole	4	0	X	47	14	9
PSA	10	4	0	X	52	26
Volume	16	7	1	0	X	44
Area	35	20	5	1	0	X

Table A.26.- The conformations identified for each step at different starting points in the search for the BAC for **pentamidine**

Function	Energy	Distance	Total Dipole	PSA	Volume	Area
Energy	X	42	25	7	2	1
Distance	1	X	43	19	4	1
Total Dipole	2	1	X	34	9	3
PSA	3	2	1	X	13	5
Volume	8	6	2	1	X	12
Area	19	11	3	1	1	X